STRUCTURE AND BONDING 126

**Series Editor** D. M. P. Mingos
**Volume Editors** P. Metrangolo · G. Resnati

# Halogen Bonding

## Fundamentals and Applications

Springer

# 126
# Structure and Bonding

**Series Editor: D. M. P. Mingos**

# Structure and Bonding
## Series Editor: D. M. P. Mingos

Recently Published and Forthcoming Volumes

**Halogen Bonding**
Fundamentals and Applications
Volume Editors: Metrangolo, P., Resnati, G.
Vol. 126, 2008

**High Energy Density Materials**
Volume Editor: Klapötke, T. H.
Vol. 125, 2007

**Ferro- and Antiferroelectricity**
Volume Editors: Dalal, N. S.,
Bussmann-Holder, A.
Vol. 124, 2007

**Photofunctional Transition Metal Complexes**
Volume Editor: V. W. W. Yam
Vol. 123, 2007

**Single-Molecule Magnets**
**and Related Phenomena**
Volume Editor: Winpenny, R.
Vol. 122, 2006

**Non-Covalent Multi-Porphyrin Assemblies**
Synthesis and Properties
Volume Editor: Alessio, E.
Vol. 121, 2006

**Recent Developments in Mercury Sience**
Volume Editor: Atwood, David A.
Vol. 120, 2006

**Layered Double Hydroxides**
Volume Editors: Duan, X., Evans, D. G.
Vol. 119, 2005

**Semiconductor Nanocrystals**
**and Silicate Nanoparticles**
Volume Editors: Peng, X., Mingos, D. M. P.
Vol. 118, 2005

**Magnetic Functions Beyond**
**the Spin-Hamiltonian**
Volume Editor: Mingos, D. M. P.
Vol. 117, 2005

**Intermolecular Forces and Clusters II**
Volume Editor: Wales, D. J.
Vol. 116, 2005

**Intermolecular Forces and Clusters I**
Volume Editor: Wales, D. J.
Vol. 115, 2005

**Superconductivity in Complex Systems**
Volume Editors: Müller, K. A.,
Bussmann-Holder, A.
Vol. 114, 2005

**Principles and Applications**
**of Density Functional Theory**
**in Inorganic Chemistry II**
Volume Editors:
Kaltsoyannis, N., McGrady, J. E.
Vol. 113, 2004

**Principles and Applications**
**of Density Functional Theory**
**in Inorganic Chemistry I**
Volume Editors:
Kaltsoyannis, N., McGrady, J. E.
Vol. 112, 2004

**Supramolecular Assembly**
**via Hydrogen Bonds II**
Volume Editor: Mingos, D. M. P.
Vol. 111, 2004

**Applications of Evolutionary Computation**
**in Chemistry**
Volume Editors: Johnston, R. L.
Vol. 110, 2004

# Halogen Bonding

## Fundamentals and Applications

Volume Editors: P. Metrangolo · G. Resnati

With contributions by

H. D. Arman · S. Biella · D. W. Bruce · M. Fourmigué · T. W. Hanks
A. Karpfen · J. K. Kochi · A. C. Legon · P. Metrangolo
W. T. Pennington · T. Pilati · G. Resnati · S. V. Rosokha

Springer

The series *Structure and Bonding* publishes critical reviews on topics of research concerned with chemical structure and bonding. The scope of the series spans the entire Periodic Table. It focuses attention on new and developing areas of modern structural and theoretical chemistry such as nanostructures, molecular electronics, designed molecular solids, surfaces, metal clusters and supramolecular structures. Physical and spectroscopic techniques used to determine, examine and model structures fall within the purview of Structure and Bonding to the extent that the focus is on the scientific results obtained and not on specialist information concerning the techniques themselves. Issues associated with the development of bonding models and generalizations that illuminate the reactivity pathways and rates of chemical processes are also relevant.
As a rule, contributions are specially commissioned. The editors and publishers will, however, always be pleased to receive suggestions and supplementary information. Papers are accepted for *Structure and Bonding* in English.
In references *Structure and Bonding* is abbeviated *Struct Bond* and is cited as a journal.

Springer WWW home page: springer.com
Visit the Struct Bond content at springerlink.com

Library of Congress Control Number: 2007936637

ISSN 0081-5993
ISBN 978-3-540-74329-3 Springer Berlin Heidelberg New York
DOI 10.1007/978-3-540-74330-9



**Springer is a part of Springer Science+Business Media**

springer.com



Cover design: WMXDesign GmbH, Heidelberg
Typesetting and Production: LE-TEX Jelonek, Schmidt & Vöckler GbR, Leipzig

Printed on acid-free paper 02/3180 YL – 5 4 3 2 1 0

## Series Editor

Prof. D. Michael P. Mingos

Principal
St. Edmund Hall
Oxford OX1 4AR, UK
*michael.mingos@st-edmund-hall.oxford.ac.uk*

## Volume Editors

Pierangelo Metrangolo

Department of Chemistry, Materials,
Chemical Engineering "Giulio Natta"
Politecnico di Milano
Via Mancinelli 7
20131 Milano, Italy
*pierangelo.metrangolo@polimi.it*

Giuseppe Resnati

Department of Chemistry, Materials,
Chemical Engineering "Giulio Natta"
Politecnico di Milano
Via Mancinelli 7
20131 Milano, Italy
*giuseppe.resnati@polimi.it*

## Editorial Board

## Structure and Bonding
## Also Available Electronically

For all customers who have a standing order to Structure and Bonding, we offer the electronic version via SpringerLink free of charge. Please contact your librarian who can receive a password or free access to the full articles by registering at:

springerlink.com

If you do not have a subscription, you can still view the tables of contents of the volumes and the abstract of each article by going to the SpringerLink Homepage, clicking on "Browse by Online Libraries", then "Chemical Sciences", and finally choose Structure and Bonding.

You will find information about the

- Editorial Board
- Aims and Scope
- Instructions for Authors
- Sample Contribution

at springer.com using the search function.

# Preface

Halogen atoms in organic compounds can typically be found at the periphery of molecules. For this reason, they are ideally positioned to be involved in intermolecular interactions. Indeed, halogen atoms are frequently involved in a wide variety of non-covalent interactions which can be remarkably different regarding their energetic and geometric features. Theoretical studies predict that the electron density distribution around halogen atoms forms an ellipsoid elongated in the direction perpendicular to the covalent bond axis. A clear trend of increasing electropositive potential develops along the covalent bond axis upon increasing the polarizability and atomic mass of the halogen. Experimental results confirm this anisotropic distribution and prove the amphoteric character of halogens. This can produce interactions in a direction perpendicular to the covalent bond axis when the halogen is the electron donor (Lewis base), and along the axis when the halogen is the electron acceptor (Lewis acid).

This book focuses on the interactions wherein halogens work as electrophilic species and interact with electron rich sites (namely, electronegative partners). Of the numerous non-covalent interactions involving halogens, this particular subset is typically referred to as halogen bonding. The book begins by introducing theoretical calculations on the characteristics of halogen bonding (A. Karpfen), then focuses on the adducts wherein the electron donor is a lone pair possessing species (n donor). The complexes formed by halogens and interhalogens in the gas (A. Legon) and solid phase (W. T. Pennington et al.) are presented and the role of halocarbons in halogen bonding-based crystal engineering is discussed (P. Metrangolo, G. Resnati et al.). A chapter exploring the complexes in which halogen atoms interact with $\pi$ electron donors (J. K. Kochi et al.) concludes the part of the book that deals with the generalities of halogen bonding. In contrast, the last two chapters of this book discuss halogen bonded adducts endowed with useful applicative properties. Among the many novel applications of halogen bonding, liquid crystals (D. Bruce) and conducting or magnetic materials (M. Fourmigue) are discussed as prototypical examples.

The findings presented throughout this book consistently converge towards the use of the term halogen bonding, independent of the energy of the interaction or its prevailing character, whether electrostatic or charge-transfer. The effectiveness of a scientific concept and the associated terminology often rest

on an optimized balance between generality, resulting in a wide applicability, and specificity, enabling it to predict specific phenomena. In this respect, it is our opinion that the concept of halogen bonding is beneficial if it is defined as comprehensively as possible, while assigning the specific role of the positive site in the interaction to the halogen. At one extreme, the term can be used for interactions in which a very strong polarity difference exists between interacting partners (as it is the case of dihalogen/halide anion complexes, *e.g.*, $I_3^-$). At the other extreme, the term halogen bonding can be used for interactions wherein the polarity difference between the interacting partners is very small (*e.g.*, in the triangular bromocarbon trimer synthon).

This book is a first in the field of halogen bonding. Focussing on interactions in which halogens work as the electrophilic sites, this book identifies the boundaries of the concept of halogen bonding. In addition, it organizes the diversified profile of intermolecular interactions involving halogens.

In order to reflect the differences in geometric and electronic parameters, a term different from halogen bonding might be used to address interactions wherein halogens work as electron donor sites. Halide bonding could be considered for this purpose, however, the best terminology to be used will emerge from the increasing interest in interactions involving halogens and will be spontaneously identified by the consensus of the scientific community.

The field of halogen bonding is still in its infancy. Nevertheless, this book proves its potential in the numerous and diverse fields in which recognition and self-assembly processes are crucial. Hopefully, this book will prompt new studies in the field that deepen the basic understanding of halogen interactions and implement its potential in the design of useful materials.

Milan,
September 2007

Pierangelo Metrangolo
Giuseppe Resnati

# Contents

**Theoretical Characterization of the Trends in Halogen Bonding**
A. Karpfen . . . . . 1

**The Interaction of Dihalogens and Hydrogen Halides with Lewis Bases in the Gas Phase: An Experimental Comparison of the Halogen Bond and the Hydrogen Bond**
A. C. Legon . . . . . 17

**Halogen Bonding with Dihalogens and Interhalogens**
W. T. Pennington · T. W. Hanks · H. D. Arman . . . . . 65

**Halogen Bonding in Crystal Engineering**
P. Metrangolo · G. Resnati · T. Pilati · S. Biella . . . . . 105

**X-ray Structures and Electronic Spectra of the π-Halogen Complexes between Halogen Donors and Acceptors with π-Receptors**
S. V. Rosokha · J. K. Kochi . . . . . 137

**Halogen-bonded Liquid Crystals**
D. W. Bruce . . . . . 161

**Halogen Bonding in Conducting or Magnetic Molecular Materials**
M. Fourmigué . . . . . 181

**Author Index Volumes 101–126** . . . . . 209

**Subject Index** . . . . . 219

## Contents of Structure and Bonding, Volume 108 and 111

## Supramolecular Assembly via Hydrogen Bonds I

ISBN: 978-3-540-20084-0

**Probing Hydrogen Bonding in Solids Using Solid State NMR Spectroscopy**
A. E. Aliev · K. D. M. Harris

**Crystal Engineering Using Multiple Hydrogen Bonds**
A. D. Burrows

**Molecular Containers: Design Approaches and Applications**
D. R. Turner · A. Pastor · M. Alajarin · J. W. Steed

## Supramolecular Assembly via Hydrogen Bonds II

ISBN: 978-3-540-20086-4

**Hydrogen Bonding Interactions Between Ions:**
**A Powerful Tool in Molecular Crystal Engineering**
D. Braga · L. Maini · M. Polito · F. Grepioni

**Hydrogen-Bonded Supramolecular Chain and Sheet Formation**
**by Coordinated Guanidine Derivatives**
P. Hubberstey · U. Suksangpanya

**Hydrogen-Bonding Templated Assemblies**
R. Vilar

**Hydrogen Bonded Network Structures Constructed**
**from Molecular Hosts**
M. J. Hardie

Struct Bond (2008) 126: 1–15
DOI 10.1007/430_2007_065

Published online: 7 September 2007

# Theoretical Characterization of the Trends in Halogen Bonding

Alfred Karpfen

Institute of Theoretical Chemistry, University of Vienna, Währinger Straße 17, 1090 Vienna, Austria
*alfred.karpfen@univie.ac.at*

**1 Introduction** . . . . . 2

**2 XY···B Complexes** . . . . . 3
2.1 XY···$NH_3$ Complexes . . . . . 4
2.2 Other XY···Amine Complexes . . . . . 10

**3 C–X···B Complexes** . . . . . 11
3.1 C–X···N Complexes . . . . . 12
3.2 C–X···H-C Complexes . . . . . 12

**4 Summary** . . . . . 13

**References** . . . . . 14

**Abstract** Theoretical investigations of the systematic trends in the spectroscopically observable properties of small intermolecular complexes bound via halogen bonding are reviewed. As a representative example of the charge-transfer or electron donor–acceptor complexes XY···B of dihalogens XY with different electron acceptors B, the case where B is an amine, in particular $NH_3$ or a methylated amine, has been selected. Additionally, a survey of the calculated properties of complexes of the type C – X···B, formed between molecules carrying the C–X group, such as halomethanes, and amines is provided. The borderline case of complexes with C – X···H – C interactions, in which halogen bonding and hydrogen bonding occur simultaneously, is included as well. The close analogy between the features characteristic of halogen bonding and those typical for hydrogen bonding is pointed out. The stabilization energies, structural parameters, theoretical vibrational spectra, and other properties useful for describing the charge transfer in these complexes are discussed in detail.

**Keywords** Halogen bonding · Hydrogen bonding · Charge-transfer complexes · Ab initio calculations

**Abbreviations**

| | |
|---|---|
| B3LYP | Becke's three-parameter exchange functionals and Lee, Yang, and Parr's correlation functionals |
| BH&HLYP | Exchange functional with equal-weighted contributions of Hartree–Fock, local spin density, and Becke functionals and Lee, Yang, and Parr's correlation functionals |
| BSSE | Basis set superposition error |

| | |
|---|---|
| CP | Counterpoise |
| CCSD(T) | Coupled cluster approach with single and double substitutions and inclusion of noniterative triple excitations |
| DFT | Density functional theory |
| MP2 | Second-order Møller–Plesset perturbation method |
| NQCC | Nuclear quadrupole coupling constant |
| RHF | Restricted Hartree–Fock method |

## 1 Introduction

Intermolecular interactions in gas-phase complexes, liquids, and organic and inorganic molecular crystals are, in general, characterized by intermolecular distances in the range of van der Waals distances. The most important exception is the case of hydrogen bonding. There, considerably shorter intermolecular distances are observed. The formation of a hydrogen bond A – H···B is usually encountered by a significant elongation of the A – H bond and an increase in the polarity of the A – H bond. Consequently, a spectroscopically observable, substantial red shift of the A – H stretching frequency occurs, accompanied by a large increase of the infrared intensity.

Among the noncovalent interactions, there is a second interesting exception with shorter intermolecular contacts: the case of halogen bonding. Originally, the term *halogen bonding* was introduced for complexes of dihalogens XY with different Lewis bases as interaction partners. Previously, complexes of this type were actually often characterized as charge-transfer complexes or as electron donor–acceptor complexes. Later, a more general definition of halogen bonding was suggested, following closely the analogy to the hydrogen bonding case. Thus, any noncovalent intermolecular arrangement A – X···B, where X is a halogen atom, is included in the definition. The characteristic structural and spectroscopic properties of the halogen bond have indeed much in common with those of the hydrogen bond. There too, the X – Y or A – X bond is usually elongated upon complex formation, the A – X stretching frequency is red-shifted, and the corresponding infrared intensity is enhanced.

In sharp contrast to the case of hydrogen bonding, most of the experimental gas-phase investigations on the complexes between dihalogens and Lewis bases stem exclusively from rotational spectroscopic investigations. For these complexes, there are hardly any vibrational spectroscopic data available. Therefore, theoretical investigations are currently the only way to obtain answers on all questions concerning the details of the intermolecular interaction, in particular, the structure changes induced by the formation of the halogen bond and the frequency shifts taking place upon complex formation in the interacting monomers.

Since the interactions in these complexes are occasionally quite weak and the interaction potentials are quite soft, only high-level quantum mechanical methods that take account of electron correlation are suitable for a reliable description of these compounds. The theoretical results obtained are indeed quite sensitive to the level of electron correlation chosen. Moreover, the inclusion of the counterpoise (CP) correction to the basis set superposition error (BSSE) in the course of the geometry optimization is often necessary, even when large basis sets are applied. Additionally, the conventional Møller–Plesset second-order (MP2) approach, which has been successfully applied to the calculation of intermolecular potential energy surfaces in the case of hydrogen bonding, has the tendency to overestimate the intermolecular interaction in these complexes. This becomes visible when comparing it to the methodically superior coupled cluster singles and doubles approach including a triples contribution via perturbational theory, CCSD(T). Quite similarly, several of the currently frequently applied density functional theory (DFT) methods may fail badly in the description of these complexes while others produce quite promising results.

## 2 XY···B Complexes

The interaction strength of complexes of dihalogens XY with different acceptors B spans a very wide range. The weakest complexes are those where the acceptor is a rare gas atom. Experimental and theoretical results on the structure, energetics, and dynamics of these rare gas–dihalogen complexes in the electronic ground and excited states have been summarized in recent review articles [1–3]. Their binding energies are all well below 1 kcal/mol, quite often even substantially below 100 $cm^{-1}$. In the electronic ground state, there are mostly two minima present, one for a linear arrangement and one for a T-shaped structure. Quite apart from the interesting dynamical questions connected with these weakly bound complexes, the rare gas–dihalogen interactions are of importance for all spectroscopic investigations of XY···B complexes and halogenated organic molecules in inert rare gas matrices. Nevertheless, the intermolecular interaction in these complexes is too weak to justify the notion of a halogen bond. Therefore, they are excluded from this review.

The interaction of dihalogen molecules XY with different acceptors B quite often leads to vicious chemical reactions. In most cases, the 1 : 1 complexes are extremely short-lived. To investigate these *prereactive* complexes experimentally in a collision-free environment, pulsed-nozzle, Fourier-transform microwave spectroscopy has turned out to be the ideal technique. Legon and coworkers prepared a large number of these complexes and performed detailed rotational spectroscopic analyses. Several series of simple molecules

have been chosen as Lewis bases B, among them CO, $C_2H_2$, $C_2H_4$, $H_2O$, $H_2S$, HCN, $NH_3$, $N(CH_3)_3$, $CH_3CN$, $H_2CO$, $PH_3$, aromatic rings like benzene, furan, thiophene, and saturated rings like oxirane and thiirane. These data have been discussed in two extensive reviews [4, 5] and are also treated in the contribution by Legon to this volume [6]. Of particular importance is the series of complexes between dihalogens and the ammonia molecule, since in these cases rich experimental data exist. Equally, a substantial number of theoretical calculations are already available. Therefore, the series of $XY\cdots NH_3$ complexes with $X,Y \in \{F,Cl,Br\}$ is chosen as a representative example of analogous series with other Lewis bases. The most important structural and vibrational spectroscopic properties of these complexes are thus discussed in some detail in the following sections.

## 2.1
## $XY\cdots NH_3$ Complexes

Five out of the six conceivable $XY\cdots NH_3$ complexes have previously been investigated with the aid of rotational spectroscopy by the group of Legon [7–11]. Only the complex with BrF is missing because of the known instability of this molecule toward a disproportionation reaction. A large number of theoretical calculations have already been devoted to these complexes, ranging in quality from conventional restricted Hartree–Fock (RHF) to MP2, and various DFT calculations [12–33]. The trends in the calculated equilibrium structures, stabilization energies, vibrational frequencies, dipole moments, and nuclear quadrupole coupling constants (NQCCs) within the series have been discussed by various groups [23, 26, 29–34]. Calculations beyond the MP2 approximation are, however, quite rare. CCSD(T) calculations including geometry optimizations are so far only available for the complexes with $F_2$, ClF, and $Cl_2$ [26].

In the following, a new set of data for the dihalogens BrF, BrCl, and $Br_2$, as obtained with MP2 and CCSD(T) calculations applying the aug-cc-pVTZ basis set, is presented. Comparison is made with the earlier MP2 and CCSD(T) data for $F_2$, ClF, and $Cl_2$ [26]. Two of the currently often used DFT variants, B3LYP and BH&HLYP, are also included. Because of the well-known BSSE error, optimized complex structures, as evaluated with and without CP correction, are reported. The BSSE error is negligible for the RHF and DFT calculations when using extended basis sets like aug-cc-pVTZ. However, for the MP2 and CCSD(T) approaches the BSSE error for structures and stabilization energies is definitely nonnegligible. The set of data necessary for the characterization of the halogen bond, namely intramolecular X-Y and intermolecular $Y\cdots N$ distances, harmonic vibrational frequencies, frequency shifts, and infrared intensity changes as obtained with MP2 and DFT methods, is also discussed.

The most important calculated and experimental monomer data, such as equilibrium distances, dipole moments, polarizabilities, and the harmonic vibrational frequencies of the dihalogens XY, are reported in Tables 1–4.

Overall, the trends in the calculated XY properties are satisfactorily reproduced with all four approaches: MP2, CCSD(T), B3LYP, and BH&HLYP. For the harmonic vibrational frequencies, the CCSD(T) data are far superior.

**Table 1** Calculated equilibrium bond distances [Å] of the dihalogens as obtained with different methods applying the aug-cc-pVTZ basis set [35]

| | MP2 | CCSD(T) | B3LYP | BH&HLYP | Exp. | Refs. |
|---|---|---|---|---|---|---|
| $F_2$ | 1.401 | 1.418 | 1.397 | 1.361 | 1.412 | [26] |
| ClF | 1.638 | 1.647 | 1.649 | 1.615 | 1.628 | [26] |
| $Cl_2$ | 1.999 | 2.020 | 2.024 | 1.996 | 1.988 | [26] |
| BrF | 1.758 | 1.765 | 1.775 | 1.742 | 1.759 | |
| BrCl | 2.138 | 2.160 | 2.170 | 2.141 | 2.136 | |
| $Br_2$ | 2.279 | 2.303 | 2.317 | 2.286 | 2.281 | |

**Table 2** Calculated dipole moments [D] of the dihalogens ClF, BrF, BrCl, and $NH_3$ as obtained with different methods applying the aug-cc-pVTZ basis set [36]

| | MP2 | B3LYP | BH&HLYP | Exp. | Refs. |
|---|---|---|---|---|---|
| ClF | 1.64 | 1.65 | 1.62 | 1.63 | [36] |
| BrF | 1.32 | 1.39 | 1.41 | 1.29 | [36] |
| BrCl | 0.45 | 0.49 | 0.48 | 0.57 | [36] |
| $NH_3$ | 1.52 | 1.49 | 1.51 | 1.47 | [36] |

**Table 3** MP2/aug-cc-pVTZ calculated polarizabilities ($\alpha$, $\alpha_{zz}$, $\alpha_{xx}$) [a.u.] of the dihalogens $F_2$, ClF, $Cl_2$, BrF, BrCl, and $Br_2$

| | MP2 | Exp. or calc.[a] | Refs. |
|---|---|---|---|
| $F_2$ | 7.83, 11.21, 6.14 | 9.31[b] | [37] |
| ClF | 17.94, 22.39, 15.71 | 22.48[c] | [38] |
| $Cl_2$ | 30.33, 41.55, 24.72 | 30.98[b] | [37] |
| BrF | 23.61, 28.08, 21.38 | 27.82[c] | [38] |
| BrCl | 36.98, 50.54, 30.20 | 51.50[c] | [38] |
| $Br_2$ | 44.08, 60.83, 35.70 | 47.37[b] | [37] |

[a] Experiment or superior calculation
[b] $\alpha$ from experiment
[c] $\alpha_{zz}$ calculated (MBPT(4))

**Table 4** Calculated harmonic vibrational frequencies and infrared intensities of the dihalogens as obtained with different methods applying the aug-cc-pVTZ basis set[a] [35]

| | MP2 | CCSD(T) | B3LYP | BH&HLYP | Exp. | Refs. |
|---|---|---|---|---|---|---|
| $F_2$ | 1003 | 916 | 1050 | 1158 | 917 | [26] |
| ClF | 800 (27)[b] | 771 | 787 (29) | 854 (36) | 786 | [26] |
| $Cl_2$ | 573 | 542 | 537 | 580 | 560 | [26] |
| BrF | 693 (30) | 672 | 676 (32) | 728 (41) | 671 | |
| BrCl | 461 (1.5) | 434 | 430 (1.5) | 461 (2.0) | 444 | |
| $Br_2$ | 341 | 322 | 316 | 338 | 325 | |

[a] Frequencies in $cm^{-1}$, infrared intensities in km/mol
[b] Intensities in parentheses

From these monomer properties alone it is not quite clear how the trends in the interaction strength with a fixed given acceptor B will develop. For the $X_2$ molecules the polarizabilities rise in the series $F_2$, $Cl_2$, and $Br_2$. The dipole moments of the interhalogens XY decrease in the series ClF, BrF, and BrCl, whereas the polarizabilities increase in this series.

In agreement with experiment, all XY···$NH_3$ complexes have the expected $C_{3v}$ equilibrium structure, irrespective of the computational level chosen, and in all XY···$NH_3$ complexes, the heavier halogen atom forms the halogen bond Y···N. The presence of the $C_{3v}$ symmetry is verified via vibrational frequency analyses. Hence, the XY···N substructure is perfectly linear. Assuming standard van der Waals radii values of 1.6 Å for N, and 1.5, 1.8, 1.9, and 2.1 Å for the halogens F, Cl, Br, and I, respectively, one arrives at intermolecular distances of 3.1, 3.4, 3.5, and 3.7 Å for the hypothetical intermolecular van der Waals distances of the XY···$NH_3$ complexes. The experimental [7–11] and calculated interatomic distances of all six XY···$NH_3$ complexes, as compiled in Table 5, demonstrate conclusively that the Y···N distances are significantly shorter by about 0.4–1.1 Å, thus fulfilling one criterion that resembles the behavior of hydrogen-bonded complexes. The comparison between optimized structures obtained with and without CP correction shows once more that the CP corrections are still substantial (0.02–0.07 Å) and nearly identical for MP2 and CCSD(T), but are entirely negligible for both DFT variants. The encouraging and amazingly good performance of the BH&HLYP method for the halogen-bonded cases, judged by the agreement with CCSD(T) and with experiment, has already been noted earlier by several other groups [20–22, 27–30, 32, 34].

The calculated intramolecular XY distances and the lengthening relative to the unperturbed monomers are given in Table 6. In all cases, the XY distances are elongated in the complex and these elongations range from about 0.01 Å in $F_2$···$NH_3$ to about 0.07 Å in BrF···$NH_3$. With the exception of $F_2$···$NH_3$, all methods predict quite similar modifications of the XY distances

**Table 5** Calculated intermolecular distances $R$(Y–N) [Å] of the XY$\cdots$NH$_3$ complexes as obtained with different methods applying the aug-cc-pVTZ basis set

| XY | | MP2 | CCSD(T) | B3LYP | BH&HLYP | Exp. | Refs. |
|---|---|---|---|---|---|---|---|
| $F_2$ | $R$(F–N) | 2.61 | 2.63 | 2.10 | 2.73 | | [26] |
| | $R_{CP}$(F–N) | 2.65 | 2.67 | 2.10 | 2.73 | 2.708 | [7] |
| ClF | $R$(Cl–N) | 2.24 | 2.32 | 2.27 | 2.34 | | [26, 27] |
| | $R_{CP}$(Cl–N) | 2.26 | 2.35 | 2.27 | 2.35 | 2.37 | [8] |
| $Cl_2$ | $R$(Cl–N) | 2.59 | 2.65 | 2.52 | 2.68 | | [26] |
| | $R_{CP}$(Cl–N) | 2.63 | 2.72 | 2.52 | 2.69 | 2.73$\pm$0.03 | [9] |
| BrF | $R$(Br–N) | 2.29 | 2.34 | 2.35 | 2.37 | | |
| | $R_{CP}$(Br–N) | 2.33 | 2.38 | 2.35 | 2.37 | | |
| BrCl | $R$(Br–N) | 2.47 | 2.54 | 2.50 | 2.57 | | |
| | $R_{CP}$(Br–N) | 2.53 | 2.57 | 2.50 | 2.57 | 2.627 | [10] |
| $Br_2$ | $R$(Br–N) | 2.54 | 2.60 | 2.56 | 2.66 | | |
| | $R_{CP}$(Br–N) | 2.61 | 2.64 | 2.57 | 2.66 | 2.72$\pm$0.03 | [11] |

**Table 6** Calculated intramolecular distances $R$(X–Y) [Å] of the XY$\cdots$NH$_3$ complexes as obtained with different methods applying the aug-cc-pVTZ basis set

| XY | | MP2 | CCSD(T) | B3LYP | BH&HLYP | Exp. | Refs. |
|---|---|---|---|---|---|---|---|
| $F_2$ | $R_{CP}$(F–F) | 1.415 | 1.430 | 1.518 | 1.369 | | [26] |
| | $\Delta R_{CP}$(F–F) | 0.014 | 0.012 | 0.121 | 0.008 | | |
| ClF | $R_{CP}$(Cl–F) | 1.712 | 1.702 | 1.733 | 1.668 | | [26, 27] |
| | $\Delta R_{CP}$(Cl–F) | 0.077 | 0.056 | 0.084 | 0.053 | | |
| $Cl_2$ | $R_{CP}$(Cl–Cl) | 2.034 | 2.044 | 2.088 | 2.023 | 2.00 | [9, 26] |
| | $\Delta R_{CP}$(Cl–Cl) | 0.035 | 0.024 | 0.064 | 0.027 | | |
| BrF | $R_{CP}$(Br–F) | 1.824 | 1.821 | 1.851 | 1.801 | | |
| | $\Delta R_{CP}$(Br–F) | 0.066 | 0.056 | 0.076 | 0.059 | | |
| BrCl | $R_{CP}$(Br–Cl) | 2.194 | 2.211 | 2.249 | 2.192 | 2.186 | [10] |
| | $\Delta R_{CP}$(Br–Cl) | 0.056 | 0.051 | 0.079 | 0.051 | | |
| $Br_2$ | $R_{CP}$(Br–Br) | 2.324 | 2.341 | 2.385 | 2.327 | 2.335 | [11] |
| | $\Delta R_{CP}$(Br–Br) | 0.045 | 0.038 | 0.068 | 0.041 | | |

in the complex. $F_2\cdots NH_3$ is so far a special case as it constitutes an instance of a very weak interaction, dominated by the dispersion contribution [25]. Therefore, in this case the deviation of the DFT methods from the CCSD(T) results is larger. The widening of the XY distances is actually slightly larger than in comparable (judged by the size of the interaction energy) hydrogen-bonded complexes.

The calculated interaction energies are collected in Table 7. Experimental data on the stability of these complexes are not available. The CP-

**Table 7** Calculated stabilization energies [kcal/mol] of the XY···$NH_3$ complexes as obtained with different methods applying the aug-cc-pVTZ basis set

| XY | | MP2 | CCSD(T) | B3LYP | BH&HLYP | Refs. |
|---|---|---|---|---|---|---|
| $F_2$ | $\Delta E$ | – 2.0 | – 2.0 | – 4.6 | – 1.2 | [26] |
| | $\Delta E_{CP}$ | – 1.8 | – 1.7 | – 4.5 | – 1.2 | |
| ClF | $\Delta E$ | – 11.8 | – 10.1 | – 12.6 | – 9.7 | [26, 28] |
| | $\Delta E_{CP}$ | – 11.0 | – 9.4 | – 12.4 | – 9.5 | |
| $Cl_2$ | $\Delta E$ | – 5.5 | – 4.9 | – 5.9 | – 4.2 | [26] |
| | $\Delta E_{CP}$ | – 4.9 | – 4.4 | – 5.8 | – 4.1 | |
| BrF | $\Delta E$ | – 16.8 | – 15.0 | – 15.8 | – 13.8 | |
| | $\Delta E_{CP}$ | – 14.6 | – 13.2 | – 15.6 | – 13.6 | |
| BrCl | $\Delta E$ | – 10.1 | – 9.0 | – 9.5 | – 7.6 | |
| | $\Delta E_{CP}$ | – 8.5 | | – 9.4 | – 7.5 | |
| $Br_2$ | $\Delta E$ | – 8.6 | | – 7.6 | – 5.9 | |
| | $\Delta E_{CP}$ | – 6.9 | | – 7.5 | – 5.8 | |

corrected CCSD(T) stabilization energies of the XY···$NH_3$ complexes range from –1.7 kcal/mol for $F_2$–$NH_3$ to about –13 kcal/mol for BrF–$NH_3$. This range is also typical for weak to medium strong hydrogen bonds. The differences between $\Delta E$ and $\Delta E_{CP}$, as evaluated with MP2 and CCSD(T), are very systematic. Apart from $F_2$···$NH_3$, the agreement between CCSD(T) and BH&HLYP is again excellent. The interaction strength increases in the series of $X_2$···$NH_3$ in the order $F_2$, $Cl_2$, and $Br_2$, as dictated by the trends in polarizabilities, and in the series of XY···$NH_3$ in the order ClF, BrCl, and BrF,

**Table 8** Calculated dipole moments ($\mu$) [D] and dipole moment enhancements ($\Delta\mu$) relative to monomers of the XY–$NH_3$ complexes as obtained with different methods applying the aug-cc-pVTZ basis set

| XY | | MP2 | B3LYP | BH&HLYP | Refs. |
|---|---|---|---|---|---|
| $F_2$ | $\mu$ | 1.99 | 4.57 | 1.95 | [26] |
| | $\Delta\mu$ | 0.47 | 3.08 | 0.44 | |
| ClF | $\mu$ | 5.68 | 5.98 | 5.10 | [26, 28] |
| | $\Delta\mu$ | 2.50 | 2.80 | 1.97 | |
| $Cl_2$ | $\mu$ | 3.40 | 4.41 | 3.26 | [26] |
| | $\Delta\mu$ | 1.88 | 2.92 | 1.65 | |
| BrF | $\mu$ | 6.48 | 6.64 | 6.19 | |
| | $\Delta\mu$ | 3.68 | 3.67 | 3.27 | |
| BrCl | $\mu$ | 5.23 | 5.77 | 4.93 | |
| | $\Delta\mu$ | 3.26 | 3.79 | 2.96 | |
| $Br_2$ | $\mu$ | 4.59 | 5.16 | 4.22 | |
| | $\Delta\mu$ | 3.07 | 3.67 | 2.57 | |

thus following neither purely the trends in XY dipole moments nor in XY polarizabilities. Overall, the interaction energies follow the order $F_2$, $Cl_2$, $Br_2$, BrCl, ClF, and BrF. The calculated dipole moments and the dipole moment enhancements relative to the sum of monomer dipole moments, displayed in Table 8, show a somewhat different trend. $\Delta\mu$ increases in the order $F_2$, $Cl_2$, ClF, $Br_2$, BrCl, and BrF and varies from about 0.4 D in $F_2\cdots NH_3$ to about 3.6 D in $BrF\cdots NH_3$. These quantities are probably also a more reliable guideline to the relative importance of charge transfer than the notoriously basis set dependent atomic charges.

Finally, MP2 and DFT calculated intramolecular X–Y stretching frequencies, their red shifts relative to the monomers, and the intermolecular $Y\cdots N$ stretching frequencies are collected in Table 9, together with the corresponding infrared intensities. Although there are no experimental gas-phase data available, the predictions can be considered as reliable. The MP2 calculated red shifts of the X–Y stretching mode are in the range of $-37\,cm^{-1}$ for $Br_2\cdots NH_3$ to $-174\,cm^{-1}$ for $ClF\cdots NH_3$. Their infrared intensities are quite large. Comparable intensities are also predicted for the intermolecular stretching vibrations.

**Table 9** Calculated harmonic X–Y and $X\cdots N$ stretching frequencies, frequency shifts, and infrared intensities of the $XY\cdots NH_3$ complexes as obtained with different methods applying the aug-cc-pVTZ basis set[a]

| XY | | MP2 | B3LYP | BH&HLYP | Refs. |
|---|---|---|---|---|---|
| $F_2$ | $\nu_{F-F}$ | 932 (10) | 631 (328) | 1109 (48) | [26] |
| | $\Delta\nu_{F-F}$ | – 106 | – 419 | – 49 | |
| | $\nu_{F-N}$ | 96 (2) | 191 (132) | 89 (2) | |
| ClF | $\nu_{Cl-F}$ | 626 (232) | 607 (249) | 711 (241) | [26, 28] |
| | $\Delta\nu_{Cl-F}$ | – 174 | – 180 | – 144 | |
| | $\nu_{Cl-N}$ | 237 (104) | 253 (66) | 206 (57) | |
| $Cl_2$ | $\nu_{Cl-Cl}$ | 505 (45) | 435 (90) | 525 (42) | [26] |
| | $\Delta\nu_{Cl-Cl}$ | – 68 | – 102 | – 55 | |
| | $\nu_{Cl-N}$ | 138 (34) | 164 (57) | 130 (23) | |
| BrF | $\nu_{Br-F}$ | 598 (133) | 554 (164) | 618 (181) | |
| | $\Delta\nu_{Br-F}$ | – 95 | – 122 | – 110 | |
| | $\nu_{Br-N}$ | 247 (58) | 258 (52) | 237 (58) | |
| BrCl | $\nu_{Br-Cl}$ | 393 (48) | 359 (56) | 405 (52) | |
| | $\Delta\nu_{Br-Cl}$ | – 68 | – 71 | – 56 | |
| | $\nu_{Br-N}$ | 186 (87) | 195 (70) | 164 (57) | |
| $Br_2$ | $\nu_{Br-Br}$ | 294 (23) | 266 (29) | 301 (23) | |
| | $\Delta\nu_{Br-Br}$ | – 37 | – 50 | – 28 | |
| | $\nu_{Br-N}$ | 168 (76) | 174 (65) | 145 (47) | |

[a] Frequencies and shifts relative to the XY monomers in $cm^{-1}$, infrared intensities in km/mol in parentheses

**Table 10** BH&HLYP/aug-cc-pVTZ calculated nuclear quadrupole coupling constants $\chi$(N) and $\chi$(Hal) [MHz] of the complexes XY···$NH_3$ [a]

| Molecule | $\chi$(N) | $\chi$(Cl) | $\chi$(Br) |
|---|---|---|---|
| $NH_3$ | – 4.34 | | |
| ClF | | – 143.40 | |
| $Cl_2$ | | – 110.96 | |
| BrCl | | – 102.5 | 878.5 |
| $Br_2$ | | | 808.2 |
| ClF···$NH_3$ | – 3.26 | – 146.95 | |
| $Cl_2$···$NH_3$ | – 3.97 | – 116.5/ – 100.0 | |
| BrCl···$NH_3$ | – 3.59 | – 84.2 | 932.4 |
| $Br_2$···$NH_3$ | – 3.74 | | 863.0/690.6 |

[a] Taken from [30]

Other key properties of these complexes relevant for comparison with experiment are the nuclear quadrupole coupling constants. Theoretical NQCC values, as calculated via electric field gradients, are discussed exhaustively in several recent theoretical investigations [26, 28, 30, 33, 34] and in experimental work [4–11]. BH&HLYP/aug-cc-pVTZ calculated NQCCs [30, 34], as evaluated for XY···$NH_3$ complexes, are listed in Table 10.

The complexes XY···$NH_3$ with Y = I have also already been investigated theoretically [29, 31, 33, 34] and for the case of ICl···$NH_3$ an experimental investigation has been reported [39]. Summarizing the experimental and theoretical results on XY···$NH_3$ complexes, one may characterize them all as "outer" complexes in the terminology suggested by Mulliken [40], i.e., they all have "intermolecular" equilibrium structures in which the dihalogens $X_2$ or XY are still recognizable as molecular entities, and in which the intermolecular Y···N distances are distinctly larger than the covalent N–Y distances in halogenated amines.

## 2.2 Other XY··· Amine Complexes

Experimental information on the complexes between dihalogens and methylated amines is still comparatively scarce. Gas-phase investigations are available only for the complexes of trimethylamine with $F_2$ [41] and with ClF [42]. So far only a few theoretical investigations on XY···amine complexes have been presented [16, 17, 22, 24, 28, 32, 34, 43, 44]. On the basis of rotational spectroscopic analysis, the $N(CH_3)_3$···ClF complex was described as being dominated by a significant contribution of an ionic $[(CH_3)NCl]^+\cdots F^-$ valence bond structure [41]. For the $(CH_3)_3N\cdots F_2$ complex an even stronger tendency toward an ionic $[(CH_3)NF]^+\cdots F^-$ structure was reported [40].

**Table 11** MP2/6-311++G(3df,2p) calculated intermolecular Y···N distances and intramolecular X–Y distances [Å] of XY···amine complexes[a]

| XY | $NH_3$ | $CH_3NH_2$ | $(CH_3)_2NH$ | $(CH_3)N$ |
|---|---|---|---|---|
| $F_2$ | 2.69/1.409[b] | 1.83/1.734 | 1.84/1.763 | 1.85/1.774 |
| ClF | 2.27/1.703 | 2.14/1.743 | 2.08/1.769 | 2.06/1.787 |
| $Cl_2$ | 2.71/2.010 | 2.51/2.037 | 2.30/2.093 | 2.20/2.138 |
| BrF | 2.34/1.837 | 2.26/1.859 | 2.22/1.874 | 2.21/1.881 |
| BrCl | 2.57/2.184 | 2.42/2.218 | 2.34/2.248 | 2.30/2.263 |
| $Br_2$ | 2.66/2.320 | 2.49/2.353 | 2.39/2.384 | 2.34/2.403 |

[a] Taken from [32]
[b] Notation $R$(Y–N)/$R$(X–Y)

A systematic theoretical study of XY···$(CH_3)_{3-n}NH_n$ complexes performed at the MP2/6-311++G(3df,2p) level and with several DFT variants [32] revealed that the structural trends taking place upon consecutive methylation (with increasing base strength) are highly systematic. As an illustration, the MP2 calculated intermolecular N···Y and intramolecular XY distances are shown in Table 11. It is evident that upon increasing the base strength of the amine, the N···Y distances are shortened considerably. Simultaneously, the dihalogen distances are widened, thus moving the equilibrium structure in the direction of an "inner" complex [40]. However, most of the complexes are still best described as "intermediate". Among all the complexes considered, the $(CH_3)_3N\cdots F_2$ complex is probably closest to Mulliken's "inner"-type charge-transfer complex. The $(CH_3)_3N\cdots$XY complexes are significantly more stable than their $H_3N\cdots$XY analogs. The calculated interaction energies are close to 20 kcal/mol for the $(CH_3)_3N\cdots$BrF complex [32].

## 3 C–X···B Complexes

C-X···B interactions play an important role in supramolecular chemistry, particularly in the self-assembly of molecular crystals [45–47]. C–X···O and C–X···N interactions are quite typical examples and are often responsible for the specific architecture of organic crystals. An interesting series of complexes are those with an A–X···H-C intermolecular contact. Adopting the currently accepted definition of halogen bonding advocated in other contributions to this volume, the latter complexes do not belong to the class of halogen-bonded complexes. These complexes are more often discussed in the context of hydrogen bonding, in particular *blue-shifted* hydrogen bonds. However, in view of the structural and spectroscopic consequences of C–X···B halogen

bonding, lengthening of the C–X bond, red shift, and intensity increase of the C–X stretching vibration, they may equally be treated as a separate group within the family of halogen-bonded complexes.

### 3.1 C–X···N Complexes

The interaction of a series of fluoroalkyl halides, $CH_3I$, $CH_2FI$, $CHF_2I$, $CF_3I$, $CF_3Br$, and $CF_3Cl$, with the ammonia molecule was investigated theoretically with MP2 and DFT methods [48]. A linear C–X···N arrangement was assumed for all these complexes. In all cases, the calculated X···N distances are shorter than the sum of van der Waals distances, and the interaction energies of the complexes are in a range of about 2–6 kcal/mol with comparatively small charge-transfer contributions. With increasing fluorine substitution the complexes become significantly more stable. The same trend was also found for a broader range of C–X molecules interacting with ammonia [33]. Contrary to the interaction of XY dihalogens with methylated amines discussed in Sect. 2.2, the interaction energy of molecules with C–X bonds and methylated amines decreases upon successive methylation [33]. The same result was also found in a study of $CF_3I$ interacting with trimethylamine and related acceptors [49].

Among other halogen-bonded C–X···B complexes, theoretical vibrational frequencies of the complexes $CF_3Cl\cdots NH_3$ and $CF_3Br\cdots NH_3$ were investigated too, with the interesting result that the calculated C–X stretching frequencies turned out to be shifted to higher wavenumbers [50]. Because of the analogy to the blue-shifting hydrogen bonds [51, 52], these particular C–X···B complexes have been called *blue-shifting halogen bonds*.

Comparing C–X bonds with different hybridization states of the carbon atom revealed that *sp*-hybridized C–X bonds form the strongest halogen bonds, followed by $sp^2$- and $sp^3$-hybridized C–X bonds [33], again a trend similar to the relative hydrogen bonding ability of C–H bonds. Ab initio and DFT studies on halogen bonding between appropriately substituted aromatic molecules, such as halobenzenes and pyridines or Schiff bases, mimicking the bonding situation in molecular crystals, are also available [53–56]. These investigations confirm that halogen bonds are highly directional. Although in most cases the interaction energies appear to be quite small, of the order of 2 kcal/mol, they are sufficiently strong to have a prominent influence on crystal packing.

### 3.2 C–X···H-C Complexes

Among the C–X···H–C complexes, the case of C–F···H–C is the best investigated. The C–F···H–C moiety is not linear. From the experimental side,

the gas-phase structures of a few dimers formed between fluoromethanes were investigated, e.g., the difluoromethane dimer $(CH_2F_2)_2$ [57, 58] and the $CHF_3$ — $CH_3F$ dimer [59, 60]. For the latter, cryospectroscopic investigations on the FTIR spectra have recently been reported [61]. Theoretical investigations are also available for the $(CH_2F_2)_2$ dimer [57, 62], the $CHF_3$ — $CH_3F$ dimer [59–61, 63], and the $(CHF_3)_2$ dimer [64]. All conceivable dimers that can be formed between $CH_4$, $CH_3F$, $CH_2F_2$, $CHF_3$, and $CF_4$ were studied at the MP2/6-31+G(d,p) level [65]. The interaction of molecules carrying $sp^3$-hybridized C–F bonds ($CH_3F$, fluorocyclopropane $C_3H_5F$) with small molecules carrying either *sp*-, $sp^2$-, or $sp^3$-hybridized C–H bonds was also recently studied [66].

There are several features common to the interaction of fluoromethanes. In the case of $sp^3$-hybridized C–F and C–H bonds a single C–F···H–C contact is comparatively weak (about 0.5 kcal/mol [65, 66]). However, the calculations showed that some of these dimers have interaction energies in the 2–3 kcal/mol range. This can be traced back to multiple C–F···H–C contacts in the cyclic equilibrium structures of these dimers. The strongest bound of these complexes is the dimer formed between $CHF_3$ and $CH_3F$ with an equilibrium structure with three C–F···H–C contacts. Most of the investigations on the various fluoromethane dimers were actually carried out to learn more about weak hydrogen bonds or about blue-shifting hydrogen bonds. As a general structural feature, the C–H bonds in these complexes are contracted, while the C–F bonds are all elongated. Since this kind of interaction, the C–F···H–C contact, can be viewed as a hydrogen bond and, simultaneously, also as a halogen bond, the term *halogen–hydrogen bond* has been coined in the related case of the interaction of fluoromethanes with hydrogen fluoride clusters, in which the C–F···H–F contact plays a leading role [67]. C–F···H–C contacts are considerably stronger when the C–H bond is adjacent to a C=C or a C≡C bond. The calculated interaction energy between $CH_3F$ and ethyne is close to 1.6 kcal/mol [66].

## 4 Summary

Different types of halogen bonding as they occur in the interaction of small molecules have been reviewed. In all cases studied so far, the halogen bond turned out to have a number of characteristic properties reminiscent of the well-known hydrogen bond. The best investigated cases are those in which a dihalogen XY interacts with a Lewis base B.

Depending on the type of dihalogen and the chosen Lewis base, the interaction can vary from very weak, e.g., as in $F_2$···$NH_3$, to about 20 kcal/mol in the complex of trimethylamine with BrF. The XY···amine complexes are of "outer" or "intermediate" types. The molecular entity XY can still be recog-

nized. Among the complexes considered, the complex of trimethylamine with $F_2$ is probably closest to the Mulliken "inner"-type complexes.

The other types of halogen bonds, C–X···B or C–X···H–C are all considerably weaker. The interaction energies of the C–X···B contacts rarely exceed 5 kcal/mol, and those of the C–X···H–C contacts are even weaker. Nevertheless, in most cases they show all the structural and vibrational spectroscopic features also encountered in the case of hydrogen bonding. The intermolecular distances are all consistently shorter than those expected from the sum of van der Waals radii. Even the case of blue-shifting halogen bonds, in analogy to the blue-shifting hydrogen bonds, may occur. In both cases, the blue shift is a consequence of the intramolecular coupling in the monomer [68].

## References

1. Rohrbacher A, Williams J, Janda KC (1999) Phys Chem Chem Phys 1:5263
2. Rohrbacher A, Halberstadt N, Janda KC (2000) Ann Rev Phys Chem 51:405
3. Delgado-Barrio G, Prosmiti R, Valdés Á, Villareal P (2005) Phys Scripta 73:C57
4. Legon AC (1999) Angew Chem Int Ed 38:2686
5. Legon AC (1998) Chem Eur J 4:1891
6. Legon AC (2007) Prereactive Complexes of Dihalogens with Lewis Bases in the Gas Phase (Chapter 2, this volume). Springer, Heidelberg
7. Bloemink HI, Hinds K, Holoway JH, Legon AC (1995) Chem Phys Lett 245:598
8. Bloemink HI, Evans CM, Holoway JH, Legon AC (1996) Chem Phys Lett 248:260
9. Legon AC, Lister DG, Thorn JC (1994) J Chem Soc Faraday Trans 90:3205
10. Bloemink HI, Legon AC, Thorn JC (1995) J Chem Soc Faraday Trans 91:781
11. Bloemink HI, Legon AC (1995) J Chem Phys 103:876
12. Lucchese RR, Schaefer HF III (1975) J Am Chem Soc 91:3409
13. Umeyama H, Morokuma H, Yamabe S (1977) J Am Chem Soc 99:330
14. Reed AE, Weinhold F, Curtiss LA, Pochatko DJ (1986) J Chem Phys 84:5687
15. Røeggen I, Dahl T (1992) J Am Chem Soc 114:511
16. Kobayashi T, Matsuzaa H, Iwata S (1994) Bull Chem Soc Jpn 67:3172
17. Tachikawa H, Komatsu E (1995) Inorg Chem 34:6546
18. Latajka Z, Berski S (1996) J Mol Struct (Theochem) 371:11
19. Latajka Z, Scheiner S, Bouteiller Y, Ratajczak H (1996) J Mol Struct (Theochem) 376:343
20. Ruiz E, Salahub DR, Vela A (1996) J Phys Chem 100:12265
21. Zhang Z, Zhao C-Y, You X-Z (1997) J Phys Chem A 101:2879
22. Salai Cheetu Ammal S, Ananthavel SP, Venuvanalingam P, Hedge MSJ (1997) J Phys Chem A 101:1155
23. Alkorta I, Rozas I, Elguero J (1998) J Phys Chem A 102:9278
24. Karpfen A (1999) Chem Phys Lett 299:493
25. Karpfen A (2000) Chem Phys Lett 316:483
26. Karpfen A (2000) J Phys Chem A 104:6871
27. Garcia A, Elorza JM, Ugalde JM (2000) J Mol Struct (Theochem) 501–502:207
28. Karpfen A (2001) J Phys Chem A 105:2064
29. Zhang Y, You X-Z (2001) J Comput Chem 22:327
30. Poleshchuk OK, Legon AC (2002) Z Naturforsch A 57:537

31. Poleshchuk OK, Kalinina EL, Legon AC (2003) Russ J Coord Chem 29:60
32. Karpfen A (2003) Theor Chem Acc 110:1
33. Zou J-W, Jiang Y-J, Guo M, Hu G-X, Zhang B, Liu H-C, Yu Q-S (2005) Chem Eur J 11:740
34. Poleshchuk OK, Branchadell V, Brycki B, Fateev AV, Legon AC (2006) J Mol Struct (Theochem) 760:175
35. Huber KP, Herzberg G (1979) Molecular spectra and molecular structure, vol 4. Van Nostrand Reinhold, New York
36. McClellan AL (1963) Tables of experimental dipole moments. Freeman, San Francisco
37. Lide DR (ed) (1999) Handbook of chemistry and physics. CRC, Boca Raton
38. Sadlej AJ (1992) J Chem Phys 96:2048
39. Waclawik ER, Legon AC (1999) Phys Chem Chem Phys 1:4961
40. Mulliken RS, Person WB (1969) J Am Chem Soc 91:3409
41. Bloemink HI, Cooke SA, Holloway JH, Legon AC (1997) Angew Chem Int Ed 36:1340
42. Bloemink HI, Holloway JH, Legon AC (1996) Chem Phys Lett 254:59
43. Matsuzawa H, Iwata S (1992) Chem Phys 163:297
44. Tachikawa H, Komatsu E (1998) Inorg Chim Acta 281:85
45. Metrangolo P, Resnati G (2001) Chem Eur J 7:2511
46. Metrangolo P, Neukirch H, Pilati T, Resnati G (2005) Acc Chem Res 38:386
47. Metrangolo P, Resnati G (2007) Halogen Bonding in Supramolecular Chemistry (Chapter 5, this volume). Springer, Heidelberg
48. Valerio G, Raos G, Meille SM, Metrangolo P, Resnati G (2000) J Phys Chem A 104:1617
49. Romaniello P, Lelj F (2002) J Phys Chem A 106:9114
50. Wang W, Wong N-B, Zheng W, Tian A (2004) J Phys Chem A 108:1799
51. Hobza P, Havlas Z (2000) Chem Rev 100:4253
52. Hobza P, Havlas Z (2002) Theor Chem Acc 108:325
53. Lommerse JPM, Stone AJ, Taylor R, Allen FH (1996) J Am Chem Soc 118:3116
54. Walsh BR, Padgett CW, Metrangolo P, Resnati G, Hanks TW, Pennington WT (2001) Cryst Growth Des 1:165
55. Bianchi R, Forni A, Pilati T (2003) Chem Eur J 9:1631
56. Berski S, Ciunik Z, Drabent K, Latajka Z, Panek J (2004) J Phys Chem B 108:12327
57. Caminati W, Melandri S, Moreschini P, Favero P (1999) Angew Chem Int Ed 38:2924
58. Blanco S, López JC, Lesarri A, Alonso JL (2002) J Mol Struct 612:255
59. Futami S, Kudoh S, Takayanagi M, Nakata M (2002) 357:209
60. Caminati W, López JC, Alonso JL, Grabow J-U (2005) Angew Chem Int Ed 44:3840
61. Rutkowski KS, Rodziewicz P, Melikova S, Herrebout WA, van der Veken BJ, Koll A (2005) Chem Phys 313:225
62. Ebrahimi A, Roohi H, Habibi SM (2004) J Mol Struct (Theochem) 684:87
63. Rodziewicz P, Rutkowski KS, Melikova S, Koll A (2005) Chem Phys Chem 6:1282
64. Tsuzuki S, Uchimaru T, Mikami M, Urata S (2004) J Phys Chem A 107:7962
65. Kryachko ES, Scheiner S (2004) J Phys Chem A 108:2527
66. Hyla-Krispin I, Haufe S, Grimme S (2004) Chem Eur J 10:3411
67. Karpfen A, Kryachko ES (2005) Chem Phys 310:77
68. Kryachko ES, Karpfen A (2006) Chem Phys 329:313

Struct Bond (2008) 126: 17–64
DOI 10.1007/430_2007_063

Published online: 19 September 2007

# The Interaction of Dihalogens and Hydrogen Halides with Lewis Bases in the Gas Phase: An Experimental Comparison of the Halogen Bond and the Hydrogen Bond

A. C. Legon

School of Chemistry, University of Bristol, Bristol BS8 1TS, UK
*A.C.Legon@Bristol.ac.uk*

**1 Introduction** . . . . . 18
1.1 Historical Background . . . . . 18
1.2 Definitions and Nomenclature . . . . . 19
1.3 Summary . . . . . 21

**2 Properties of Isolated Complexes B···XY: How to Measure Them** . . . . 21

**3 Comparison of the Angular and Radial Geometries of Halogen-Bonded Complexes B···XY and their Hydrogen-Bonded Analogues B···HX** . . . . . 23
3.1 Angular Geometries of B···ClF and B···HCl in Which B is a n-Pair Donor . . . . . 25
3.1.1 B Carries a Single n-Pair . . . . . 25
3.1.2 B Carries Two Equivalent n-Pairs . . . . . 26
3.1.3 B Carries Two Inequivalent n-Pairs . . . . . 35
3.2 Angular Geometries of B···ClF and B···HCl in Which B is a π-Pair Donor . . . . . 36
3.2.1 B Carries a Single-π-Pair . . . . . 36
3.2.2 B Carries Pseudo-π-Pairs . . . . . 38
3.2.3 B Carries Several-π-Pairs . . . . . 39
3.3 Angular Geometries of B···ClF and B···HCl in Which B is a Mixed n-Pair/π-Pair Donor . . . . . 43
3.4 Radial Geometries of Complexes B···XY and B···HX: A Summary . . . . 47

**4 Intermolecular Binding Strength in Halogen-Bonded Complexes: Systematic Behaviour of $k_\sigma$** . . . . . 47

**5 Extent of Electron Transfer in Halogen-Bonded Complexes B···XY** . . . 50
5.1 Electron Transfer in Weak (Outer) Complexes B···XY . . . . . 50
5.2 Do Mulliken Inner Halogen-Bonded Complexes Exist in the Gas Phase? . 54

**6 Conclusions: A Model for the Halogen Bond in B···XY** . . . . . 56

**References** . . . . . 59

**Abstract** This chapter is concerned exclusively with the experimentally determined properties of halogen-bonded complexes of the type B···XY in isolation in the gas phase and their relationship with those of the corresponding hydrogen-bonded complexes B···HX.

B is one of a series of simple Lewis bases and XY is a homo- or hetero-dihalogen molecule $F_2$, $Cl_2$, $Br_2$, ClF, BrCl or ICl. The method used to determine these properties (angular and radial geometry, binding strength, and the extent of electric charge redistribution on formation of B···XY) is first outlined. A comparison of the angular geometries of the pair of halogen-bonded and hydrogen-bonded complexes B···ClF and B···HCl as B is systematically varied follows. Systematic relationships among the radial geometries of the two series are also summarised. The intermolecular stretching force constants $k_\sigma$ and the extent of electron transfer (both inter- and intramolecular) on formation of B···XY, for XY = $Cl_2$, $Br_2$, ClF, BrCl or ICl, are shown to vary systematically as B is varied. A striking similarity noted among the properties of halogen-bonded complexes B···XY and their hydrogen-bonded analogues B···HX demonstrates that rules for predicting the angular geometries of hydrogen-bonded complexes (and other generalisations) may also be applied to the halogen-bonded series, but with the caveat that while the hydrogen bond shows a propensity to be non-linear when B···HX has appropriate symmetry, the halogen bond tends to remain close to linearity. A model for the halogen bond, successfully applied earlier to the hydrogen bond, is proposed.

**Keywords** Lewis bases · Dihalogens · Halogen bond · Angular geometry · Electric charge transfer

**Abbreviations**

| | |
|---|---|
| Efg | Electric field gradient |
| n-pair | Non-bonding electron pair |
| π-pair | π-bonding electron pair |
| XY | Generalised dihalogen molecules |
| HX | Generalised hydrogen halide |

## 1 Introduction

This chapter is restricted to a discussion of halogen-bonded complexes B···XY that involve a homo- or hetero-dihalogen molecule XY as the electron acceptor and one of a series of simple Lewis bases B, which are chosen for their simplicity and to provide a range of electron-donating abilities. Moreover, we shall restrict attention to the gas phase so that the experimental properties determined refer to the isolated complex. Comparisons with the results of electronic structure calculations are then appropriate. All of the experimental properties of isolated complexes B···XY considered here result from interpreting spectroscopic constants obtained by analysis of rotational spectra.

### 1.1 Historical Background

The first report of an adduct of the type to be discussed here was that of Guthrie in 1863 [1], who described the compound $H_3N\cdots I_2$. The spectroscopy of the interaction of benzene with molecular iodine in the UV/visible

region carried out by Benesi and Hildebrand in 1949 [2] was the initial focus of the important work of Mulliken [3] on the theory of electron donor–acceptor complexes in the 1950s and 1960s. During that period, Hassel and co-workers [4, 5] carried out X-ray diffraction studies of crystals of addition complexes formed by dihalogen molecules with Lewis bases. They concluded that the hydrogen bridge and halogen bridge were closely related. Of particular interest in the context of the work to be described here is Hassel's statement that, in complexes formed between halogen molecules and electron-donor molecules possessing lone pairs of electrons, it is to be assumed "that halogen atoms are directly linked to donor atoms with bond directions roughly coinciding with the axes of the orbitals of the lone pairs in the non-complexed donor molecule". Hassel's investigations involved crystals of the adducts, so that the complexes were therefore mutually interacting, albeit quite weakly. Complexes in effective isolation in cryogenic matrices were studied by infrared spectroscopy in the 1980s, particulary by Pimentel [6], Ault [7–10] and Andrews [11–14]. The so-called fast-mixing nozzle [15] incorporated into a pulsed-jet, Fourier-transform microwave spectrometer [16, 17] allowed complexes formed from simple Lewis bases (such as $NH_3$, $H_2CCH_2$, etc.) and dihalogen molecules to be isolated and probed by microwave radiation before they could undergo the (sometimes violent) reaction that attends normal mixing. This technique allowed the power and precision of rotational spectroscopy to be brought to bear on many simple complexes. Moreover, the Lewis base and the dihalogen molecule could be systematically varied to reveal conclusions of general interest about the binding that holds the two components together.

## 1.2 Definitions and Nomenclature

The aim of this chapter is to show that there is a strong parallelism between the measured properties of halogen-bonded and hydrogen-bonded complexes and, consequently, that the terms *halogen bond* and *hydrogen bond* carry similar connotations. After extensive consultations and discussions, the IUPAC Working Party on the hydrogen bond, and other molecular interactions, put forward the following definition of the hydrogen bond for consideration by the Chemistry community [18]:

"*The hydrogen bond is an attractive interaction between a group X–H and an atom or a group of atoms, in the same or different molecule(s), when there is evidence of bond formation.*"

Of several properties simultaneously recommended as providing criteria of such evidence, the most important in the present context are:

1. The physical forces involved in the hydrogen bond must include electrostatic and inductive forces in addition to London dispersion forces

2. The atoms H and X are covalently bound to one another, and B···HX is polarised so that the H atom becomes more electropositive (i.e. the partial positive charge $^{\delta+}$ increases)
3. The lengths of the H–X bond and, to a lesser extent, the bonds involved in B deviate from their equilibrium values
4. The stronger the hydrogen bond, the more nearly linear is the Z···H – X arrangement and the shorter the B···H distance
5. The interaction energy per hydrogen bond is greater than at least a few times $kT$, where $T$ is the temperature of the observation, in order to ensure its stability

We shall show both from experimental evidence about gas-phase complexes and, to a lesser extent, from the results of electronic structure calculations that a parallel definition of the intermolecular halogen bond is appropriate:

"*The halogen bond is an attractive interaction between a halogen atom X and an atom or a group of atoms in different molecule(s), when there is evidence of bond formation.*"

The atom X may be attached to another halogen atom Y or some other group of atoms R and the criteria (1–5) can be used with appropriate modification.

This definition was implied by the author [19, 20], who used the terms halogen bond or chlorine bond in these and in earlier articles referred to therein. The definition is also similar to that proposed by Metrangolo et al. [21], who used the term halogen bond (with XB as an abbreviation analogous to HB for the hydrogen bond) to describe any non-covalent interaction involving halogens as electron acceptors. Thus, the general notation for the halogen bond would be B···XY, where B is a Lewis base (electron donor), X is a halogen atom (electron acceptor) and Y can be a halogen atom or some other atom that is a constituent of a group R attached to X. The Lewis base B and XY might undergo a chemical reaction when mixed under normal conditions of temperature and pressure. This is especially so when XY is $F_2$ or ClF, both of which are notoriously reactive. To obtain the experimental results discussed here, pre-mixing of the components was avoided and instead we used a coaxial flow technique [15] to form B···XY but to preclude chemical reaction of B and XY. Accordingly, the phrase *pre-reactive complexes* is used to describe such species [22].

Mulliken [3] presented a classification of electron donor–acceptor complexes based on the extent of intermolecular charge transfer that accompanies complex formation. An *outer* complex is one in which the intermolecular interaction B···XY is weak and there is little intra- or intermolecular electric charge redistribution, while an *inner* complex is one in which there is extensive electric charge (electrons or nuclei) redistribution to give $[BX]^+\cdots Y^-$. Inner complexes are presumably more strongly bound in general than outer complexes.

### 1.3 Summary

The structure of the remainder of this chapter is as follows: First, in Sect. 2, we shall summarise briefly how the various properties of isolated complexes B···XY may be derived from the molecular constants that are determinable by analysis of rotational spectra. Then, in Sects. 3, 4 and 5, we shall present some generalisations about the halogen bond through the discussion of pre-reactive, outer complexes of the type B···XY. The approach will be to compare the properties of halogen-bonded complexes B···XY, as determined from rotational spectroscopy, with those of the corresponding hydrogen-bonded analogues B···HX, similarly determined. We shall show by systematic variation of both B and XY that there is a striking parallelism of the properties (angular geometry in Sect. 3, intermolecular stretching force constant in Sect. 4, electric charge redistribution on complex formation in Sect. 5) between the two types of complex. We shall also show in Sect. 5, by a comparison of the series $H_3N\cdots HX$ and $(CH_3)_3N\cdots HX$ with corresponding members of the series $H_3N\cdots XY$ and $(CH_3)_3N\cdots XY$, that hydrogen- and halogen-bonded complexes that tend towards the limiting Mulliken inner type can be identified in the gas phase and that there is here also a strong analogy between the two classes of complex. In conclusion, in Sect. 6, we shall indicate that a simple, essentially electrostatic model for the hydrogen bond is also appropriate for the halogen bond in outer complexes.

## 2 Properties of Isolated Complexes B···XY: How to Measure Them

Rotational spectroscopy is a precise means by which the properties of molecules in effective isolation in the gas phase may be measured. Only for strong complexes (particularly those linked by a hydrogen bond) have rotational spectra been detected by using equilibrium gas mixtures of the two components at normal or slightly lower temperatures [23]. Techniques that involve supersonic jets or beams are usually employed when the rotational spectra of more weakly bound species are sought. The two methods most used in this context are molecular beam electric resonance spectroscopy (MBERS) and pulsed-jet, Fourier-transform (F-T) microwave spectroscopy, both of which have been described in detail elsewhere [16, 17, 24]. A supersonic jet or beam of gas mixture is formed by expanding a mixture of the components of interest (e.g. B and XY here) in, e.g., excess argon through a small circular hole (nozzle) into a vacuum. When the gas pulse enters the vacuum chamber it is rich in weakly bound complexes, which achieve collisionless expansion after ca. 10 μs. Thereafter, the target species are frozen in their lowest rotational states and usually in the zero-point vibrational state

until they undergo collision with the walls of the vacuum chamber. The complexes can absorb microwave radiation while in the collisionless expansion phase and their rotational spectra can be detected. The results presented here have been established mainly by using a pulsed-nozzle, F-T microwave spectrometer, but modified to incorporate a so-called fast-mixing nozzle [15]. The latter device allows complexes of B···XY to be formed from two reactive components B and XY (e.g. ethyne and ClF) and achieve collisionless expansion in the vacuum chamber before the reaction (often violent) that would attend mixing under normal conditions. A detailed description of this nozzle is available elsewhere [25].

The form of the observed spectrum of B···XY can often give a clue to the symmetry of the species responsible for it. Thus asymmetric-top molecules, symmetric-top molecules and linear molecules give rise to different spectral patterns. Once the rotational spectrum of a complex B···XY has been assigned, the observed transition frequencies may be fitted to give a range of precise spectroscopic constants, usually for the zero-point state, which can then be interpreted to give various molecular properties of B···XY. Of principal interest here are the rotational constants, centrifugal distortion constants and nuclear quadrupole coupling constants.

Rotational constants $G = A$, $B$ or $C$ are inversely proportional to principal moments of inertia $I_\alpha$ through the expressions $G = h/8\pi^2 I_\alpha$, where $\alpha$ refers to one of the three principal inertia axis directions $a$, $b$ or $c$. The $I_\alpha$ are related to the coordinates of the atoms $i$ in the principal axis system via the relations $I_\alpha = \sum_i m_i(\beta_i^2 + \gamma_i^2)$, where $\alpha$, $\beta$ and $\gamma$ are to be cyclically permuted over $a$, $b$ and $c$. Hence, the principal moments of inertia are simple functions of the distribution of the masses of the atoms of the complex in space. Accordingly, these quantities can be used to determine the separation of the two subunits B and XY and their relative orientation in space, i.e. the radial and angular geometries of the complex, respectively. All molecular geometries of B···XY considered here are of the $r_0$-type, that is, are obtained by fitting the zero-point principal moments of inertia of a limited number of isotopomers as though they are equilibrium quantities. Moreover, the geometry of each component is assumed to survive complex formation.

Although there are several centrifugal distortion constants that can be determined from the rotational spectrum of a complex B···XY, one is of special importance, namely, $D_J$ ( for linear or symmetric top molecules) or, equivalently, $\Delta_J$ (for an asymmetric-rotor molecule). Both $D_J$ and $\Delta_J$ are inversely proportional to the intermolecular stretching force constant $k_\sigma$, according to simple and convenient expressions presented by Millen [26] in the approximation of rigid, unperturbed subunits B and X and with the neglect of terms higher than quadratic in the intermolecular potential energy function. Thus, $k_\sigma$ offers a measure of the strength of the interaction, given that it is the restoring force per unit infinitesimal extension of the weak bond.

The final spectroscopic constants of particular interest here are the halogen nuclear quadrupole coupling constants $\chi_{\alpha\beta}(X)$ and $\chi_{\alpha\beta}(Y)$ [27], where $\alpha$ and $\beta$ are to be permuted over the principal inertial axis directions *a*, *b* and *c*. Halogen nuclei (with the exception of $^{19}F$) have an intrinsic (or spin) angular momentum, $\boldsymbol{I}_X$, with a spin quantum number $I_X \geq 3/2$ and therefore with a non-zero electric quadrupole moment $\mathbf{Q}_X$. The nuclear spin vector $\boldsymbol{I}_X$ can couple in only a limited number of discrete orientations to the rotational angular momentum vector $\boldsymbol{J}$ of the molecular framework. Each allowed orientation of the angular momentum and spin vector corresponds to different orientations of the nuclear electric quadrupole moment with respect to the electric field gradient $\nabla\mathbf{E}_X$ at X and therefore to a different interaction energy. Hence, rotational energy levels (and therefore transitions) carry a hyperfine structure. Analysis of this nuclear quadrupole hyperfine structure gives various components (depending on the molecular symmetry) of the nuclear quadrupole coupling tensor $\chi_{\alpha\beta}(X)$, where $\alpha$ and $\beta$ are to be permuted over the principal inertial axes *a*, *b* and *c*. The importance of this tensor follows from its definition $\chi_{\alpha\beta}(X) = -(eQ_Xh)\partial^2 V_X/\partial\alpha\partial\beta$ where $Q_X$ is the conventional electric quadrupole moment of nucleus X and $-\partial^2 V/\partial\alpha\partial\beta$ is a component of the electric field gradient (efg) tensor at the nucleus X. This direct proportionality of $\chi_{\alpha\beta}(X)$ and $\chi_{\alpha\beta}(Y)$ to the efgs at the nuclei X and Y, respectively, means that the changes $\Delta\chi_{\alpha\beta}(X)$ and $\Delta\chi_{\alpha\beta}(Y)$ in $\chi_{\alpha\beta}(X)$ and $\chi_{\alpha\beta}(Y)$ that accompany formation of B···XY lead directly to the changes in the efgs at X and Y. Hence $\Delta\chi_{\alpha\beta}(X)$ and $\Delta\chi_{\alpha\beta}(Y)$ carry quantitative information about the electric charge redistribution associated with the process. We shall see in Sect. 5 that intra- and intermolecular electron transfer on formation of B···XY can be estimated from these quantities. For an asymmetric rotor of $C_S$ symmetry, only one off-diagonal element (*ab* or *ac* normally) of the tensor $\chi_{\alpha\beta}(X)$ or $\chi_{\alpha\beta}(Y)$ is non-zero but its value provides important information about the orientation of the XY subunit with respect to the principal inertial axis system (*a*, *b*, *c*) in complexes B···XY (and indeed of the HX subunit in hydrogen-bonded complexes B···HX [28, 29]). This leads to an estimate of the deviation of the Z···X – Y (or Z···H — X) atoms from collinearity, where Z is the electron-donor atom of B, as discussed in Sect. 3.

## 3
## Comparison of the Angular and Radial Geometries of Halogen-Bonded Complexes B···XY and their Hydrogen-Bonded Analogues B···HX

In this section, we discuss the observed geometries, both angular (the relative orientation of the components B and XY in space) and radial (the distance between B and XY at the observed orientation) of complexes B···XY.

Attention will be paid to the systematic relationship of the geometries of B···XY to those of hydrogen-bonded complexes in the corresponding series B···HX, especially for angular geometries, which are dealt with in detail in Sects. 3.1, 3.2 and 3.3. Radial geometries are treated only in summary (Sect. 3.4) here, but a detailed analysis is available in [19].

Many complexes B···XY, where B is a Lewis base and XY is $F_2$, [30–37], $Cl_2$ [22, 38–48], BrCl [49–58], ClF [34, 59–85], $Br_2$ [86–92] or ICl [93–102], have been investigated by means of their rotational spectra. Those in the group B···ClF cover the largest range of Lewis bases B, mainly because ClF contains only a single quadrupolar nucleus and the rotational spectra are relatively simple. Except for $F_2$, all the other dihalogen molecules contain two quadrupolar nuclei and hence the rotational transitions of the B···XY complexes display complicated nuclear quadrupole hyperfine structure. For this reason, the complexes B···$Cl_2$, B···BrCl, B···$Br_2$ and B···ICl investigated have been limited mainly to those of relatively high symmetry (molecular point groups $C_{\infty v}$, $C_{2v}$ and $C_{3v}$), which simplifies the spectral analysis. Necessarily, these complexes yield more information about the electric charge redistribution that accompanies complex formation (Sect. 5).

It will be shown in Sect. 5.1 that the extent of electron transfer to XY from B and the extent of electron transfer within XY when B···XY is formed are both small in most complexes so far investigated in the gas phase. Members of this group also have small intermolecular stretching force constants $k_\sigma$ and are weakly bound (see Sect. 4). Such complexes are therefore of the Mulliken outer type and the discussion of geometries here will be limited to these. There are a few complexes B···XY that exhibit significant electric charge rearrangement and are strongly bound. This group can be categorised as approaching the Mulliken inner complex limit and will be discussed in Sect. 5.2.

The discussions of Sects. 3.1, 3.2 and 3.3 are structured by reference to a set of rules that were proposed some years ago [103, 104] for rationalising the angular geometries of hydrogen-bonded complexes of the type B···HX, where X is a halogen atom. These rules are as follows:

---

The equilibrium angular geometry of a hydrogen-bonded complex B···HX can be predicted by assuming that the axis of the HX molecule lies:

1. Along the axis of a non-bonding (n) electron pair carried by the acceptor atom of B, with $^{\delta+}$H closer to the n-pair than $X^{\delta-}$, or
2. Along the local symmetry axis of a π- or pseudo-π orbital (with $^{\delta+}$H interacting with the π-density) when B carries no n-pairs, or
3. Along the axis of a n-pair, when B carries both n- and π-pairs (i.e. rule 1 takes precedence over rule 2 in this case)

---

Guided by these rules, we shall compare in most detail the observed angular geometries of pairs of complexes B···ClF and B···HCl for a wide range of Lewis bases B, although we shall also refer to other B···XY and B···HX. The reasons for choosing B···HCl and B···ClF as the series of halogen- and hydrogen-bonded complexes for comparison are: (i) that these are by far the most systematically studied of all the pairs of B···HX/B···XY series and (ii) that deviations of the hydrogen bond atoms Z···H – Cl from collinearity have been determined for a number of B···HCl of $C_S$ symmetry and are available for comparison with the corresponding quantity for B···ClF, similarly determined. For each complex, the geometry was obtained by fitting the principal moments of inertia of one or more isotopomers under the assumption of unperturbed monomer geometries.

## 3.1
## Angular Geometries of B···ClF and B···HCl in Which B is a n-Pair Donor

We begin by comparing pairs of B···ClF and B···HCl that test rule 1. We shall show a diagram comparing the experimental geometries, drawn to scale, of B···ClF and B···HCl for each B, together with a representation of B, also to scale but with its n-pair(s) drawn in the form of an exaggerated electron density distribution that is traditionally used among chemists. We shall then employ a similar approach for various prototype π-electron donors to test rule 2 and for mixed n- and π-donors appropriate to rule 3 in Sects. 3.2 and 3.3, respectively.

### 3.1.1
### B Carries a Single n-Pair

The prototype Lewis base that carries a single n-pair and no π-pairs is ammonia. The observed geometries of $H_3N···ClF$ [63] and $H_3N···HCl$ [105] are shown in Fig. 1, as is the n-pair model of $NH_3$. Both complexes are symmetric-top molecules belonging to the $C_{3v}$ molecular point group and clearly both obey rule 1. The geometries of the complexes $H_3N···F_2$ [30], $H_3N···Cl_2$ [45], $H_3N···BrCl$ [52], $H_3N···Br_2$ [86] and $H_3N···ICl$ [97] were found also to be of $C_{3v}$ symmetry and isomorphous with their $H_3N···HX$ counterparts (X = F [1], Cl [105], Br [106] and I [107]). The halogen atom of higher atomic number acts as the electron acceptor in complexes containing a heteronuclear dihalogen molecule. The same conclusions have been reached for the pairs $H_3P···XY$, for XY = $Cl_2$ [40], BrCl [55], $Br_2$ [88] and ICl [102], and their H-bonded analogues $H_3P···HX$, where X = Cl [108], Br [109] and I [110].

[1] Howard BJ, Langridge-Smith PPR, unpublished observations

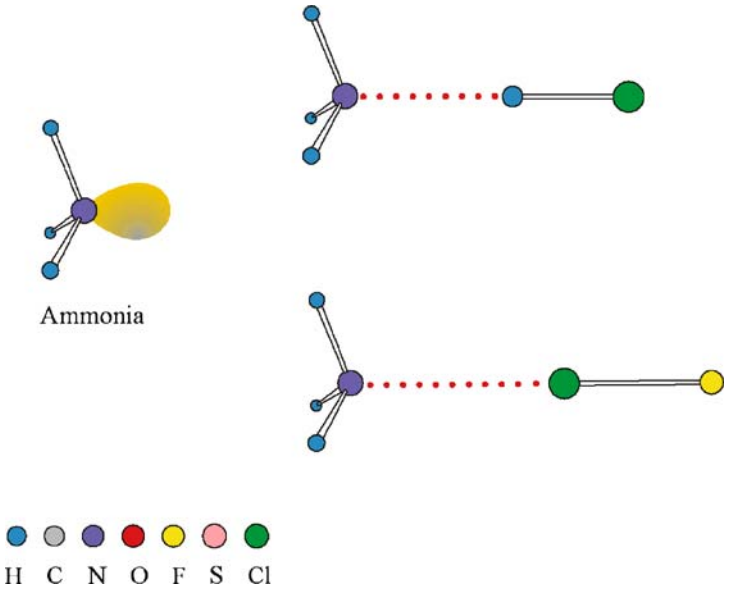


**Fig. 1** Comparison of the experimentally determined geometries of the hydrogen-bonded complex $H_3N\cdots HCl$ and its halogen-bonded analogue $H_3N\cdots ClF$ (both drawn to scale) with a non-bonding electron-pair (n-pair) model of $NH_3$. Here, and in other figures, the n-pair electron distribution is drawn in the exaggerated style favoured by chemists. The key to the colour coding of atoms used in this and similar figures is also displayed

### 3.1.2
### B Carries Two Equivalent n-Pairs

#### 3.1.2.1
#### Linear Halogen Bonds and Hydrogen Bonds

The prototype Lewis bases in this category are $H_2O$ and $H_2S$. The complex $H_2O\cdots HF$ is sufficiently strongly bound to have been investigated in an equilibrium mixture of $H_2O$ and HF held at 200 K in the cell of a conventional Stark-modulation microwave spectrometer [111, 112]. This allowed vibrational satellites associated with low-frequency, intermolecular stretching and bending modes to be observed and analysed and vibrational wavenumbers for these modes to be determined. It was not only possible to conclude that in the zero-point state this complex is effectively planar but also to determine the potential energy (PE) as a function of the out-of-plane, low-frequency, hydrogen-bond bending co-ordinate. The mode in question inverts the configuration at the oxygen atom and is shown schematically in Fig. 2. The $O\cdots H-F$ nuclei were assumed to remain collinear during this motion. The energy levels associated with the motion were calculated by using the ex-

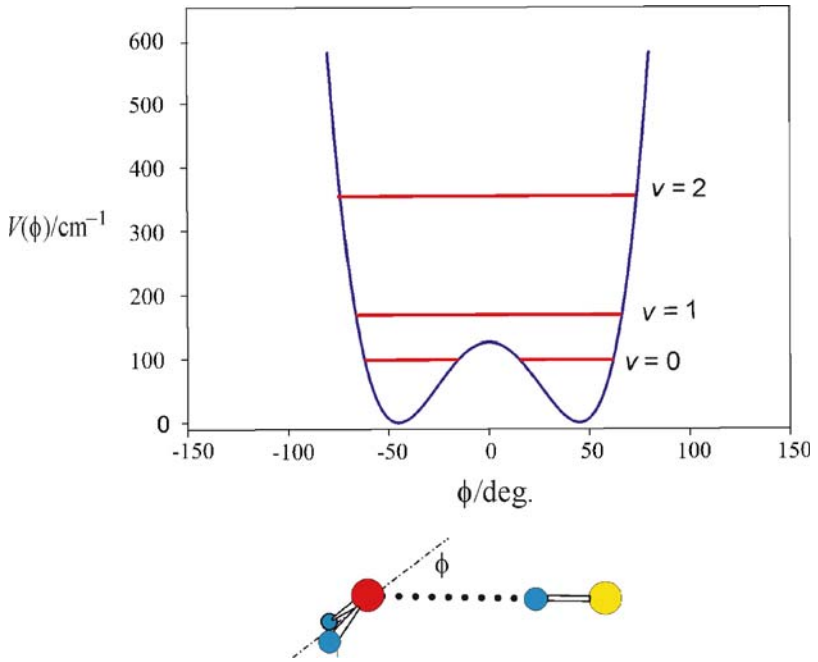


**Fig. 2** The experimentally determined potential energy $V(\phi)$, expressed as a wavenumber for convenience, as a function of the angle $\phi$ in the hydrogen-bonded complex $H_2O\cdots HF$. The definition of $\phi$ is shown. The first few vibrational energy levels associated with this motion, which inverts the configuration at the oxygen atom, are drawn. The PE barrier at the planar conformation ($\phi = 0$) is low enough that the zero-point geometry is effectively planar (i.e. the vibrational wavefunctions have $C_{2v}$ symmetry, even though the equilibrium configuration at O is pyramidal with $\phi_e = 46°$ (see text for discussion)). See Fig. 1 for key to the colour coding of atoms

pression for the conventional quartic/quadratic PE function in terms of the dimensionless reduced coordinate $z$ given in Eq. 1. This function was fitted to a range of experimental data to give the potential constants $a$ and $b$ and then converted to the equivalent $\phi$-dependent form of the type given in Eq. 2, where $\phi$ is the inversion angle defined in Fig. 2. The form of the reduced mass for the inversion motion and details of the calculation are given in [112]:

$$V(z) = a(z^4 - bz^2) \tag{1}$$

$$V(\phi) = A\phi^4 - B\phi^2 \tag{2}$$

We note from Fig. 2 that the hypothetical equilibrium conformation is pyramidal, with $\phi_e = 46(8)°$, even though the geometry of the complex is effectively planar in the zero-point state (i.e. the vibrational wavefunction has $C_{2v}$ symmetry) because the PE barrier at the planar ($\phi = 0$) form is low. At the time of the publication of [112] this was a critical result because it demon-

strated that rule 1 is appropriate in the case of the important prototype Lewis base $H_2O$, given that half the angle between the n-pairs in the n-pair model of $H_2O$ should be ~54° (See Fig. 2).

It was not possible to determine experimental PE functions for $H_2O\cdots HCl$ [113] and $H_2O\cdots ClF$ [72] in same way. However, another approach was possible. The energy of each complex was obtained by carrying out a full geometry optimisation at fixed values of the out-of-plane bending coordinate $\phi$ in the range 0 to ~70°. The aug-cc-pVDZ/MP2 level of theory was used and correction for basis set superposition error was applied. This ab initio potential function was then fitted numerically to the expression of Eq. 1 to give the coefficients $A$ and $B$ and thence $a$ and $b$. Once $a$ and $b$ were available, the matrix of the Hamiltonian $H = p_z^2/2\mu + V(z)$ was set up using a basis composed of 100 harmonic oscillator functions and was diagonalised to give the vibrational energy levels. This approach for $H_2O\cdots HF$ gave values of $\phi_{min}$ and the PE barrier height in good agreement with those of the experimentally determined function. Thus we can have some confidence in the results obtained when the same procedure was applied to $H_2O\cdots HCl$ [114] and $H_2O\cdots ClF$ [34]; the plots of $V(\phi)$ versus $\phi$ and the energy levels are displayed in Fig. 3. The equilibrium values of the angle $\phi$ are 45.7° and 57.4° for $H_2O\cdots HCl$ and $H_2O\cdots ClF$, respectively, and the two equivalent minima are separated by PE barriers of $V_0 = 80$ and 174 $cm^{-1}$, respectively. These values are similar to the experimental results 46(8)° and 126(70) $cm^{-1}$

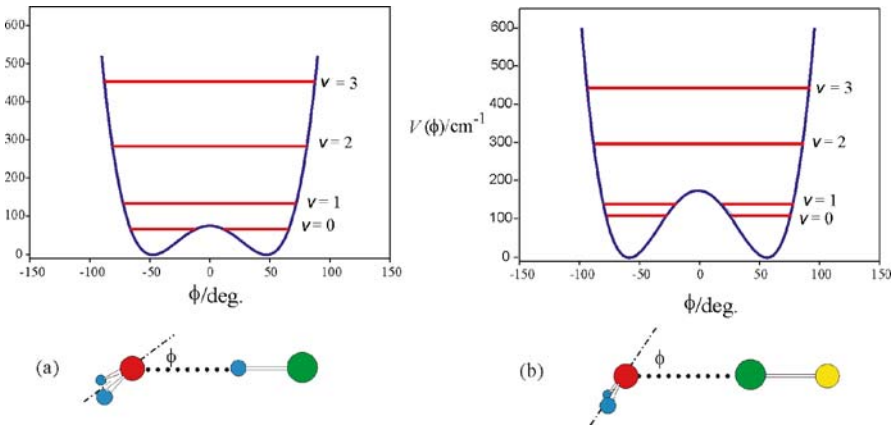


**Fig. 3** The potential energy $V(\phi)$, expressed as a wavenumber, as a function of the angle $\phi$ for **a** $H_2O\cdots HCl$ and **b** $H_2O\cdots ClF$. These have been obtained using ab initio calculations, by the method discussed in the text. The same approach reproduces the experimental function of $H_2O\cdots HF$ (Fig. 2) very well. Several vibrational energy levels associated with the motion in $\phi$ are also shown. As for $H_2O\cdots HF$, the PE barrier at $\phi = 0$ is low enough that both molecules are effectively planar in the zero-point state, even though the molecules are pyramidal at equilibrium. See Fig. 1 for key to the colour coding of atoms

for $H_2O\cdots HF$ [112]. Indeed, when the zero-point rotational constants of all isotopomers investigated for each of $H_2O\cdots HCl$ or $H_2O\cdots ClF$ were fitted under the assumption of unchanged monomer geometries and collinear $O\cdots H-Cl$ and $O\cdots Cl-F$ arrangements, the results for the effective angle $\phi$ were 36.5(3)° and 58.9(16)°, respectively. Thus, there seems little doubt that the configuration at O in these complexes is pyramidal, a result consistent with rule 1 and the chemist's simple n-pair model of $H_2O$. Similar analyses have been applied with similar results to $H_2O\cdots F_2$ [34] $H_2O\cdots Cl_2$ [48], $H_2O\cdots BrCl$ [56], $H_2O\cdots Br_2$ [91] and $H_2O\cdots ICl$ [101]. In each case, the lowest vibrational energy level lies near to or above the PE maximum at the planar geometry, so the zero-point geometry is effectively planar while the equilibrium geometry is pyramidal at O. The hydrogen-bonded complexes $H_2O\cdots HX$, where X = Br [115] and I [116], are both effectively planar, but the above-described treatment is yet to be applied to give the form of the PE function.

The situation for the complexes $H_2S\cdots HX$ and $H_2S\cdots XY$ is different from that of their $H_2O$ analogues. It has been shown by rotational spectroscopy that the conformation at S is much more steeply pyramidal, with $\phi \approx 90°$, and that there is no evidence of inversion in $H_2S\cdots HF$ [117], $H_2S\cdots HCl$ [118] or $H_2S\cdots HBr$ [119], i.e. each is permanently pyramidal at S on the time scale of the microwave experiment. Similar conclusions hold for $H_2S\cdots ClF$ [60], $H_2S\cdots BrCl$ [54], $H_2S\cdots Br_2$ [90] and $H_2S\cdots ICl$ [98]. The experimental zero-point geometries of $H_2S\cdots HCl$ and $H_2S\cdots ClF$ (derived under the assumption of unchanged monomer geometries) are compared in Fig. 4. A collinear arrangement of the $S\cdots Cl-F$ nuclei was demonstrated in the case of $H_2S\cdots ClF$ but assumed for $S\cdots H-Cl$ in $H_2S\cdots HCl$. The 90° structures seen in Fig. 4 suggest that for $H_2S$ the n-pairs can be modelled as occupying sp hybridised valence orbitals whose axis is perpendicular to the nuclear plane, as illustrated in Fig. 4. The PE as a function of the angle $\phi$ for each of $H_2S\cdots HCl$ and $H_2S\cdots ClF$, as calculated[2] by the method outlined for $H_2O\cdots HCl$ and $H_2O\cdots ClF$ earlier, is shown in Fig. 5. The first few vibrational energy levels are drawn on each function. Each energy level is actually a pair having a very small separation, which indicates that the inversion motion between the two equivalent forms of each complex is very slow as a result of the relatively high PE barrier and the large separation of the two minima, in agreement with the experimental conclusion. We note that minima are at $\phi \approx \pm 90°$ in both cases, as expected from the proposed n-pair model, thereby providing evidence for the isostructural nature of pairs of hydrogen- and halogen-bonded complexes $B\cdots HCl$ and $B\cdots ClF$ when B is $H_2S$. For $H_2S\cdots HI$[3] and $H_2S\cdots F_2$ [35], on the other hand, there is evidence of a lower barrier to the $\phi = 0°$(planar) structure, both through the observation of vibrational satellites in the rotational

[2] Davey JB, Legon AC, unpublished calculations

[3] Legon AC, Suckley AP, unpublished observations

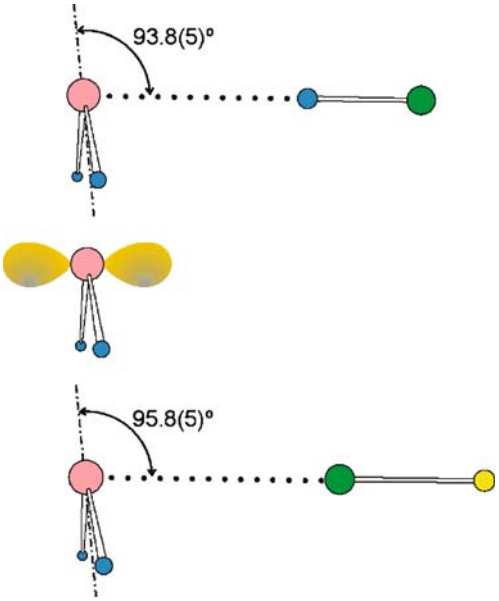


**Fig. 4** The experimentally determined geometries of $H_2S\cdots HCl$ and $H_2S\cdots ClF$ drawn to scale. The n-pair model of $H_2S$, as discussed in the text, is shown for comparison. See Fig. 1 for key to the colour coding of atoms

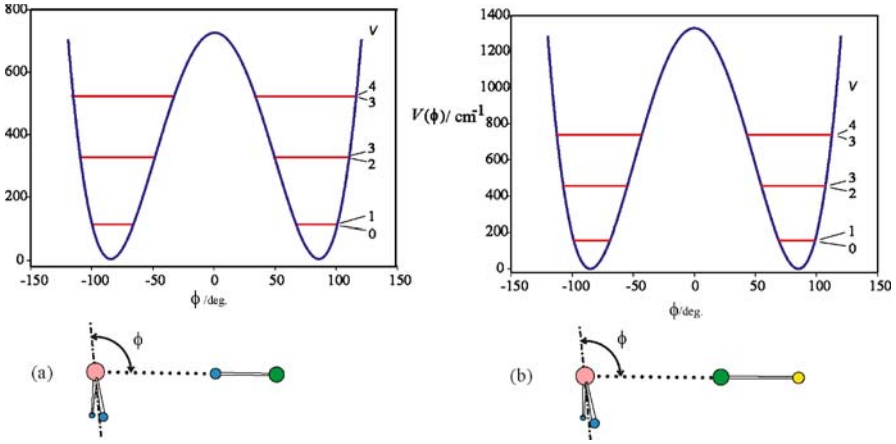


**Fig. 5** The potential energy $V(\phi)$, expressed as a wavenumber, as a function of the angle $\phi$ for **a** $H_2S\cdots HCl$ and **b** $H_2S\cdots ClF$. These have been obtained using ab initio calculations, by the method discussed in the text. Several vibrational energy levels associated with the motion in $\phi$ are also shown. The PE barrier at $\phi = 0$ is high in both molecules, so that in each case the $v = 0$ and $v = 1$ vibrational energy levels are negligibly separated and hence both molecules are pyramidal in the zero-point state and at equilibrium. The values of $\phi_e$ and the effective values $\phi_0$ determined experimentally (see Fig. 4) are in good agreement. See Fig. 1 for key to the colour coding of atoms

spectra and the angle $\phi$ determined by fitting rotational constants. This observation can be readily rationalised when we note that, in general, complexes B···$F_2$ and B···HI are more weakly bound for a given B than those involving other HX or XY molecules.

### 3.1.2.2 Non-linear Halogen Bonds and Hydrogen Bonds

The ab initio calculations for $H_2Z\cdots HCl$ and $H_2Z\cdots ClF$, where Z is O or S, (referred to in Sect. 3.1.2.1) reveal that the nuclei Z···H – Cl and Z···Cl – F deviate insignificantly from collinearity. For example, the angular deviations $\theta$ are less than 2° in $H_2O\cdots F_2$, $H_2O\cdots ClF$ and $H_2O\cdots HCl$ [34, 114]. Is this always the case and, if not, can the deviation from a linear arrangement be measured experimentally?

The position of the subunit HX in the principal inertia axes system of an effectively planar complex $H_2O\cdots HX$ is difficult to determine from zero-point rotational constants because of the large amplitude motion of the $H_2O$ and HX subunits, which involves mainly the H atoms, and the small contributions that the H atoms make to the principal moments of inertia. If $H_2O$ is replaced by the cyclic ether oxirane, $(CH_2)_2O$, to yield the complex $(CH_2)_2O\cdots HX$, the inversion motion is quenched and the complex has a pyramidal configuration at O and $C_S$ symmetry, even in the zero-point state [120]. This allows the orientation of the oxirane subunit in the principal inertia axis system of the complex to be established. Moreover, if the atom X has a quadrupolar nucleus, determination of the complete nuclear quadrupole coupling tensor $\chi_{\alpha\beta}(X)$ of X from the rotational spectrum of the complex gives the orientation of HX in the principal inertia axis system. If *a* is the principal inertia axis (which passes almost through the centre of the oxirane ring and close to the centre of mass of the HX subunit), *ab* is the molecular symmetry plane and *z* the HX internuclear axis, it can be shown [28, 29] that the angle $\alpha_{az}$ between *a* and *z* is given in terms of the elements of $\chi_{\alpha\beta}(X)$ by the expression:

$$\alpha_{az} = \tan^{-1}\left(\frac{-\chi_{ab}}{\chi_{aa} - \chi_{bb}}\right). \tag{3}$$

Of primary interest here is the important result that $\alpha_{az}$ so obtained is independent of the large amplitude, zero-point angular oscillation of the HX subunit even when components of the zero-point coupling tensor are used in Eq. 3. The assumptions made in deriving Eq. 3 are that the electric field gradient at X is unperturbed on complex formation and that the effect of the intermolecular stretching motion on the coupling tensor is negligible. Once $\alpha_{az}$ is available, the principal moments of inertia of sufficient isotopomers of, for example, $(CH_2)_2O\cdots HCl$ can be fitted under the constraint that the result-

ing structure must also reproduce this angle. The geometry of $(CH_2)_2O\cdots HCl$ so obtained [28, 120] is shown in Fig. 6.

The angle $\theta$ defines the non-linearity of the hydrogen bond and $\phi$ is the angle O–H–Cl, as indicated. Also shown in Fig. 6 is the geometry similarly determined for the halogen-bond analogue of $(CH_2)_2O\cdots HCl$, namely $(CH_2)_2O\cdots ClF$ [67]. We note immediately a striking similarity between the angles $\phi$ of these two complexes [69.1(1)° and 67.3(1)°, respectively], a result that can be understood on the basis of rule 1 if the oxygen atom of oxirane carries two equivalent n-pairs, as drawn schematically in Fig. 6. By contrast, there is a significant difference in the non-linearities [$\theta$ = 16.5(1)° and 2.9(1)°] of the hydrogen bond $O\cdots H-Cl$ and the halogen bond $O\cdots Cl-F$ in the two complexes. We shall see that this relationship between $(CH_2)_2O\cdots HCl$ and $(CH_2)_2O\cdots ClF$ is an example of a common property of the two series $B\cdots HCl$ and $B\cdots ClF$ and, moreover, that the propensity to be non-linear is an important characteristic of the hydrogen bond.

Other Lewis bases in which the electron donor atom Z carries two equivalent n-pairs and which form complexes of $C_S$ symmetry with HCl and ClF have been investigated by the same approach. The resulting geometries when B is formaldehyde are shown, together with the conventional n-pair model of $CH_2O$, in Fig. 7. The angle $\phi$ is virtually identical in $H_2CO\cdots HCl$ [121] and $H_2CO\cdots ClF$ [79] and is close to that expected from the n-pair model in which the angle between the n-pairs is ∼120°. The hydrogen bond again deviates significantly from linearity [$\theta$ = 20.3(8)°] but the $O\cdots Cl-F$ system is essentially collinear [$\theta$ = 3.2(7)°].

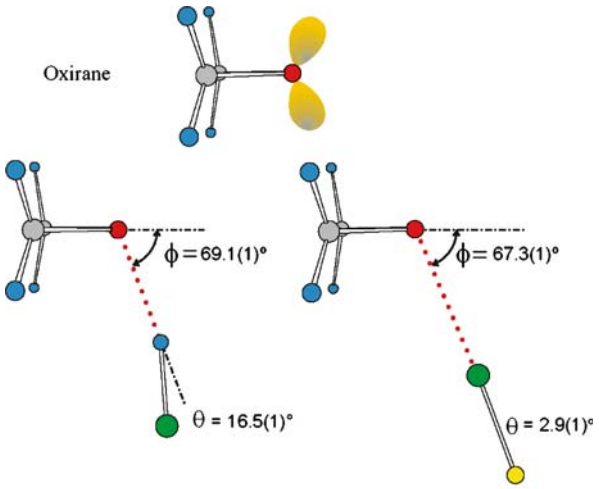


**Fig. 6** The experimentally determined geometries of oxirane···HCl and oxirane···ClF drawn to scale. The n-pair model of oxirane is shown for comparison. While the angle $\phi$ is similar in both complexes, the non-linearity $\theta$ of the hydrogen bond is much greater than that of the halogen bond. See Fig. 1 for key to the colour coding of atoms

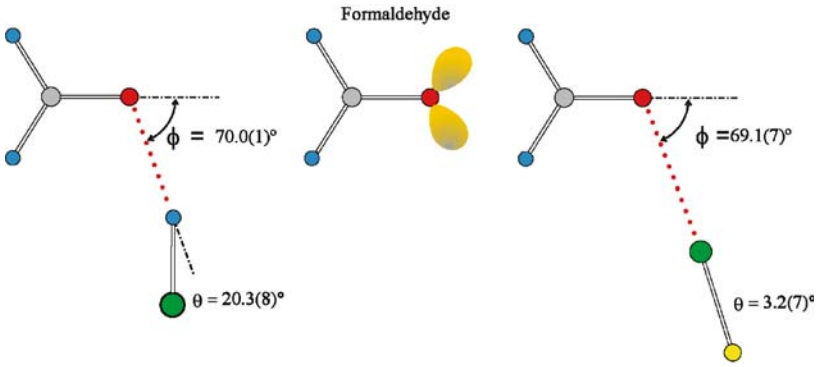


**Fig. 7** The experimentally determined geometries of $CH_2O\cdots HCl$ and $CH_2O\cdots ClF$, drawn to scale, are shown in comparison to the n-pair model of formaldehyde. The angle $\phi$ is again similar in both complexes but the non-linearity $\theta$ of the hydrogen bond is much greater than that of the halogen bond. See Fig. 1 for key to the colour coding of atoms

It is possible to test the n-pair model more precisely when O is the electron donor atom. In the series of cyclic ethers oxirane $[(CH_2)_2O]$, oxetane $[(CH_2)_3O]$, and 2,5-dihydrofuran $[(CHCH_2)_2O]$, the internal ring angle COC increases from ∼60° through ∼90° to ∼109° (the tetrahedral angle). It is generally accepted that this increase is accompanied by a corresponding decrease in the angle between the n-pairs carried by O; if so the angle $\phi$ should decrease correspondingly. The n-pair models of these three Lewis bases are shown in Fig. 8 together with the observed geometries of their complexes with HCl. Table 1 gives the angles $\phi$ and $\theta$ for the two series $B\cdots HCl$ and $B\cdots ClF$, where B is oxirane [67, 120], oxetane [122] or 2,5-dihydrofuran [29, 77], all determined from their rotational spectra under assumptions identical to those described earlier for the oxirane complexes [$(CH_2)_3O\cdots ClF$ has not yet been investigated].

It is clear from Fig. 8 and Table 1 that the angle $\phi$ does indeed decrease as expected if the n-pair models and rule 1 were applicable. Moreover, the hydrogen bond non-linearity $\theta$ decreases along the series B = oxirane, oxetane, 2,5-dihydrofuran. On the other hand, the values of $\theta$ for oxirane$\cdots ClF$ and 2,5-dihydrofuran$\cdots ClF$ (included in Fig. 8) reveal that the halogen bond shows little propensity to be non-linear.

Oxirane is an important Lewis base in the present context. The O atom carries two equivalent n-pairs of electrons, as it does in $H_2O$, but oxirane has the advantage over water in that it is possible to determine both angles $\phi$ and $\theta$ for its complexes with HCl and ClF because the non-zero off-diagonal element $\chi_{ab}$(Cl) of the Cl nuclear quadrupole coupling tensor is available. The corresponding Lewis base in which an S atom carries two equivalent n-pairs is thiirane. Each of the pair of complexes $(CH_2)_2S\cdots HCl$ and $(CH_2)_2S\cdots ClF$ has $C_S$ symmetry and here it is the off-diagonal element $\chi_{ac}$(Cl) that is non-zero

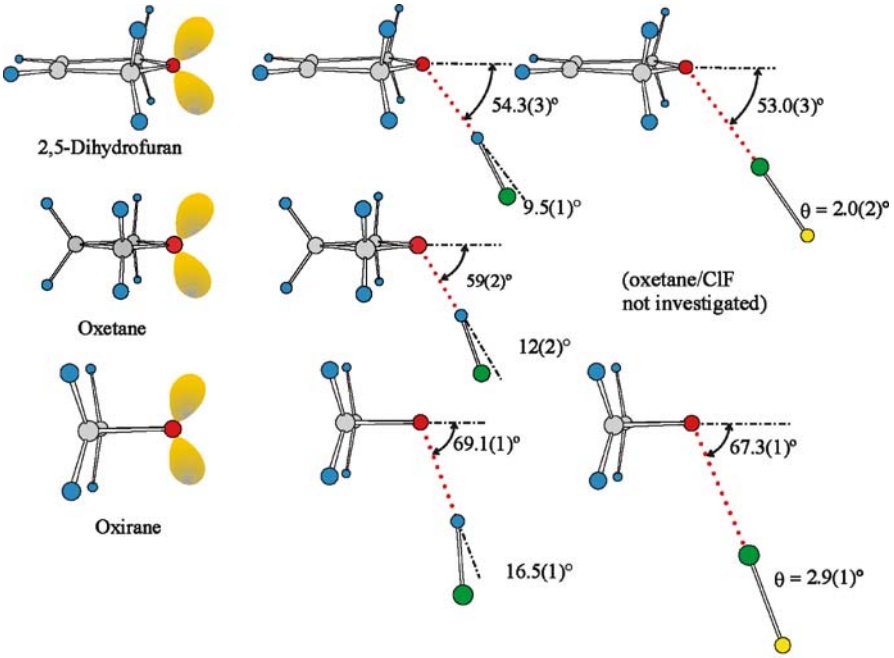


**Fig. 8** The n-pair models of 2,5-dihydrofuran, oxetane and oxirane (*first column*) and the experimental geometries of their complexes with HCl (*second column*) and ClF (*third column*), each drawn to scale. The angle $\phi$ is almost identical in B···HCl and B···ClF for a given B but increases from 2,5-dihydrofuran, through oxetane, to oxirane, as expected from the model (see text). The non-linearity of the hydrogen bond increases monotonically from 2,5-dihydrofuran to oxirane. See Fig. 1 for key to the colour coding of atoms

**Table 1** The angles $\phi$ and $\theta$ (in degrees; see Fig. 8 for definitions) in complexes B···HCl and B···ClF, where B is one of the cyclic ethers 2,5-dihydrofuran, oxetane or oxirane

| B | B···HCl | | B···ClF | |
|---|---|---|---|---|
| | $\phi$ | $\theta$ | $\phi$ | $\theta$ |
| Oxirane | 69.1(1) | 16.5(1) | 67.3(1) | 2.9(1) |
| Oxetane | 59(2) | 12(2) | ··· | ··· |
| 2,5-Dihydrofuran | 54.3(3) | 9.5(1) | 53.0(3) | 2.0(2) |

because the axis *a* and *c* lie in the molecular symmetry plane. Thus both $\phi$ and $\theta$ can be determined for each complex, in contrast to the position for the $H_2S$ analogues, for which only in $H_2S\cdots ClF$ was it possible to establish the collinearity of the $S\cdots Cl-F$ nuclei. The determined geometries (drawn to scale) of $(CH_2)_2S\cdots HCl$ [28, 123] and $(CH_2)_2S\cdots ClF$ [69] are displayed in Fig. 9.

The values of $\phi$ are both close to 90°, which suggests an n-pair model of thiirane (see Fig. 9) similar to that described for $H_2S$ earlier. A reason for the

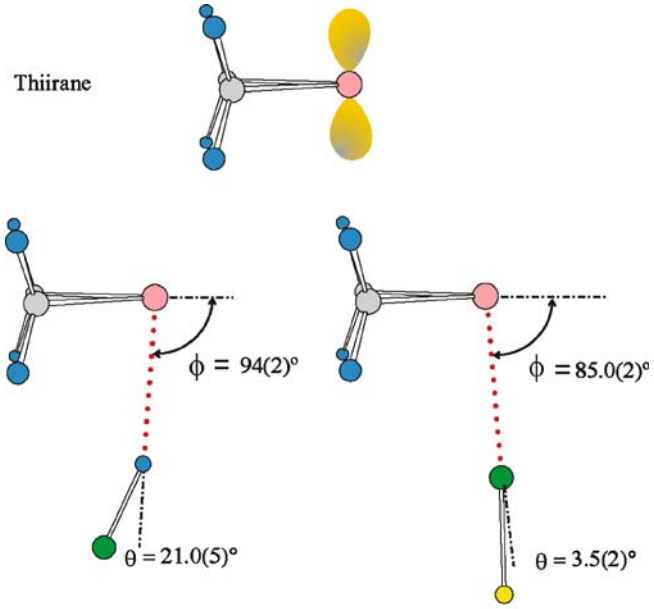


**Fig. 9** The experimentally determined geometries of thiirane···HCl and thiirane···ClF drawn to scale. The n-pair model of thiirane is shown for comparison. The angle $\phi$ is slightly different in the two complexes for reasons discussed in [69]. The non-linearity $\theta$ of the hydrogen bond is again greater than that of the halogen bond. See Fig. 1 for key to the colour coding of atoms

slightly smaller angle in the case of $(CH_2)_2S\cdots ClF$ is discussed in [69]. It is clear that the hydrogen bond in $(CH_2)_2S\cdots HCl$ deviates significantly from linearity [$\phi = 21.0(5)°$] while the halogen bond in $(CH_2)_2S\cdots ClF$ is close to linear[$\phi = 3.5(2)°$]. The hydrogen bonds in the complexes $(CH_2)_2S\cdots HF$ [124] and $(CH_2)_2S\cdots HBr$ [28, 125] are also significantly non-linear.

### 3.1.3 B Carries Two Inequivalent n-Pairs

Sulfur dioxide is an example of a simple Lewis base that carries two sets of inequivalent n-pairs, one set on each O atom. The n-pair model (in which the π bonding pairs are not drawn and are ignored here) is shown in Fig. 10. The geometries of $SO_2\cdots HF$ [126, 127], $SO_2\cdots HCl$ [28, 126] and $SO_2\cdots ClF$ [70] have all been determined from investigations of their rotational spectra. Each molecule is planar and belongs to the $C_S$ point group. Scale drawings for $SO_2\cdots HCl$ and $SO_2\cdots ClF$ are displayed in Fig. 10.

We note that the HCl and ClF molecules attach, approximately at least, along the axis of the *cis* n-pair, as required by rule 1, with angles $\phi$ of 143.0(1)° and 131.9(6)°, respectively, although the former value may be influenced by

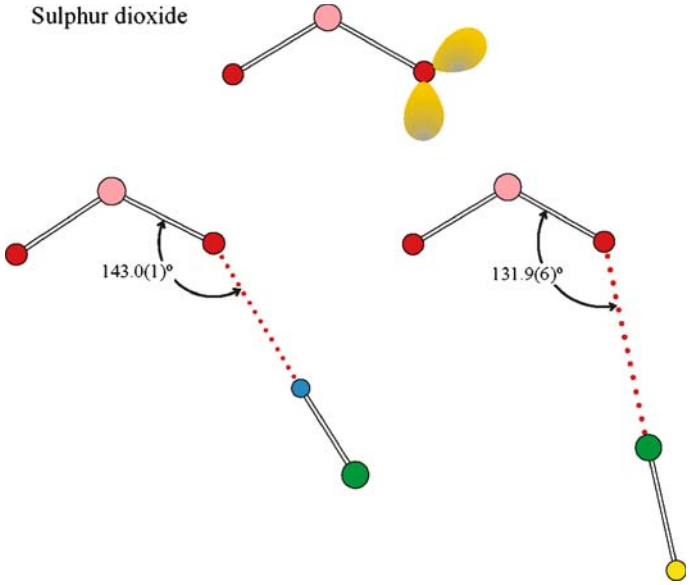


**Fig. 10** The n-pair model of sulfur dioxide and the experimental geometries of $SO_2\cdots HCl$ and $SO_2\cdots ClF$. Note that neither the hydrogen bond nor the halogen bond deviate significantly from linearity. See Fig. 1 for key to the colour coding of atoms

the non-rigid behaviour noted in $SO_2\cdots H-Cl$. The hydrogen bond and the chlorine bond are both nearly linear [$\theta = -2.5(7)^\circ$ and $-0.7(2)^\circ$, respectively], a result which is different from those obtained for other B···HCl and B···ClF pairs belonging to the $C_S$ point group. This will be discussed when the rules for rationalising the geometries of hydrogen- and halogen-bonded complexes are refined in Sect. 6.

### 3.2 Angular Geometries of B···ClF and B···HCl in Which B is a π-Pair Donor

According to the rules for predicting angular geometries of hydrogen-bonded complexes B···HX, given earlier, the HX molecule lies along the local symmetry axis of a π orbital when B carries no non-bonding electron pairs and only π pairs. In this section, we examine whether this rule also applies to halogen-bonded complexes B···XY. We consider first Lewis bases that offer only a single π pair.

#### 3.2.1 B Carries a Single-π-Pair

The experimentally determined geometries of the complexes of the simplest π electron donor, ethene, with HCl [128] and ClF [65] are displayed in Fig. 11.

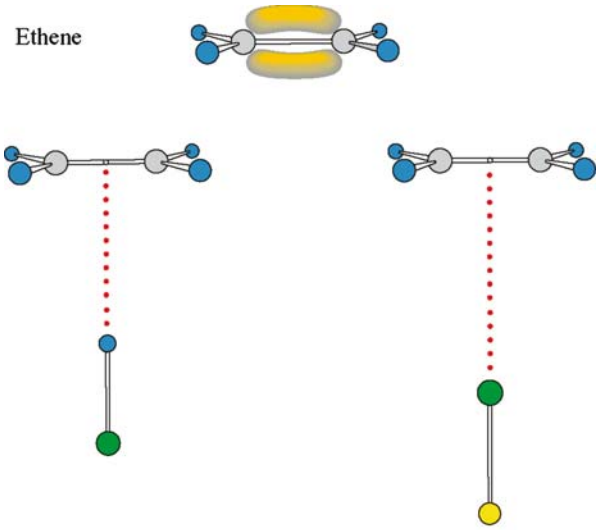


**Fig. 11** The experimental geometries of ethene···HCl and ethene···ClF (drawn to scale) and the π-electron model of ethene. See Fig. 1 for key to the colour coding of atoms

These two molecules are clearly isostructural and of $C_{2v}$ symmetry, with the XY or HX molecule lying along the $C_2$ axis of ethene that is perpendicular to the plane containing the $C_2H_4$ nuclei. Other complexes ethene···XY, where XY = $Cl_2$ [46], BrCl [51], $Br_2$ [89] and ICl [96], and other complexes ethene···HX, where X is F [129] or Br [130], have also been shown to have the form illustrated in Fig. 11. It is of interest to note that $C_2H_4$···$Cl_2$ was detected through its UV spectrum many years ago [131] and that the pre-reactive complex $C_2H_4$···$Br_2$ has recently been shown to be important on the overall reaction coordinate for bromination through autocatalytic action of bromine [132].

Each angular geometry can be rationalised on the basis of rule 2 (see earlier) with the aid of the familiar π bonding electron density distribution of ethene, which is included in Fig. 11. In all cases, the electron acceptor molecule XY or HX lies along the symmetry axis of the π orbital of the Lewis base. The electrophilic end, $^{\delta+}$X of XY or $^{\delta+}$H of HX, as appropriate, interacts with the π-electron density. There is no evidence that the hydrogen bonds or the halogen bonds in these complexes are not strictly linear in the equilibrium geometry (i.e. that the arrangements ∗···H–X or ∗···X–Y are not collinear, where ∗ is the midpoint of the C – C bond). In view of the symmetry of ethene, non-linear hydrogen or halogen bonds are not expected.

Ethyne has two π bonding orbitals at right angles to each other and a resultant π electron density that is cylindrically symmetric with respect to the internuclear axis. Complexes of ethyne with HF [133], HCl [134], HBr [135], ClF [66], $Cl_2$ [47], BrCl [50], $Br_2$ [92] and ICl [95] have been characterised by

rotational spectroscopy. Each complex has the planar, T-shaped geometry of $C_{2v}$ symmetry that is predicted by applying rule 2 using the π-bonding model of ethyne.

### 3.2.2 B Carries Pseudo-π-Pairs

Cyclopropane resembles an alkene in its chemical behaviour. This fact led Coulson and Moffitt [136] to propose a model for cyclopropane in which a pseudo-π carbon–carbon bond is formed by overlap of a pair of $sp^3$ hybrid orbitals on adjacent carbon atoms. A schematic diagram showing the electron density distribution between a pair of C atoms in cyclopropane resulting from such a model is shown in Fig. 12. The symmetry axis of the pseudo-π orbital coincides with a median of the cyclopropane equilateral triangle. Hence, according to rule 2, the angular geometry of cyclopropane···ClF [73], or of cyclopropane···HCl [137], is predicted to have $C_{2v}$ symmetry, with ClF, or HCl, lying along the extension of the median. The electrophilic end $^{\delta+}$Cl of ClF, or $^{\delta+}$H of HCl, is expected to interact with the pseudo-π electron dens-

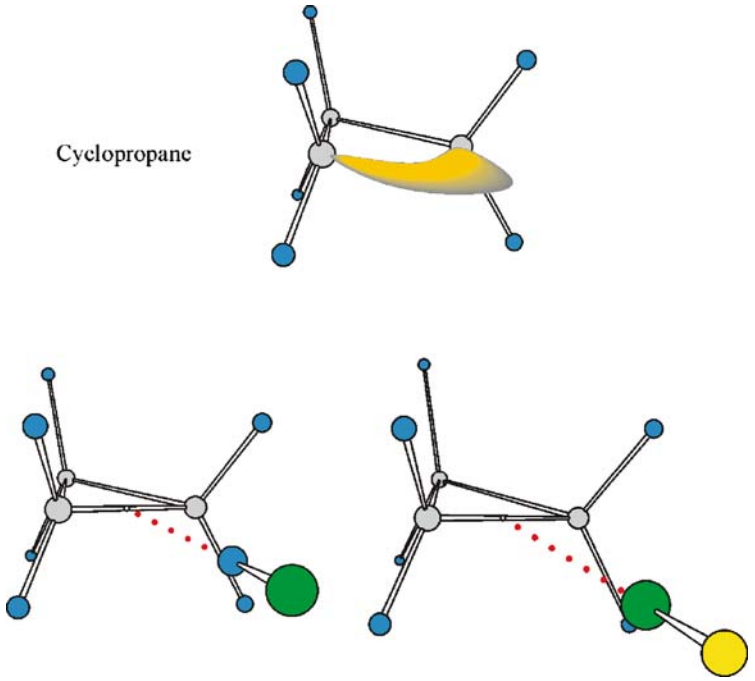


**Fig. 12** The experimental geometries of cyclopropane···HCl and cyclopropane···ClF (drawn to scale) and the Coulson–Moffitt pseudo-π-electron model of cyclopropane. See Fig. 1 for key to the colour coding of atoms

ity of the C – C bond in preference to $F^{\delta-}$ or $Cl^{\delta-}$, respectively. The observed geometries of the two complexes, included in Fig. 12, are clearly as predicted by rule 2. Cyclopropane···HF has a similar angular geometry [138].

### 3.2.3
### B Carries Several-π-Pairs

Rule 2 can also be tested when the Lewis base B carries no n-pairs but two or more π-electron pairs, either conjugated or cumulative. Strictly, cyclopropane might be considered in this category but has been discussed in Sect. 3.2.2 as the prototype of a pseudo-π donor for convenience.

#### 3.2.3.1
#### B is a Conjugated π-bonded System

*trans*-1,3-Butadiene is the prototype Lewis base offering a pair of conjugated, but non-aromatic, π bonds as electron donors. According to rule 2, the axis of a ClF or HCl molecule, for example, should lie along the local symmetry axis of one of the π-orbitals in the equilibrium geometry of a complex with *trans*-1,3-butadiene. There will be four equivalent geometries because there are two equivalent π orbitals and either may be approached from above or below the molecular plane. Two possibilities then exist, however. If the potential energy barriers to tunnelling between the four equivalent positions are sufficiently high, the ClF/HCl molecule will be localised at one of the π bonds. On the other hand, if the PE barriers are low enough, the diatomic molecule might tunnel quantum mechanically through them and sample the four equivalent positions. The geometry of the 1,3-butadiene···ClF complex, as determined from its ground-state rotational spectrum [76], is shown, drawn to scale, in Fig. 13. There was no evidence from the observed spectrum of tunnelling between the equivalent structures and therefore it was concluded that the ClF molecule is localised at one site. The geometry displayed in Fig. 13 is consistent with rule 2. Thus, the ClF axis lies perpendicular to the plane of the nuclei in 1,3-butadiene and the angle $\phi$ ($\angle C_2 - * \cdots Cl$) is 95°, where $*$ is the mid-point of a terminal C – C bond. The rotational spectrum of 1,3-butadiene···HCl exhibits the characteristics of non-rigid-rotor behaviour, probably as a result of a low potential energy barrier between equivalent conformers[4], but the analysis is incomplete and therefore comparison of the geometries of the ClF and HCl complexes with 1,3-butadiene is unavailable.

Benzene is the prototype aromatic Lewis base. It offers formally three pairs of equivalent, conjugated π bonds as the potential electron donor. Symmetric-top-type rotational spectra have been observed for the benzene···HX complexes, where X is F [139], Cl [140] or Br [141], by methods (molecular-beam

[4] Kisiel Z, Legon AC, unpublished observations

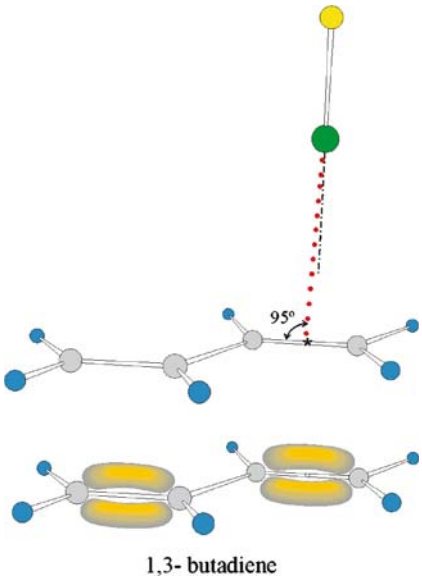


**Fig. 13** The experimental geometry of 1,3-butadiene···ClF drawn to scale and the π-electron model of 1,3-butadiene. The geometry of 1,3-butadiene···HCl is not yet available for comparison. See Fig. 1 for key to the colour coding of atoms

electric resonance spectroscopy and pulsed-jet, Fourier-transform microwave spectroscopy) involving supersonic expansion of gas mixtures of benzene and HX in argon. In each case, only information about the vibrational ground state is available. Benzene···ClF also has a symmetric top-type spectrum but exhibits evidence of non-rigid-rotor behaviour [80]. The ground-state spectrum is accompanied by a single vibrational satellite spectrum which is presumably associated with a low-energy vibrationally excited state, given the low effective temperature of the experiment. A possible interpretation of these observations for benzene···ClF is that the geometry of the complex is as shown in Fig. 14, that is, in the zero-point state, the ClF subunit executes the motion defined by the angle $\phi$, with a PE maximum at the $C_{6v}(\phi = 0°)$ conformation. Thus, the electrophilic end $^{\delta+}$Cl of the ClF subunit interacts with the π-electron density as it traces out the nearly circular path in the $\phi$ coordinate, as indicated, encompassing the six carbon atoms. This path presumably corresponds to a potential energy minimum relative to a maximum at the $C_{6v}(\phi = 0°)$ conformation but is itself likely to present small maxima at the carbon atoms.

It is possible that the complexes benzene···HX can be described in a similar way, but in the absence of any observed non-rigid-rotor behaviour or a vibrational satellite spectrum, it is not possible to distinguish between a strictly $C_{6v}$ equilibrium geometry and one of the type observed for benzene···ClF. In either case, the vibrational wavefunctions will have $C_{6v}$ symmetry, however.

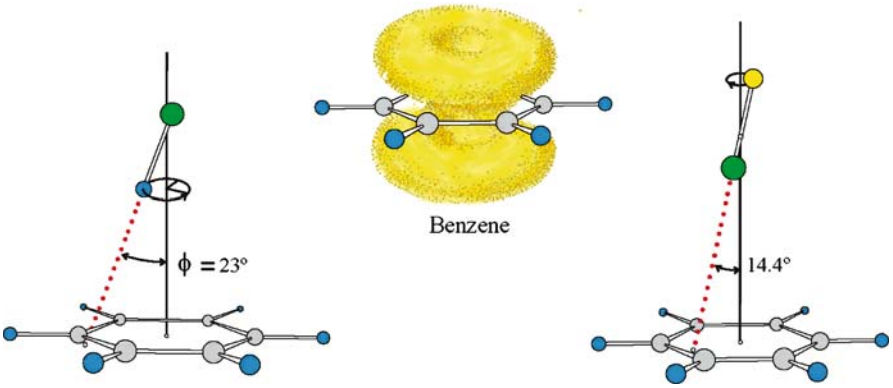


**Fig. 14** The experimental geometries of benzene···HCl and benzene···ClF (to scale) and the π-electron model of benzene. See text for discussion of the motion of the ClF subunit, as inferred from an analysis of the rotational spectrum of benzene···ClF. See Fig. 1 for key to the colour coding of atoms

### 3.2.3.2
### B is a Cumulative π-Bonded System

The π-electron density model of allene, the prototype of molecules that carry two cumulative π bonds, is shown in Fig. 15. According to rule 2, complexes of allene with either HCl or ClF should have the diatomic subunit lying along an axis that passes through, or close to, the midpoint of one of the C – C bonds and is perpendicular to the plane formed by the two C atoms involved and the two H atoms attached to one of them. The geometries of allene···HCl[5] and allene···ClF [75], as determined by means of their rotational spectra, are included in Fig. 15. The angle of rotation $\psi$ about the C = C = C axis cannot be determined spectroscopically because allene is a symmetric-top molecule. The angle $\psi$ would be 0° if, as seems likely, the electrophilic end $^{\delta+}$H of HCl or $^{\delta+}$Cl of ClF interacts with the maximum of π electron density, but $\psi = 90°$ would require that HCl or ClF lies in the nodal plane of the π orbital. Hence, the angle $\psi$ was set to zero. It is possible to determine both the angles $\theta$ and $\phi$ for these molecules of $C_S$ symmetry by the methods outlined in Sect. 3.1.2.2 because the off-diagonal element $\chi_{ab}$ of the Cl nuclear quadrupole coupling tensor is non-zero and determinable. We note from Fig. 15 that the angle $\phi$ for each complex is close to the value of 90°, as required by rule 2. The non-linearity is $\theta \approx 7°$ for the hydrogen bond in allene···HCl[6] and $\theta = 4.9(15)°$ [75] for the halogen bond in allene···ClF. Both these observations indicate only a minor secondary interaction of $^{\delta-}$Cl and $^{\delta-}$F, respectively, with the nearest H atom on the C atom

[5] Fillery-Travis AJ, Legon AC, unpublished observations
[6] Fillery-Travis AJ, Legon AC, unpublished observations

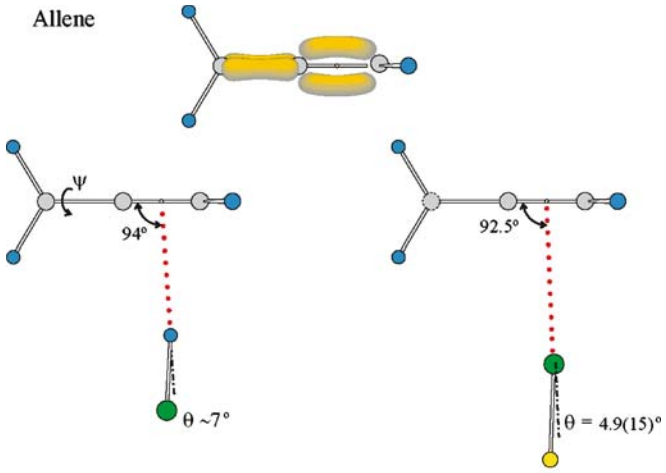


**Fig. 15** The experimental geometries of allene···HCl and allene···ClF, drawn to scale. The π-electron model for allene is also shown. The angles $C_2{-}{*}\cdots H$ and $C_2{-}{*}\cdots Cl$, respectively, where $*$ is the centre of the C – C bond, are both close to 90°, as required by rule 2. The hydrogen and halogen bonds both show small non-linearities. See Fig. 1 for key to the colour coding of atoms

remote from the primary interaction. Allene···HF exhibits a similar geometry [142].

### 3.2.3.3
### B Carries Both-π- and Pseudo-π-Pairs

Methylenecyclopropane has two pseudo-π C – C bonds of its cyclopropane ring adjacent to the π bond between $C_1$ and $C_2$. It is therefore the prototype for a Lewis base that offers cumulative π and pseudo-π-bonds in competition as electron donors. The observed geometries of complexes of methylenecyclopropane with ClF [78] and HCl [143], as determined from spectroscopic constants obtained by analysis of rotational spectra, are shown in Fig. 16. Each has $C_S$ symmetry, with the *ab* principal inertia plane coincident with the plane of symmetry. Accordingly, the off-diagonal element $\chi_{ab}$(Cl) of the Cl nuclear quadrupole coupling tensor was found to be non-zero and was accurately measured in each case. By applying the approach set out in Sect. 3.1.2.2, it was possible to determine both the angles $\phi$ and $\theta$, as defined in Fig. 16. The hydrogen and halogen bonds clearly involve the interaction of $^{\delta+}$H and $^{\delta+}$Cl, respectively, with the $C_1 - C_2$ π bond rather than with a pseudo-π bond of the cyclopropane ring. Moreover, the angles $\phi$ are close to 90° in both complexes, as would be predicted from rule 2, but we note that while the hydrogen bond is significantly non-linear [$\theta = 17.5(2)°$] the halogen bond is much less so [$\theta = 4.9(1)°$]. It is now established for several such pairs of complexes of $C_S$

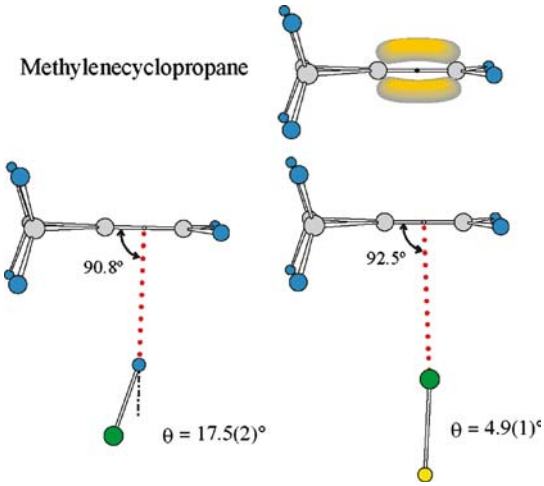


**Fig. 16** The experimental geometries of methylenecyclopropane···HCl and methylenecyclopropane···ClF, drawn to scale. The π-electron model for the Lewis base is also shown. The angles C–∗···H and C–∗···Cl, respectively, where ∗ is the centre of the C – C double bond, are both close to 90°, as required by rule 2. The halogen bond again exhibits a smaller non-linearity $\theta$ than the hydrogen bond. See Fig. 1 for key to the colour coding of atoms

symmetry that the hydrogen bond is significantly non-linear while the corresponding halogen bond is not. We shall return later (Sect. 6) to this important difference between the two types of intermolecular bond. Other complexes of methylenecyclopropane with HX (X = F [144] and Br [145]) have geometries similar to that for X = Cl.

### 3.3 Angular Geometries of B···ClF and B···HCl in Which B is a Mixed n-Pair/π-Pair Donor

According to rule 3, if a Lewis base B carries both non-bonding and π-bonding electron pairs, the n-pairs are definitive of the angular geometry. There are many examples of simple Lewis bases B that can in principle act as either n- or π-electron pair donors. These include CO, HCN, $H_2CO$, furan, thiophene, pyridine, etc. We note that, for convenience, we considered $H_2CO$ earlier as an example of a Lewis base carrying a pair of equivalent n-pairs and ignored the π pair. In fact, $H_2CO$···HCl [121] and $H_2CO$···ClF [79] are examples that obey rule 3. The complexes HX with carbon monoxide when X = F [146], Cl [147], Br [148], and I [149] have all been investigated through their rotational spectra. Each is linear, with the order of the atoms OC···HX in the lowest energy conformer, so that the n-pair on the C atom takes precedence over the π pairs (and indeed the n-pair on O), as predicted by rule 3.

Likewise, the complexes of CO with the dihalogen molecules XY = ClF, [61] $Cl_2$, [39], BrCl [49], $Br_2$ [87] and ICl [94] are all linear in their equilibrium geometries with atoms in the order OC···XY and with X as the more electropositive halogen atom when XY is a heteronuclear dihalogen. Thus, the n-pair carried by C again defines the angular geometry in preference to the π pair. Complexes of the type $N_2$···HX, where X = F [150], Cl [151, 152] and Br [153] are all linear, as are $N_2$···XY, where XY is ClF [71], BrCl [58] and ICl [100]. Thus the complexes of $N_2$ also obey rule 3. The same pattern emerges for the series of complexes formed by hydrogen cyanide with hydrogen halide molecules and with dihalogen molecules. Thus, each complex has been shown to have a linear equilibrium geometry, with atoms in the order HCN···HX, when X = F [154, 155], Cl, [156], Br [157] or I [158], or HCN···XY, when XY = $F_2$ [32], ClF [64],$Cl_2$ [41], BrCl [53] or ICl [99]. Again, when XY is a heteronuclear dihalogen, X is always the more electropositive atom. Those members of the two series $CH_3CN$···HX and $CH_3CN$···XY so far investigated (namely HX = HF [159, 160] and HCl [161] and XY = $F_2$ [31] and ClF [84]) indicate that the same conclusion appears to hold when methyl cyanide is the electron donor. So, there is ample evidence that rule 3 holds for both hydrogen- and halogen-bonded complexes.

Is there any evidence that this rule can be contravened? To answer this question, the complexes of vinyl fluoride, furan and thiophene with HCl and ClF will be considered. Vinyl fluoride, $CH_2CHF$, is an example of a mixed n-pair/π-pair donor in which, unlike CO, HCN, $CH_3CN$ or $CH_2O$, the pairs of electrons (a π-pair shared between $C_1$ and $C_2$ and an n-pair on F) do not have an atom in common. In addition, its complexes with HCl and ClF are important in the context of linear/non-linear hydrogen and halogen bonds. On the other hand, furan and thiophene are examples of mixed n-pair/π-pair aromatic donors in which the n-pair can be withdrawn into the ring.

The geometries of complexes $CH_2CHF$···HCl [85, 162] and $CH_2CHF$···ClF [85], as determined from their ground-state spectroscopic constants, are displayed in Fig. 17. Each complex is effectively planar and we note that in each case the F atom of vinyl fluoride acts as the electron donor. The simple electron density model showing the three n-pairs on F (see Fig. 17) leads to the prediction of a value of ∼115° for the angles C – F···H and C – F···Cl in $CH_2CHF$···HCl and $CH_2CHF$···ClF, respectively. The observed values $\phi$ = 123.7(1)° and 125.7(3)°, respectively, are very similar and reasonably close to 115°. This indicates that rule 3 is again obeyed. The angular deviations of the F···H – Cl nuclei and the F···Cl – F nuclei from a collinear arrangement (defined as $\theta$ in Fig. 17) are different, however. As is the case for several complexes of $C_S$ symmetry discussed earlier, the halogen bond is strictly linear [$\theta$ = 0.6(1)°] while the hydrogen bond deviates by $\theta$ = 18.3(1)° from linearity. The complexes vinyl fluoride···HF [163] and vinyl fluoride···HBr [164] are isostructural with vinyl fluoride···HCl and exhibit similarly non-linear hydrogen bonds.

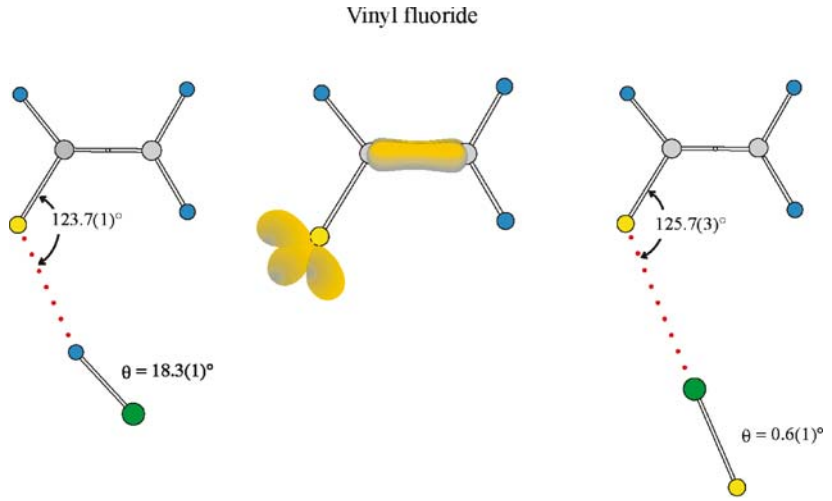


**Fig. 17** The n-pair/π-pair model of vinyl fluoride and scale drawings of the experimental geometries of vinyl fluoride···HCl and vinyl fluoride···ClF. Note that rule 3 is obeyed, with the n-pair taking precedence over the π-pair in defining the angular geometry in both cases. The angles $C_1$–F···H and $C_1$–F···Cl of the HCl and ClF complexes, respectively, are similar, but the non-linearity of the hydrogen bond is large compared with that of the halogen bond, which is negligible. See Fig. 1 for key to the colour coding of atoms

Furan is the prototype of molecules that carry both non-bonding and aromatic π bonding electron pairs. The usual model for the n-pair and π electron density in this molecule is shown in Fig. 18. The oxygen atom is taken to have a non-bonding electron pair in an orbital whose symmetry axis coincides with the $C_2$ axis of furan.

If rule 3 is applied to complexes of furan with HCl or ClF, the predicted geometry would be one that retains $C_{2v}$ symmetry, with the HCl or ClF molecule lying along the axis of the n-pair, and hence along the furan $C_2$ axis, with $^{\delta+}$H or $^{\delta+}$Cl, respectively, nearest to O. The experimentally determined geometry of furan···HCl [165], which is shown in Fig. 18, is indeed precisely as predicted, as is that of furan···HF [166]. The geometry of furan···ClF [81], established by rotational spectroscopy, is strikingly different, as may be seen from Fig. 18. It is obviously not the analogue of that obtained for furan···HCl. Instead, the end $^{\delta+}$Cl of ClF appears to interact with the π electron density associated with carbon atoms $C_2$ and $C_3$, so that this geometry violates rule 3. When furan was replaced by its sulfur analogue thiophene, *both* thiophene···HCl [167] and thiophene···ClF [83] were shown to posses a face-on geometry and both violate rule 3. Thiophene···HF [168] and thiophene···HBr [169] have face-on geometries similar to that of thiophene···HCl.

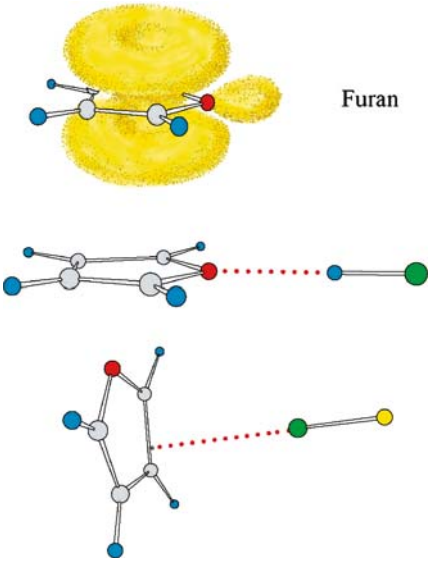


**Fig. 18** The n-pair/π-pair model of furan together with the experimental geometries of furan···HCl and furan···ClF. Furan···HCl, which has a planar geometry of $C_{2v}$ symmetry with HCl lying along the $C_2$ axis, clearly obeys rule 3 but the observed face-on arrangement for furan···ClF demonstrates that rule 3 is violated in this case. See Fig. 1 for key to the colour coding of atoms

The behaviour of the n-pair/aromatic π-pair donors can be understood by considering the electric charge distributions for the series of heterocyclic molecules pyridine, furan and thiophene. A convenient tabulation of the molecular electric dipole and quadrupole moments of these compounds is given in ref. [19]. The electric dipole moment decreases along the series, an observation which has been interpreted as indicating a progressive withdrawal of the n-pair on the heteroatom into the ring. On the other hand, the magnitude of out-of-plane component, $Q_{cc}$, of the electric quadrupole moment, which is a measure of the extension of the π cloud above and below the molecular plane, increases along this series. Thus, thiophene is the member of the series most likely to violate rule 3 and pyridine the least likely. Certainly, both the HCl and ClF complexes of thiophene are of the π-type. The complexes pyridine···HX, for X = F [170], Cl [171] and Br [172] are all of the n-type, with HX lying along the $C_2$ axis and forming a strong hydrogen bond to the heteroatom. Furan is the intermediate case and whether the n- or π-electron pairs define the geometry of the complex is evidently sensitive to the precise nature of the electron acceptor. Thus, furan···HCl is an n-pair complex while furan···ClF has a π-type interaction. Interestingly, furan···HBr [173] also has the face-on conformation, so there is a changeover between X = Cl and Br in the furan complexes.

### 3.4
### Radial Geometries of Complexes B···XY and B···HX: A Summary

Radial geometries of B···XY and B···HX are also systematically related. Only a summary will be given here; the reader is referred to earlier publications for detailed discussion [19, 174–178].

There are two general conclusions of importance. First, the distance $r(Z\cdots X)$, where Z is the electron donor atom/centre in the complex B···XY, is smaller than the sum of the van der Waals radii $\sigma_Z$ and $\sigma_X$ of these atoms. This result has been shown [179] to be consistent with the conclusion that the van der Waals radius of the atom X in the dihalogen molecule X is shorter along the XY internuclear axis than it is perpendicular to it, i.e. there is a polar flattening of the atom X in the molecule XY of the type suggested by Stone et al. [180]. This result has been shown to hold for the cases XY = $Cl_2$ [174], BrCl [175], ClF [176] and ICl [178], but not for $F_2$, in which the F atom in the molecule appears (admittedly on the basis of only a few examples) to be more nearly spherical [177].

The second conclusion concerns the difference $\Delta r = r_{B\cdots HX}(Z\cdots X) - r_{B\cdots XY}(Z\cdots X)$ between the Z to X distances in the two series B···HX and B···XY. $\Delta r$ is positive and nearly constant for a given B and X, when XY is $Cl_2$, $Br_2$, BrCl or ClF. Since the order of the internuclear distances is $r(XY) > r(HX)$ for any given atom X, this result means the outer atom Y of the dihalogen molecule XY is always more distant from a given point in B for the complex B···XY than is the atom X from the same reference point in B for the complex B···HX. This second general result is relevant to the discussion of linear versus non-linear hydrogen and halogen bonds in Sect. 6.

## 4
## Intermolecular Binding Strength in Halogen-Bonded Complexes: Systematic Behaviour of $k_\sigma$

The quadratic intermolecular stretching force constant $k_\sigma$ provides a measure of the force required for a unit infinitesimal increase in the separation of the subunits B and XY along the intermolecular bond in complexes B···XY and hence is one criterion of binding strength. Values can be determined from centrifugal distortion constants $D_J$ or $\Delta_J$ using the expressions set out by Millen [26], who assumed a model involving rigid, unperturbed subunits. In practice, this model implies that the complexes are weakly interacting, that the intermolecular stretching mode has a much smaller force constant than any other stretching mode, and that the geometrical perturbations of the subunits are negligible. Strictly, the expressions apply only to complexes in which the halogen bond coincides with the principal inertia axis $a$ (e.g. to complexes of $C_{2v}$ and $C_{3v}$ symmetry here). The heavy atoms S···X – Y in $H_2S$···XY com-

plexes lie so nearly along the *a* axis that the expressions can also be applied in such cases with insignificant error. We seek the answers to two questions: (1) Are the complexes B···XY weakly bound according to the $k_\sigma$ criterion? (2) Are there any systematic relationships between the $k_\sigma$ values as B and XY are varied?

Table 2 displays the values of $k_\sigma$ for some B···XY complexes of either axial symmetry or $C_{2v}$ symmetry and also those for $H_2S$···XY, where B is one of several Lewis bases and X is $F_2$, ClF, $Cl_2$, BrCl, $Br_2$ or ICl. These values are taken from papers referred to earlier. It is evident from Table 2 that, for a given XY, the order of $k_\sigma$ is $N_2 < OC < HCCH \sim H_2CCH_2 \sim HCN < H_2O \sim PH_3 < H_2S < NH_3$. Moreover, for a given B, the order of $k_\sigma$ is $F_2 < Cl_2 < Br_2 < BrCl < ClF < ICl$, although the number of data for complexes B···$F_2$ is small.

It has been shown [181] that the hydrogen bond interaction in complexes B···HX are of the weak, predominantly electrostatic type and that the $k_\sigma$ values in a large number of complexes can be reproduced by means of the empirical equation:

$$k_\sigma = cNE\,, \tag{4}$$

where *N* and *E* are numbers representing the gas-phase nucleophilicities and electrophilicities of the individual molecules B and HX, respectively, and *c* is a constant arbitrarily assigned the value $0.25\,\mathrm{N\,m^{-1}}$. Values of *N* and *E* for a range of B and HX [181] are given in Table 3. The observed and predicted values of $k_\sigma$ for various B···HX are included in [181] and illustrate that Eq. 4 gives good agreement with the experimental values. Examination of the data in [181] and Table 2 shows that the $k_\sigma$ for two types of complex B···HX and B···XY are similar in magnitude and that most complexes B···XY are weakly

**Table 2** Values of $k_\sigma$ (in $\mathrm{N\,m^{-1}}$) for series of complexes B···XY and those (in parentheses) calculated using the values of $N_B$ and $E_{XY}$ from Table 4 and Eq. 4

| B | XY | | | | | |
|---|---|---|---|---|---|---|
| | $F_2$ | $Cl_2$ | $Br_2$ | BrCl | ClF | ICl |
| $N_2$ | ··· | ···(2.1) | ···(3.2) | 4.4(3.9) | 5.0(4.3) | 5.4(5.3) |
| CO | ··· | 3.7(3.3) | 5.1(4.8) | 6.3(5.9) | 7.0(6.6) | 8.0(8.0) |
| $C_2H_2$ | ··· | 5.6(4.9) | 7.8(7.2) | 9.4(8.9) | 10.0(9.8) | 12.1(12.0) |
| $C_2H_4$ | ··· | 5.9(5.7) | 8.8(8.4) | 10.5(10.4) | 11.0(11.5) | 14.0(14.0) |
| HCN | 2.6 | 6.6(5.9) | ···(8.7) | 11.1(10.7) | 12.3(11.9) | 14.5(14.5) |
| $H_2O$ | 3.7 | 8.0(6.4) | 9.8(9.4) | 12.1(12.2) | 14.2(13.5) | 15.7(16.5) |
| $H_2S$ | 2.4 | 6.3(6.8) | 9.8(9.9) | 12.2(12.2) | 13.3(13.5) | 16.6(16.5) |
| $PH_3$ | ··· | 5.6(6.4) | 9.8(9.5) | 11.6(11.7) | ···(25.0) | 20.7(15.8) |
| $NH_3$ | 4.7 | 12.7(12.5) | 18.5(18.3) | 26.7(22.6) | 34.3(25.0) | 30.4(30.5) |

**Table 3** Nucleophilicities $N_B$ of Lewis bases B and electrophilicities $E_{HX}$ of hydrogen halides HX

| B | $N_2$ | CO | $C_2H_2$ | $C_2H_4$ | $H_2S$ | $PH_3$ | HCN | $H_2O$ | $NH_3$ |
|---|---|---|---|---|---|---|---|---|---|
| $N_B$ | 2.1 | 3.4 | 5.1 | 4.7 | 4.8 | 5.4 | 7.3 | 10.0 | 12.2 |
| HX | HF | HCl | HBr | | | | | | |
| $E_{HX}$ | 10.0 | 5.0 | 4.2 | | | | | | |

bound according to this criterion. It is of interest to examine whether the $k_\sigma$ of the B···XY series can be reproduced by assigning electrophilicities to the various dihalogen molecules. The complexes B···$F_2$ are excluded from this analysis because of insufficient $k_\sigma$ values. We assume that $c$ in Eq. 4 has the same value (0.25 N m$^{-1}$) for both the B···HX and B···XY series and make the arbitrary choice that $E_{ICl} = 10.0$. We then use $k_\sigma$ for the B···ICl series [93–102] in Eq. 4 to obtain the $N_B$ values for $N_2$, CO, $C_2H_2$, $C_2H_4$, HCN, $H_2O$, $H_2S$ and $NH_3$ shown in Table 4.

**Table 4** Nucleophilicities $N_B$ of Lewis bases B and electrophilicities $E_{XY}$ of dihalogens XY

| B | $N_2$ | CO | $C_2H_2$ | $C_2H_4$ | HCN | $H_2O$ | $PH_3$ | $H_2S$ | $NH_3$ |
|---|---|---|---|---|---|---|---|---|---|
| $N_B$ | 2.1 | 3.2 | 4.8 | 5.6 | 5.8 | 6.3 | 6.3 | 6.6 | 12.2 |
| XY | | $Cl_2$ | $Br_2$ | BrCl | ClF | ICl | | | |
| $E_{XY}$ | | 4.1 | 6.0 | 7.4 | 8.2 | 10.0 | | | |

We do not use $k_\sigma$ for $H_3P$···ICl [102] to obtain $N_{PH_3}$ because the $k_\sigma$ for this complex is anomalously high [20.7(1) N m$^{-1}$]. Figure 19 shows the straight line that necessarily results for the B···ICl series when $k_\sigma$ is plotted against $N_B$. Also shown in Fig. 19 are the results for the other series B···XY, where XY is $Cl_2$, ClF, BrCl and $Br_2$, when the $N_B$ values determined from the series B···ICl are used with the appropriate $k_\sigma$ values. We note that for each series the points lie on a reasonable straight line, the slope of which is, according to Eq. 4, $cE_{XY}$. Each line drawn results from a least-squares fit and leads to the values $E_{XY}$ for XY = $Cl_2$, $Br_2$, BrCl and ClF included in Table 4. The value of $N_B = 6.3$ used for $PH_3$ was that obtained by requiring that the $k_\sigma$ for $H_3P$···$Cl_2$, $H_3P$···$Br_2$ and $H_3P$···BrCl fitted best onto the existing straight lines for B···$Cl_2$, B···$Br_2$ and B···BrCl, respectively. The anomalous nature of the point for $H_3P$···ICl (added subsequently) is then obvious. The $k_\sigma$ values for $H_3N$···ClF and $H_3N$···BrCl were not included in the least-squares fit for the series B···ClF and B···BrCl, respectively, because they also appear to be anomalously high. These high values are thought to arise from a non-negligible charge transfer, as represented by a small contribution of the ionic structure $[H_3NX]^+$···$Y^-$ to the valence bond description of these complexes (discussed in Sect. 5.2) [52, 63].

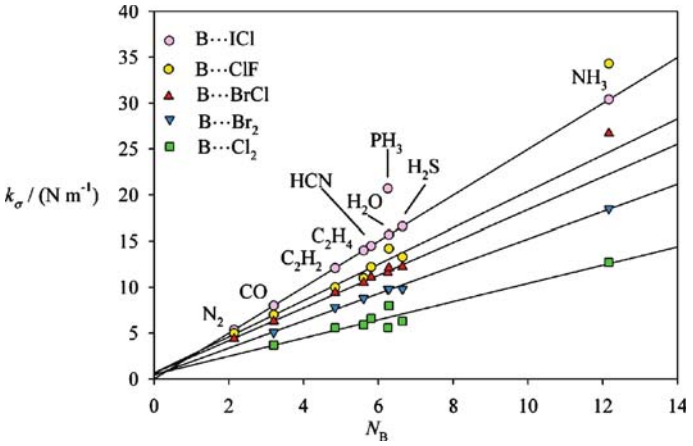


**Fig. 19** Variation of the intermolecular stretching force constant $k_\sigma$ with nucleophilicity $N_B$ for several series of halogen-bonded complexes B···XY, where B is one of a series of Lewis bases and XY is $Cl_2$, $Br_2$, BrCl, ClF or ICl. $N_B$ were assigned by use of Eq. 4 with the choice of $E_{ICl} = 10.0$, hence the perfect straight line for the B···ICl series. The lines for the other series are those obtained by least-squares fits to the $k_\sigma$ values using the $N_B$ determined from the B···ICl series. Points for $H_3P$···ICl, $H_3N$···ClF and $H_3N$···BrCl are anomalous and were excluded from the fits (see text for discussion)

A comparison of the $N_B$ values determined from the B···HX series (Table 3) with those determined here for the B···XY series (Table 4) reveals that the magnitude of $N_B$ obtained in the two different ways is similar for a given B. The notable exception is $H_2O$, which appears to have a significantly greater nucleophilicity when determined using the B···HX series than it has with respect to halogen or interhalogen diatomic molecules. The order of the electrophilicities of the dihalogen molecules determined as outlined above is $E_{Cl_2} < E_{Br_2} < E_{BrCl} < E_{ClF} < E_{ICl}$ and is reasonable in view of the fact that ICl, ClF and BrCl have small electric dipole moments of $4.14(6) \times 10^{-30}$ C m [182], $2.962 \times 10^{-30}$ C m [183] and $1.731(12) \times 10^{-30}$ C m [184], respectively, while $Cl_2$ and $Br_2$ are non-polar but have electric quadrupole moments of $10.79(54) \times 10^{-40}$ C m$^2$ [185] and $17.52 \times 10^{-40}$ C m$^2$ [186], respectively.

## 5
## Extent of Electron Transfer in Halogen-Bonded Complexes B···XY

### 5.1
### Electron Transfer in Weak (Outer) Complexes B···XY

In Sect. 2, it was indicated that changes $\Delta\chi_{\alpha\beta}(X)$ and $\Delta\chi_{\alpha\beta}(Y)$ in halogen nuclear quadrupole coupling constants $\chi_{\alpha\beta}(X)$ and $\chi_{\alpha\beta}(Y)$ of a dihalogen

molecule XY that accompany formation of B···XY lead directly to the changes in the efgs at X and Y. In turn, the changes in the efgs at X and Y can be interpreted in terms of a simple model to give quantitative information about the electric charge redistribution within XY that attends formation of B···XY. We briefly discuss how the extents of intermolecular electron transfer $\delta_i(B \rightarrow X)$ and intramolecular molecular electron transfer $\delta_p(X \rightarrow Y)$ can be extracted from the observed nuclear quadrupole coupling constants of X and Y. Townes and Dailey [187] developed a simple model for estimating efgs at nuclei, and hence nuclear quadrupole coupling constants, in terms of the contributions from the electrons in a molecule such as XY. First, they assume that filled inner shells of electrons remained spherically symmetric when a molecule XY is formed from the atoms X and Y and, second, they make a similar assumption for valence-shell s electrons. Accordingly, filled inner shells and valence s electrons contribute nothing to efgs, which therefore arise only from p, d, ... valence shell electrons. Moreover, because the contribution of a particular electron to the efg at a given nucleus varies as $\langle r^{-3} \rangle$, where $r$ is the instantaneous distance between the nucleus and the electron, only electrons centred on the nucleus in question contribute significantly to the efg at that nucleus.

We assume that, on formation of B···XY, a fraction $\delta_i$ (i = intermolecular) of an electronic charge is transferred from the electron donor atom of Z of the Lewis base B to the $np_z$ orbital of X and that similarly a fraction $\delta_p$ (p = polarisation) of an electronic charge is transferred from $np_z$ of X to $n'p_z$ of Y, where $z$ is the XY internuclear axis and $n$ and $n'$ are the valence-shell principal quantum numbers of X and Y. Within the approximations of the Townes–Dailey model [187], the nuclear quadrupole coupling constants at X and Y in the hypothetical equilibrium state of B···XY can be shown [178] to be given by:

$$\chi^{e}_{zz}(X) = \chi_0(X) - (\delta_i - \delta_p)\chi_A(X) \tag{5}$$

and

$$\chi^{e}_{zz}(Y) = \chi_0(Y) - \delta_p \chi_A(Y)\,. \tag{6}$$

In Eqs. 5 and 6, $\chi_0(X)$ and $\chi_A(X)$ are the coupling constants associated with the free molecule XY and the free atom X, respectively, and similar definitions hold for $\chi_0(Y)$ and $\chi_A(Y)$. The free molecule values are known for $Cl_2$ [188], BrCl [189], $Br_2$ [190] and ICl [93], as are the free atom coupling constants for Cl, Br and I [191]. The equilibrium coupling constants $\chi^{e}_{zz}(X)$ and $\chi^{e}_{zz}(Y)$ are not observables. The observed (zero-point) coupling constant $\chi_{aa}(X)$ for B···XY is the projection of the equilibrium value $\chi^{e}_{zz}(X)$ onto the principal inertia axis $a$ resulting from the angular oscillation $\beta$ of the XY subunit about its own centre of mass when within the complex B···XY. If the motion of the B subunit does not change the efgs at X and Y (which is likely to be a good approximation here) $\chi_{aa}(X)$ and $\chi_{aa}(Y)$ are given by the

expressions:

$$\chi_{aa}(\mathrm{X}) = \chi^{\mathrm{e}}_{zz}(\mathrm{X})\,\langle P_2(\cos\beta)\rangle \ , \tag{7}$$

$$\chi_{aa}(\mathrm{Y}) = \chi^{\mathrm{e}}_{zz}(\mathrm{Y})\,\langle P_2(\cos\beta)\rangle \ , \tag{8}$$

in which $\beta$ is the instantaneous angle between $a$ axis and the XY internuclear axis $z$ and $\langle P_2(\cos\beta)\rangle$ is the second Legendre coefficient. Substitution of Eqs. 7 and 8 into Eqs. 5 and 6 leads to the following expressions for $\delta_{\mathrm{i}}$ and $\delta_{\mathrm{p}}$, the fractions of an electronic charge transferred from B to X and from X to Y, respectively, when B···XY is formed:

$$\delta_{\mathrm{p}} = \frac{\chi_0(\mathrm{Y})}{\chi_{\mathrm{A}}(\mathrm{Y})} - \frac{\chi_{aa}(\mathrm{Y})}{\chi_{\mathrm{A}}(\mathrm{Y})}\,\langle P_2(\cos\beta)\rangle^{-1} \tag{9}$$

$$\delta_{\mathrm{i}} = \frac{\chi_0(\mathrm{X})}{\chi_{\mathrm{A}}(\mathrm{X})} + \frac{\chi_0(\mathrm{Y})}{\chi_{\mathrm{A}}(\mathrm{Y})} - \left\{ \frac{\chi_{aa}(\mathrm{X})}{\chi_{\mathrm{A}}(\mathrm{X})} + \frac{\chi_{aa}(\mathrm{Y})}{\chi_{\mathrm{A}}(\mathrm{Y})} \right\} \langle P_2(\cos\beta)\rangle^{-1} \ . \tag{10}$$

Hence, the inter- and intramolecular electron transfer $\delta_{\mathrm{i}}e$ and $\delta_{\mathrm{p}}e$ can be determined once the value of $P_2(\cos\beta)$ is available. It has been possible to make good estimates of the last quantity for members of each of the series B···$Cl_2$, B···BrCl, B···$Br_2$ and B···ICl as follows. By making the reasonable assumption that $\delta_{\mathrm{i}} = 0$ in the weak complexes Ar···BrCl [57] and Ar···ICl [93], the values $\beta_{\mathrm{av}} = \cos^{-1}\left\langle\cos^2\beta\right\rangle^{1/2} = 6.4°$ and 5.4°, respectively, and $\delta_{\mathrm{p}} = 0.0035(6)$ and 0.0054(1), respectively, are determined. The very small values of $\delta_{\mathrm{p}}$ justify, a posteriori, the assumption $\delta_{\mathrm{i}} = 0$ initially. All other complexes B···BrCl and B···ICl considered are much more strongly bound than Ar···BrCl and Ar···ICl, respectively, and so smaller values of $\beta_{\mathrm{av}}$ (in the range of 5.0(5)° and 4.0(5)°, respectively) were assumed. Moreover, $\langle P_2(\cos\beta)\rangle$ is close to unity even for the Ar complexes and changes so slowly as $\beta_{\mathrm{av}}$ deceases that any errors incurred by such assumptions are negligible. A similar treatment was employed for B···$Br_2$ and B···$Cl_2$ complexes using OC···$Br_2$ [87] and OC···$Cl_2$ [39] as the complexes appropriate to the weak limit having $\delta_{\mathrm{i}} = 0$, in the absence of experimental knowledge of linear complexes Ar···$Br_2$ and Ar···$Cl_2$. Hence, values of $\delta_{\mathrm{i}}$ and $\delta_{\mathrm{p}}$ have been determined for the four series B···XY, where B is $N_2$, CO, $C_2H_2$, $C_2H_4$, $PH_3$, $H_2S$, HCN, $H_2O$ and $NH_3$ and XY is $Cl_2$, $Br_2$, BrCl and ICl. Some systematic trends are evident in $\delta_{\mathrm{i}}$ and $\delta_{\mathrm{p}}$.

Figure 20 displays plots of $\delta_{\mathrm{i}}$ against the first ionisation potential $I_{\mathrm{B}}$ of the Lewis base B for each of the three series B···$Cl_2$, B···BrCl [55] and B···ICl [178]. Each set of points can be fitted reasonably well by a function $\delta_{\mathrm{i}} = A\exp(-\,a\,I_{\mathrm{B}})$. This function is shown by a continuous line in each case. The points for the series B···$Br_2$ lie very close to those for the B···BrCl series and are omitted for clarity.

Figure 20 demonstrates that there is a family relationship among the curves and that the smaller the energy required to remove the most loosely

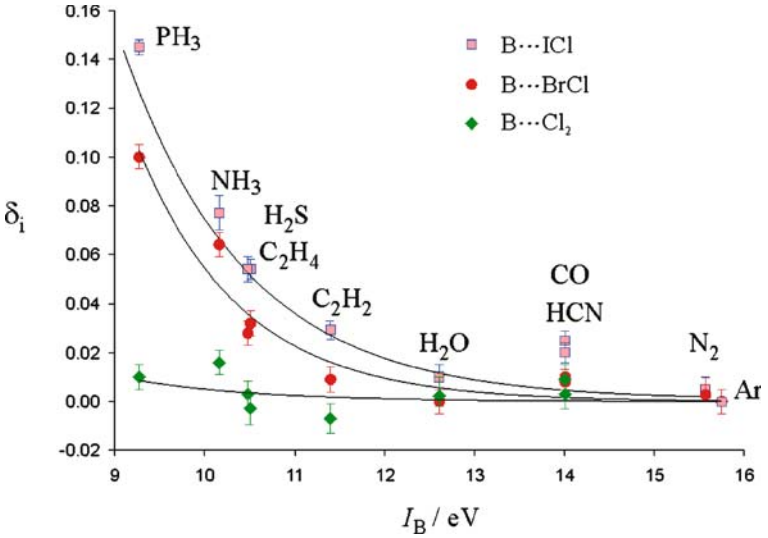


**Fig. 20** Variation of the fraction $\delta_i$ of an electronic charge transferred from B to XY on formation of B···XY with the ionisation energy $I_B$ of B for the series XY = $Cl_2$, BrCl and ICl. See text for the method of determination of $\delta_i$ from observed XY nuclear quadrupole coupling constants. The *solid curves* are the functions $\delta_i = A \exp(-aI_B)$ that best fit the points for each series B···XY. Data for B···$Br_2$ are nearly coincident with those of B···BrCl and have been excluded for the sake of clarity

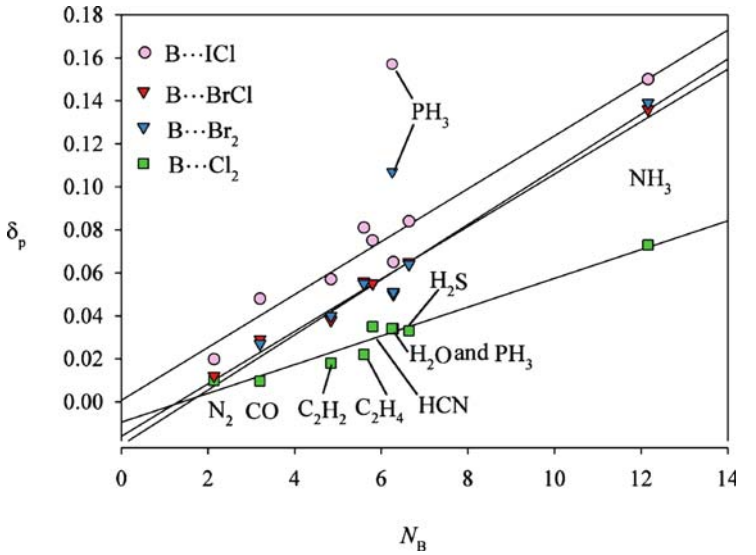


**Fig. 21** Variation of the fraction $\delta_p$ of an electronic charge transferred from X to Y on formation of B···XY with $k_\sigma$ for the series XY = $Cl_2$, $Br_2$, BrCl and ICl. See text for the method of determination of $\delta_p$ from observed XY nuclear quadrupole coupling constants. The *solid line* represents the least-squares fit of the points for each B···XY series

bound electron (n-type or π-type) from B, the greater is the extent of electron transfer from B to XY on formation of B···XY. It is also clear that for all members of the B···$Cl_2$ series the intermolecular charge transfer is negligible, except possibly for B = $NH_3$. For a given B, the order of the extent $\delta_i e$ of electron transfer is $Cl_2$ < $Br_2$∼BrCl < ICl. Values of $\delta_i$ have also been calculated using ab initio methods by several authors [132, 192–195]. In summary, these ab initio calculations lead to values of $\delta_i$ of the same order of magnitude as those obtained experimentally and show similar trends as B and XY are varied. The conclusion from both experiments and ab initio calculations is that the extent of electron transfer is generally < 0.06 *e*, except when B = $NH_3$ and $PH_3$ and XY = BrCl and ICl.

The values of $\delta_p$ also behave systematically, as shown in Fig. 21, in which $\delta_p$ is plotted against $k_\sigma$ for the various series B···XY. It is evident that, for a given XY, $\delta_p$ is an approximately linear function of $k_\sigma$ and hence of the strength of the interaction. Moreover, for a given B the order of $\delta_p$ is ICl > BrCl ∼ $Br_2$ > $Cl_2$, which is the order of the polarisabilities of the leading atoms X in B···XY and therefore seems reasonable from the definition (see earlier) of $\delta_p$.

## 5.2
## Do Mulliken Inner Halogen-Bonded Complexes Exist in the Gas Phase?

A detailed analysis of the halogen and nitrogen nuclear quadrupole coupling constants for the series of hydrogen-bonded complexes$(CH_3)_{3-n}H_nN\cdots HX$, where $n = 0$ and 3 and X = F, Cl, Br and I, has allowed conclusions about how the extent of proton transfer changes with both $n$ and X. The work has been reviewed in detail elsewhere [196] and only a summary is given here. It was concluded that progressive methylation of ammonia, which leads to a monotonic increase in the gas-phase proton affinity of the base, coupled with a decrease in the energy change accompanying the gas-phase process $HX = H^+ + X^-$ along the series X = F, Cl, Br and I, allows the Mulliken inner complex $[(CH_3)_{3-n}H_nNH]^+\cdots X^-$ to become more stable than the Mulliken outer complex $(CH_3)_{3-n}H_nN\cdots HX$ when X = Br and I and $n = 0$. In fact, the extent of proton transfer was crudely estimated to be ∼0%, ∼60%, ∼80% and ∼100% for the series $(CH_3)_3N\cdots HX$, when X is F, Cl, Br and I, respectively, a result which indicates that the proton is gradually transferred as HX becomes progressively easier to dissociate in the case when the proton affinity of the base is greatest. Is there any evidence for Mulliken inner complexes $[BX]^+\cdots Y^-$?

Evidence for a significant contribution from the ionic form $[BX]^+\cdots Y^-$ in a gas-phase complex B···XY was first deduced from the spectroscopic constants of $H_3N\cdots ClF$, as obtained by analysis of its rotational spectrum [63]. In particular, the value $k_\sigma = 34.3\ N\ m^{-1}$ of the intermolecular stretching force constant (obtained from the centrifugal distortion constant $D_J$ in the man-

ner outlined in Sect. 2 is large compared with that (ca. 25 N m$^{-1}$) expected from the plot of $k_\sigma$ versus $N_B$ shown in Fig. 19. Similarly, the Cl-nuclear quadrupole coupling constant is smaller in magnitude than those of more weakly bound B···ClF complexes. A detailed analysis suggested [63, 68] a contribution of $H_3NCl^+\cdots F^-$ of roughly 20% to the valence bond description of $H_3N\cdots ClF$.

In view of the fact that complete methylation of $H_3N\cdots HX$ to give $(CH_3)_3N\cdots HX$ leads to an increased extent of proton transfer from HX to the base when X is Cl and essentially complete transfer when X is I, it seemed reasonable to seek a more significant contribution from the ionic valence bond structure $[(CH_3)_3NCl]^+\cdots F^-$ in $(CH_3)_3N\cdots ClF$ by examining properties similarly derived from its rotational spectrum [68].

It was found that $(CH_3)_3N\cdots ClF$ has a centrifugal distortion constant $D_J$ consistent with the large value $k_\sigma \sim 70$ N m$^{-1}$ for the intermolecular stretching force constant. The distance $r(N\cdots Cl) = 2.090$ Å, as obtained by isotopic substitution at N and Cl, is very short compared with that predicted for an intermolecular N···Cl bond in an analogous complex in which little ionic character is expected, for example HCN···ClF [64], which is weakly bound ($k_\sigma = 12.3$ N m$^{-1}$) and has $r(N\cdots Cl) = 2.639(3)$ Å. The Cl nuclear quadrupole coupling constant of $(CH_3)_3N\cdots ClF$ is significantly smaller in magnitude than expected of a weakly bound complex. A detailed analysis of the observed coupling constant leads to an estimated contribution of ca. 60% for the ionic valence bond structure $[(CH_3)_3NCl]^+\cdots F^-$. In addition, the $^{14}$N nuclear quadrupole coupling constant of $(CH_3)_3N\cdots ClF$ is consistent with a substantial (roughly 70%) contribution of the ion-pair form. It should be emphasised that the models used to interpret the Cl and N nuclear quadrupole coupling constants were crude and that the percentage ionic characters deduced thereby are only semi-quantitative. Nevertheless, there is evidence of a substantial (∼50%) contribution from the ionic structure $[(CH_3)_3NCl]^+\cdots F^-$ in a valence-bond description. Hence, $(CH_3)_3N\cdots ClF$ appears to be intermediate between a Mulliken outer and inner complex. These experimental conclusions are consistent with the results of ab initio calculations [197, 198].

A detailed examination of the rotational spectrum $(CH_3)_3N\cdots F_2$ led [37] to molecular properties that suggest that this complex too has significant ion-pair character. Thus, the behaviour of the spectral intensity as a function of microwave radiation power led to an estimate of ∼10 D for the electric dipole moment, a value which is an order of magnitude large than that (∼1 D) expected on the basis of the vector sum of the component dipole moments (i.e. with no charge transfer). The centrifugal distortion constant $D_J$ is consistent with a large intermolecular stretching force constant $k_\sigma$. The value of the $^{14}$N-nuclear quadrupole coupling constant implies a substantial contribution from $[(CH_3)_3NF]^+\cdots F^-$, as do all the other properties mentioned. If the complex is assumed to be entirely $[(CH_3)_3NF]^+\cdots F^-$ and the geom-

etry of trimethylamine is assumed to be unchanged when $F_2$ approaches it along the $C_3$ axis to form $[(CH_3)_3NF]^+\cdots F^-$, the observed ground-state moments of inertia of the three isotopomers $(CH_3)_3{}^{14}N\cdots F_2$, $(CH_3)_3{}^{15}N\cdots F_2$ and $(CD_3)_3{}^{14}N\cdots F_2$ can be fitted to give the distances $r(N-F) = 1.29(4)$ Å and $r(F-F) = 2.32(4)$ Å, a result consistent with significant covalent character of the N – F bond, with a substantially lengthened F – F bond, and therefore with an ion-pair type of structure. Subsequent ab initio calculations [197–199] showed that this approach overestimates the ionic character, largely because the trimethylamine geometry is significantly perturbed on formation of the complex. If this perturbed geometry of trimethylamine is used in place of the unperturbed geometry and the observed experimental moments of inertia are refitted, the revised bond lengths involving fluorine are $r(N-F) = \sim 1.7$ Å and $r(F-F) = \sim 1.9$ Å, which are in good agreement with the ab initio values [199]. Evidently the $(CH_3)_3N\cdots F_2$ complex has a significant ion-pair character. We conclude therefore that even in the gas phase there are complexes, such as $(CH_3)_3N\cdots ClF$ and $(CH_3)_3N\cdots F_2$, for which the description "inner complex" is partially appropriate.

## 6
## Conclusions: A Model for the Halogen Bond in B···XY

We have established in Sect. 3 a strong case to support the conclusion that a complex B···XY involving a given Lewis base B and a dihalogen molecule XY has an angular geometry that is isomorphous with that of the corresponding member of the series of hydrogen-bonded complexes B···HX. This was achieved mainly by a comparison of pairs of complexes B···HCl and B···ClF for a given B, coupled with the systematic variation of the Lewis base, although there is also similar, but less complete, evidence from comparisons of other series B···HX and B···XY, where X is Cl, Br or I and Y is Cl or Br. The observed parallelism among angular geometries of B···HX and B···XY suggests that the empirical rules [103, 104] for predicting angular geometries of hydrogen-bonded complexes B···HX can be extended to halogen-bonded complexes B···XY. The polarity of the heteronuclear dihalogen molecules ClF, BrCl and ICl is such that the more electropositive atom of each pair, i.e. Cl, Br and I, respectively, carries a small net positive charge $^{\delta+}$ while the other atom carries a corresponding net negative charge $^{\delta-}$. Although the homonuclear dihalogen molecules $F_2$, $Cl_2$ and $Br_2$ have no electric dipole moment, each has a non-zero electric quadrupole moment that can be represented by the following electric charge distribution: $^{\delta+}X\underline{\overline{^{\delta-}}}X^{\delta+}$. Thus we can envisage the partial positive charge $^{\delta+}$ associated with the atom X in XY or $X_2$ as interacting with a n- or a $\pi$-electron pair on the Lewis base B when we restate the rules for halogen-bonded complexes B···XY as follows:

The equilibrium angular geometry of a halogen-bonded complex B···XY can be predicted by assuming that the internuclear axis of a XY or $X_2$ molecule lies:

1. Along the axis of a non-bonding (n) electron pair carried by the acceptor atom Z of B, with order of atoms $Z\cdots{}^{\delta+}X - Y^{\delta-}$, or
2. Along the local symmetry axis of a π or pseudo-π orbital if B carries only π-pairs, or
3. Along the axis of a n-pair when B carries both n- and π-pairs (i.e. rule 1 takes precedence)

The main difference between hydrogen bond and the halogen bond lies in the propensity of the hydrogen bond to be non-linear [28, 29], when symmetry of the complex is appropriate (molecular point group $C_S$ or $C_1$). In so far as complexes B···ClF are concerned, the nuclei Z···Cl – F, where Z is the acceptor atom/centre in B, appear to be nearly collinear in all cases, while the nuclei Z···H – Cl in complexes B···HCl of appropriate symmetry often show significant deviations from collinearity. This propensity for the hydrogen-bonded species B···HCl to exhibit non-linear hydrogen bonds can be understood as follows.

We imagine that $^{\delta+}H–Cl^{\delta-}$ approaches B, $^{\delta+}H$ first, along the axis of, e.g., an n-pair, as required by the rules. Then a secondary attraction, between the nucleophilic end $Cl^{\delta-}$ of HCl and the most electrophilic region E of B, causes $Cl^{\delta-}$ to move towards E but with $^{\delta+}H$ fixed, so that the motion is pivoted at $^{\delta+}H$. The angle Z···H – Cl (defined as $\phi$ in most of the figures) therefore remains constant in first approximation, which explains why the values of $\phi$ in complexes B···HCl are those predicted by the rules even though the hydrogen bond is non-linear. In the new equilibrium position the force of attraction between E and $Cl^{\delta-}$ is balanced by the force tending to restore the hydrogen bond to linearity. There are three factors that conspire to keep the Z···Cl – F nuclei in B···ClF more nearly collinear than the nuclei Z···H – Cl in the corresponding complex B···HCl:

1. For a given B, the Z···Cl bond in B···ClF is stronger than the Z···H bond in B···HCl (as measured by $k_\sigma$) and is presumably more difficult to bend
2. $Cl^{\delta-}$ in HCl is probably a better nucleophile than $F^{\delta-}$ of ClF
3. $F^{\delta-}$ is further away from the electrophilic region E of B than is $Cl^{\delta-}$ (see Sect. 3.4)

It is of interest to note that systematic studies [200–204] of complexes B···HCCH involving weak primary hydrogen bonds Z···HCCH have revealed large non-linearities, but with an angle $\phi$ that remains reasonably close to those predicted by the rules. Figure 22 illustrates this result through the experimentally determined geometries for the cases when B is 2,5-dihydrofuran [200], oxirane [201], formaldehyde [202], thiirane [203], and vinyl fluoride [204]. On the other hand, as noted in Sect. 3.1.3, both

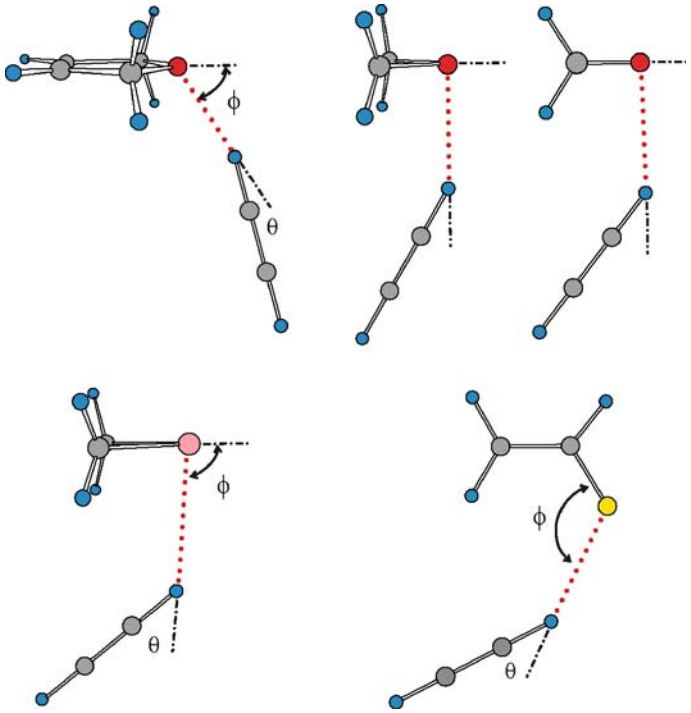


**Fig. 22** Experimentally determined geometries, drawn to scale, for a series of weak, hydrogen-bonded complexes B···HCCH, where B is 2,5-dihydrofuran, oxirane, formaldehyde, thiirane or vinyl fluoride. The values of [$\phi$ and $\theta$] are [57.8(18)° and 16.2(32)°], [90.4(12)° and 29.8(4)°], [92.0(15)° and 39.5(10)°], [96.0(5)° and 42.9(23)°] and [122.6(4)° and 36.5(2)°], respectively. The non-linearities of the hydrogen bonds are large because the primary Z···H hydrogen bonds are weak. The exception is 2,5-dihydrofuran···HCCH, in which the distance between the centre of the ethyne π bond and the most electrophilic region of B is larger because the angle $\phi$ is smaller than for other B, thus making the secondary interaction correspondingly weaker. See Fig. 1 for key to the colour coding of atoms

$SO_2$···ClF [70] and $SO_2$···HCl [28, 126] have negligible non-linearity of the halogen and hydrogen bonds, respectively, even though weakly bound. Examination of Fig. 10 reveals that the $F^{\delta-}$ and $Cl^{\delta-}$ are far away from the centre $S^{\delta+}$ in each case and that, therefore, the linear arrangements are to be expected.

The rules for predicting angular geometries of halogen-bonded complexes B···XY have recently received support from a wide ranging analysis of X-ray diffraction studies in the solid state by Laurence and co-workers [205]. This study not only confirms the validity of the rules in connection with complexes B···XY, where XY is $Cl_2$, $Br_2$, $I_2$, ICl and IBr, with many Lewis bases B but also reinforces the conclusion that halogen bonds Z···X – Y show a smaller propensity to be non-linear that do hydrogen bonds Z···H — X.

There are other parallels between the series of complexes B···XY and B···HX. We established in Sect. 4 that B···XY and B···HX have, in general, similar binding strengths, as measured by the intermolecular stretching force constant $k_\sigma$, and both are, for the most part, weakly bound. We have also shown in Sect. 5 that the electric charge redistribution that occurs when B···XY is formed from its components B and XY is generally small (exceptions among both halogen- and hydrogen-bonded complexes were discussed).

The striking parallel behaviour among the various properties of B···XY and B···HX suggests that the origin of the halogen-bond interaction might be similar to that of the hydrogen bond interaction. An electrostatic model has had much success in predicting angular geometries, both qualitatively [103, 104] and quantitatively [206]. In first approximation, an electrostatic model is one which takes into account only the interaction of the unperturbed electric charge distributions of the two component molecules as they come together to form the complex in its equilibrium conformation, with contributions from interactions of any induced moments assumed minor. The empirical rules set out in Sect. 3 and this section for hydrogen-bonded and halogen-bonded complexes, respectively, are inherently electrostatic in origin. The reason why the electrostatic component of the energy is definitive of the angular geometry has been investigated in detail through ab initio calculations [207] for $H_2O\cdots HF$. The systematic behaviour of the intermolecular force constants $k_\sigma$ of hydrogen-bonded complexes has been discussed in terms of a predominantly electrostatic interpretation [181].

## References


1. Guthrie F (1863) J Chem Soc 16:239
2. Benesi HA, Hildebrand JH (1949) J Am Chem Soc 71:2703
3. Mulliken RS, Person WB (1969) Molecular complexes: A lecture and reprint volume. Wiley-Interscience, New York
4. Hassel O, Rømming C (1962) Quart Rev Chem Soc 16:1
5. Hassel O (1970) Science 170:497
6. Frei H, Pimentel GC (1985) Annu Rev Phys Chem 36:491
7. Bai H, Ault BS (1990) J Phys Chem 94:199
8. Bai H, Ault BS (1990) J Mol Struct 238:223
9. Machara NP, Ault BS (1988) J Mol Struct 172:126
10. Machara NP, Ault BS (1988) Inorg Chem 27:2383
11. Andrews L, Hunt RD (1988) J Chem Phys 89:3502
12. Andrews L, Lascola R (1987) J Am Chem Soc 109:6243
13. Andrews L, McInnis TC, Hannachi Y (1992) J Phys Chem 96:4248
14. McInnis TC, Andrews L (1992) J Phys Chem 96:2051
15. Legon AC, Rego CA (1990) J Chem Soc Faraday Trans 86:1915
16. Balle TJ, Flygare WH (1981) Ann Rev Sci Instrum 52:33
17. Legon AC (1992) In: Scoles G (ed) Atomic and molecular beam methods, vol 2. Oxford University Press, New York, p 289

18. Arunan E et al. (2007) Chemistry International, March–April 2007, available at http://www.iupac.org/publications/ci/2007/2902/pp1_2004-026-2-100.html
19. Legon AC (1999) Angew Chem Int Ed 38:2686
20. Legon AC (1998) Chem Eur J 4:1890
21. Metrangolo P, Neukirch H, Pilati T, Resnati G (2005) Acc Chem Res 38:386
22. Bloemink HI, Dolling SJ, Legon AC (1995) J Chem Soc Faraday Trans 91:2059
23. Legon AC, Millen DJ (1986) Chem Rev 86:635
24. Leopold KR, Fraser GT, Novick SE, Klemperer W (1994) Chem Rev 94:1807
25. Legon AC (1992) J Mol Struct 266:21
26. Millen DJ (1985) Can J Chem 63:1477
27. Townes CH, Schawlow AL (1955) Microwave spectroscopy. McGraw-Hill, New York, p 149
28. Legon AC (1994) Faraday Discuss Chem Soc 97:19
29. Legon AC, Thorn JC (1994) Chem Phys Lett 227:472
30. Bloemink HI, Hinds K, Holloway JH, Legon AC (1995) Chem Phys Lett 245:598
31. Cooke SA, Cotti G, Evans CM, Holloway JH, Legon AC (1996) Chem Phys Lett 260:388
32. Cooke SA, Cotti G, Evans CM, Holloway JH, Legon AC (1996) Chem Phys Lett 262:308
33. Cooke SA, Cotti G, Holloway JH, Legon AC (1997) Angew Chem Int Ed 36:129
34. Cooke SA, Cotti G, Evans CM, Holloway JH, Kisiel Z, Legon AC, Thumwood JMA (2001) Chem Eur J 7:2295
35. Cotti G, Evans CM, Holloway JH, Legon AC (1997) Chem Phys Lett 264:513
36. Evans CM, Holloway JH, Legon AC (1997) Chem Phys Lett 267:281
37. Bloemink HI, Cooke SA, Holloway JH, Legon AC (1997) Angew Chem Int Ed 36:1340
38. Baiocchi FA, Dixon TA, Klemperer W (1982) J Chem Phys 77:1632
39. Jäger W, Xu Y, Gerry MCL (1993) J Chem Phys 97:3685
40. Legon AC, Warner HE (1993) J Chem Phys 98:3827
41. Legon AC, Thorn JC (1993) J Chem Soc Faraday Trans 89:4157
42. Legon AC, Lister DG, Thorn JC (1994) J Chem Soc Chem Commun, p 757
43. Bloemink HI, Hinds K, Legon AC, Thorn JC (1994) J Chem Soc Chem Commun, p 1321
44. Bloemink HI, Hinds K, Legon AC, Thorn JC (1994) Chem Phys Lett 223:162
45. Legon AC, Lister DG, Thorn JC (1994) J Chem Soc Faraday Trans 90:3205
46. Bloemink HI, Hinds K, Legon AC, Thorn JC (1995) Chem Eur J 1:17
47. Bloemink HI, Cooke SA, Hinds K, Legon AC, Thorn JC (1995) J Chem Soc Faraday Trans 91:1891
48. Davey JB, Legon AC, Thumwood JMA (2001) J Chem Phys 114:6190
49. Blanco S, Legon AC, Thorn JC (1994) J Chem Soc Faraday Trans 90:1365
50. Bloemink HI, Hinds K, Legon AC, Thorn JC (1994) J Chem Soc Chem Commun, p 1229
51. Bloemink HI, Hinds K, Legon AC, Thorn JC (1994) Angew Chem Int Ed 33:1512
52. Bloemink HI, Legon AC, Thorn JC (1995) J Chem Soc Faraday Trans 91:781
53. Hinds K, Legon AC (1995) Chem Phys Lett 240:467
54. Bloemink HI, Legon AC (1996) Chem Eur J 2:265
55. Legon AC, Thumwood JMA, Waclawik ER (2000) J Chem Phys 113:5278
56. Davey JB, Legon AC (2001) Phys Chem Chem Phys 3:3006
57. Davey JB, Legon AC, Waclawik ER (2001) Chem Phys Lett 346:103
58. Legon AC, Ottaviani P (2002) Phys Chem Chem Phys 4:441
59. Janda KC, Steed JM, Novick SE, Klemperer W (1977) 67:5162

60. Bloemink HI, Hinds K, Holloway JH, Legon AC (1995) Chem Phys Lett 242:113
61. Hinds K, Holloway JH, Legon AC (1995) Chem Phys Lett 242:407
62. Bloemink HI, Hinds K, Legon AC, Holloway JH (1995) J Chem Soc Chem Commun, p 1833
63. Bloemink HI, Evans CM, Holloway JH, Legon AC (1996) Chem Phys Lett 248:260
64. Hinds K, Legon AC, Holloway JH (1996) Mol Phys 88:673
65. Bloemink HI, Holloway JH, Legon AC (1996) Chem Phys Lett 250:567
66. Hinds K, Holloway JH, Legon AC (1996) J Chem Soc Faraday Trans 92:1296
67. Bloemink HI, Evans CM, Holloway JH, Legon AC (1996) Chem Phys Lett 251:275
68. Bloemink HI, Holloway JH, Legon AC (1996) Chem Phys Lett 254:59
69. Evans CM, Holloway JH, Legon AC (1996) Chem Phys Lett 255:119
70. Cotti G, Holloway JH, Legon AC (1996) Chem Phys Lett 255:401
71. Cooke SA, Cotti G, Hinds K, Holloway JH, Legon AC, Lister DG (1996) J Chem Soc Faraday Trans 9:2671
72. Cooke SA, Cotti G, Evans CM, Holloway JH, Legon AC (1996) Chem Commun, p 2327
73. Hinds K, Holloway JH, Legon AC (1996) J Chem Soc Faraday Trans 93:373
74. Cooke SA, Holloway JH, Legon AC (1997) J Mol Struct 406:15
75. Cooke SA, Holloway JH, Legon AC (1997) Chem Phys Lett 266:61
76. Cooke SA, Holloway JH, Legon AC (1997) J Chem Soc Faraday Trans 93:2361
77. Cooke SA, Corlett GK, Evans CM, Holloway JH, Legon AC (1997) Chem Phys Lett 275:269
78. Cooke SA, Holloway JH, Legon AC (1997) J Chem Soc Faraday Trans 93:4253
79. Cooke SA, Corlett GK, Evans CM, Legon AC, Holloway JH (1998) J Chem Phys 108:39
80. Cooke SA, Evans CM, Holloway JH, Legon AC (1998) J Chem Soc Faraday Trans 94:2295
81. Cooke SA, Corlett GK, Holloway JH, Legon AC (1997) J Chem Soc Faraday Trans 94:2675
82. Waclawik ER, Legon AC, Holloway JH (1998) Chem Phys Lett 295:289
83. Cooke SA, Holloway JH, Legon AC (1998) Chem Phys Lett 298:151
84. Page MD, Waclawik ER, Holloway JH, Legon AC (1999) J Mol Struct 509:55
85. Davey JB, Holloway JH, Legon AC, Waclawik ER (1999) Phys Chem Chem Phys 1:2415
86. Bloemink HI, Legon AC (1995) J Chem Phys 103:876
87. Waclawik ER, Thumwood JMA, Lister DG, Fowler PW, Legon AC (1999) Mol Phys 97:159
88. Waclawik ER, Legon AC (2000) Chem Eur J 6:3968
89. Legon AC, Thumwood JMA (2001) Phys Chem Chem Phys 3:1397
90. Legon AC, Thumwood JMA (2001) Phys Chem Chem Phys 3:2758
91. Legon AC, Thumwood JMA, Waclawik ER (2002) Chem Eur J 8:940
92. Davey JB, Legon AC (2001) Chem Phys Lett 350:39
93. Davey JB, Legon AC, Waclawik ER (1999) Chem Phys Lett 306:133
94. Davey JB, Legon AC, Waclawik ER (1999) Phys Chem Chem Phys 1:3097
95. Davey JB, Legon AC (1999) Phys Chem Chem Phys 1:3721
96. Thumwood JMA, Legon AC (1999) Chem Phys Lett 310:88
97. Waclawik ER, Legon AC (1999) Phys Chem Chem Phys 1:4695
98. Legon AC, Waclawik ER (1999) Chem Phys Lett 312:385
99. Herrebout WA, Legon AC, Waclawik ER (1999) Phys Chem Chem Phys 1:4961
100. Davey JB, Legon AC, Waclawik ER (2000) J Mol Struct 500:391
101. Davey JB, Legon AC, Waclawik ER (2000) Phys Chem Chem Phys 2:1659

102. Davey JB, Legon AC, Waclawik ER (2000) Phys Chem Chem Phys 2:2265
103. Legon AC, Millen DJ (1982) Faraday Discuss Chem Soc 73:71
104. Legon AC, Millen DJ (1987) Chem Soc Rev 16:467
105. Howard NW, Legon AC (1988) J Chem Phys 88:4694
106. Howard NW, Legon AC (1987) J Chem Phys 86:6722
107. Legon AC, Stephenson D (1992) J Chem Soc Faraday Trans 88:761
108. Legon AC, Thumwood JMA, Waclawik ER, Willoughby LC (2000) Phys Chem Chem Phys 2:4918
109. Willoughby LC, Legon AC (1983) J Phys Chem 87:2085
110. Howard NW, Legon AC, Luscombe GJ (1991) J Chem Soc Faraday Trans 87:507
111. Bevan JW, Kisiel Z, Legon AC, Millen DJ (1980) Proc Roy Soc Lond A 372:441
112. Kisiel Z, Legon AC, Millen DJ (1982) Proc Roy Soc Lond A 381:419
113. Legon AC, Willoughby LC (1983) Chem Phys Lett 95:449
114. Kisiel Z, Pietrewicz BA, Fowler PW, Legon AC, Steiner E (2000) J Phys Chem 104:6970
115. Legon AC, Suckley AP (1988) Chem Phys Lett 150:153
116. McIntosh A, Walther T, Lucchese RR, Bevan JW, Suenram RD, Legon AC (1999) Chem Phys Lett 314:57
117. Willougby LC, Fillery-Travis AJ, Legon AC (1984) J Chem Phys 81:20
118. Goodwin EJ, Legon AC (1984) J Chem Soc Faraday Trans 2 80:51
119. Jaman AI, Legon AC (1986) J Mol Struct 145:261
120. Legon AC, Rego CA, Wallwork AL (1992) J Chem Phys 97:3050
121. Legon AC (1996) J Chem Soc Faraday Trans 92:2677
122. Antolinez S, Lopez JC, Alonso JL (2001) Chem Phys Lett 334:250
123. Evans CM, Legon AC (1995) Chem Phys 198:119
124. Atkins MJ, Legon AC, Warner HE (1994) Chem Phys Lett 229:267
125. Legon AC, Wallwork AL, Warner HE (1991) J Chem Soc Faraday Trans 87:3327
126. Fillery-Travis AJ, Legon AC (1986) Chem Phys Lett 123:4
127. Fillery-Travis AJ, Legon AC (1986) J Chem Phys 85:3180
128. Aldrich PD, Legon AC, Flygare WH (1981) J Chem Phys 75:2126
129. Shea JA, Flygare WH (1982) J Chem Phys 76:4857
130. Fowler PW, Legon AC, Thumwood JMA, Waclawik ER (2000) Coord Chem Rev 197:231
131. Dubois JE, Garnier F (1967) Spectrochim Acta 23A:2279
132. Lenoir D, Chiappe C (2003) Chem Eur J 9:1037
133. Read WG, Flygare WH (1982) J Chem Phys 76:292
134. Legon AC, Aldrich PD, Flygare WH (1981) J Chem Phys 75:625
135. Cole GC, Davey JB, Legon AC, Lyndon AF (2003) Mol Phys 101:603
136. Coulson CA, Moffitt WE (1949) Philos Mag 40:1
137. Legon AC, Aldrich PD, Flygare WH (1982) J Am Chem Soc 104:1486
138. Buxton LW, Aldrich PD, Shea JA, Legon AC, Flygare WH (1981) J Chem Phys 75:2681
139. Baiocchi FA, Williams JH, Klemperer W (1983) J Phys Chem 87:2079
140. Read WG, Campbell EJ, Henderson G (1983) J Chem Phys 78:3501
141. Cooke SA, Corlett GK, Evans CM, Legon AC (1997) Chem Phys Lett 272:61
142. Legon AC, Willoughby LC (1988) Chem Phys Lett 143:214
143. Kisiel Z, Fowler PW, Legon AC (1994) J Chem Phys 101:4635
144. Kisiel Z, Fowler PW, Legon AC (1995) Chem Phys Lett 232:187
145. Legon AC, Lister DG (1999) Phys Chem Chem Phys 1:4175
146. Legon AC, Soper PD, Flygare WH (1981) J Chem Phys 74:4944
147. Soper PD, Legon AC, Flygare WH (1981) J Chem Phys 74:2138

148. Keenan MR, Minton TK, Legon AC, Balle TJ, Flygare WH (1981) Proc Nat Acad Sci USA 77:5583
149. Wang Z, Lucchese RR, Bevan JW, Suckley AP, Rego CA, Legon AC (1993) J Chem Phys 98:1761
150. Soper PD, Legon AC, Read WG, Flygare WH (1982) J Chem Phys 76:292
151. Altmann RS, Marshall MD, Klemperer W (1983) J Chem Phys 79:57
152. Howard NW, Legon AC (1988) Chem Phys Lett 149:57
153. Howard NW, Legon AC (1989) J Chem Phys 90:672
154. Legon AC, Millen DJ, Rogers SC (1980) Proc Roy Soc Lond A 370:213
155. Legon AC, Millen DJ, Willoughby LC (1985) Proc Roy Soc Lond A 401:327
156. Legon AC, Campbell EJ, Flygare WH (1982) J Chem Phys 76:2267
157. Campbell EJ, Legon AC, Flygare WH (1983) J Chem Phys 78:3494
158. Fowler PW, Legon AC, Peebles SA (1994) Chem Phys Lett 226:501
159. Bevan JW, Legon AC, Millen DJ, Rogers SC (1980) Proc Roy Soc Lond A 370:239
160. Soper PD, Legon AC, Read WG, Flygare WH (1981) J Phys Chem 85:3440
161. Legon AC, Millen DJ, North HM (1987) J Phys Chem 91:5210
162. Kisiel Z, Fowler PW, Legon AC (1990) J Chem Phys 93:3054
163. Cole GC, Legon AC (2004) Chem Phys Lett 400:419
164. Legon AC, Ottaviani P (2002) Phys Chem Chem Phys 4:4103
165. Shea JA, Kukolich SG (1983) J Chem Phys 78:3545
166. Lesarri A, Lopez JC, Alonso JL (1998) J Chem Soc Faraday Trans 94:729
167. Cooke SA, Corlett GK, Legon AC (1998) J Chem Soc Faraday Trans 94:1565
168. Cooke SA, Corlett GK, Legon AC (1998) Chem Phys Lett 291:269
169. Legon AC, Ottaviani P (2004) Phys Chem Chem Phys 6:488
170. Cooke SA, Corlett GK, Legon AC (1998) J Mol Struct 448:107
171. Cooke SA, Corlett GK, Lister DG, Legon AC (1998) J Chem Soc Faraday Trans 94:837
172. Cole GC, Legon AC (2004) J Chem Phys 121:10467
173. Cole GC, Legon AC, Ottaviani P (2002) J Chem Phys 117:2790
174. Legon AC (1995) Chem Phys Lett 237:291
175. Legon AC (1995) J Chem Soc Faraday Trans 91:1881
176. Legon AC (1997) Chem Phys Lett 279:55
177. Legon AC (1998) Chem Commun, p 2737
178. Legon AC (1999) Chem Phys Lett 314:472
179. Peebles SA, Fowler PW, Legon AC (1995) Chem Phys Lett 240:130
180. Price SL, Stone AJ, Lucas J, Rowland RS, Thornley AE (1994) J Am Chem Soc 116:4910
181. Legon AC, Millen DJ (1987) J Am Chem Soc 109:356
182. Herbst E, Steinmetz WE (1972) J Chem Phys 56:5346
183. Fabricant B, Muenter JS (1977) J Chem Phys 66:5274
184. Nair KPR, Hoeft J, Tiemann E (1978) Chem Phys Lett 58:153
185. Buckingham AD, Graham C, Williams JH (1983) Mol Phys 49:703
186. Fowler PW, Legon AC, Peebles SA (1997) Adv Quant Chem 28:247
187. Townes CH, Schawlow AL (1955) Microwave spectroscopy. McGraw-Hill, New York, p 225
188. Xu Y, Jäger W, Ozier I, Gerry MCL (1993) J Chem Phys 98:3726
189. Legon AC, Thorn JC (1993) Chem Phys Lett 215:554
190. Bettin N, Knöckel H, Tiemann E (1981) Chem Phys Lett 80:386
191. Gordy W, Cook RL (1983) Microwave molecular spectra. In: Weissberger A (ed) Techniques of chemistry, vol XVIII, 3rd edn. Wiley, New York, pp 725–802
192. Alkorta I, Rozas I, Elguero E (1998) J Phys Chem A 102:9278

193. Karpfen A (2000) J Phys Chem A 104:6871
194. Zhang Y, Xiao-Zeng Y (2001) J Computat Chem 22:327
195. Zou J-W, Jiang Y-J, Gou M, Hu G-X, Zhang B, Liu H-C, Yu Q-S (2005) Chem Eur J 11:740
196. Legon AC (1993) Chem Soc Rev 22:153
197. Karpfen A (1999) Chem Phys Lett 299:493
198. Domene C, Fowler PW, Legon AC (1999) Chem Phys Lett 309:463
199. Karpfen A (2003) Theor Chem Acc 110:1
200. Cole GC, Hughes RA, Legon AC (2005) J Chem Phys 122:134311
201. Legon AC (1995) Chem Phys Lett 247:24
202. Howard NW, Legon AC (1988) J Chem Phys 88:6793
203. Batten RC, Cole GC, Legon AC (2003) J Chem Phys 119:7903
204. Cole GC, Legon AC (2003) Chem Phys Lett 369:31
205. Ouvrard C, Le Questel J-Y, Berthelot M, Laurence C (2003) Acta Cryst B 59:512
206. Buckingham AD, Fowler PW (1985) Can J Chem 63:2018
207. Hurst GJB, Fowler PW, Stone AJ, Buckingham AD (1986) Int Rev Phys Chem 5:107

Struct Bond (2008) 126: 65–104
DOI 10.1007/430_2007_067

Published online: 31 October 2007

# Halogen Bonding with Dihalogens and Interhalogens

William T. Pennington[1] (✉) · Timothy W. Hanks[2] · Hadi D. Arman[1]

[1]Department of Chemistry, Hunter Chemistry Laboratory,
Clemson University, Clemson, SC 29634-1905, USA
*billp@clemson.edu*

[2]Department of Chemistry, Furman University, Greenville, SC 29613, USA

**1 Introduction** . . . . . 66
1.1 Historical Background . . . . . 66
1.2 Significance of Halogen Bonding with Dihalogens . . . . . 68

**2 Crystal Structures** . . . . . 69
2.1 General Observations . . . . . 69
2.2 Nitrogen and Oxygen Electron Donors . . . . . 87
2.3 Phosphorus and Sulfur Electron Donors . . . . . 88
2.4 Arsenic and Selenium Electron Donors . . . . . 89

**3 Computation Studies** . . . . . 90
3.1 General Observations . . . . . 90
3.2 Oxygen Electron Donors . . . . . 92
3.3 Nitrogen Electron Donors . . . . . 93
3.4 Sulfur and Selenium Electron Donors . . . . . 95
3.5 π-Electron Donors . . . . . 97

**References** . . . . . 98

**Abstract** The fact that iodine forms complexes with Lewis bases has been recognized since at least the middle of the nineteenth century. With the development of X-ray crystallography and modern spectroscopic techniques, the directionality and strength of halogen bonds has been determined. Halogen bonds between dihalogens and Lewis bases fall into four main categories: simple adducts, bridging adducts, amphoteric adducts, and adducts that are both bridging and amphoteric. In the case of very strong interactions between the electron donor and the dihalogen, the halogen–halogen bond is broken, leading to ionic or oxidative addition products. The theoretical description of the halogen bond has also progressed, in parallel with the development of increasingly sophisticated theories of bonding. Relatively accurate predictions of structural parameters and interaction energies are now possible, but they present a challenge to available computational hardware and software.

**Keywords** Halogen bond · Crystallography · Molecular modeling · ab initio · Charge transfer

**Abbreviations**

| | |
|---|---|
| BSSE | Basis set superposition error |
| DFT | Density functional theory |

| | |
|---|---|
| ECP | Effective core potential |
| GGA | Generalized gradient approach |
| HF | Hartree–Fock |
| HOMO | Highest occupied molecular orbital |
| IRC | Intrinsic reaction coordinate |
| LCAO | Linear combination of atomic orbitals |
| LSDA | Local spin density approximation |
| LUMO | Lowest unoccupied molecular orbital |
| MO | Molecular orbital |
| MP2 | Second order Møller–Plesset perturbation theory |
| NBO | Natural bond order analysis |
| NERP | Negative eigenvalues progression reduction |
| QCC | Nuclear quadrupole coupling constants |
| RHF | Restricted Hartree–Fock |
| UPS | Ultraviolet photoelectron spectroscopy |
| $V_{OC}$ | Open circuit voltage |
| ZORA | Zero order regular approximation |

# 1 Introduction

## 1.1 Historical Background

It has long been known that iodine dissolves in solvents possessing electron lone pairs and that the colors of these solutions are related to the solvent's basicity. Explaining this simple observation has required decades of work and has consistently required the application of the most sophisticated experimental tools available. The observation has also continually challenged theories of bonding, and even today taxes the capabilities of the fastest computers in efforts to provide accurate descriptions of its origin.

In 1863, Guthrie added iodine to a saturated solution of ammonium nitrate to give a material that he formulated as $NH_3I_2$ [1]. This complex spontaneously decomposed to give ammonia and iodine when isolated, and was decidedly different from products obtained from combinations of the two compounds under different conditions. This study highlighted several questions that were to become central to the study of halogen bonded complexes. These include (1) the nature and structure of the donor–acceptor complex; (2) the origin of the changes in the electronic (and later vibrational, rotational, nuclear magnetic, and microwave) spectra; (3) the strength of the donor–acceptor interaction; and 4) the role of the halogen bonded complex in other reactions.

For most of the next century, studies of halogen bonded systems in solution were of primary interest. It was soon learned that the non-halogen com-

ponent of the complex contained lone pairs of electrons (or π systems). The complexes that were initially formed were not ionic, but with time or stronger bases, salts could be isolated. On the theoretical front, halogen bonded systems were found to be inconsistent with Lewis' theories of valence [2]. In response, Mulliken [3, 4] and others developed a classification system and conceptual framework for donor–acceptor complexes.

A major breakthrough in the field began with the elucidation of the solid-state structure of a 1 : 1 complex between molecular bromine and 1,4-dioxane using X-ray crystallography [5]. This, and subsequent structures determined by Hassel and others, provided dramatic evidence that complex formation involved short intramolecular contacts between electron pair donors and one or both atoms of the dihalogen. This interaction was found to be accompanied by a lengthening of the halogen–halogen bond. By the late 1960s, several functional groups were found to serve as electron pair donors, while a variety of halogens, interhalogens, organohalogens, and others were found to act as electron acceptors. A comprehensive review by Bent in 1968 indicated that most of the gross structural features of electron donor–dihalogen complexes were well-described at this time [6]. Like a hydrogen bond, a halogen bond was recognized as being relatively strong (on the order of 40 kJ/mol) and highly directional. Bent also suggested that the halogen bonded complex was related to the transition state of the $S_N2$ reaction, going so far as to describe the complex as akin to the first step in a "Walden inversion".

Bent lists some 20 descriptive phrases used during the "first century" of halogen bonding that illustrate the struggle to understand the phenomenon. These include purely geometrical descriptions ("bumps-in-hollows", "pairs-in-pockets"), chemical descriptions ("exaltation of valency", "donor–acceptor interactions"), physical descriptions ("electron clutching", "charge-transfer interactions"), and descriptions arising from the emerging theory of quantum mechanics ("complex resonance", "filling of antibonding orbitals") [6]. Some of these terms are still common today, while others are obsolete and even amusing. Yet all of them necessitate an anisotropic distribution of electron density around the halogen atoms.

By the beginning of the "second century" of the halogen bond story it had become clear that quantum mechanical treatments would be required to provide a conceptual framework for eventual application of the interaction to practical problems. An important contribution was the early work by Flurry to develop a simple MO theory using the linear combination of atomic orbitals (LCAO) approach [7, 8]. This work provided a semiempirical method for predicting complex geometry, bond strengths, and spectroscopic features. Along with the collection of large quantities of experimental data, the refinement of theoretical models has been a hallmark of modern halogen bonding research.

## 1.2 Significance of Halogen Bonding with Dihalogens

Much of the current research into halogen bonding involves organohalogen or inorganic halide acceptors. However, the dihalogens ($X_2$) and interhalogens (XY) continue to attract attention. This review will focus specifically on structural and theoretical studies of such systems over the past decade. While polyhalide anions are closely related to the neutral donor–acceptor concepts that are the focus here, they will be discussed only when necessary to elaborate on the central theme of the review.

Spectroscopic studies of the $X_2$ and XY charge-transfer systems have provided fundamental insights into the nature of the interaction. The charge-transfer band of organoiodine halogen bonded complexes typically lies in the UV region and is obscured by other chromophores in the system [9]. These are readily observed, however, in complexes of the dihalogens. The C–X and halogen bond vibrations are also difficult to identify unambiguously in the organoiodines, and vibrational spectroscopy has not been commonly used in the study of such complexes [10]. This is not the case with $X_2$ and XY, where valuable structural information is readily obtained [11, 12]. Microwave studies of organohalogen complexes are also rare. Conversely, such studies are a powerful tool for examining gas phase bond energies and geometries of $X_2$ and XY complexes [13–15], and a chapter from A.C. Legon in this book specifically deals with this topic [16].

Halogen bonding is increasingly being discovered to play an important role in biochemical systems, particularly in thyroid biochemistry. While halogen bonding involving the halogenated thyroid enzymes is often the focus of studies in this area, the role of $I_2$ is also of interest [17, 18]. Closely related to this are investigations into the interaction of various antithyroid drugs with $I_2$ [19]. Recently, it has also been found that certain psychotropic drugs also affect thyroid function, with halogen bonding potentially playing a major role [20]. Interestingly, halogen bonding has also been used as a spectroscopic tool for the determination of drug concentrations in tablets and formulations [21–23].

Other applications involving $X_2$ and XY halogen bonding include dye-sensitized solar cells [24–26], batteries [27–29], membrane electrodes [30], and polymorph control [31]. Iodine has been used to evaluate the active electron donor sites in zeolites by monitoring changes in the visible absorption band [32]. Halogen bonding was even found to play an important role in the rheology and carbonization of coal tar pitch [33] and in the recovery of metals such as gold [34] and mercury [35]. In some cases, it is the complex itself that is of interest, while in others, the complex is an initial intermediate that instigates a chemical reaction. No matter what the process, a better understanding of halogen bond strength and structure is desirable.

# 2
# Crystal Structures

## 2.1
## General Observations

Structural results for N-donor Lewis base molecules (B) with dihalogens ($X_2$) and interhalogens (XY) began to appear with regularity in the late 1950s and 1960s with the extensive work of Hassel [36–42], Stromme [39–42], Romming [42, 45, 46], McCullough [47–51], and others [52–54]. Since then, a large number of such complexes have been studied. This interest has been driven in large part by research in two areas: the unusual electric properties imparted to materials when doped with dihalogens (particularly iodine) [55], and the study of dihalogen and interhalogen complexes with potential antithyroid drugs and related derivatives, including dithiole thiones [56–65], imidazole thiones [19, 66–73] and selones [68, 74–76], thiazole thiones [77] and selones [78–80], oxazole thiones [81], and various thiourea derivatives [77, 82]. Additional activity has involved the fundamental study of halogen bonding in particular classes of compounds, such as aromatic nitrogen heterocycles [31, 83–94, 96], thioethers [95–106], phosphines [107–118] and arsines [119–124], and phosphine sulfides [125–132] and selenides [133–136].

A recent study of halogen bond geometry based on 141 homo- and heteronuclear dihalogens provides a thorough investigation of the metric data for halogen bond geometry, and supports the generally recognized similarities between this interaction and hydrogen bonding [137]. In particular, the authors verify that halogen bonding in the solid state and for a wide assortment of interhalogens (XY) and Lewis bases (B) is essentially identical to that for gas phase complexes as reported earlier [138–142]. For the complexes studied, the following was found. (1) The mean B···X–Y bond angle is 176°, which is 11–38° more linear than the corresponding O–H···B hydrogen bonds. (2) The direction of the halogen bond is very close to the axis of the nonbonding electron pair for $sp^3$-hybridized N, P, and As, and $sp^2$-hybridized N bases. (3) For thio- and selenoethers and carbonyl bases, the halogen bond is quasi-perpendicular to the $R_1S(Se)R_2$ plane or to the plane bisector of the $R_1CR_2$ angle. But for thio- or selenoamides, the NCS(Se)···X torsion angle changes from ~0 or 180° to ~90° when bulky R groups crowd the S or Se lone pairs. (4) For $R_3P=S$ or $=Se$ bases, the chalcogen lone pairs of electrons are staggered relative to the substituents on P. (5) The lengthening of the X–Y bond obeys a bond order model [$n$(X–Y)+$n$(B···X) = 1]. (6) The Lewis acid strength ($Br_2 < I_2 < IBr < ICl$) is independent of the softness of the base. (7) The length of the B···X halogen bond and the elongation of the X–Y bond are significantly related to the donation strength of the Lewis base.

For the structural discussion of this report, a CCDC search [143] for compounds containing $X_2$ or XY molecules with intermolecular B···X (B = N, O, P, S, As, Se; X = Cl, Br, I; Y = Cl, Br, I)[1] distances less than the sum of their van der Waals radii was performed. Results which did not include atomic coordinates, or those reporting crystallographically disordered or otherwise structurally suspect results, were ignored. Ionic salts were included only if they also contained halogen bonded adducts, or served as interesting data points along the complex–ionic salt continuum. Metric data for the resulting 210 complexes are reported in Tables 1–3 for nitrogen and oxygen, phosphorus and sulfur, and arsenic and selenium, respectively.

Depending on a complex balance of the strength of the electron donor–halogen interaction, packing requirements resulting from the size and shape of the electron donor B, the presence, strength, and directionality of other attractive interactions, and the ability, particularly of iodine, but also to more limited extents of bromine and chlorine, to catenate through halogen–halogen donor–acceptor interactions, several different structural modes are observed.

Electron donors which interact at only one end of the $X_2$ or XY molecule form simple adducts (Fig. 1, mode *A*), often referred to as a "spoke" structure. The diiodine complex of tris(diethylamino)phosphine selenide (PAQKIB) [135] shown in Fig. 2a is an excellent example of this mode, as the Se···I distance at one end of the $I_2$ molecule is 2.715 Å, while at the other end there are no close contacts with any other atom.

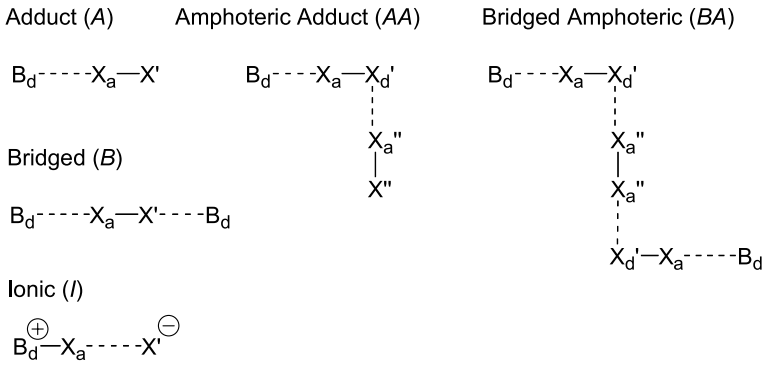


**Fig. 1** Dihalogen interaction modes

When B···X interactions occur at either end of the dihalogen, the electron acceptor molecule serves as a bridge (Fig. 1, mode *B*). This interaction more typically occurs with weaker electron donors, as a strong donor polarizes the dihalogen to the extent that the Lewis acidity of the second halogen atom is

[1] Despite a recent computational article suggesting that organofluorine compounds could participate in halogen bonding [190], to date no $F_2$ complexes have been observed in the solid state.

**Table 1** Geometric parameters for halogen bonded complexes with nitrogen and oxygen electron donors

| REFCODE | Compound name | $B_d \cdots X_a$ (Å)[a] | $X_a$–Y (Å) | $B_d \cdots X_a$–Y (°) | Mode |
|---|---|---|---|---|---|
| N···I–I | | | | | |
| CHXADI10 | 9-Cyclohexyladenine diiodine | 2.520 | 2.764 | 177.14 | *A* |
| GAWXEH | *N*-Iodine-2,3-diazabicyclo(2.2.2)oct-2-ene | 2.431 | 2.807 | 175.49 | *A* |
| HMCPZI | Hexamethylcyclotriphosphazene diiodine | 2.418 | 2.823 | 177.80 | *A* |
| HXMIOD | Hexamethylenetetramine bis(diiodine) | 2.497 | 2.791 | 173.92 | *A* |
| | | 2.498 | 2.771 | 173.85 | |
| NULBEB | 2,3-Bis(2′-pyridyl)quinoxaline diiodine | 2.530 | 2.759 | 173.80 | *A* |
| NULBIF | 4-Cyanopyridine diiodine | 2.543 | 2.745 | 175.47 | *A* |
| | | 2.554 | 2.750 | 175.50 | |
| NULBOL | 4,4′-Dipyridyl bis(diiodine) | 2.407 | 2.796 | 177.83 | *A* |
| NULCEC | 2,3,5,6-Tetrakis(2′-pyridyl)pyrazine bis(diiodine) | 2.563 | 2.750 | 173.02 | *A* |
| PICOLI | 4-Picoline diiodine | 2.322 | 2.823 | 175.51 | *A* |
| QIHBOY | 1,2-Bis(4-pyridyl)ethylene bis(diiodine) | 2.422 | 2.802 | 178.78 | *A* |
| TMEAMI | Trimethylamine diiodine | 2.271 | 2.830 | 178.33 | *A* |
| WEKGIC | (Triphenylphosphonio(trimethylsilyl)imino)diiodine | 2.432 | 2.833 | 178.93 | *A* |
| YUYNUB | 1,3,5,7-Tetraazatricyclo(3.3.1.1$^{3,7}$)decane tris(diiodide) | 2.593 | 2.746 | 177.58 | *A* |
| HMTNTI | Hexamethylenetetramine tri-iodo-nitrogen diiodine | 2.475 | 2.808 | 175.41 | *B* |
| | | 3.247 | | 178.10 | |
| HXMTDI | Hexamethylenetetramine diiodine | 2.439 | 2.830 | 173.07 | *B* |
| | | 3.482 | | 179.75 | |
| NULBUR | Quinoxaline diiodine | 2.949 | 2.724 | 178.77 | *B* |
| | | 2.918 | | 175.77 | |
| PHNAZI01 | Phenazine diiodine | 2.986 | 2.726 | 180.00 | *B* |
| | | 3.099 | | 180.00 | |
| QARGUL | Bis(9-chloroacridine) diiodine | 2.981 | 2.741 | 178.75 | *B* |

**Table 1** (continued)

| REFCODE | Compound Name | $B_d \cdots X_a$ (Å)[a] | $X_a$-Y (Å) | $B_d \cdots X_a$-Y (°) | Mode |
|---|---|---|---|---|---|
| VUKDIO | Pyrazine diiodine | 2.817 | 2.733 | 175.18 | *B* |
| VUKDOU | Tetramethylpyrazine diiodine | 3.086 | 2.718 | 177.45 | *B* |
| VUKDOU01 | Tetramethylpyrazine diiodine | 3.075 | 2.721 | 177.72 | *B* |
| CECZAL[b] | 2,2′-Bipyridine tris(diiodide) | 2.604 | 2.746 | 179.41 | *BA* |
| DARZAY[c] | 2,3,5,6-tetrakis(2-Pyridyl)pyrazine hexakis(diiodine) | 2.498 | 2.760 | 174.46 | *BA* |
| | | 2.568 | 2.755 | 168.30 | |
| QARGIZ[d] | bis(Acridine) tris(diiodine) | 2.440 | 2.813 | 175.08 | *BA* |
| QARGOF[e] | bis(9-Chloroacridine) tris(diiodine) | 2.613 | 2.754 | 179.21 | *BA* |
| | 2.619 | 2.749 | 176.94 | | |
| N···I–Br | | | | | |
| TAGNIZ | cis-*N*,*N*-bis(Bromoiodo)-2,2′-bipyridine | 2.461 | 2.577 | 175.84 | *A* |
| TASPEJ | 2,5-bis(2-Pyridiniumyl)-3,6-bis(2-pyridyl)pyrazine bis(iodobromide) | 2.405 | 2.595 | 175.14 | *A* |
| | | 2.410 | 2.588 | 173.99 | |
| N···I–Cl | | | | | |
| CLQUIC | 2-Chloroquinoline iodomonochloride | 2.432 | 2.446 | 179.93 | *A* |
| GANXAV | 3-Bromo-1-chloroiodopyridine | 2.344 | 2.473 | 178.43 | *A* |
| GANXOJ | 1-Chloroiodo-4-(dimethylamino)pyridine | 2.246 | 2.562 | 179.24 | *A* |
| PMTTIC | Pentamethylenetetrazole iodine monochloride | 2.347 | 2.437 | 176.11 | *A* |
| PYRIIC10 | Pyridine iodomonochloride | 2.290 | 2.510 | 178.72 | *A* |
| REWWUL | Triphenylphosphane(trimethylsilyl)imide iodochloride | 2.327 | 2.554 | 178.64 | *A* |
| TAGNEV | trans-*N*,*N*′-bis(Chloroiodo)-2,2′-bipyridine | 2.343 | 2.478 | 176.16 | *A* |
| | | 2.336 | 2.459 | 179.32 | |
| TAGNEV01 | *N*,*N*′-bis(Chloroiodo)-2,2′-bipyridine | 2.321 | 2.488 | 175.33 | *A* |
| | | 2.337 | 2.497 | 179.40 | |

**Table 1** (continued)

| REFCODE | Compound name | $B_d \cdots X_a$ (Å)[a] | $X_a$–Y (Å) | $B_d \cdots X_a$–Y (°) | Mode |
|---|---|---|---|---|---|
| TMEICL | Trimethylamine iodomonochloride | 2.303 | 2.524 | 176.88 | *A* |
| ZAVDAB | (Chloro-iodo)-trimethylsilyl-trimethylphosphoranimine | 2.228 | 2.651 | 177.39 | *A* |
| ZAVDEF | (Chloro-iodo)-*N*-chloro-triphenylphosphoranimine | 2.294 | 2.512 | 176.49 | *A* |
| N···Br–Br | | | | | |
| ICUGES | *N*-Bromo-*N*-(bromine)-triphenylphosphineimine | 2.245 | 2.484 | 177.24 | *A* |
| TEYPES | 1,3-Bis(dibromo)-*s*-triazine | 2.515 | 2.338 | 174.94 | *A* |
| ACTNBM | Bis(acetonitrile) dibromine | 2.837 | 2.327 | 179.40 | *B* |
| O···I–I | | | | | |
| ATICEL | *catena*-(Dodecakis(m3-formato-O,O,O′)-hexamanganese diiodine clathrate) | 2.827 | 2.687<br>2.643 | 174.49<br>174.58 | *A* |
| CDEXTI10 | Cyclohexaamylose-iodine tetrahydrate | 3.070<br>3.315 | 2.677 | 167.21<br>167.46 | *B* |
| QOJKEF | 1,4-Dioxane diiodine | 2.808 | 2.693 | 178.74 | *B* |
| VAMDOD | *catena*-(Bis($\mu_2$-isonicotinato)-copper diiodide) | 2.947 | 2.692 | 174.23 | *B* |
| O···Br–Br | | | | | |
| ACETBR | Acetone dibromine | 2.818 | 2.282 | 178.36 | *B* |
| DOXABR | 1,4-Dioxane dibromine | 2.723 | 2.303 | 178.34 | *B* |
| METHOB | Bis(methanol) bromine complex | 2.705<br>2.907<br>2.676<br>2.826 | 2.324<br><br>2.252<br> | 179.10<br>175.09<br>178.06<br>173.75 | *B* |

**Table 1** (continued)

| REFCODE | Compound name | $B_d \cdots X_a$ (Å)[a] | $X_a$–Y (Å) | $B_d \cdots X_a$–Y (°) | Mode |
|---|---|---|---|---|---|
| O$\cdots$Cl–Cl | | | | | |
| ULISAJ | 1,4-Dioxane dichlorine | 2.647 | 2.025 | 178.08 | *B* |

[a]$B_d$ represents the electron donor; $X_a$ represents the electron acceptor

| REFCODE | $X'_d$–$X''_a$ (Å) | $X''_a$–X″ (Å) | $X_a$–$X'_s \cdots X''_d$ (°) | $X'_s \cdots X''_a$–X″ (°) |
|---|---|---|---|---|
| [b]CECZAL | 3.550 | 2.711 | 83.04 | 175.54 |
| [c]DARZAY | 3.530 | 2.730 | 97.17 | 173.21 |
| | 3.379 | 2.730 | 106.83 | 178.09 |
| [d]QARGIZ | 3.475 | 2.731 | 80.82 | 177.15 |
| [e]QARGOF | 3.876 | 2.719 | 85.47 | 176.07 |
| | 3.595 | | 100.91 | 175.20 |

**Table 2** Geometric parameters for halogen bonded complexes with phosphorus and sulfur electron donors

| P···I–I<br>REFCODE | Compound name | $B_d \cdots X_a$ (Å)[a] | $X_a$–Y (Å) | $B_d \cdots X_a$–Y (°) | Mode |
|---|---|---|---|---|---|
| REFCODE | Compound name | $B_d \cdots X_a$ (Å)[a] | $X_a$–Y (Å) | $B_d \cdots X_a$–Y (°) | Mode |
| CENYEA | 1,2-Bis((di-iodo)diphenylphosphino) ethane | 2.471 | 3.148 | 177.34 | *A* |
| JITSIO | Triphenylphosphine diiodine | 2.480 | 3.161 | 178.23 | *A* |
| QAMZAF | (2-Methyl-1,2-dicarba-*closo*-dodecaboranyl)-bis(isopropyl)-(diiodine)phosphane | 2.598 | 3.021 | 177.50 | *A* |
| ECISIT | 1-Diphenylphosphino-2-methyl-1,2-dicarbadodecaborane(10) hemikis(iodine) | 3.334 | 2.775 | 173.81 | *B* |
| REFCODE | Compound name | $B_{d^-} - X^+$ (Å) | $X^+ \cdots X^-$ (Å) | $B_d$-$X^+ \cdots X^-$ (°) | Mode |
| FILTEZ | Bis(triphenylphosphine-iodo)-triiodine triiodide | 2.399 | 3.507 | 177.39 | *I* |
| FILTID | (Triphenylphosphine-iodo)-triiodine | 2.394 | 3.551 | 156.79 | *I* |
| LOBKOC | (Tetraiodo)-triphenylphosphite | 2.367 | 3.389 | 170.28 | *I* |
| LOBKUI | 1,8-Bis(tri-*p*-tolylphosphito)octaiodide | 2.361 | 3.345 | 170.77 | *I* |
| LOBLAP | (Tetraiodo)-tris(2,4-di-*t*-butylphenyl)phosphate | 2.390 | 3.227 | 170.80 | *I* |
| SORPUK | Tris(2,4,6-trimethoxyphenyl)(diiodine)phosphine dichloromethane solvate | 2.483 | 3.340 | 174.50 | *I* |
| ZEKMOR | Dimethylphenyl(diiodo)phosphorus | 2.410 | 3.408 | 177.01 | *I* |
| P···I–Br | | | | | |
| PESJOM | Triphenylphosphine iodinebromide | 2.461 | 3.062 | 178.06 | *I* |
| P···Br–Br | | | | | |
| JOMSEJ | Triphenylphosphine dibromine | 2.181 | 3.123 | 177.15 | *I* |
| SUHJIO | Bromo-triphenylphosphonium tribromide | 2.144 | 3.492 | 151.54 | *I* |
| | | 2.134 | 3.549 | 153.89 | |

**Table 2** (continued)

| S···I–I REFCODE | Compound name | $B_d \cdots X_a$ (Å) | $X_a$–Y (Å) | $B_d \cdots X_a$–Y (°) | Mode |
|---|---|---|---|---|---|
| BENZSI | Benzyl sulfide-iodine | 2.779 | 2.819 | 178.93 | *A* |
| BIMMEP | 4,4-Bis(methylsulfanyl)-1,3-dithiole-2-thione-diiodine | 2.716 | 2.808 | 177.45 | *A* |
| BZHTIC10 | 1,5-Diphenylthiocarbazone diiodine | 2.663 | 2.917 | 178.49 | *A* |
| DAXXIK | Bis(benzimidazole-2-thione)iodonium (benzimidazole-2-thione-diiodine) triiodide | 2.670 | 2.887 | 178.34 | *A* |
| DAXXOQ | *N*-Methylbenzothiazole-2-thione-diiodine | 2.808 | 2.791 | 176.95 | *A* |
| DAYBOU | 1,3-Dithiacyclohexane-2-thione-diiodine | 2.755 | 2.812 | 175.41 | *A* |
| DAYCIP | 4,5-Ethylenedithio-1,3-dithiole-2-thione-diiodine | 2.805 | 2.812 | 175.44 | *A* |
| DTHINI | 1,4-Dithiane bis(iodine) | 178.49 | 2.789 | 177.89 | *A* |
| FAJPUB | Dithia(3.3.1)propellane bis(iodine) | 2.825 | 2.797 | 176.71 | *A* |
| | | 2.806 | 2.796 | 176.08 | |
| FAJRAJ | Dithia(3.3.2)propellane bis(iodine) | 2.803 | 2.794 | 173.00 | *A* |
| | | 2.901 | 2.767 | 176.97 | |
| FOJPIE | Diferrocenyl(phenyl)(diiodosulfido)phosphine | 2.761 | 2.823 | 176.31 | *A* |
| GEGNUB | 1,3-Dimethyl-2-thioimidazolium diiodine | 2.616 | 2.967 | 175.08 | *A* |
| GEGNUB01 | 1,3-Dimethyl-2-thioimidazolium diiodine | 2.607 | 2.984 | 177.11 | *A* |
| GIDYOH | Bis(1,3-diethylimidazolidine-2-thione-4,5-dithionato)-palladium diiodine chloroform solvate | 2.874 | 2.811 | 179.61 | *A* |
| GIGLOX | *N*,*N*′-Bis(morpholino)-dithio-oxadiamide bis(diiodine) | 2.920 | 2.751 | 175.53 | *A* |
| | | 2.789 | 2.805 | 174.73 | |
| | | 2.801 | 2.787 | 176.50 | |
| | | 2.892 | 2.738 | 173.89 | |

**Table 2** (continued)

| | | | | | |
|---|---|---|---|---|---|
| HAFLAC | (6-Propylthiouracil)-diiodine | 2.780 | 2.826 | 175.85 | *A* |
| HAFLEG | (5-Chloro-2-mercaptobenzothiazole)-diiodine | 2.634 | 2.920 | 173.78 | *A* |
| HEMDIM | Bis(($\mu^2$-diiodosulfido-*S*,*S*)-($\eta^5$-cyclopentadienyl)-*t*-butylimino-molybdenum) | 2.720 | 2.853 | 175.24 | *A* |
| HIZLOR | *N*-(2-Diiodomercapto-2-methylpropyl)-*N*′-(2-mercapto-2-methylpropyl)-1,5-diazacyclooctane-nickel(II) | 2.602 | 3.026 | 176.91 | *A* |
| HOJLOH | *S*-Diiodo-hexamethylthiophosphoramide | 2.704 | 2.704 | 177.99 | *A* |
| ISBCLS | 1,4-Dithiane trichloro-antimony iodine | 2.717 | 2.818 | 178.63 | *A* |
| KUWDEL | 5,5-Dimethylimidazolidine-2,4-dithione diiodine | 2.748 | 2.817 | 176.88 | *A* |
| KUWDIP | 5,5-Dimethylimidazolidine-2,4-dithione bis(diiodine) | 2.843 | 2.767 | 173.74 | *A* |
| | | 2.738 | 2.849 | 177.94 | |
| KUWDOV | 5,5-Dimethyl-2-thioxoimidazolidin-4-one diiodine | 2.773 | 2.802 | 176.14 | *A* |
| LOPQIQ | 1,3-Bis(thiourea)triiodonium thiourea-diiodine diiodine triiodide | 2.507 | 3.056 | 173.69 | *A* |
| MURQEV | (*Z*)-2-Chloro-3,3-diphenyl-3-thioxo-1-(2,4,6-tri-*t*-butylphenyl)-1,3-diphosphapropene *S*-diiodine | 2.809 | 2.812 | 174.91 | *A* |
| NENRON | Bis(bis(diphenylthiophosphinoyl)methane) tris(diiodine) | 2.823 | 2.801 | 176.39 | *A* |
| NENRUT | 1,2-Bis(diphenylthiophosphinoyl)ethane bis(diiodine) | 2.872 | 2.772 | 177.78 | *A* |
| NICSIB | 1,4,7,10,13,16-Hexathiacyclooctadecane tris(diiodine) | 2.747 | 2.825 | 177.56 | *A* |
| NIGHUG | *S*,*S*′-Bis(diiodo)-2,11-dithia(3.3)paracyclophane | 2.796 | 2.799 | 176.68 | *A* |
| | | 2.812 | 2.803 | 175.63 | |
| NOFKOI | Triphenylphosphinesulfide diiodide | 2.753 | 2.823 | 175.51 | *A* |
| OHORUY | (1,3-Dithiole-2-diiodothione-4-yl)ferrocenium pentaiodide | 2.705 | 2.857 | 176.33 | *A* |
| PEJKIY | 1,3-Dithiolan-2-thione-diiodine | 2.715 | 2.823 | 176.47 | *A* |
| PELXUZ | Tetrakis($\mu^2$-diiodo)-bis(1,4,7-trithiacyclononane) | 2.760 | 2.816 | 174.86 | *A* |
| | | 2.870 | 2.785 | 178.36 | |
| | | 2.862 | 2.799 | 177.28 | |

**Table 2** (continued)

| | | | | | |
|---|---|---|---|---|---|
| PELXUZ01 | Tetrakis($\mu_2$-diiodo)-bis(1,4,7-trithiacyclononane) | 2.792 | 2.818 | 174.83 | *A* |
| | | 2.886 | 2.781 | 178.19 | |
| | | 2.878 | 2.792 | 177.54 | |
| PIGXUY | 1,3-Dithiole-2-thione diiodine | 2.715 | 2.843 | 176.71 | *A* |
| PUSREA | 1,4,7-Tris(iodine)-1,4,7,10,13-pentathiacyclopentadecane iodine | 2.885 | 2.765 | 171.13 | *A* |
| | | 2.796 | 2.798 | 178.39 | |
| | | 2.840 | 2.674 | 172.90 | |
| | | 2.828 | 2.779 | 178.82 | |
| PUSROK | 1,4,10,13-Tetrakis(iodine)-1,4,7,10,13,16-hexathiacyclooctadecane | 2.792 | 2.787 | 174.95 | *A* |
| PUSSAX | 1,4,7,13,16,19-Hexakis(iodine)-1,4,7,10,13,16,19,22-octathiatetracosane | 2.815 | 2.807 | 177.42 | *A* |
| | | 2.822 | 2.794 | 170.17 | |
| | | 2.741 | 2.787 | 177.23 | |
| PYITCC | Tetrapyridine-bis(diiodothiocyanato)-cobalt(II) | 2.797 | 2.804 | 178.83 | *A* |
| REBZON | 1,2,4,5-Tetrakis(isopropylthio)benzene tris(diiodine) | 3.025 | 2.745 | 178.36 | *A* |
| REMSAD | 1,4,8,11-Tetrakis(diiodine)-1,4,8,11-tetrathiacyclotetradecane | 2.803 | 2.789 | 177.71 | *A* |
| | | 2.881 | 2.757 | 172.50 | |
| RUKKEN | *S*-Diiodo-1,4,8,11-tetrathiacyclotetradecane | 2.859 | 2.810 | 178.57 | *A* |
| RUKEN01 | 1,5,8,12-Tetrathiacyclotetradecane diiodine | 2.876 | 2.808 | 178.50 | *A* |
| RUKKIR | 1,8-Bis(diiodo)-1,4,8,11-tetrathiacyclotetradecane | 2.800 | 2.821 | 177.58 | *A* |
| | | 2.841 | 2.808 | 177.86 | |
| RUKKUD | 1,5,9,13-Tetrakis(diiodo)-1,5,9,13-tetrathiacyclohexadecane | 2.756 | 2.811 | 174.74 | *A* |
| | | 2.848 | 2.792 | 171.71 | |
| SUTTIK | Bis(iodo-(1,4,7,10,13-tetrathiacyclopentadecane)-silver(I)) bis(diiodide) tris(diiodine) | 3.130 | 2.755 | 175.87 | *A* |
| | | 2.986 | 2.770 | 173.29 | |
| | | 3.057 | 2.756 | 168.39 | |
| | | 3.497 | 2.760 | 168.50 | |

**Table 2** (continued)

| | | | | | |
|---|---|---|---|---|---|
| TCAPLI | *N*-Methyl-thiocaprolactam-iodine complex | 2.687 | 2.879 | 176.23 | *A* |
| TOTWUU | 1,1′-Methylenebis(*S*-iodine-3-methyl-4-imidazoline-2-thione) | 2.683 | 2.897 | 175.71 | *A* |
| TOTXAB | 1,1′-Ethylenebis(*S*-iodine-3-methyl-4-imidazoline-2-thione) | 2.642 | 2.903 | 177.05 | *A* |
| UJEVOU | Dimethyl 2-thioxo-1,3-dithiole-4,5-dicarboxylate-*S*-diiodine | 2.912 | 2.790 | 177.93 | *A* |
| VARCIA10 | 1,3,6,7-Tetrathiapentalene-2,5-dione iodine | 2.711 | 2.832 | 176.63 | *A* |
| VARCIA11 | 1,3,6,7-Tetrathiapentalene-2,5-bisthione diiodine | 2.697 | 2.866 | 178.02 | *A* |
| VEBCEK | 4,5,6,7-Tetrathiocino(1,2-b : 3,4-b′)diimidazolyl-1,3,8,10-tetraethyl-2,9-dithione bis(diiodine) | 2.774 | 2.822 | 174.82 | *A* |
| VUTPEF | Bis(1,10-bis(diiodo)-4,7,13,16-tetraoxa-1,10-dithiacyclooctadecane) diiodine | 2.762<br>2.848 | 2.810<br>2.774 | 178.04<br>173.46 | *A* |
| XOVRIJ | Benzothiazole-2-thione-(diiodine) | 2.729 | 3.077 | 174.19 | *A* |
| YESHAF | *N*,*N*′-Dimethylperhydro-1,4-diazepine-2,3-dithione *S*,*S*′-bis(diiodine) | 2.583 | 2.964 | 175.11 | *A* |
| YEWPAR | 1,3-Diisopropyl-4,5-dimethylimidazolium-dithiocarboxylate diiodide | 2.880 | 2.772 | 173.49 | *A* |
| YANLEF | 1,4,7-Trithiacyclononane tris(diiodine) | 2.786 | 2.818 | 175.07 | *A* |
| ZARDOL | 4,5,6,7-Tetrathiocino(1,2-b : 3,4-b′)diimidazolyl-1,3,8,10-tetra-*n*-butyl-2,9-dithione-bis(diiodine) | 2.783 | 2.840 | 175.30 | *A* |
| LINHEV | 1,4,7,10-Tetrathiacyclododecane diiodide | 3.220 | 2.736 | 170.54 | *B* |
| MSNROD | 5-(2-Methylmercapto-4-methyl-4,5-dihydro-1′,3′,4′-thiadiazol-5-ylidene)-3-ethyl-rhodanine-iodine | 3.099 | 2.751 | 178.46 | *B* |
| MUJBIC | Tris(dimethyldithiocarbamato)-cobalt(III) bis(diiodine) | 3.148<br>3.144 | 2.754<br>2.778 | 175.70<br>175.42 | *B* |
| NENRON | Bis(bis(diphenylthiophosphinoyl)methane) tris(diiodine) | 3.204 | 2.740 | 175.50 | *B* |
| NICSIB | 1,4,7,10,13,16-Hexathiacyclooctadecane tris(diiodine) | 3.123 | 2.773 | 170.26 | *B* |

**Table 2** (continued)

| | | | | | |
|---|---|---|---|---|---|
| OBIWOM | Bis(1-methyl-3-isopropylimidazolidine-2,4,5-trithione-*S*,*S*′)-nickel diiodine | 3.098 | 2.790 | 176.28 | *B* |
| PELXUZ | Tetrakis($\mu^2$-diiodo)-bis(1,4,7-trithiacyclononane) | 3.239<br>3.055 | 2.754 | 176.18<br>168.39 | *B* |
| PELXUZ01 | Tetrakis($\mu_2$-diiodo)-bis(1,4,7-trithiacyclononane) | 3.197<br>3.089 | 2.755 | 176.14<br>168.86 | *B* |
| PUSRIE | 1,4,7,10,13,16-Hexathiacyclooctadecane iodine | 3.099 | 2.788 | 178.68 | *B* |
| PUSRUQ | 1,4,7,10,13,16,19,22-Octathiacyclotetracosane iodine | 3.213 | 2.757 | 172.66 | *B* |
| REBZON | 1,2,4,5-Tetrakis(isopropylthio)benzene tris(diiodine) | 3.149 | 2.761 | 173.29 | *B* |
| ROHXAN | *cis*-Bis(*N*,*N*-diethyldithiocarbamato)-dicarbonyl-ruthenium(II) iodine | 3.177 | 2.745 | 172.34 | *B* |
| RUKKAJ | *catena*-(($\mu^2$-Diiodine)-1,4,7,10-tetrathiacyclododecane) | 3.148<br>3.174<br>3.203 | 2.755<br><br>2.750 | 170.27<br>175.00<br>164.99 | *B* |
| RUKKOX | *catena*(9-Diiodine-1,2-bis(1,5,9,13-tetrathiacyclo-hexadecane)-diiodine) | 3.115 | 2.774 | 173.01 | *B* |
| RUQPIC | *catena*(($\mu^2$-Diiodo)-1,3,5-trithiacyclohexane) | 3.169 | 2.754 | 169.03 | *B* |
| RUQPIC01 | 1,3,5-Trithiacyclohexane (diiodine) | 3.147 | 2.760 | 168.59 | *B* |
| TOTSEA | Bis(tetra-*n*-butylammonium) bis(2-dicyanomethylene-4,5-disulfanylcyclopent-4-ene-1,3-dionate)-palladium iodine | 3.169 | 2.735 | 171.23 | *B* |
| CEWMIA[b] | 2-Imidazolidinethione bis(diiodine) | 2.487 | 3.148 | 177.90 | *AA* |
| HAMCAA[c] | 4,5-Bis(bromomethyl)-1,3-dithole-2-thione-diiodine diiodine | 2.562 | 2.963 | 173.94 | *AA* |
| VUTPEF[d] | Bis(1,10-bis(diiodo)-4,7,13,16-tetraoxa-1,10-dithiacyclooctadecane) diiodine | 2.653<br>2.774 | 2.902<br>2.821 | 175.97<br>175.26 | *AA* |
| ZEBQOM[e] | 2-(3*H*)-(Diiodothio)benzoxazole diiodine | 2.873<br>3.298 | 2.769 | 178.44<br>169.79 | *AA* |

**Table 2** (continued)

| | | | | | |
|---|---|---|---|---|---|
| BAQTOC[f] | Triphenylphosphine sulfide tris(diiodine) | 2.591 | 2.982 | 178.11 | *BA* |
| CEWMOG[g] | Bis(2-imidazolidinethione) tris(diiodine) | 2.580 | 2.984 | 177.67 | *BA* |
| ICUXAG[h] | 2-Thioxo-1,3-dithiole-4-carboxylic acid-*S*-diiodine hemikis(diiodine) | 2.733 | 2.819 | 175.72 | *BA* |
| LOPQEM[i] | Bis(thiourea-diiodine) diiodine | 2.503 | 3.054 | 176.04 | *BA* |
| TPHPSI10[j] | Bis(*S*-iodine-triphenylphosphinesulfide) iodine | 2.729 | 2.837 | 175.24 | *BA* |
| TURMEY[k] | Bis(1,3-diisopropylimidazolidine-2,4,5-trithionato)-nickel(II) diiodine | 2.824 | 2.815 | 177.48 | *BA* |
| TURMIC[l] | Diiodo-bis(1,3-diisopropylimidazolidine-2,4,5-trithionato)-nickel(II) bis(1,3-diisopropylimidazolidine-2,4,5-trithionato)-nickel(II) diiodine | 2.849 | 2.790 | 178.78 | *BA* |
| XOVREF[m] | Bis(benzimidazole-2-thione-(diiodine)) diiodine dihydrate | 2.572 | 2.989 | 176.76 | *BA* |
| XOVROP[n] | Benzothiazole-2-thione-(diiodine) diiodine | 2.588 | 2.969 | 177.79 | *BA* |
| REFCODE | Compound name | $B_d$-$X^+$ (Å) | $X^+ \cdots X^-$ (Å) | $B_d$-$X^+ \cdots X^-$ (°) | Mode |
| LOPQIQ | 1,3-Bis(thiourea)triiodonium thiourea-diiodine diiodine triiodide | 2.437 | 3.168 | 171.59 | *I* |
| | | 2.466 | 3.145 | 176.08 | |
| S···I–Br | | | | | |
| REFCODE | Compound name | $B_d \cdots X_a$ (Å) | $X_a$–Y (Å) | $B_d \cdots X_a$–Y (°) | Mode |
| BIBQUY | 1,4,8,11-Tetrathiacyclotetradecane bis(iodobromide) | 2.679 | 2.654 | 175.52 | *A* |
| BIBSIO | 1,5,9,13-Tetrathiacyclohexadecane tetrakis(iodobromide) | 2.617 | 2.705 | 177.64 | *A* |
| | | 2.687 | 2.645 | 177.59 | |
| BIBSOU | (1,4,7,10,13,16-Hexathiacyclooctadecane) bis(iodobromide) | 2.620 | 2.694 | 174.95 | *A* |
| BIMNUG | 4,5,-Bis(methylsulfanyl)-1,3-dithiole-2-thione-iodine monobromide | 2.589 | 2.714 | 175.62 | *A* |
| DTHIBR10 | 1,4-Dithiane bis(iodine monobromide) | 2.687 | 2.646 | 178.16 | *A* |
| HAMCEE | 4,5-Bis(bromomethyl)-1,3-dithiole-2-thione-bromoiodine | 2.597 | 2.747 | 178.13 | *A* |
| | | 2.564 | 2.765 | 176.13 | |

**Table 2** (continued)

| | | | | | |
|---|---|---|---|---|---|
| IPOGUP | 4,5-Bis(2-cyanoethanesulfanyl)-1,3-dithiole-2-bromiodothione | 2.605<br>2.607 | 2.709<br>2.706 | 177.24<br>177.71 | *A* |
| JADYAP | (*N*,*N*′-Dimethylperhydrodiazepine-2,3-dithione)-(iodobromide-*S*) | 2.574 | 2.752 | 175.90 | *A* |
| LOSWEV | Dimethyl 1,3,-dithiole-2-(bromoiodo)thione-4,5-dicarboxylate iodomonobromide | 2.605 | 2.711 | 178.01 | *A* |
| NAHQOD | Dibenzylthio iodine bromide | 2.616 | 2.690 | 174.80 | *A* |
| QAQTAE | *S*-(Bromoiodo)-*N*,*N*′-dimethylbenzimidazole-2(3*H*)-thione | 2.607 | 2.751 | 173.28 | *A* |
| ZZZHUE01 | Bromoiodo-triphenylphosphine sulfide | 2.665 | 2.668 | 175.08 | *A* |
| ZZZHUE02 | Bromoiodo-triphenylphosphine sulfide | 2.656 | 2.683 | 175.13 | *A* |
| S···I–Cl | | | | | |
| ICUWUZ | Dimethyl 2-thioxo-1,3-dithiole-4,5-dicarboxylate-*S*-iodine chloride | 2.591 | 2.603 | 176.11 | *A* |
| LIFXIH | *N*-Methylbenzothiazole-2(3*H*)-thione iodine chloride | 2.556 | 2.604 | 179.89 | *A* |
| NAHQIX | Dibenzylthio iodine chloride | 2.575 | 2.558 | 176.14 | *A* |
| SIBJOC | Chloroiodo-triphenylphosphine sulfide | 2.641 | 2.586 | 174.86 | *A* |
| HAMCII[o] | 4,5-Bis(bromomethyl)-1,3-dithiole-2-thione-chloroiodine hemikis(diiodine) | 2.534 | 2.761 | 176.57 | *BA* |
| S···Br–Br | | | | | |
| RORNIV | Dimethylsulfide-dibromide | 2.299 | 2.717 | 175.05 | *A* |
| RORNIV01 | Dibromo-dimethyl sulfide | 2.328 | 2.705 | 176.05 | *A* |
| TEBKIU | 1,2,4,5-Tetrakis(ethylthio)benzene bis(dibromine) | 2.808<br>3.239 | 2.408 | 171.54<br>164.45 | *B* |
| REFCODE | Compound name | $B_d$-$X^+$ (Å) | $X^+ \cdots X^-$ (Å) | $B_d$-$X^+ \cdots X^-$ (°) | Mode |
| BEMLIO | 5-Bromosulfenyl-1,3,2,4-dithiadiazolium tribromide | 2.206 | 3.204 | 174.53 | *I* |
| FIMDOU | Bromodimethyl sulfide bromide tetrabromodiide | 2.260 | 2.969 | 178.67 | *I* |

**Table 2** (continued)

| | | | | | |
|---|---|---|---|---|---|
| YESGUY | 1,3-Diisopropyl-4,5-dimethylimidazolium-2-bromodithiocarboxylate tribromide | 2.167 | 3.217 | 155.59 | *I* |

[a] $B_d$ represents the electron donor; $X_a$ represents the electron acceptor

| REFCODE | $X'_d$–$X''_a$ (Å) | $X''_a$–$X''$ (Å) | $X_a$–$X'_s \cdots X''_d$ (°) | $X'_s \cdots X''_a$–$X''$ (°) |
|---|---|---|---|---|
| [b]CEWMIA | 3.003 | 2.849 | 92.42 | 177.13 |
| [c]HAMCAA | 3.270 | 2.747 | 81.70 | 175.53 |
| [d]VUTPEF | 3.403 | 2.736 | 80.44 | 176.13 |
| | 3.550 | | 79.03 | |
| [e]ZEBQOM | 3.453 | 2.729 | 88.39 | 178.44 |
| [f]BAQTOC | 3.373 | 2.744 | 93.02 | 175.35 |
| | 3.561 | 2.710 | 86.30 | 178.53 |
| | 3.503 | | 82.75 | 177.27 |
| | 3.582 | | 86.06 | 171.24 |
| [g]CEWMOG | 3.475 | 2.760 | 85.12 | 177.70 |
| [h]ICUXAG | 3.441 | 2.725 | 80.90 | 175.50 |
| [i]LOPQEM | 3.407 | 2.754 | 84.64 | 175.20 |
| [j]TPHPSI10 | 3.570 | 2.757 | 96.30 | 176.67 |
| [k]TURMEY | 3.213 | 2.755 | 93.68 | 168.98 |
| [l]TURMIC | 3.671 | 2.786 | 86.56 | 176.24 |
| | | | 102.09 | 175.75 |
| [m]XOVREF | 3.399 | 2.767 | 88.74 | 176.02 |
| [n]XOVROP | 3.423 | 2.750 | 102.71 | 174.04 |
| | 3.445 | | 78.46 | 172.26 |
| [o]HAMCII | 3.257 | 2.708 | 84.67 | 174.57 |

**Table 3** Geometric parameters for halogen bonded complexes with arsenic and selenium electron donors

| As···I–I<br>REFCODE | Compound name | $B_d \cdots X_a$ (Å)[a] | $X_a$–Y (Å) | $B_d \cdots X_a$–Y (°) | Mode |
|---|---|---|---|---|---|
| FESKAP | Diiodo-triphenylarsane | 2.641 | 3.004 | 174.81 | *A* |
| FESKAP01 | (Triphenylarsine)-diiodine | 2.653 | 3.005 | 174.32 | *A* |
| FESKAP02 | (Triphenylarsine)-diiodine | 2.615 | 3.013 | 180 | *A* |
| FESKAP10 | (Triphenylarsine)-diiodine | 2.641 | 3.005 | 174.79 | *A* |
| FUTTAP | (Triphenylarsine)-diiodine toluene solvate | 2.638 | 3.002 | 180 | *A* |
| ZODJOR | Diiodo-trimethyl-arsenic | 2.271 | 3.392 | 180 | *B* |
| As···I–Br | | | | | |
| CUXCON | (Iodobromo)-triphenyl-arsenic(III) | 2.590 | 2.855 | 174.78 | *A* |
| As···Br–Br | | | | | |
| REFCODE | Compound name | $B_a \cdots X_d$ (Å) | $X_d$–Y (Å) | $B_a \cdots X_d$–Y (°) | Mode |
| TMASBR01 | Dibromo-trimethyl-arsenic | 2.275 | 3.363 | 180 | *I* |
| Se···I–I | | | | | |
| REFCODE | Compound name | $B_d \cdots X_a$ (Å) | $X_a$–Y (Å) | $B_d \cdots X_a$–Y (°) | Mode |
| DSEIOD | 1,4-Diselenane bis(iodine) | 2.830 | 2.870 | 178.67 | *A* |
| EZOXUM | Bis(tri-*t*-butylphosphine)-bis(diiodo)-diselenium<br>(m2-iodo)-bis(tri-*t*-butylphosphine)-diselenium triiodide | 2.760 | 2.914 | 171.69 | *A* |
| GIHZIG | Diphenyldiselenide iodine | 2.992 | 2.774 | 174.21 | *A* |
| HECMOR | Di-*t*-butyliodophosphane selenidediiodine | 2.782 | 2.878 | 175.84 | *A* |
| KUWDUB | 5,5-Dimethyl-2-selenoimidazolidine-4-one diiodine | 2.699 | 2.962 | 170.73 | *A* |
| OXSELI | 1,4-Oxaselenane iodine | 2.755 | 2.955 | 174.77 | *A* |
| PAQKAT | Triphenylphosphineselenido-diiodine | 2.802 | 2.881 | 173.67 | *A* |
| PAQKEX | (Tris(dimethylamino)phosphine)selenide-diiodide | 2.721<br>2.711 | 2.965<br>2.960 | 176.78<br>177.35 | *A* |

**Table 3** (continued)

| | | | | | |
|---|---|---|---|---|---|
| PAQKIB | (Tris(diethylamino)phosphine)selenido-diiodide | 2.715 | 2.985 | 178.05 | *A* |
| PELHUK | 6-Propyl-2-(diiodoseleno)uracil | 2.781 | 2.893 | 176.75 | *A* |
| REBNER | Bis(*N*,*N*′-dimethylimidazolidin-2-yl)-di-selenone bis(triiodide) *N*,*N*-dimethylimidazolidine-2-selone iodine | 2.683 | 3.025 | 175.52 | *A* |
| RIZMES | Dimethyl-selenium diiodine | 2.768 | 2.915 | 174.31 | *A* |
| RUQPOI | 1,3,5-Triselenacyclohexane diiodine | 2.734 | 2.944 | 179.31 | *A* |
| THSEL01 | Tetrahydroselenophene iodine | 2.765 | 2.913 | 179.06 | *A* |
| YEYFEN | (*N*-Methyl-1,3-thiazolidine-2(3*H*)-selenone)-diiodine | 2.725 | 2.983 | 173.27 | *A* |
| ZOBDOJ | 1,1′-Bis(3-methyl-4-imidazolin-2-selenone)methane bis(diiodine) | 2.716<br>2.776 | 2.996<br>2.912 | 175.63<br>176.86 | *A* |
| KIGFEL | Bis(2,4,6-triisopropylphenyl) diselenide diiodide | 3.483 | 2.722 | 169.18 | *B* |

| REFCODE | Compound name | $B_d \cdots X_a$ (Å) | $X_a$–Y (Å) | $B_d \cdots X_a$–Y (°) | Mode |
|---|---|---|---|---|---|
| RIJQAC[b] | (Tris(dimethylamino)phosphaneselenide)iodine(I) triiodide | 2.596 | 3.215 | 174.78 | *AA* |
| RIJQEG[c] | (Tris(*N*-morpholyl)phosphane-selenide)iodine(I) triiodide di-iodine | 2.590 | 3.186 | 172.01 | *AA*<br>*BA* |
| YEYFOX[d] | | 2.639 | 3.071 | 176.66 | *AA* |
| | | 2.639 | 3.071 | 176.66 | *BA* |
| | | 2.662 | 3.059 | 178.84 | *BA* |
| | | 2.662 | 3.059 | 178.84 | *BA* |
| | | 2.720 | 2.960 | 171.52 | *BA* |

Se· · · I–Br

| REFCODE | Compound name | $B_d \cdots X_a$ (Å) | $X_a$–Y (Å) | $B_d \cdots X_a$–Y (°) | Mode |
|---|---|---|---|---|---|
| NOWLOA | Se,Se-Diphenylselenium bromoiodide | 2.808 | 2.641 | 177.29 | *A* |
| NOWLUG | Se,Se-Dimethylselenium bromoiodide | 2.664 | 2.797 | 175.82 | *A* |
| WIPPAM | Se-(Bromoiodo)-*N*-methylbenzothiazole-2-selone | 2.636 | 2.813 | 177.10 | *A* |

**Table 3** (continued)

| REFCODE | Compound name | $B_d \cdots X_a$ (Å) | $X_a$–Y (Å) | $B_d \cdots X_a$–Y (°) | Mode |
|---|---|---|---|---|---|
| YEYFUD[e] Se$\cdots$I–Cl | *N*-Methylbenzothiazole-2(3*H*)-selenone-iodine dibromoiodide | 2.564 | 3.129 | 174.31 | *AA* |
| REFCODE | Compound name | $B_d \cdots X_a$ (Å) | $X_a$–Y (Å) | $B_d \cdots X_a$–Y (°) | Mode |
| LIGFIQ | *N*-Methylbenzothiazole-2(3*H*)-selenone iodinechloride | 2.625 | 2.690 | 178.89 | *A* |
| LIGFIQ01 | Se-(Chloroiodo)-*N*-methylbenzothiazole-2-selone | 2.618 | 2.690 | 178.75 | *A* |
| OXSEIC | 1-Oxa-4-selenacyclohexane iodine monochloride complex | 2.630 | 2.731 | 175.76 | *A* |
| Se$\cdots$Br–Br | | | | | |
| IRABEI | 5 : 5′-Tribromo-5, 10′-dibromo-5,10-bromo-bis(5,10-selenanthrene) bis(5,5-dibromoselenanthrene) | 2.645 | 2.358 | 174.19 | *A* |

[a] $B_d$ represents the electron donor; $X_a$ represents the electron acceptor

| REFCODE | $X'_d$-$X''_a$ (Å) | $X''_a$-X″ (Å) | $X_a$-$X'_s \cdots X''_d$ (°) | $X'_s \cdots X''_a$-X″ (°) |
|---|---|---|---|---|
| [b]RIJQAC | 3.175 | 2.778 | 80.59 | 173.44 |
| [c]RIJQEG | 3.100 | 2.786 | 89.29 | 179.35 |
| | 3.338 | 2.754 | 165.87 | 174.43 |
| [d]YEYFOX | 3.155 | 2.746 | 85.46 | 178.25 |
| | 3.670 | 2.762 | 73.95 | 165.11 |
| | 3.341 | 2.762 | 117.98 | 173.28 |
| | 3.525 | 2.764 | 97.20 | 176.44 |
| | 3.380 | 2.764 | 108.99 | 176.48 |
| [e]YEYFUD | 2.803 | 2.645 | 89.27 | 175.37 |

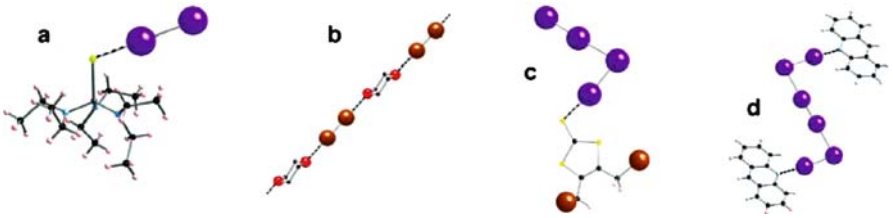


**Fig. 2** Structures illustrating bonding modes from Fig. 1. **a** PAQKIB, mode *A*; **b** DOXABR, mode *B*; **c** HAMCAA, mode *AA*; **d** QARGIZ, mode *BA*

reduced. This mode is illustrated in Fig. 2b for the dioxane complex of dibromine (DOXABR), in which interactions at either end of the $Br_2$ molecule with oxygen electron donors of two different dioxane molecules result in an extended donor–acceptor chain.

For some strong electron donor molecules the polarization of the $X_2$ molecule may be sufficient that the X atom not complexed to B serves as an electron donor to a second $X_2$ molecule, i.e., the dihalogen is "amphoteric", acting as a Lewis acid to Lewis base B, and as a Lewis base to the second $X_2$ molecule, acting as a Lewis acid. For a $1:1\ B \cdot X_2 : X_2$ ratio, an extended adduct (Fig. 1, mode *AA*) is formed, as illustrated in Fig. 2c for 4,5-bis(bromomethyl)-1,3-dithiole-2-thione-diiodine diiodine (HAMCAA) [58]. This is often referred to as an "extended spoke" structure. If the second $X_2$ acts as Lewis acid acceptor at either end of the molecule, then a bridged amphoteric adduct (Fig. 1, mode *BA*) is formed, as illustrated for $(\text{acridine} \cdot I_2)_2 \cdot I_2$ (QARGIZ) [31] in Fig. 2d.

## 2.2 Nitrogen and Oxygen Electron Donors

Second only to sulfur-based systems, nitrogen complexes are relatively well represented in the structural literature with 41 complexes reported. Of these, 25 are with $I_2$ as the electron acceptor, 11 are with the interhalogen ICl, three are with $Br_2$, and two are with IBr. As expected, in every case the halogen bond forms between the nitrogen and the softest halogen atom, i.e., iodine, in all of the complexes except those with dibromine. Most $N \cdot I_2$ complexes, and all $N \cdot Br_2$, N · IBr, and N · ICl complexes are simple adducts, mode *A*. Exceptions for the diiodine complexes include: bridging mode (*B*) observed for diazines, such as pyrazine [86], tetramethylpyrazine [86], phenazine, and quinoxaline [87], and for 9-chloroacridine [89] and the 1 : 1 complex of diiodine with hexamethylenetetramine [144]; and amphoteric bridging mode (*BA*) observed for 2,2′-bipyridine [85], acridine [89], 9-chloroacridine [89], and 2,3,5,6-tetra-2′-pyridylpyrazine [91]. The occurrence of both *B* and *BA* complexes with 9-chloroacridine, and of *B* and *A* complexes and an

ionic salt [145] for tetramethylenetetramine, highlights the obvious difficulty in predicting which mode will be favored for a given donor–acceptor pair.

Oxygen complexes with dihalogens are relatively rare, with only eight complexes known, and none of these involves interhalogens. Diiodine and dibromine complexes are equally represented with four and three known examples of each, respectively, and one dichlorine complex is known. It should be pointed out that this complex, dioxane dichlorine [41], is the only halogen bonded complex of dichlorine that has been structurally characterized. As opposed to those observed for nitrogen, all of the oxygen complexes except one crystallize with bridging dihalogens (mode *B*). The sole exception is a relatively complex manganese formate salt, in which an $I_2$ molecule interacts as a simple adduct [146].

## 2.3 Phosphorus and Sulfur Electron Donors

True halogen bonded complexes with phosphorus as the electron donor atom are even more rare than those with oxygen, and all of these involve diiodine as the electron acceptor. Three examples of simple adducts and one with a bridging diiodine were found. All other phosphorus halogen complexes are better described as salts with ion pairs closely associated through X···X interactions. One bromo- (JOMSEJ) and two iodo salts (SORPUK and ZEKMOR) are related to simple adduct (mode *A*, Eq. 1) complexes, in which the P···X interaction has strengthened to a covalent bond, while the X–X bond has weakened to the point of being an interaction. Likewise, one bromo- (SUHJIO) and five iodo- (LOBKOC, LOBKUI, LOBLAP, FILTEZ, and FILTID) salts with trihalide anions can be considered as coming from extended adducts (mode *AA*, Eq. 2).

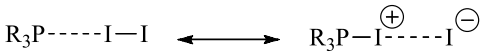

**Equation 1**

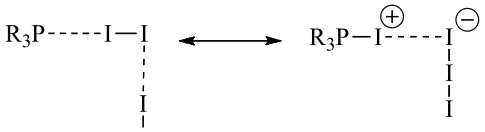

**Equation 2**

With 112 structurally characterized complexes, sulfur-based electrons are by far the most commonly encountered. This is attributed to its importance in antithyroid drugs, as described above. The majority of these complexes

(87) have diiodine-based electron acceptors, but all of the halogens and interhalogens except for dichlorine are represented. Of the diiodine complexes, 60 are simple adducts, 17 are bridging, four are extended adducts, and nine are bridged extended adducts. One ionic salt is included (LOPQIQ) due to the presence of a simple adduct structure in the asymmetric unit in addition to two iodonium cations closely linked to one $I_3^-$ and an additional discrete $I_3^-$ anion. All of the interhalogen IBr complexes are simple adducts, as are all of the ICl complexes, except one (HAMCII) [59] which is a bridged extended adduct, with the chlorine atoms acting as Lewis base donors to a bridging $I_2$ molecule. Two of the three known $Br_2$ complexes are simple adducts, while the third is bridging. In addition, three bromo salts are known, two with $S-Br^+$ cations and $Br_3^-$ anions (BEMLIO and YESGUY), and one with bis-donor-iodonium cations and an $I^-\cdots I_2\cdots I^-$ anion (FIMDOU).

## 2.4 Arsenic and Selenium Electron Donors

Few arsenic based complexes have been characterized. Three sets of structural data (FESKAP, FESKAP01, FESKAP02), a set for a second polymorph (FESKAP10), and a set for a toluene solvate (FUTTAP) have been reported for triphenylarsine·$I_2$, and all are simple adducts, as is the same electron donor complexed with the interhalogen IBr (CUXCON). For trimethylarsine, on the other hand, two electron donors are bridged by a single diiodine (ZODJOR), but with dibromine a simple ionic salt, $Me_3AsBr^+\cdots Br^-$ (TMASBR01), is formed.

Like sulfur, selenium based electron donors are heavily studied due to their potential as antithyroid agents. Of the 28 complexes reported, the majority (20) are diiodine based, and most of these (16) are simple adducts. One diiodine complex is bridged, one contains only extended adducts, one contains only bridged adducts, and one contains both bridged and extended adducts. All of the interhalogen complexes are simple adducts except one with iodine monobromine, which forms an extended adduct.

In addition to halogen bonded complexes or ionic salts, it is also possible for sulfur and selenium electron donors to form complexes in which the electron donor atom inserts into the $X_2$ bond, giving a hypervalent donor atom with a T-shaped geometry. It has been recently reported [147] that for dibromine and selenium, this type of complex is favored over halogen bonded complexes. While no purely halogen bonded complex is reported for dibromine, there is one complex (IRABEI) in which one selenium atom of each of several selenanthrene molecules in the asymmetric unit does insert into a $Br_2$ bond, but for one of the molecules, the other selenium atom forms a halogen bond with a $Br_2$ molecule to form a simple adduct (*A*).

# 3
# Computation Studies

## 3.1
## General Observations

The Lewis dot formalism shows any halogen in a molecule surrounded by three electron lone pairs. An unfortunate consequence of this perspective is that it is natural to assume that these electrons are equivalent and symmetrically distributed (i.e., that the iodine is $sp^3$ hybridized). Even simple quantum mechanical calculations, however, show that this is not the case [148]. Consider the diiodine molecule in the gas phase (Fig. 3). There is a region directly opposite the I–I sigma bond where the nucleus is poorly shielded by the atoms' electron cloud. Allen described this as "polar flattening", where the effective atomic radius is shorter at this point than it is perpendicular to the I–I bond [149]. Politzer and coworkers simply call it a "sigma hole" [150, 151]. This area of positive electrostatic potential also coincides with the LUMO of the molecule (Fig. 4).

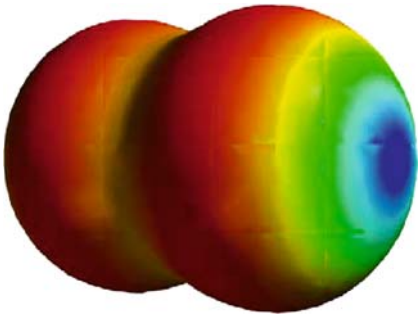

**Fig. 3** The electron density map (0.002 au contour) for diiodine, colored by the electrostatic potential. *Red* is the most negative potential and *blue* is the most positive

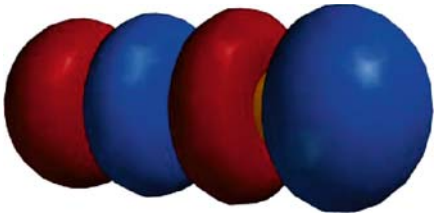

**Fig. 4** The lowest unoccupied molecular orbital for diiodine

The sigma hole is the key to understanding halogen bonding. Based upon the crystallographic and spectral data presented in the literature and the computational studies outlined below, the following generalizations may be made:

1. Halogen bonding is largely an electrostatic phenomenon. Therefore, when the halogen is bound to a more electronegative element, it becomes a better electron acceptor. Conversely, base strength parallels (at least to the first order of approximation) the effectiveness of a given species as a halogen bond electron donor.
2. Halogen bond electron acceptor ability decreases in the order I > Br > Cl. Fluorine (acting as an electron acceptor) forms only very weak halogen bonds, if at all.
3. When a halogen is in close contact with another atom approximately 180° from the halogen–halogen sigma bond, it is acting as an electron acceptor. When the contact is approximately 90°, it is acting as an electron donor.
4. Formation of a halogen bond at one atom of a dihalogen does not preclude the second atom from also acting as an electron acceptor. The stronger the electron donor, however, the less likely that a D···X–X···D complex will be formed.
5. Halogen bond formation results in partial occupation of a $\sigma^*$ antibonding orbital, weakening the bond. Depending on the electron donor strength and the environment, this can result in heterolytic fragmentation of the bond, leading to ionic products.

While the general features of halogen bonding are now well known, it has proven challenging to develop models with sufficient accuracy to predict spectroscopic features and bond energies. This is particularly problematic with iodine, where high quality basis sets are not readily available and are computationally expensive. There have been numerous approaches taken to address this issue during the past decade, many of which are discussed below.

Some surveys of computational methods involving charge-transfer complexes of dihalogens have recently been reported. Alkorta and coauthors looked at $F_2$, $Cl_2$, $Br_2$, FBr, FCl, and ClBr interacting with several $\sigma$ and $\pi$ electron donors and using both the B3YLP DFT and MP2 methods [152]. Two basis sets were used in this study: a 6-31G* was used with the DFT method, while a 6-311++G** basis set (which includes diffuse and additional polarization functions) was used with both the DFT and MP2 methods. Where possible, the calculated halogen bond geometries were compared with experimental values.

MP2 calculations gave better halogen bond distance estimations than did DFT, with the latter method consistently underestimating the bond length with both basis sets. The electron donor X–Y angle was found to be nearly linear in all cases, with a maximum deviation of 8° in the case of HF···$Cl_2$. Bond energy calculations followed the trends noted above, and the results correlate with hydrogen bond strengths with the same electron donor. However, there were significant variations in the values predicted from each approach. This is not surprising, given the different equilibrium geometries used; however, the correlation with bond distance was not consistent. The authors noted

that basis set superposition errors (BSSEs) [153, 154] could be large in these calculations, particularly at the 6-31G* level.

More recently, Zhao and Truhlar created a benchmark database of non-bonding interactions, including halogen bonded complexes, and compared a large number of computational methods [155, 156]. Neither iodine nor bromine electron acceptors were included in the surveys, but the results do reveal some of the challenges that exist in this area. For example, it was shown that all local spin density approximation (LSDA), generalized gradient approach (GGA), and hybrid GGA (GGA with HF exchange) functionals systematically overestimate binding energies, though the latter approach was typically more successful. The best functionals were found to be the MPWB1K and MPW1B95, which are hybrid meta GGA functions (where the functional also depends on kinetic energy density). These are recently developed functionals [157] that outperform the MP2 approach with these test complexes. Other functionals, including BHandHLYP [158] and the widely used B3LYP (both hybrid GGA) [159], also performed well.

### 3.2 Oxygen Electron Donors

While the first observations of halogen bonding were probably complexes formed in aqueous solutions, there are relatively few investigations of the oxygen halogen bond in the recent literature.

Davey, Legon, and Thumwood have studied several classes of donor–acceptor interactions through combinations of rotational spectroscopy and ab initio calculations. In a recent paper, they investigate the $H_2O\cdots Cl_2$ complex, noting that it probably plays a role in both the ozone depletion cycle (through the reaction $HOCl + HCl \rightarrow Cl_2 + H_2O$) and in water treatment through the reverse reaction to form hypochlorous acid [160]. They examined seven isotopomers resulting from various combinations of deuterium and $^{35}Cl/^{37}Cl$ labeled complexes by pulsed-jet microwave spectroscopy. Analysis of the spectra provided rotational and nuclear quadrupole coupling constants that were used in conjunction with models to give the geometry, binding energy, and estimations of electron transfer in the complex. The authors noted that the geometry of the complex is virtually identical to that of the hydrogen bonded analogue $H_2O\cdots HCl$, though the binding is not as strong. They also suggest that the extent of charge transfer from $H_2O$ to chlorine is very small, but the charge transfer of the bound chlorine to the unbound chlorine is significantly larger. Thus the interaction is primarily electrostatic in nature. Similar studies with ICl or IBr and a series of electron donors have shown that the extent of electron transfer decreases with the order $PH_3 > NH_3 > C_2H_4 \sim H_2S > C_2H_2 > H_2O > CO \sim HCN$ [142, 161].

Grabowski and Bilewicz have found an interesting effect in the study of halogen bonding between formaldehyde and ClF (**1**) [162]. Using MP2/

6-311++G(d,p) and correcting for BSSEs using the counterpoise method, the authors examined the effect of cooperativity on the halogen bond strength. That is, after performing a full geometry optimization of the 1 : 1 complex, they added a second ClF molecule to the system. Geometry optimization of the new complex gave structure **2**, where the fluorine on the first ClF acts as an electron donor to the second ClF. Interestingly, the calculated O···Cl bond length decreases as the second halogen bond is formed. Extension of the ClF···ClF chain out to six interhalogen units (**3**, where $n = 5$) resulted in further shortening of the O···Cl bond, and a corresponding increase in the halogen bond energy. The authors conclude that cooperativity in halogen bonding is similar to the effect observed in hydrogen bonded systems.

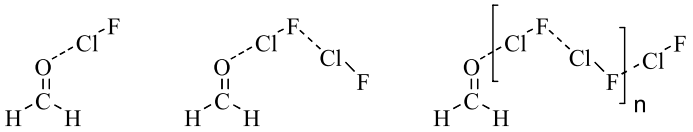

1 2 3

**Structure 1**

## 3.3 Nitrogen Electron Donors

The pyridine-$I_2$ system has received considerable attention over the years. While the single crystal diffraction data for this complex have not been reported, closely related structures are known, including 4-methylpyridine-$I_2$ [42] and pyridine-ICl [163]. Studies of pyridine-$I_2$ in solution give a dipole moment of 4.5–6.3 D and a binding energy of 7.4–8.6 kcal/mol, depending on the solvent [164–168]. Bopp and coworkers have studied the systems using ab initio methods (MP2) and compared several basis sets, including both all-electron and effective core potential basis sets [169]. In addition to examining the geometry and binding energies of the system, the vibrational frequencies were also computed and compared to experiment [170]. While ultimately unsatisfied with the level of accuracy obtainable with the available computers, the group was able to show that inclusion of electron correlation is important. The smaller effective core potential basis sets were not particularly accurate, but the authors suggest they might be used if their shortcomings were well described and could be taken into account.

Karpfen published a study of trends in halogen bonding between a series of amines and halogens and interhalogens [171]. Iodine-containing electron acceptors were not included. This study involved the use of RHF, MP2, and various DFT methods using extended, polarized basis sets and made extensive use of pulsed-nozzle, FT-microwave spectroscopic data (similar to that

discussed above) collected by the Legon group [172]. The calculated bond strengths ranged from 6.7 to nearly 85 kJ/mol. Bond strength increases with increasing gas-phase basicity of the amine, larger dipole moment, and polarizability of the halogen. All of the complexes can be described as "outer"-type charge-transfer complexes in the Mulliken terminology [173]. The RHF approach was found to be unsatisfactory for calculating equilibrium geometries, while MP2 and DFT (particularly using the BHandHLYP functionals) were found to be of comparable accuracy.

The Legon group, in addition to their extensive work in studying complexes of N bases and halogens by rotational spectroscopy, have also explored computational strategies for studying them. In a very recent paper [13], they used both the GAUSSIAN98W [174] and ADF2004 program packages in an effort to accurately calculate both halogen bond strength and the nuclear quadrupole coupling constants (QCC, as obtained from microwave data). For the former, geometry optimizations were carried out using the BHandHLYP density functional in conjunction with such extended standard basis set as aug-cc-pVTZ and the small-core relativistic pseudopotential correlation consistent basis sets for iodine.[2] For ADF calculations, they used the OPTX exchange functional combined with the PBE correlation functional using an all-electron triple-$\zeta$+ polarization basis set of uncontracted Slater orbitals. Scalar relativistic effects were considered using the zero order regular approximation (ZORA) [175]. The authors found good correlation between both methods and gas phase geometries (though not solid-state N–X bond lengths from X-ray diffraction). The experimental QCCs correlate well with those predicted by the BHandHLYP density functional, with the exception of iodine. The pseudopotential used in this treatment did not reproduce the effect of the occupied core orbitals particularly well. The less computationally expensive ZORA model was shown to give acceptable results for the QCCs, including iodine. The halogen bond energies in these complexes were best described as being more electrostatic than covalent.

In a particularly interesting investigation, Kusama and Sugihara [25] used MP2(full)/LANL2DZ* calculations to try to understand the influence of six nitrogen heterocycles on the performance of some dye-sensitized solar cells. The heterocycles have been shown to increase the open circuit voltage ($V_{OC}$) as well as the solar energy conversion efficiency. The authors suggest this effect results from a shift in the $I^-/I_3^-$ redox electrolyte equilibrium due to the formation of a charge-transfer complex (Eq. 3).

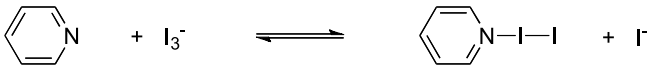


**Equation 3**

[2] Basis sets were obtained from the extensible computational chemistry environment basis set database, version 02/25/04. Pacific Northwest Laboratory, P.O. Box 999, Richland, WA 99352.

The LANL2DZ basis set was augmented by a set of six d polarization functions as successfully used by Bopp [169] and others. Complex geometries were optimized and the effects of the acetonitrile solvent were modeled using the polarized continuum model of Tomasi and coworkers [176, 177]. The nature of the halogen bond was described using NBO analysis. The authors found a rough correlation between the electron donor HOMO and the $V_{OC}$. The higher the HOMO, and thus the smaller the energy difference between that orbital and the $I_2$ LUMO, the higher the $V_{OC}$. Likewise, decreasing $\Delta G$ of complex formation (increasing halogen bond strength) also correlated with $V_{OC}$.

Valdes and Sordo have studied the interaction of $PH_3$ and $NH_3$ with BrCl using either all-electron or effective core potential (ECP) MP2 methods, and several different basis sets [178]. They found that ECPs could give results nearly equivalent to their all-electron counterparts. $PH_3$ was found to form weaker halogen bonds than $NH_3$.

### 3.4 Sulfur and Selenium Electron Donors

The interaction of dihalogens, particularly diiodine, with sulfur and selenium electron donors has been an area of increasing interest over the past decade because of potential biological, pharmaceutical, and electronic materials applications [35, 179]. Devillanova and coworkers have recently reviewed the solution behavior of a large number of chalcogenides and $I_2$, particularly thiones, selones, sulfides, and selenides [180]. Correlations between computational methods, thermodynamic parameters, and spectroscopic data (UV/Vis, $^{13}C$ NMR, Raman, UPS) were discussed.

The interaction of chalcogenides and dihalogens can lead to a large variety of complexes and salts. The initial interaction in both the gas phase [15] and in solution [180] seems to be the formation of a halogen bonded structure. The available literature shows that Se electron donors bind $I_2$ more strongly than do S electron donors, and that thiones and selones bind more strongly than the corresponding sulfides and selenides. The electron donor ability of S or Se depends greatly on the environment, and the formation constants vary widely. For compounds containing the framework R – C(= X) – R (X=S, Se), the *K* values decrease according to the following sequence of R: NR $\geq$ alkyl $\geq$ aromatic $\geq$ S $\geq$ O.

Bouab, Yanez, and coworkers have noted that thiocarbonyl electron donors can form two distinctly different charge-transfer complexes in solution [181]. Calculations at the HF/LANL2DZ* and MP2(full)/LANL2DZ*//LANL2DZ* levels indicate that a charge-transfer band in the 300-nm region results when the halogen bond lies in the plane of the C = S group, while a band at 350 nm results when the bond is perpendicular to that plane (**4** and **5**, respectively). The halogen bond in both types of complexes is primarily

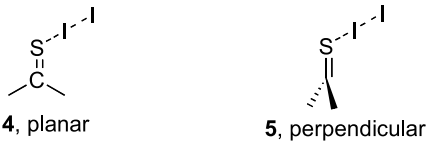


electrostatic in nature. The perpendicular arrangement arises primarily from steric interactions at the α positions.

The reactivity of the initial halogen bonded complex has also received considerable attention. Husebye and coworkers have suggested a process whereby the dihalogen bond is cleaved to give a key cation intermediate and a halide anion (Eq. 4) [182]. This mechanism is consistent with that often proposed for nitrogen electron donor systems.

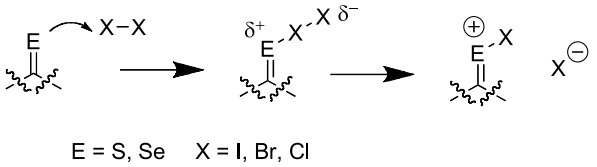


**Equation 4**

Devillanova and coworkers have also addressed this issue with some simple thiones and selones. Using spectroscopic analysis and quantum mechanical calculations, they examined the various possible reaction pathways shown in Fig. 5 [72, 183]. The geometries and relative stabilities of the charge-transfer and "T-shaped" hypervalent adducts were compared using DFT cal-

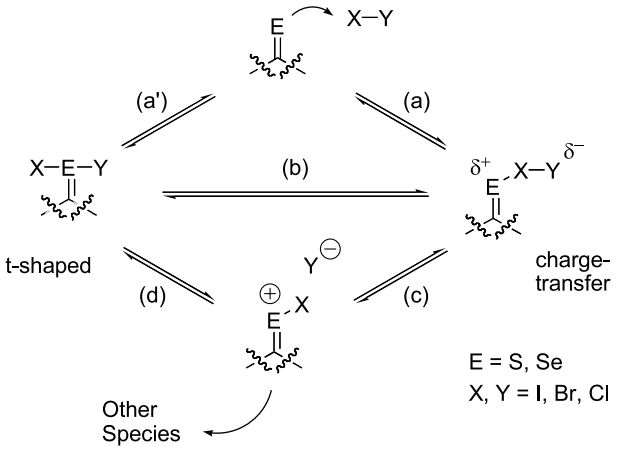


**Fig. 5** Pathways for the reaction of thiones and selones with dihalogens

culations with the Becke3LYP functional and LANL2DZ basis set as well as the mPW1PW [184] functional. The latter adds diffuse and polarization functions for halogen atoms to the LANL2DZ basis set [186].

The calculated optimized geometries were found to be in good agreement with available experimental data. In general, the T-shaped hypervalent structures were found to be of lower energy than the charge-transfer structures. This energy difference was greater with chlorine than bromine and even smaller (or reversed) with iodine. Stronger electron donors also encouraged formation of hypervalent complexes. These results are consistent with the Husebye model, where initial formation of the charge-transfer complex is followed by X–Y bond cleavage to give ions (Fig. 5 pathways (a) and (c), respectively).

The possibility that the hypervalent complex might be formed directly from the starting fragments in an oxidative addition reaction (pathway (a′)) or by rearrangement of the charge-transfer complex (pathway (b)) was investigated using the negative eigenvalues progression reduction (NERP) [183] and the intrinsic reaction coordinate (IRC) techniques [187]. Both methods identified reasonable transition states for (b) (see, for example, adduct **6**), but not for (a′). In fact, attempts to find a saddle point for the conversion of the starting fragments into the hypervalent complex inevitably identified only the transition state for pathway (b), leading the authors to conclude that direct addition of the dihalogen to the electron donor is unfeasible. However, pathway (b) is predicted to be lower in energy than the Husebye route (pathways (c) and (d)). The authors did note that solvent effects would be expected to play a major role in the reaction.

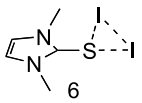


6

## 3.5 π-Electron Donors

Other electron donor systems have received attention over the past decade. In 1949, Benesi and Hildebrand observed an absorption band in solutions of iodine in benzene that they attributed to a charge-transfer complex. The structure(s) contributing to this band have been a matter of some debate ever since. In this book, the chapter of J.K. Kochi and coworker discusses these adducts in the solid and in solution [185]. Figure 6 shows various geometries that have been proposed. Grozema and coworkers examined the potential energy surface of the benzene-$I_2$ system at the MP2 level, correcting for counterpoise errors across the entire surface rather than only at energy minima, as had been the case for earlier studies [188].

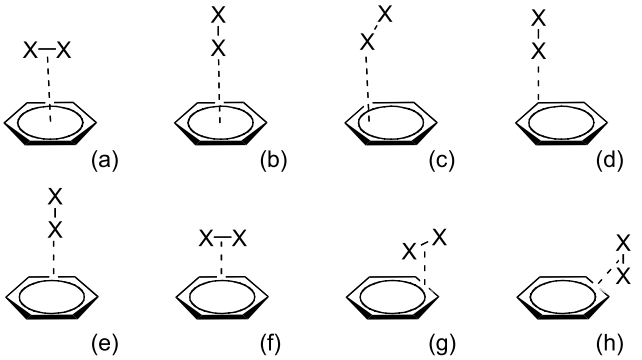


**Fig. 6** Proposed structures for iodine–benzene complex: **a** resting, **b** axial, **c** oblique (turned 30° around center of mass), **d** above carbon, **e** above bond, **f** resting on bond, **g** displaced resting, and **h** T-shaped [79]

The lowest energy structures were found to be the above carbon and above bond geometries (Fig. 6d and e, respectively). This is a function of the anisotropy of the electron density around the iodine and the geometry dependent polarization of the dihalogen.

More recently, Mukherjee et al. [189] applied time dependent HF and DFT methods to examine the ground- and excited-state geometries of the benzene–ICl complex optimized at the HF, B3LYP, and MPW1PW91 levels in both the gas phase and in $CCl_4$ solution. The experimental $CCl_4$ CT absorption was not well reproduced by HF methods due to inadequate electron correlation, but DFT calculations using B3LYP and MPW1PW91 functionals did reproduce the values closely. The optimized geometry closely resembles the "above bond" geometry for the ground state and the "above carbon" geometry for the excited state (Fig. 6e and d, respectively).

## References

1. Guthrie F (1863) J Chem Soc 16:239
2. Lewis GN (1938) J Franklin Inst 226:301
3. Mulliken RS (1952) J Phys Chem 56:801
4. Mulliken RS, Person WB (1969) Molecular complexes. Wiley-Interscience, New York, p 498
5. Hassel O, Hvoslef J (1954) Acta Chem Scand 8:873
6. Bent HA (1968) Chem Rev 68:587
7. Flurry RL (1966) J Phys Chem 69:1927
8. Flurry RL (1969) J Phys Chem 73:2111
9. Rosokha SV, Neretin IS, Rosokha TY, Hecht J, Kochi JK (2006) Heteroatom Chem 17:449
10. Messina MT, Metrangolo P, Navarrini W, Radice S, Resnati G, Zerbi G (2000) J Mol Struct 524:87

11. Al-Hashimi NA, Hassan KA, Nour E-M (2005) Spectrochim Acta A 62A:317
12. Baruah SK (2004) Asian J Chem 16:706
13. Poleshchuk OK, Branchadell V, Brycki B, Fateev AV, Legon AC (2006) J Mol Struct Theochem 760:175
14. Davey JB, Legon AC (2001) Phys Chem Chem Phys 3:3006
15. Legon AC, Thumwood JMA (2001) Phys Chem Chem Phys 3:2758
16. Legon AC (2007) The Interaction of Dihalogens and Hydrogen Halides with Lewis Bases in the Gas Phase: An Experimental Comparison of the Halogen Bond and the Hydrogen Bond (in this volume). Springer, Heidelberg
17. Lagorce JF, Thomes JC, Catanzano G, Buxeraud J, Raby M, Raby C (1991) Biochem Pharm 42:S89
18. Lagorce JF, Comby F, Rousseau A, Buxeraud J, Raby C (1993) Chem Pharm Bull 41:1258
19. Corban CJ, Hadjikakou SK, Hadjiliadis N, Kubicki M, Tiekink ERT, Butler IS, Drougas E, Kosmas AM (2005) Inorg Chem 44:8617
20. Sauvage MF, Marquet P, Rousseau A, Raby C, Buxeraud J, Lachatre G (1998) Toxicol Appl Pharmacol 149:127
21. Karuna T, Neelima K, Venkateshwarlu G, Yadagiri Swamy P (2006) J Sci Ind Res 65:808
22. Mostafa AA, Bebawy LI, Refaat HH (2002) J Pharm Biomed Anal 27:889
23. Cardoso SG, Ieggli CVS, Pomblum SCG (2007) Pharmazie 2007 62:34
24. Nazeeruddin MK, Klein C, Liska P, Gratzel M (2005) Coord Chem Rev 249:1460
25. Kusama H, Sugihara H (2006) J Photochem Photobiol A 181:268
26. Kusama H, Arakawa H, Sugihara H (2005) J Photochem Photobiol A 171:197
27. Sen S, Pal P, Misra TN (1993) J Mater Sci 28:1367
28. Srivastava ON, Singh RA (1999) Bull Electrochem 15:372
29. Gupta RK, Singh RA (2005) J Polym Res 12:189
30. Ganjali MR, Norouzi P, Shirvani-Arani S, Kakanezhadifard A (2007) J Anal Chem 62:279
31. Bailey RD, Grabarczyk M, Hanks TW, Pennington WT (1997) J Chem Soc Perkin Trans II 2781
32. Choi SY, Park YS, Hong SB, Yoon KB (1996) J Am Chem Soc 118:9377
33. Miyajima N, Akatsu T, Ikoma T, Ito O, Rand B, Tanabe Y, Yasuda E (2000) Carbon 38:1831
34. Cau L, Deplano P, Marchio L, Mercuri ML, Pilia AS, Trogu EF (2003) Dalton Trans 1969
35. Bigoli F, Cabras MC, Deplano P, Mercuri ML, Marchio L, Serpe A, Trogu EF (2004) Eur J Inorg Chem 960
36. Hassel O, Hope H (1960) Acta Chem Scand 12:391
37. Hassel O, Hope H (1961) Acta Chem Scand 15:407
38. Groth P, Hassel O (1964) Acta Chem Scand 18:402
39. Hassel O, Stromme KO (1958) Acta Chem Scand 12:1146
40. Hassel O, Stromme KO (1959) Acta Chem Scand 13:275
41. Hassel O, Stromme KO (1959) Acta Chem Scand 13:1775
42. Hassel O, Romming C, Tufte T (1961) Acta Chem Scand 15:967
43. Marstokk K-M, Stromme KO (1968) Acta Crystallogr B 24:713
44. Ahlsen EL, Stromme KO (1974) Acta Chem Scand 28:175
45. Romming C (1960) Acta Chem Scand 14:2145
46. Romming C (1972) Acta Chem Scand 26:1555
47. Chao GY, McCullough JD (1960) Acta Crystallogr 13:727

48. Chao GY, McCullough JD (1961) Acta Crystallogr 14:940
49. Hope H, McCullough JD (1964) Acta Crystallogr 17:712
50. Maddox H, McCullough JD (1966) Inorg Chem 5:522
51. Knobler C, McCullough JD (1968) Inorg Chem 7:365
52. Uchida T (1967) Bull Chem Soc Jpn 40:2244
53. Uchida T, Kimura K (1984) Acta Crystallogr C 40:139
54. Baenziger NC, Nelson AD, Tulinsky A, Bloor JH, Popov AI (1967) J Am Chem Soc 89:6463
55. Svensson PH, Kloo L (2003) Chem Rev 103:1649
56. Bricklebank N, Skabara PJ, Hibbs DE, Hursthouse MB, Malik KMA (1999) J Chem Soc Dalton Trans 3007
57. Skabara PJ, Bricklebank N, Berridge R, Long S, Light ME, Coles SJ, Hursthouse MB (2000) J Chem Soc Dalton Trans 3235
58. Lee L, Crouch DJ, Wright SP, Berridge R, Skabara PJ, Bricklebank N, Coles SJ, Allen DW, Berridge R, Bricklebank N, Forder SD, Palacio F, Coles SJ, Hursthouse MB, Skabara PJ (2003) Inorg Chem 42:3975
59. Light ME, Hursthouse MB (2004) Cryst Eng Commun 6:612
60. Skabara PJ, Berridge R, Bricklebank N, Lath H, Coles SJ, Horton PN (2006) Polyhedron 25:989
61. Bigoli F, Deplano P, Mercuri ML, Pellinghelli MA, Trogu EF (1992) Phosphorus Sulfur Silicon Relat Elem 72:65
62. Bigoli F, Deplano P, Mercuri ML, Pellinghelli MA, Trogu EF (1992) Phosphorus Sulfur Silicon Relat Elem 70:175
63. Bigoli F, Deplano P, Ienco A, Mealli C, Mercuri ML, Pellinghelli MA, Pintus G, Saba G, Trogu EF (1999) Inorg Chem 38:4626
64. Lu FL, Keshavarz M, Srdanov G, Jacabson RH, Wudl F (1989) J Org Chem 54:2165
65. Beck J, Daniels J, Roloff A, Wagner N (2006) Dalton Trans 1174
66. Daga V, Hadjikakou SK, Hadjiliadis N, Kubicki M, dos Santos JHZ, Butler IS (2002) Eur J Inorg Chem 1718
67. Antoniadis CD, Corban GJ, Hadjikakou SK, Hadjiliadis N, Kubicki M, Warner S, Butler IS (2003) Eur J Inorg Chem 1635
68. Atzei D, Deplano P, Trogu EF, Bigoli F, Pellinghelli MA, Sabatini A, Vacca A (1989) Can J Chem 67:1416
69. Bigoli F, Deplano P, Mercuri ML, Pellinghelli MA, Sabatini A, Trogu EF, Vacca A (1995) Can J Chem 73:380
70. Bigoli F, Deplano P, Mercuri ML, Pellinghelli MA, Sabatini A, Trogu EF, Vacca AJ (1996) J Chem Soc Dalton Trans 3583
71. Cristiani F, Demartin F, Devillanova FA, Isaia F, Saba G, Verani GJ (1992) Chem Soc Dalton Trans 3553
72. Aragoni MC, Arca M, Demartin F, Devillanova FA, Garau A, Isaia F, Lippolis V, Verani G (2005) Dalton Trans 2252
73. Freeman F, Ziller JW, Po HN, Keindl MC (1988) J Am Chem Soc 110:2586
74. Bigoli F, Pellinghelli MA, Deplano P, Devillanova FA, Lippolis V, Mercuri ML, Trogu EF (1994) Gazz Chim Ital 124:445
75. Kuhn N, Fawzi R, Kratz T, Steimann M, Henkel G (1996) Phosphorus Sulfur Silicon Relat Elem 112:225
76. Antoniadis CD, Blake AJ, Hadjikakou SK, Hadjiliadis N, Hubberstey P, Schroder M, Wilson C (2006) Acta Crystallogr B 62:580
77. Boyle PD, Christie J, Dyer T, Godfrey SM, Howson IR, McArthur C, Omar B, Pritchard RG, Williams GR (2000) J Chem Soc Dalton Trans 3106

78. Cristina F, Demartin F, Devillanova FA, Isaia F, Lippolis V, Verani G (1994) Inorg Chem 33:6315
79. Demartin F, Devillanova FA, Garau A, Isaia F, Lippolis V, Verani G (1999) Polyhedron 18:3107
80. Boyle PD, Cross WI, Godfrey SM, McAuliffe CA, Pritchard RG, Teat S (1999) J Chem Soc Dalton Trans 2219
81. Cristina F, Devillanova FA, Isaia F, Lippolis V, Verani G, Demartin F (1995) Polyhedron 14:2937
82. Herbstein FH, Schwotzer W (1984) J Am Chem Soc 106:2367
83. Bernardinelli G, Gerdil R (1976) Acta Crystallogr B 32:1906
84. Soled S, Carpenter GB (1974) Acta Crystallogr B 30:910
85. Pohl SZ (1983) Z Naturforsch B Chem Sci 38:1535
86. Bailey RD, Buchanan ML, Pennington WT (1992) Acta Crystallogr C 48:2259
87. Bailey RD, Drake GW, Grabarczyk M, Hanks TW, Pennington WT (1997) J Chem Soc Perkin Trans II 2773
88. Rimmer EL, Bailey RD, Pennington WT, Hanks TW (1998) J Chem Soc Perkin Trans II 2557
89. Rimmer EL, Bailey RD, Hanks TW, Pennington WT (2000) Chem Eur J 6:4071
90. Walsh RD, Padgett CW, Metrangolo P, Resnati G, Hanks TW, Pennington WT (2001) Cryst Growth Des 1:165
91. Padgett CW, Walsh RD, Drake GW, Hanks TW, Pennington WT (2005) Cryst Growth Des 5:745
92. Batsanov AS, Howard JAK, Lightfoot AP, Twiddle SJR, Whiting A (2005) Eur J Org Chem 1876
93. Aragoni MC, Arca M, Devillanova FA, Hursthouse MB, Huth SL, Isaia F, Lippolis V, Mancini A, Ogilvie HR, Verani G (2005) J Organomet Chem 690:1923
94. Mascal M, Richardson JL, Blake AJ, Li W-S (1996) Tetrahedron Lett 37:3505
95. Cristiani F, Devillanova FA, Isaia F, Lippolois V, Verani G, Demartin F (1993) Heteroatom Chem 4:571
96. Blake AJ, Gould RO, Radek C, Schroder M (1993) Chem Commun, p 1191
97. Blake AJ, Li W-S, Lippolis V, Schroder M (1997) Acta Crystallogr C 53:886
98. Blake AJ, Cristiani F, Devillanova FA, Garau A, Gilby LM, Gould RO, Isaia F, Lippolis V, Parsons S, Radek C, Schroder M (1997) J Chem Soc Dalton Trans 1337
99. Arca M, Cristiani F, Devillanova FA, Garau A, Isaia F, Lippolis V, Verani G, Demartin F (1997) Polyhedron 16:1983
100. Blake AJ, Devillanova FA, Garau A, Gilby LM, Gould RO, Isaia F, Lippolis V, Parsons S, Radek C, Schroder M (1998) J Chem Soc Dalton Trans 2037
101. Blake AJ, Devillanova FA, Isaia F, Lippolis V, Parsons S, Schroder M (1999) J Chem Soc Dalton Trans 525
102. Herbstein FH, Ashkenazi P, Kaftory M, Kapon M, Reisner GM, Ginsburg D (1986) Acta Crystallogr B 42:575
103. Baker PK, Harris SD, Durrant MC, Hughes DL, Richards RL (1995) Acta Crystallogr C 51:697
104. Bock H, Nagel N, Seibel A (1997) Liebigs Ann Chem 2151
105. Yamamoto M, Wu LP, Kuroda-Sowa T, Maekawa M, Suenaga Y, Munakata M (1997) Inorg Chim Acta 258:87
106. Tipton AI, Lonergan MC, Stern CL, Shriver DF (1992) Inorg Chim Acta 201:23
107. Godfrey SM, Kelly DG, McAuliffe CA, Mackie AG, Pritchard RG (1991) Chem Commun, p 1163

108. Bricklebank N, Godfrey SM, Mackie AG, McAuliffe CA, Pritchard RG (1992) Chem Commun, p 355
109. Bricklebank N, Godfrey SM, Lane HP, McAuliffe CA, Pritchard RG (1995) J Chem Soc Dalton Trans 2421
110. Cross WI, Godfrey SM, McAuliffe CA, Pritchard RG, Sheffield JM, Thompson GM (1999) J Chem Soc Dalton Trans 2795
111. Godfrey SM, McAuliffe CA, Peaker AT, Pritchard RG (2000) J Chem Soc Dalton Trans 1287
112. Pritchard RG, Moreland L (2006) Acta Crystallogr C 62:o656
113. Teixidor F, Nunez R, Vinas C, Sillanpaa R, Kivekas R (2000) Angew Chem Int Ed 39:4290
114. Nunez R, Farras P, Teixidor F, Vinas C, Sillanpaa R, Kivekas R (2006) Angew Chem Int Ed 45:1270
115. Ruthe F, Jones PG, du Mont W-W, Deplano P, Mercuri ML (2000) Z Anorg Allg Chem 626:1105
116. Cotton FA, Kibala PA (1987) J Am Chem Soc 109:3308
117. Ellis BD, MacDonald CLB (2006) Inorg Chem 45:6864
118. Vogt H, Trijanov VB, Rybakov VB (1993) Z Naturforsch B Chem Sci 48:258
119. McAuliffe CA, Beagley B, Gott GA, Mackie AG, MacRory PP, Pritchard RG (1987) Angew Chem Int Ed 26:264
120. Beagley B, Colburn CB, El-Sayrafi O, Gott GA, Kelly DG, Mackie AG, McAuliffe CA, MacRory PP, Pritchard RG (1988) Acta Crystallogr C 44:38
121. Abbas S, Godfrey SM, McAuliffe CA, Pritchard RG (1994) Acta Crystallogr C 50:717
122. Bricklebank N, Godfrey SM, Lane HP, McAuliffe CA, Pritchard RG, Moreno JM (1995) J Chem Soc Dalton Trans 3873
123. Cross WI, Dahalan MZ, Godfrey SM, Jaiboon N, McAuliffe CA, Pritchard RG, Thompson GM (2000) Acta Crystallogr C 56:140
124. Hursthouse MB, Steer IA (1971) J Organomet Chem 27:C11
125. Arca M, Demartin F, Devillanova JA, Garau A, Isaia F, Lippolis V, Verani GJ (1999) J Chem Soc Dalton Trans 3069
126. Arca M, Devillanova JA, Garau A, Isaia F, Lippolis V, Verani G, Demartin F (1998) Z Anorg Allg Chem 624:745
127. Bricklebank N, Coles SJ, Forder SD, Hursthouse MB, Poulton A, Skabara PJ (2005) J Organomet Chem 690:328
128. Apperley DC, Bricklebank N, Hursthouse MB, Light ME, Coles SJ (2001) Polyhedron 20:1907
129. Apperley DC, Bricklebank N, Burns SL, Hibbs DE, Hursthouse MB, Malik KMA (1998) J Chem Soc Dalton Trans 1289
130. Cross WI, Godfrey SM, Jackson SL, McAuliffe CA, Pritchard RG (1999) J Chem Soc Dalton Trans 2225
131. Ito S, Liang H, Yoshifuji M (2003) Chem Commun, p 398
132. Bransford JW, Meyers EA (1978) Cryst Struct Commun 7:697
133. Seppala E, Ruthe F, Jeske J, du Mont W-W, Jones PG (1999) Chem Commun, p 1471
134. Jeske J, Jones PG, du Mont W-W (1999) Chem Eur J 5:385
135. Godfrey SM, Jackson SL, McAuliffe CA, Pritchard RG (1997) J Chem Soc Dalton Trans 4499
136. Rudd MD, Lindeman SV, Husebye S (1997) Acta Chem Scand 51:689
137. Ouvrard C, Le Questel JY, Berthelot M, Laurence C (2003) Acta Crystallogr B 59:512
138. Legon AC (1995) J Chem Soc Faraday Trans 91:1881
139. Legon AC (1998) Chem Commun, p 2737

140. Legon AC (1998) Chem Eur J 4:1890
141. Legon AC (1999) Angew Chem Int Ed 38:2686
142. Legon AC (1999) Chem Phys Lett 314:472
143. Allen FH (2002) Acta Crystallogr B 58:380 (CSD version 5 28, Nov 2006 and updates Jan 2007)
144. Pritzkow H (1975) Acta Crystallogr B 31:1589
145. Pritzkow H (1975) Acta Crystallogr B 31:1505
146. Wang Z, Zhang B, Fujiwara H, Kbayashi H, Kurmoo M (2004) Chem Commun, p 416
147. Aragoni MC, Arca M, Demartin F, Devillanova FA, Garau A, Isaia F, Lelj F, Lippolis V, Verani G (2005) Dalton Trans 2252
148. Hanks TW, Pennington WT, Bailey RD (2001) In: Glaser R, Kaszynski P (eds) Anisotropic organic materials approaches to polar order. Am Chem Soc, Washington DC
149. Lommerse JPM, Stone AJ, Taylor R, Allen FH (1996) J Am Chem Soc 118:3108
150. Clark T, Hennemann M, Murray JS, Politzer P (2007) J Mol Model 13:291
151. Politzer P, Lane P, Concha MC, Ma Y, Murray JS (2007) J Mol Model 13:305
152. Alkorta I, Rozas I, Elguero J (1998) J Phys Chem A 102:9278
153. Paizs B, Suhai S (1998) J Comput Chem 19:575
154. Kestner NR, Combariza JE (1999) Rev Comput Chem 13:99
155. Zhao Y, Truhlar DG (2005) J Chem Theory Comput 1:415
156. Zhao Y, Truhlar DG (2006) J Chem Theory Comput 2:1009
157. Zhao Y, Truhlar DG (2004) J Phys Chem A 108:6908
158. Frisch MJ, Trucks GW, Schlegel HB, Gill PMW, Johnson BG, Wong MW, Foresman JB, Robb MA, Head-Gordon M, Replogle ES, Gomperts R, Andres JL, Raghavachari K, Binkley JS, Gonzalez C, Martin RL, Fox DJ, Defrees DJ, Baker J, Stewart JJP, Pople JA (1993) Gaussian 92/DFT, Revision F.2. Gaussian Inc, Pittsburgh
159. Stephens PJ, Devlin FJ, Chabalowski CF, Frisch MJ (1994) J Phys Chem 98:11623
160. Davey JB, Legon AC, Thumwood JMA (2001) J Chem Phys 114:6190
161. Legon AC, Thumwood JMA, Waclawik ER (2000) J Chem Phys 113:5278
162. Grabowski SJ, Bilewicz E (2006) Chem Phys Lett 427:51
163. Hassel O, Romming C (1956) Acta Chem Scand 10:696
164. Hamilton AJ, Suton LE (1968) J Chem Soc Chem Commun, p 460
165. Reid S, Mulliken RS (1954) J Am Chem Soc 76:6008
166. Toyoda K, Person WB (1966) J Am Chem Soc 88:1629
167. Kortum G, Waltz H (1958) Z Elektrochem 57:73
168. Barton SS, Pottier RH (1984) J Chem Soc Perkin Trans II 731
169. Reiling S, Besnard M, Bopp PA (1997) J Phys Chem A 101:4409
170. Kiefer W, Bernstein HJ (1972) J Mol Spectrosc 43:366
171. Karpfen A (2003) Theor Chem Acc 110:1
172. Legon AC (1996) Chem Commun, p 109
173. Mulliken RS (1950) J Am Chem Soc 72:600
174. Frisch MJ, Trucks GW, Schlegel HB, Gill PMW, Johnson BG, Robb MA, Cheeseman JR, Keith T, Petersson GA, Montgomery JA, Raghavachari K, Al-Laham MA, Zakrzewski V, Ortiz JV, Foresman JB, Closlowski J, Stefanov BB, Nanayakkara A, Challacombe M, Peng CY, Ayala PY, Chen W, Wong MW, Andress JL, Replogle ES, Gomperts R, Martin RL, Fox DJ, Binkley JS, Defress DJ, Baker J, Stewart JP, Head-Gordon M, Gonzales C, Pople JA (1998) GAUSSIAN 98, Revision A. Gaussian Inc, Pittsburg
175. van Lenthe E, Ehlers AE, Baerends EJ (1999) J Chem Phys 110:8943
176. Cances E, Mennucci B, Tomasi J (1997) J Chem Phys 107:3032

177. Mennucci B, Cammi R, Tomasi J (1998) J Chem Phys 109:2798
178. Valdes H, Sordo JA (2003) Chem Phys Lett 371:386
179. Laurence C, El-Ghomari MJ, Le Questel J-Y, Berthelot M, Mokhlisse R (1998) J Chem Soc Perkin Trans II 1545
180. Aragoni MC, Arca M, Devillanova FA, Garau A, Isaia F, Lippolis V, Verani G (1999) Coord Chem Rev 184:271
181. Esseffar M, Bouab W, Lamsabhi A, Abboud J-LM, Notario R, Yanez M (2000) J Am Chem Soc 122:2300
182. Rudd MD, Linderman SV, Husebye S (1997) Acta Chem Scand 51:689
183. Aragoni MC, Arca M, Demartin F, Devillanova FA, Garau A, Grimaldi P, Isaia F, Lelj F, Lippolis V (2006) Eur J Inorg Chem 2006:2166
184. Adamo C, Barone V (1998) J Chem Phys 108:664
185. Rosokha SV, Kochi JK (2007) X-ray Structures and Electronic Spectra of the π-Halogen Complexes between Halogen Donors and Acceptors with π-Receptors (in this volume). Springer, Heidelberg
186. Check CE, Faust TO, Bailey JM, Wright BJ, Gilbert TM, Sunderlin LS (2001) J Phys Chem A 105:8111
187. Gonzales C, Schlegel HB (1990) J Chem Phys 94:5523
188. Grozema FC, Zijlstra RWJ, Swart M, van Duijnen PT (1999) Int J Quant Chem 75:709
189. Tiwary AS, Sengupta PS, Mukherjee AK (2007) Chem Phys Lett 433:427
190. Politzer P, Murray JS, Concha MC (2007) J Mol Model 13(10):1033–1038

Struct Bond (2008) 126: 105–136
DOI 10.1007/430_2007_060

Published online: 6 September 2007

# Halogen Bonding in Crystal Engineering

Pierangelo Metrangolo[1,2] (✉) · Giuseppe Resnati[1,2] (✉) · Tullio Pilati[3] · Serena Biella[1,2]

[1]Laboratory of Nanostructured Fluorinated Materials (NFMLab), Department of Chemistry, Materials and Chemical Engineering "Giulio Natta", Politecnico di Milano, 7, via Mancinelli, 20131 Milano, Italy
*pierangelo.metrangolo@polimi.it; giuseppe.resnati@polimi.it*

[2]Como Campus, Politecnico di Milano, 7, via Castelnuovo, 22100 Como, Italy

[3]C.N.R.-Institute of Molecular Sciences and Technologies, Università di Milano, 19, via Golgi, 20133 Milano, Italy

**1 Introduction** . . . . . 106

**2 General Features of XB** . . . . . 107
2.1 Relative Effectiveness of XB vs. HB . . . . . 109
2.2 XB and Electron Density Around Halogen Atoms . . . . . 110
2.3 Structure and Role of the Halocarbon . . . . . 114
2.4 Structure and Role of the Halocarbon Partner . . . . . 115
2.5 Directionality of XB . . . . . 116

**3 Halogen-Bonded Supramolecular Architectures** . . . . . 118
3.1 1D Architectures . . . . . 119
3.2 2D Architectures . . . . . 122
3.3 3D Architectures . . . . . 125

**4 Conclusions** . . . . . 129

**References** . . . . . 130

**Abstract** The term halogen bonding encompasses any non-covalent interaction involving halogens as electrophilic species. High strength and directionality are the remarkable features of halogen bonding that fully justify its use as a primary intermolecular interaction to dictate molecular self-assembly processes. This chapter will outline the use of halogen bonding in crystal engineering and will highlight the obtainment of heteromeric crystal structures with complex topologies. Even though the use of halogen bonding is still in its infancy, the growing interest in the field shown by the crystal engineering community promises major advances in the future.

**Keywords** Halogen bonding · Supramolecular chemistry · Crystal engineering · Tecton · Topology

**Abbreviations**

| | |
|---|---|
| BPE | (*E*)-1,2-Bis(4-pyridyl)ethylene |
| BPY | Dipyridine |
| DABCO | Diazabicyclooctane |

| | |
|---|---|
| DBTFB | Dibromotetrafluorobenzene |
| DIB | Diiodobenzene |
| DITFB | Diiodotetrafluorobenzene |
| HB | Hydrogen bonding |
| HMTA | Hexamethylenetetramine |
| PFC | Perfluorocarbon |
| TIE | Tetraiodoethylene |
| TMEDA | Tetramethylethylenediamine |
| XB | Halogen bonding |

## 1 Introduction

Following the concept introduced by Jean-Marie Lehn in 1978, supramolecular chemistry can be considered as "... the chemistry of molecular assemblies and of the intermolecular bond" [1]. This concept encompasses several poorly related disciplines, both within chemistry and at the interface of chemistry with condensed matter physics, materials science, and biology. This chapter will have a more specific focus on some of these topics and we will focus on crystal engineering involving organic compounds, a subject of the diversified topics addressed by supramolecular chemistry. Moving from the paradigm shift [2] that supramolecular chemistry generated from the focus on atoms and the bonds between atoms, to the focus on molecules and bonds between molecules, in this chapter we will concentrate on the atomic characteristics conferring to molecules, or to molecular sites, the specific properties that determine their mutual complementarity via halogen bonding.

Intermolecular recognition and self-assembly processes both in the solid, liquid, and gas phases are the result of the balanced action of steric and electronic factors related to shape complementarity, size compatibility, and specific anisotropic interactions. Rather than pursuing specific and definitive rules for recognition and self-assembly processes, we will afford some heuristic principles that can be used as guidelines in XB-based supramolecular chemistry.

The term halogen bonding (XB) [3–8] indicates any D···X–Y interaction in which X is the electrophilic halogen (Lewis acid, XB donor), D is a donor of electron density (Lewis base, XB acceptor), and Y is carbon, nitrogen, halogen, etc. (Fig. 1).

Most of the energetic or geometric trends found in hydrogen-bonded complexes (wherein hydrogen functions as the acceptor of electron density) and other interaction features known from spectroscopic or theoretical investigations are encountered in halogen-bonded complexes as well [9–12]. Expectedly, halogen atoms being much larger than hydrogen atoms, XB is more sensitive to steric hindrance than hydrogen bonding (HB) [13].

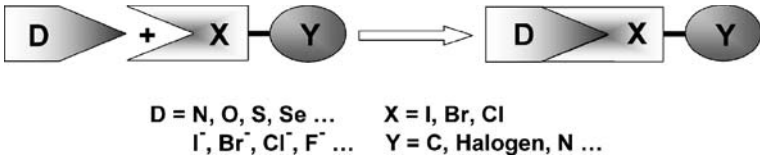


**Fig. 1** Schematic representation of XB. XB acceptors (*D*) are neutral or anionic species, while donors (*X*) are halogen atoms bound to a wide diversity of molecular arrays (*Y*)

Architectures originating from halogens and interhalogens (Fig. 1, Y = F, Cl, Br, I) gave fundamental contributions towards the identification of the interaction [14–17] and are still attracting great interest [18, 19] (see also the chapter by Legon in this volume) as it is the case, for instance, for polyhalide anions [20] or for adducts wherein sulfur, selenium, or arsenic derivatives work as electron donors [21]. Numerous architectures in which the electrophilic halogen is bound to nitrogen, phosphorous, or other elements (Fig. 1, Y = N, P, etc.) [22] present the standard XB characteristics (Table 1). However, the focus of this chapter will be limited to the supramolecular architectures formed by carbon-bound halogens (Fig. 1, Y = C).

Both n and $\pi$ electrons can be involved in XB formation [23–27] and usually the latter give weaker interactions than the former [18, 28] (see also the chapter by Legon and the chapter by Kochi in this volume). In this chapter we will consider only n XB acceptors.

The first unequivocal report on a halogen-bonded complex was made by F. Guthrie who described, in 1863, a solution-based synthesis of the $NH_3 \cdots I_2$ complex [29]. In 1881 J. W. Mallet described an alternative synthesis for the same compound based on a gas/solid protocol [30]. Two years later O. Roussopoulos described the 1 : 3 co-crystal formation between iodoform and quinoline as well as other related adducts [31, 32]. In 1893 I. Remsen and J. F. Norris demonstrated the tendency of methylamines to form similar adducts with chlorine, bromine, and iodine [33]. It can thus be stated that the basics in the topic of halogen-bonded adducts had been laid in the nineteenth century. The field begun to be systematized only after the crystallographic studies of O. Hassel in the 1950s. In his Nobel lecture, Hassel stressed the similarities between interactions wherein hydrogen and halogen work as electron acceptors, and also the similarities between interactions given by dihalogens and halocarbons [17]. Important contributions to the topic and its systematization have been given by H. A. Bent [16] and J.-M. Dumas [34].

**Table 1** Examples where the XB donor is bound to nitrogen and the acceptor is an oxygen atom **(A)**, an anion **(B)**, or a nitrogen atom **(C)**

**(A)**

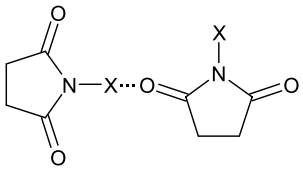

| X | N-X···O (Å) | N-X···O (°) | C = O···X (°) | Refs. |
|---|---|---|---|---|
| Cl | 2.880 | 168.87 | 136.50 | [240] |
| Br | 2.802 | 169.54 | 140.88 | [241] |
| I | 2.580 | 175.71 | 121.65 | [242] |

**(B)**

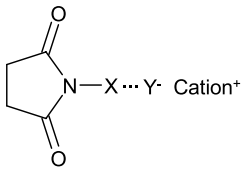

| X | $Y^-$ | Cation | N-X···$Y^-$ [Å] | N-X···$Y^-$ [deg] | Refs. |
|---|---|---|---|---|---|
| Cl | $Cl^-$ | $Ph_4P^+$ | 2.892, 2.898 | 178.64, 176.91 | [243] |
| Br | $Cl^-$ | $Ph_4P^+$ | 2.822, 2.852 | 177.50, 179.10 | [244] |
| Br | $Br^-$ | $Ph_4P^+$ | 2.900, 2.929 | 177.52, 178.35 | [244] |
| Br | $Br^-$ | $Et_4N^+$ | 2.836 | 175.80 | [245] |
| Br | $Br^-$ | $Cs^+$ | 3.038 | 178.40 | [246] |
| I | $Cl^-$ | $Ph_4P^+$ | 2.845, 2.910 | 177.59, 179.22 | [247] |
| I | $Br^-$ | $Ph_4P^+$ | 2.933, 3.007 | 177.19, 179.35 | [247] |
| I | $I^-$ | $Ph_4P^+$ | 3.103, 3.170 | 176.87, 179.18 | [247] |
| Br | $(CH_3)_2CCO_2N^-$ | $Et_4N^+$ | 2.109 | 177.40 | [248] |

**(C)**

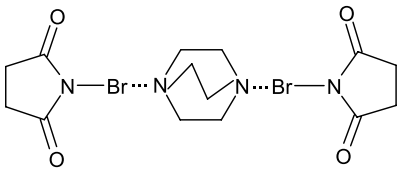

| N···Br | 2.332 Å | [249] |
|---|---|---|

## 2
## General Features of XB

### 2.1
### Relative Effectiveness of XB vs. HB

According to the definition given above, the term XB comprehensively covers a vast class of non-covalent interactions, from the weak N···Cl XB [35] to the very strong $I^-\cdots I_2$ interaction, which forms the triiodide anion; 10 and 200 kJ $mol^{-1}$ can be assumed as the energy extremes for these interactions, respectively.

The remarkable strength of some XBs allows them to prevail over HBs in identifying the modules to be involved in self-assembly. For instance, in experiments of competitive co-crystal formation, a dipyridyl derivative prefers to co-crystallize with XB donors rather than HB donors and the same occurs for *N*,*N*,*N*′,*N*′-tetramethylethylenediamine (TMEDA) [36]. In solution, solute–solute intermolecular HBs are considerably diminished if a strong XB donor co-solute is added. If haloperfluorocarbons (halo-PFCs) are used, the HB breaking potency increases moving from perfluorocarbons to chloro-, bromo-, and iodoperfluorocarbons [37–43], perfectly consistent with the order of the increasing XB donor ability of the halo-PFCs co-solutes. In aque-

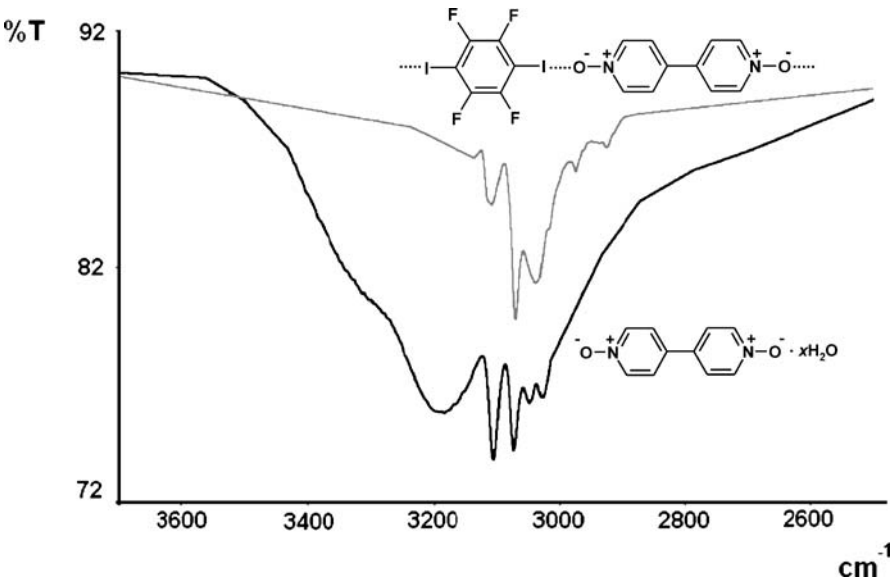


**Fig. 2** IR spectra of 4,4′-dipyridyl *N*,*N*′-dioxide in the $\nu_{O-H}$ stretching region for the hydrated compound (*black line, bottom*) and the complex it gives with 1,4-DITFB (*grey line, top*). Hydration water disappears on complex formation

ous solution, the nitrogen lone pairs of TMEDA are hydrogen-bonded to the solvent. When a stochiometric amount of 1,2-diiodotetrafluoroethane, which is insoluble in water, is added to an aqueous solution of TMEDA, N···I XB is strong enough to drive the phasing out of the diamine from the aqueous solution and the pure TMEDA/diiodoethane co-crystal rapidly precipitates [3]. From a preparative point of view, when the hydrated forms of hydrocarbon electron donors are crystallized with iodo-PFCs, no crystallization water is found in the formed complexes and this is largely independent of the solvent used for the crystallization. For instance, several diamine and dipyridyl derivatives are hygroscopic compounds (e.g. 4,4′-dipyridyl (4,4′-BPY) and its *N*,*N*′-dioxide), but crystallization of their hydrated forms in the presence of diiodoperfluoroalkanes or -arenes affords water-free halogen bonded co-crystals (Fig. 2).

This ability of halogen-bonded halo-PFCs to substitute water in the crystal packing of the hydrocarbons donors possessing a lone-pair, coupled with the easy removal of halo-PFCs from the formed perfluorocarbons-hydrocarbons-HC co-crystals through vacuum pumping, could be developed as a general, economic, and large scale way to obtain dinitrogen electron donors (or their derivatives) in anhydrous form.

## 2.2 XB and Electron Density Around Halogen Atoms

Theoretical studies explain XB occurrence in terms of anisotropic distribution of the electron density around halogen atoms. This anisotropicity determines the formation of a region of positive electrostatic potential on the outermost portion of some covalently-bonded halogen atoms [44–46] (see also the chapter by Karpfen in this volume). The electron density is represented by an ellipsoid elongated in the direction across the bonding axis, a feature called polar flattening [47]. Consistent with the directionality of the approach of the lone pair of the electron donor on the halogen [48], namely with the XB directionality, the effective atomic radius along the extended C – X bond axis is smaller than in the direction perpendicular to this axis.

Within a homogeneous series of compounds, and independent of their structure, a clear trend of increasing electropositive potential along the C – X axis occurs moving from fluorine to iodine. In halocarbons, the electrostatic potential of F remains negative all around the atom, whereas Cl, Br, and I show the emergence of an electropositive crown along the C – X axis, which is surrounded by an electroneutral ring and, further out, an electronegative belt. The size of this electropositive crown increases with the polarizability of the halogen, consistent with the experimental finding that iodocarbons give rise to the strongest D···I-C XBs [49, 50]. The presence and the magnitude of the positive halogen crown also depend on the electron-

withdrawing power of the groups neighbouring the halogen on the carbon skeleton [51]. Chlorine in $CH_3Cl$ does not present any positive electrostatic potential, but it appears in $CH_2FCl$, and becomes even greater in $CF_3Cl$; the most positive chlorine potential in $HOCH_2CH_2Cl$ is – 1.1 but it becomes 7.8 in $O_2NCH_2CH_2Cl$. Similarly, the atomic charge increases with the fluorination degree in iodomethane derivatives, being 0.009 in $CH_3I$ and 0.165 in $CF_3I$ [52].

The possibility to carefully tune the XB strength of a given halocarbon by modifying the substituents on the carbon skeleton is also confirmed experimentally. As expected, the stronger an XB, the shorter the interaction length (see onwards). The N···I-C interaction length in the infinite chain given by 1,4-BPY with 1,4-diiodobenzene (1,4-DIB) is 3.032 Å and the N···I

**Table 2** Interaction of 1,4-DIB and 1,4-DITFB with XB acceptors

| Co-crystals | I···N distance X-ray [Å] | DFT calculations [Å] | I···N interaction energy (DFT) [kcal mol$^{-1}$] |
|---|---|---|---|
| 1,4-BPY·1,4-DIB | 3.032 | 3.151 | 3.29 |
| 1,4-BPY·1,4-DITFB | 2.851 | 2.936 | 5.81 |
| BPE·1,4-DIB | 2.996 | 3.119 | 3.44 |
| BPE·1,4-DITFB | 2.810 | 2.891 | 6.02 |
| HMTA·1,4-DIB | 3.011 | 3.124 | 3.52 |
| HMTA·1,4-DITFB | 2.844 | 2.919 | 6.07 |

On interaction with a variety of XB acceptors, 1,4-DITFB forms shorter and stronger contacts than 1,4-DIB. Clearly, the electron withdrawing ability of fluorine boosts the donor ability of the iodine atoms

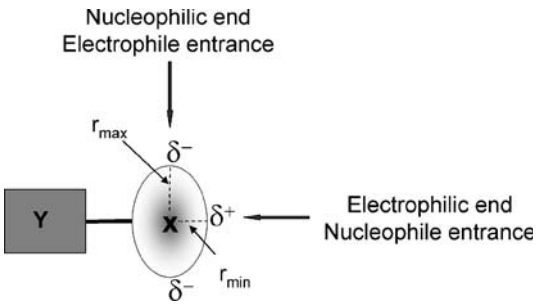


**Fig. 3** Due to the anisotropic distribution of the electron density, halogen atoms show a negative electrostatic potential and a larger radius ($r_{max}$) in the equatorial region and a positive electrostatic potential and a smaller radius ($r_{min}$) in the polar region. As a consequence of this, halogens behave as nucleophiles at the equator and as electrophiles at the pole

interaction energy (density functional theory, DFT) is 3.29 kcal mol$^{-1}$. The same parameters become 2.851 Å and 5.81 kcal mol$^{-1}$, respectively, when 1,4-diiodotetrafluorobenzene (1,4-DITFB) is used [50] (Table 2).

Similarly, the experimentally determined N···I distances in the co-crystals given by (*E*)-1,2-bis(4-pyridyl)ethylene (BPE) and hexamethylenetetramine (HMTA) with 1,4-DIB were longer than with its tetrafluorinated analogue and the computed N···I energies weaker. The I$^-$···I-C interaction length in the adduct between a cyclopropenium iodide and iodobenzene is 3.535 Å when one nitro group is on the aromatic ring and becomes 3.431 and 3.328 Å when two and three nitro groups are present, respectively [53].

In keeping with the anisotropic electrostatic potential model for the halogen atoms, halogens show an "amphiphilic" character and can work both as the electrophilic sites and the nucleophilic sites when involved in short contacts (Fig. 3).

The halogen acts as an electron-deficient site when it gives contacts towards the pole (electrophilic end) [54, 55], while the same halogen can act as an electron-rich site when it gives contacts towards the equator (nucleophilic end) (for instance with metal ions, protons [56], or halogens [57]).

**Table 3** Interaction of XB donors with different acceptors

| | C – I distance [Å] | $\Delta_{C-I}$ [a] [%] | I···donor distance Expected [b] [Å] | Observed [c] [Å] | $\Delta_{I\cdots donor}$ [d] [%] |
|---|---|---|---|---|---|
| 1,4-DITFB | 2.075 | | | | |
| 1,4-BPY···1,4-DITFB | 2.094 | 0.92 | 3.53 | 2.851 | 19.2 |
| 1,4-BPE···1,4-DITFB | 2.089 | 0.67 | 3.53 | 2.768 | 21.6 |
| TMDCN···1,4-DITFB | 2.079 | 0.19 | 3.53 | 3.061 | 13.3 |
| DABCO···1,4-DITFB | 2.119, 2.121 | 2.12, 2.22 | 3.53 | 2.739, 2.748 | 22.4, 22.1 |
| DMAB···1,4-DITFB | 2.084 | 0.43 | 3.50 | 3.097 | 11.5 |
| 2,2-BPY···1,4-DITFB | 2.086 | 0.53 | 3.53 | 3.111 | 11.9 |
| TMPDA···1,4-DITFB | 2.091 | 0.77 | 3.53 | 2.935 | 16.8 |
| TMACl···1,4-DITFB | 2.096, 2.083 | 1.01, 0.38 | 3.65 | 3.134/3.153 | 14.0, 13.6 |

When a given XB donor interacts with different acceptors, the shortening of the D···X interaction ($\Delta_{D\cdots I}$) is greater than the lengthening of the C – X bond ($\Delta_{C-I}$). This proves how the D···I distance is more sensitive to XB strength than the C – I distance.

[a] Percentage change of C – I distance, $\Delta_{C-I}$ = difference between C – I distance in the XB donor as pure compound and as an halogen bonded complex

[b] Sum of van der Waals radii of XB donor and acceptor atom

[c] From single crystal X-ray analysis

[d] Percentage change of I···donor distance, $\Delta_{I\cdots donor}$ = difference between the expected and the observed distances. *TMBDCN* 2,3,5,6-tetramethyl-1,4-benzodicarbonitrile, *DMAB* 4,4′-bis(dimethylamino)benzophenone, *TMPDA* *N*,*N*,*N*′,*N*′-tetramethyl-*p*-phenylenediamine, *TMACl* tetramethylammonium chloride

The term halogen bonding addresses exclusively the former contacts and its usefulness relies on the identification of a specific subset of the numerous and diverse non-covalent interactions that halogens can give rise to [58].

The attractive nature of XB causes D···X distances shorter than the sum of van der Waals radii of involved atoms; the stronger the interaction, the shorter the D···X interaction lengths. Consistent with the rationalization of XB as an electron donation from D to the antibonding X – Y orbital [59], XB formation results in an elongation of the X – Y covalent bond. The D···X interaction length is usually a more sensitive probe for XB strength than the X – Y covalent bond elongation (Table 3).

In many cases the XB adduct is a pre-reactive complex (or intermediate) formed prior to chemical reaction or significant charge transfer [18] (see also the chapter by Legon in this volume). The stronger interactions easily evolve into different molecular species if concentration, temperature, solvent polarity, or other parameters are changed [60]. The 1 : 1 complex that dihalogen

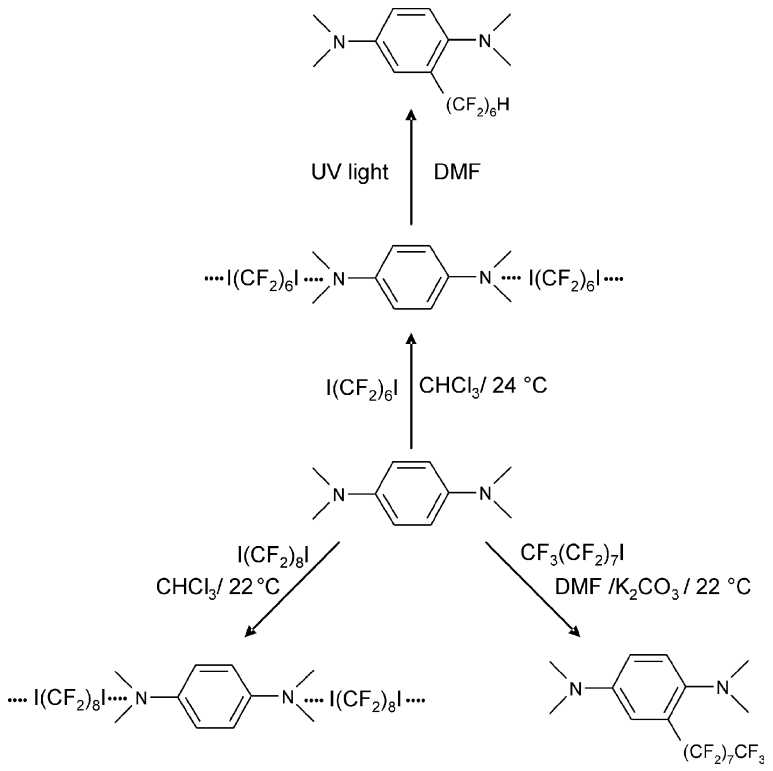


**Fig. 4** Halogen-bonded adducts are pre-reactive complexes, which, under convenient conditions, can lead to covalent bonds breaking and forming. Perfluoroalkylation occurs when the complexes between iodoperfluoroalkanes and anilines are heated or irradiated in certain solvents

molecules form with alkenes is a particularly well-known example. It lies on the way to the addition products formation and its evolution depends on solvent polarity [24]. After Mulliken's terminology, the outer complex $NH_3 \cdots I_2$ evolves into the inner complex $[NH_3I]^+ \cdots I^-$, which finally affords $NH_2I$, $NH_4^+$ and $I^-$ [61, 62]. When iodoperfluoroalkanes interact with aniline derivatives, halogen-bonded adducts or perfluoroalkylation products are formed depending on the adopted reaction conditions [63–65] (Fig. 4).

### 2.3 Structure and Role of the Halocarbon

Both theoretical and experimental data (in the solid, liquid, and gas phases) prove that the tendency of halocarbons to work as XB donors decreases in the order I > Br > Cl [66–68]. Clearly, polarizability and not electronegativity plays a key role. 3-Halo-cyanoacetylene works as self-complementary module and the N···X distance is beautifully consistent with the scale reported above, being 2.932, 2.978 and 2.984 Å in the iodo, bromo and chloro derivatives, respectively [69, 70]. The same trend is observed when a phenyl, rather than a triple bond, spaces the donor and acceptor sites. The N···Br distance in 4-bromobenzonitrile is longer than in the 4-iodo derivative [71, 72] and no XB is present in the chloro and fluoro analogues, wherein molecules are pinned by N···H and X···H short contacts [73]. PFCs have a very poor tendency, if any, to work as XB donors [74–77] and no crystal engineering can be based on such tectons. However, $F_2$ is a quite strong XB donor and several adducts have been described in the gas phase [11, 18] (see also the chapter by Legon in this volume).

Consistent with the fact that the more electron-withdrawing the atom, or the moiety, bound to a given halogen, the stronger the XB it gives rise to, the strength order C(sp)-X>C($sp^2$)-X>C($sp^3$)-X is usually followed [78]. Haloalkynes (e.g. diiodoacetylene [79–81] and bromo- or iodoethynylbenzenes [82, 83]), are particularly good XB donors. For instance, the O···I interaction length in the infinite chains that 1,4-dioxane gives with diiodoacetylene and tetraiodoethylene (TIE) are 2.668 and 3.004 Å, respectively [84, 85]. Similarly, when 1,4-diselenane interacts with the same XB donors, the Se···I distances are 3.34 and 3.43 Å, respectively [86–88]. As expected, on increasing the electron withdrawing ability of the benzene ring in iodo-ethynylbenzenes, the iodoalkyne moiety becomes a better XB donor. The $Br^- \cdots I$ interaction length in the tetrathiafulvalenium bromide/1,4-bis(iodoethynylenzene) complex is 3.266 Å and becomes 3.141 Å when the benzene ring is tetrafluorinated [83].

Haloarenes routinely form XB. The same holds for haloheteroarenes and when the heteroaromatic ring is positively charged, the halogen becomes a particularly good XB donor [89–94]. This strategy has been applied with particular success in order to control the packing of bromo- and iodo-

substituted tetrathiafulvalene derivatives, which are interesting molecular conductors [95–106]. On interacting with unfunctionalized monohaloalkanes, n electron donors usually give $S_N2$ type products rather than halogen-bonded adducts, as the entrance of electron donors from the back-side of the C – X covalent bond (nucleophilic attack at carbon) prevails over the front-side entrance (nucleophilic attack at halogen). Particularly strong electron-withdrawing residues geminal to the halogen atom of monohaloalkanes boost the Lewis acidity of the halogen and allow it to give strong XBs. This is the case, among others [107, 108], for various iodomethyl onium salts (e.g. $Ph_3P^+$-$CH_2$-I anion$^-$) wherein both the anion···I-C distances and the anion···I-C angles show the presence of strong XB [109–111]. Similarly, short $Cl^-\cdots$Cl-C XBs are present in chloromethyl onium salts [112, 113] (e.g. $Me_3N^+$-$CH_2$-Cl $Cl^-$ [114] and in $Ph_3P^+$-$CH_2$-Cl $ICl_4^-$ [115]).

For steric and electronic reasons, the entrance of n electron donors from the front-side of the C – X covalent bond is favoured over the back-side entrance in polyhaloalkanes. The latter compounds thus routinely form XBs. The interaction can further evolve into chemical reactions [63, 64, 116]. Tri- and tetrabromomethane have been extensively used to form halogen-bonded adducts [117], and iodoperfluoroalkanes are particularly tailored to XB-based crystal engineering [118]. The general rule that strong electron-withdrawing groups geminal or vicinal to the halogen atom boost its XB donor ability holds also for polyhaloalkanes [119]. The $Br^-\cdots$Br distances in tribromomethyl-triphenylphosphonium bromide ($Ph_3P^+$-$CBr_3$ $Br^-$) are shorter than in the tetraphenylphosphonium bromide/tetrabromomethane adduct ($Ph_4P^+$ $Br^-/CBr_4$) [120, 121].

## 2.4 Structure and Role of the Halocarbon Partner

Increased electron density on the XB acceptor site increases its Lewis basicity and favours XB formation. In solution, the XB acceptor ability of $sp^2$ hybridized oxygens increases moving from acetone, to dimethylsulfoxide, to hexamethylphosphortriamide [67, 68]. Nitrogen is usually a better XB acceptor than oxygen (see onwards), but the reverse is true when pyridines and corresponding *N*-oxides are compared, consistent with the electron densities on the respective electron donor sites [122]. 1,4-Dicyanobenzene does not give a co-crystal with 1,4-DITFB, but 1,4-dicyano-tetramethylbenzene does [123]. Pyrazine and its 2-methyl derivative afford solid and halogen-bonded co-crystals when interacting with 1,2-diiodotetrafluoroethane, but this is not the case starting from pyrazinecarbonitrile, even on cooling to – 20 °C [124]. Neither the oxygen nor the nitrogen atoms of ω-iodoperfluoroalkylsulfonamides form XBs [125], but when a formal negative charge is on the sulfonamide group, intermolecular O···I XB occurs and gives rise to infinite chains. Similarly, ω-iodoperfluoroalkylsulfonic salts present

in the solid intermolecular O···I XBs that connect the anions into infinite chains [126, 127].

Anions are usually better XB acceptors than neutral species [128] and the more naked they are, the stronger their XB acceptor ability is. Most of the halogen-bonded systems reported in the literature are formed by halide anions. In this series, iodide examples are the most frequently recurring, and fluoride anions are the least common. In solution, association of halide anions with XB acceptors decreases in the order $I^- > Br^- > Cl^- > F^-$ [128]. This scale contrasts with the scale based on percentage shortening of X⁻···I-C distances with respect to the sum of van der Waals radii. Clearly, the solvation energies of the starting anions, and formed superanions, as well as the strength of the formed XBs affect association processes and the relative relevance of the two parameters is different in solution and in the solid. Also polyhalide anions (e.g. $I_3^-$ [129], $Br_3^-$ [120], $ICl_2^-$ [111], $ICl_4^-$ [115]) form XBs; usually they give longer, namely weaker, XBs than the corresponding halides [112, 120, 128] and work as electron density donors at the two ends of the ion. $CN^-$ [96–98, 130–132] and $SCN^-$ [133, 134] anions have been reported to give XBs.

Typical nitrogen atoms (e.g. in amine and pyridine derivatives) give stronger XBs than typical oxygen and sulfur atoms (e.g. in ethers, alcohols, thioethers) [67, 68, 135, 136]. When 1,2-diiodotetrafluoroethane and *N*-methylmorpholine interact [124], they both work as bidentate modules and form infinite chains thanks to the formation of O···I and N···I XBs, the two interactions corresponding to 0.82 and 0.80 times the respective sum of van der Waals radii [137]. The relative effectiveness of oxygen and sulfur in XB formation often depends on the nature of the XB donor, as the pairings after the HSAB theory are favoured. A very rigorous and general scale wherein XB acceptors, or donors, are listed according to their strength cannot be filed as the relative effectiveness of a given set of XB acceptors (or donor) may also depend on the used XB donor (or acceptor, respectively). Steric hindrance around the XB acceptor site decreases its effectiveness and may affect the relative strength of two electron donor sites, as in the case for 2,2′- and 4,4′-BPY. Moreover, when subtle differences have to be compared, it may happen that scales based on thermodynamic and spectroscopic measurements (or theoretical calculations) are not identical.

## 2.5 Directionality of XB

XB is a particularly directional interaction, more directional than HB. The angle between the covalent and non-covalent bonds around the halogen in D···X-Y is approximately 180° [48]. As discussed above, the origin of this directionality is in the anisotropic distribution of electron density around the halogen atom. Figure 5 shows the Cambridge Structure Database (CSD, ver-

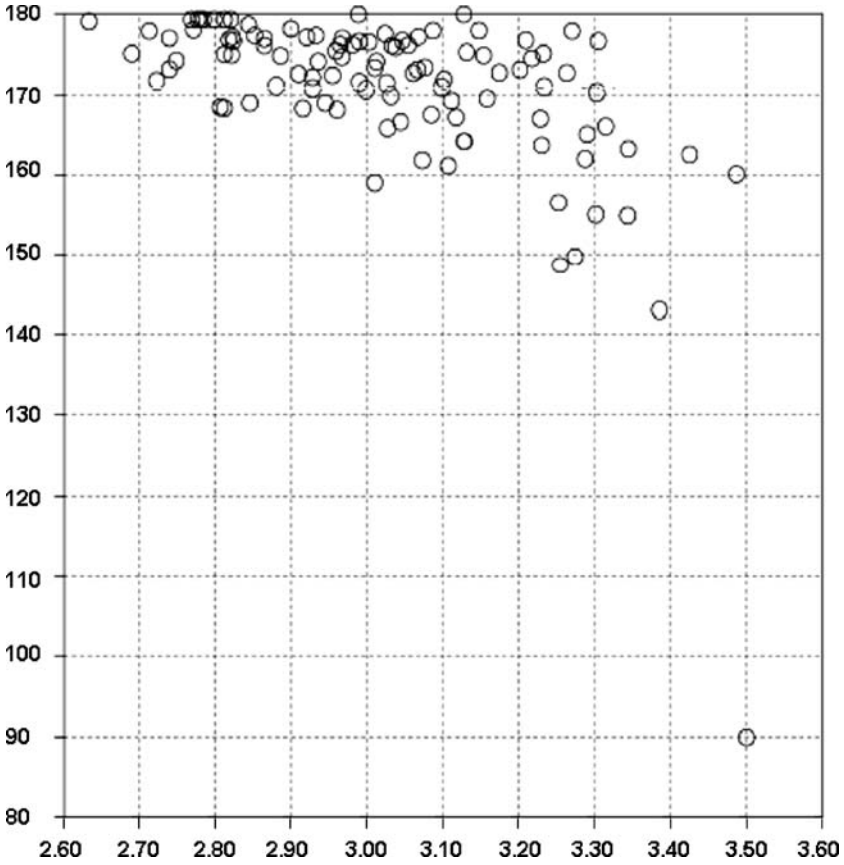


**Fig. 5** Scatterplot derived from the CSD reporting the N···I-C angle (deg) vs. the N···I distance (Å) for crystal structures containing intermolecular N···I contacts; only error-free and non-polymeric structures containing single-bonded iodine atoms and showing no disorder with $R < 0.06$ are considered. The scatterplot clearly demonstrates the high directionality of the N···I XB

sion 5.26, October 2005) scatterplots of intermolecular N···I-C interactions versus N···I distances, respectively.

Clearly, short interactions are more directional then long ones. A similar trend is observed also when bromine and chlorine atoms are the XB donor sites or when XB acceptor sites other than nitrogen and oxygen are used [138].

When n electron donors are involved, the XB is preferentially along the axis of the donated lone pair on D. For instance, XBs around ethers, thioethers, and amines feature a tetrahedral arrangement with preferential axial directions for the XBs around hexacyclic amines, and equatorial directions for hexacyclic thioethers [16, 17, 124, 139–142] (Fig. 6).

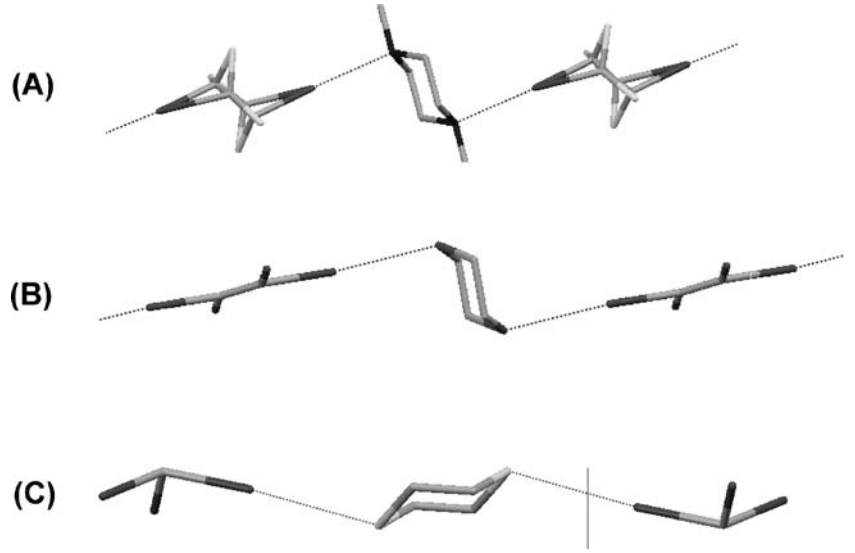


**Fig. 6** XBs around ethers, thioethers and amines feature a tetrahedral arrangement with preferential axial directions for the XBs around hexacyclic amines (*A*, co-crystal between 1,4-dimethylpiperazine and 1,2-diiodotetrafluoroethane) and ethers (*B*, co-crystal between 1,4-dioxane and tetraiodoethene), and equatorial directions for hexacyclic thioethers (*C*, co-crystal between 1,4-dithiane and iodoform)

In pyridine···X-C interactions, the C – X moiety is roughly coplanar with the pyridine and the two C-N···X angles are approximately 120° [129, 143, 144]. The same holds for other nitrogen heteroaromatics (e.g. pyrazine, quinoline, etc.) [145–147]. A carbonyl group pins the donors after a trigonal planar geometry and works either as a mono- [148, 149] or bidentate XB acceptor [150]. Sulfoxides behave similarly [151, 152] and imines form XB along the expected axis of the lone pair [153].

## 3
## Halogen-Bonded Supramolecular Architectures

After considering the atomic and molecular characteristics determining the properties of the XB given by a halocarbon and its partner, let's focus on the potential of this interaction in relating the geometries of the starting modules with the geometries of the supramolecular architectures that the halocarbon and its partner give rise to. The attention will be focussed on some prototype topologies in order to show the XB effectiveness in bridging molecular and supramolecular topologies and to formulate some basic concepts in XB-based molecular tectonics. The key starting points are the remarkable strength and the particularly high directionality (both on the donor and on the acceptor

partners) of the XB. These features give a substantial contribution to the reliability of XB-based crystal engineering and allow a precise structural control of the formation of the supramolecular aggregates to be obtained whenever reliable tectons are used.

### 3.1 1D Architectures

As discussed above, XBs tend to be linear, namely to be formed along the C – X bond axis on the XB donor module and along the lone pair axis of the heteroatom on the XB acceptor module. The angles between these axes determine the halogen-bonded adducts geometry.

For instance, pyramidal tetramers are formed when a pyramidal and tridentate XB donor interacts with a monodentate XB acceptor (e.g. the adducts $CHI_3$/isoquinoline [32] and $CHBr_3$/tris(tetrakis(4-nitrophenyl)methane) [154]). According to the same geometric paradigm, linear trimers are formed when a linear and bidentate XB donor interacts with a monodentate XB acceptor (e.g. the adducts 1,4-DITFB/$Ph_4P^+Cl^-$, 1,4-DITFB/$Ph_4P^+Br^-$ [155], 1,4-di(2-iodoethinyl)-2,5-dimethylbenzene/bis(tetrathiafulvalenium)$^+$ $Cl^-$ [83]) and when a monodentate XB donor interacts with a linear and bidentate XB acceptor (e.g. the adduct $C_6F_5I/(Me_2N)_3S^+F^-$ [156]).

When both the donor and the acceptor modules are bidentate, infinite chain (1D polymers) are formed. The simplest case is when the axes of the donor and acceptor sites are parallel and coaxial so that linear polymers are formed. This is the case in the homopolymers formed by bidentate and self-complementary tectons (e.g. 4-iodopyridine [157], 4-iodobenzonitrile [71, 72], halocyanoacetylenes [70]) and in the co-polymers formed when dihalocarbons interact with dinitrogen, or dioxygen, substituted hydrocarbons (e.g. the systems formed when 1,4-DITFB, or 1,4-DIB, interact with 4,4′-BPY [50], when 1,4-dinitrobenzene interacts with 1,4-DIB [158–162][1], and when 1,4-DITFB interacts with DABCO [163]) (Fig. 7).

Weaker XBs usually result in less linear geometries and this accounts for the waved geometry in the copolymer given by 1,4-DITFB with 1,4-dicyano,2,3,5,6-tetramethylbenzene [123] and for the reduced linearity of the homopolymer given by 4-bromobenzonitrile compared to 4-iodobenzonitrile [71].

Stepped infinite chain are formed when the binding sites, while remaining parallel, are no more collinear, but are translated from each other. Examples are the homopolymer given by 4′-bromo-2′,3′,5′,6′-tetrafluorostilbazole [163] and the copolymers obtained starting from bidentate XB donors having collinear sites, and XB acceptors with translated sites (e.g. the adducts 1,4-DITFB/BPE, 1,4-dibromotetrafluorobenzene (1,4-DBTFB)/BPE [49, 50], 1,4-

[1] M. Bolte, private communication, CCDC structure reference code ISIHUN)

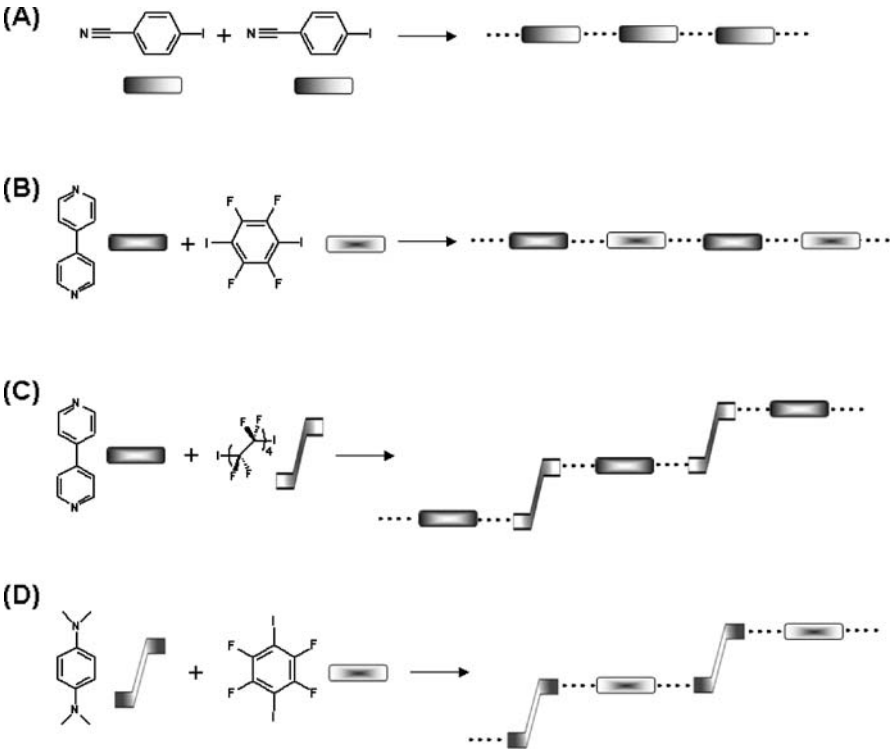


**Fig. 7** Linear 1D infinite chains formed on self-assembly of bidentate and self-complementary modules where donor and acceptor sites axes are parallel and coaxial (*A*), of bidentate donor and acceptor modules where donor and acceptor sites axes are parallel and coaxial (*B*), or are parallel and translated from each other in the XB donor (*C*) or acceptor (*D*) module, respectively

DITFB/1,4-bis(*N*,*N*-dimethylamino)benzene [64], diiodobutadiyne/dicyano and diiodobutadiyne/dipyridyl derivatives [80, 81]). Similarly, the stepped infinite chains geometry is obtained when XB acceptor tectons with collinear sites interact with stepped XB donors. Examples are the chains formed by TIE (e.g. with phenazine [129]), by (*E*)-1,2-diiododifluoroethene (e.g. with 1,4-BPY [164]), and by α,ω-diiodoperfluoroalkanes, or their dibromo analogues (e.g. with 1,4-BPY, pyrazine and its derivatives) wherein the perfluoroalkyl chain typically adopts a *trans* conformation along the carbon chain [124, 165–167]. Stepped 1D networks are generated also on self-assembly of tectons, both of which have parallel and translated binding sites (e.g. α,ω-dicyanoalkanes/α,ω-diiodoperfluoroalkane adducts [168] and TMEDA/(*E*)-1,2-diiododifluoroethene adduct [164]).

When the binding sites axes on starting modules are not parallel but form an angle, the resulting self-assembled chains assume a herringbone arrangement, the angles along the chain corresponding to the angles of binding sites

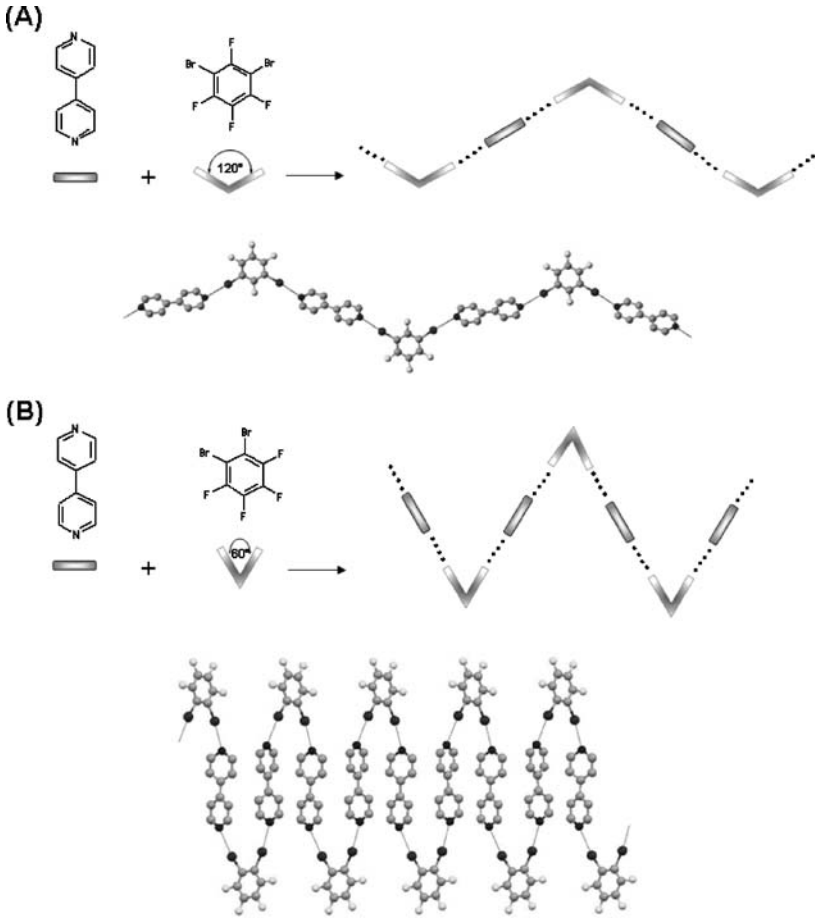


**Fig. 8** Herringbone 1D infinite chains formed on self-assembly of bidentate donor and acceptor modules wherein acceptor sites axes are parallel and coaxial and donor sites axes are angled

axes in starting modules. For instance, this happens when a linear module interacts with an angled partner, as is the case of 4,4′-BPY interacting with 1,3-DBTFB (angle 120°), 1,2-DBTFB (angle 60°) [49] or the corresponding diiodo analogues [169, 170]) (Fig. 8).

Zig-zag chains are also obtained starting from many other neutral tectons wherein the donor and/or acceptor sites have an angled geometry, e.g. (*Z*)-diazaalkenes [171][2], phosphine oxides [79], carbonyl [150], phosphoramidyl [124, 139], and sulfinyl [151] sites, tetrahedral molecules that work as bidentate modules (e.g. the adducts $CBr_4$/DABCO [172],

[2] A.L. Spek, private communication, CCDC structure reference code FEGYAR01

$CBr_4$/*N*,*N*,*N*′,*N*′-tetramethyl-*p*-phenylendiamine [134], $CBr_4$/4,4′-bis(*N*,*N*-dimethylaminophenyl)methane [134], $CHBr_3$/HMTA [173], $CHBr_3$/1,4-dimethoxybenzene [134], 1,4-DITFB/TMEDA[3], and other systems [64, 134, 147, 174–177]).

When halide anions are used as electron donors, they frequently work as bidentate modules with either linear or angled geometries. Thus, on interaction with bidentate XB donors, linear [83, 178, 179] or herringbone chains [57, 90, 92, 155, 180–185] are formed.

When the binding sites are conveniently pre-organized on the starting modules, topologies that recall 1D infinite chains are formed, also starting from polydentate modules. This is the case, for instance, of the ribbons [186, 187] given by a tetradentate module (where π–π interactions point the four arms two by two to opposite sides of the core), and the nanopillars [188] given by an hexadentate module (where a phosphazene scaffold directs the six pendants three by three to the opposite sides of the phosphazene ring). In both cases a linear bidentate partner works as connector of the polydentate modules and translates the polydentate module geometry into the supramolecular architecture geometry.

## 3.2 2D Architectures

When one, or both, the interactive modules are tridentate, bidimensional (2D) architectures can be formed. A frequently recurring pattern is the (6,3) network (honeycomb structure), which is sometimes formed when onium halides self-assemble with dihalocarbons. Halide anions work as tridentate XB acceptors and occupy the nodes while the dihalocarbons work as bidentate XB donors and form the sides that space the nodes. Such architectures are present in the co-crystals 1,4-DITFB/$Ph_4P^+Br^-$, 1,4-DITFB/$Me_4N^+I^-$ [155], and α,ω-diiodoperfluoroalkanes/K.2.2.2.⊂KI [128, 189]. The less planar the trigonal arrangement around the nodes, the more corrugated the honeycomb structure (Fig. 9).

The same (6,3) topology can be formed on self-assembly of tridentate XB donors with tridentate XB acceptors. After this self-assembly paradigm, the complementary partners alternate at the nodes of the 2D architecture. Examples are the co-crystals $CHI_3$/HMTA [190], $CHI_3$/$Ph_4P^+Cl^-$ [183], $CHI_3$/$BnMe_3N^+I^-$ [191], $CBr_4$/*n*-$Bu_4N^+Br^-$ [192], and $CBr_4$/*n*-$Bu_4N^+SCN^-$ [134]. In these structures the halomethane molecules obviously have a tetrahedral geometry and the XB linearity translates the pyramidal arrangement of these tectons, which sit at the nodes of the network, into the corrugation of the honeycomb structure (Fig. 10).

[3] M. Bolte, private communication, CCDC structure reference code QIHCOZ01

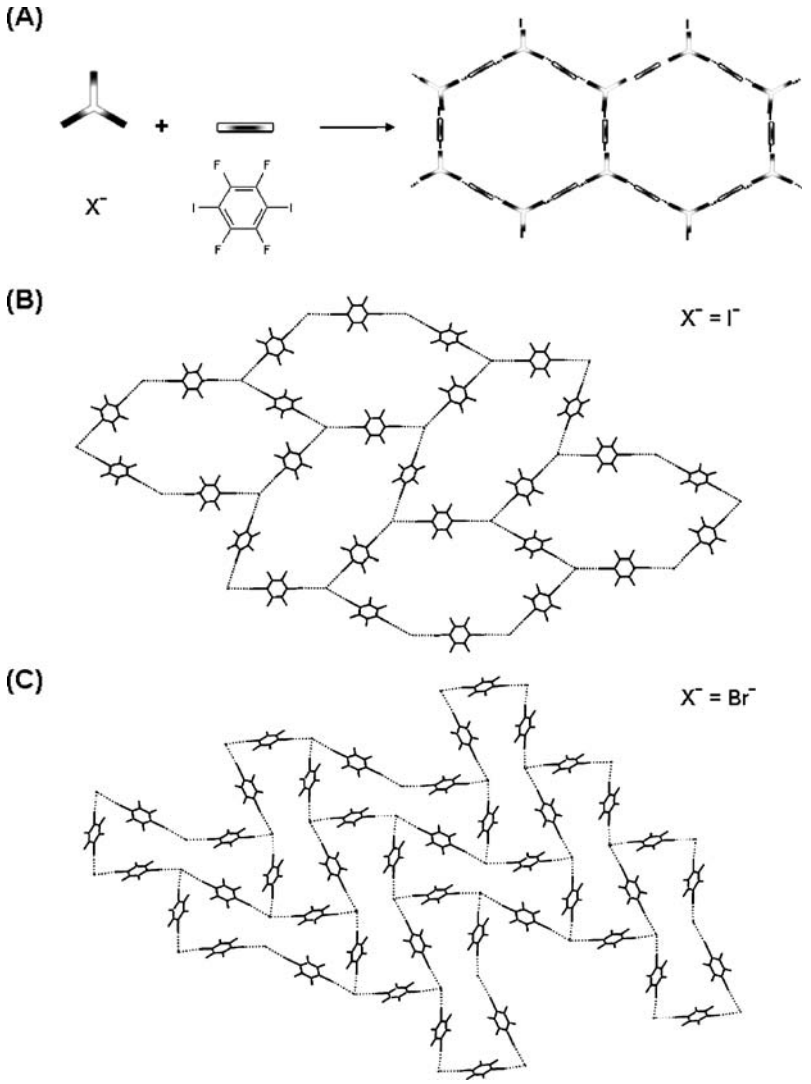


**Fig. 9** Honeycomb-like architectures formed on self-assembly of halide anions (which work as tridentate XB acceptors and sit at the networks nodes) with 1,4-DITFB (which works as bidentate donor and forms network sides) (**A**). The angles formed by the XBs around the halide anions determine the corrugation of the honeycomb architecture, a more planar arrangement around the halide anions (as is the case of the iodide anions in adduct 1,4-DITFB/$Me_4P^+I^-$ (**B**) with respect to the bromide anions in adduct 1,4-DITFB/$Ph_4P^+Br^-$ (**C**)) results in a less corrugated honeycomb architecture

The self-assembly of tridentate modules with bi- or tridentate partners may afford architectures other than the (6.3) nets described above. For instance, in the co-crystal 1,4-DITFB/$Ph_4P^+I^-$ the iodide anions work as

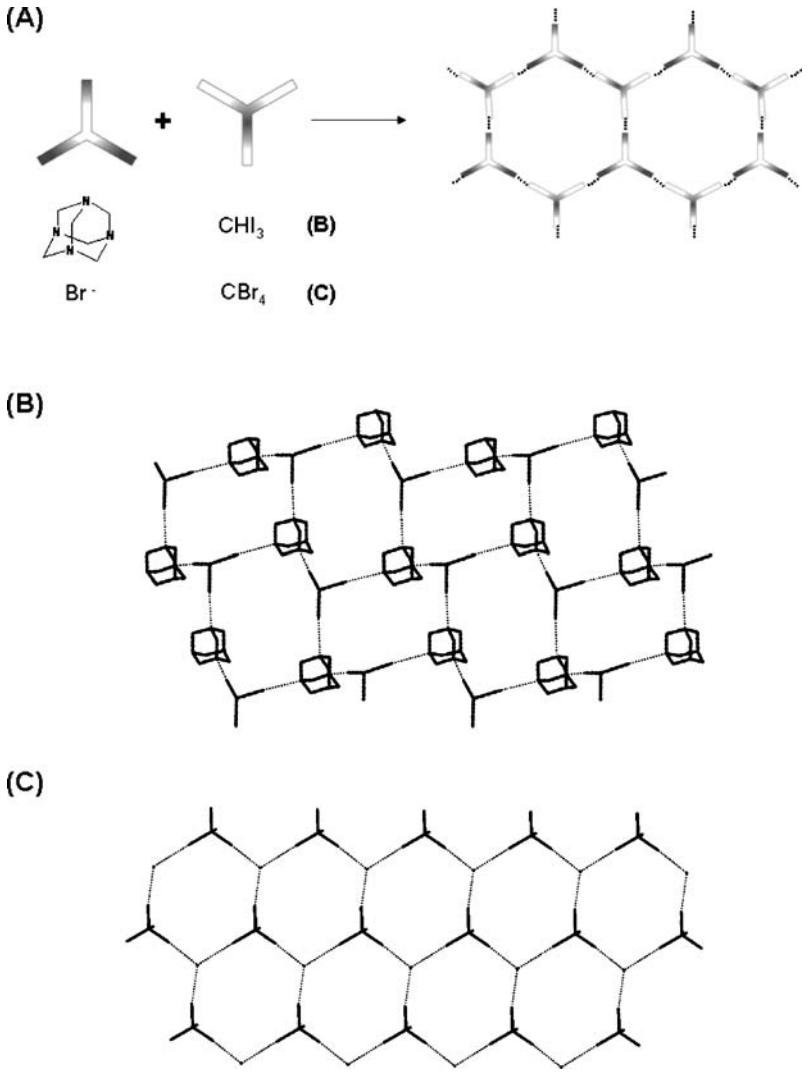


**Fig. 10** Honeycomb-like architectures formed on self-assembly of tridentate XB donors with tridentate XB acceptors

T-shaped tridentate nodes, the diiodobenzenes as linear bidentate modules that space the nodes and ribbons compounded of consecutive rectangles are formed [155] (Fig. 11). A similar topology is present in the co-crystal $CBr_4/Ph_4P^+Br^-$ where bromide anions and carbon tetrabromide both work as tridentate notes that alternate in the ribbon [121].

The overall crystal packing of both the 1D and the 2D networks described above frequently present a layered structure wherein cationic layers alternate

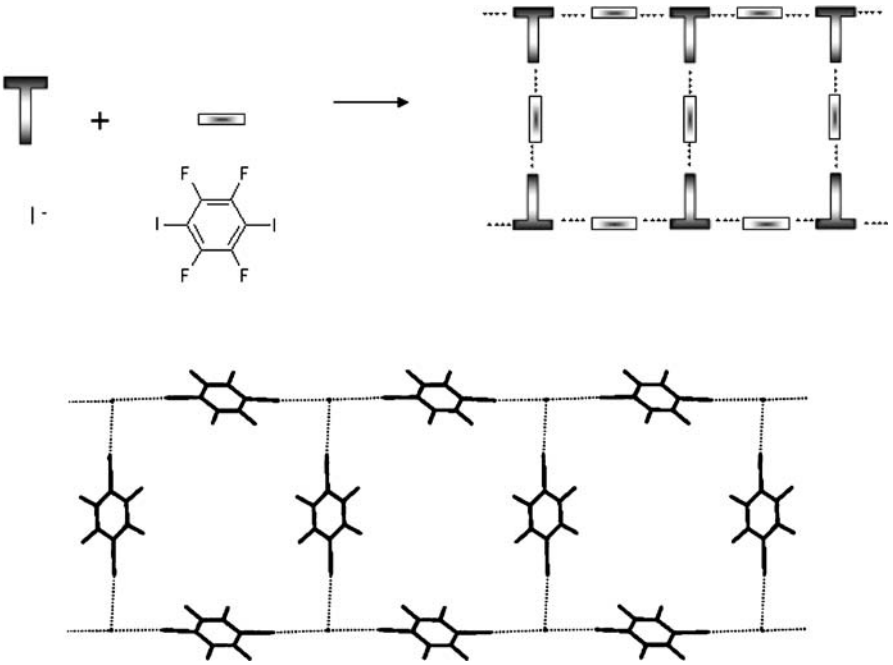


**Fig. 11** Ladder-type architecture formed by self-assembly of a tridentate module ($I^-$) with a bidentate module (1,4-DITFB)

with layers formed by the halogen-bonded supramolecular anions [83, 128, 155, 156, 178, 189, 193] (Fig. 12).

The layer thickness usually depends on the compounding module's size and an accurate metric engineering can be done according to which the length of starting module determines the thickness of the layer. This holds for self-assembled architectures wherein the XB acceptor is both an anionic [189] (Fig. 13) and a neutral tecton [168].

### 3.3 3D Architectures

When one, or both, of the interactive modules are tetradentate, bi- or tridimensional (3D) architectures can be formed. An example of 2D architecture is the (4,4) network present in the complex diiodoacetylene/$Ph_4P^+$ $Cl^-$ (and the analogous complexes formed by bromide or iodide anions) [194] as well as in the complex 1,6-diiodoperfluorohexane/tetrakis(4-pyridyl)pentaerythritol [195]. In all these complexes, the XB acceptor works as the tetradentate tecton sitting at the node of the network and the XB donor works as the linear bidentate module that spaces the nodes.

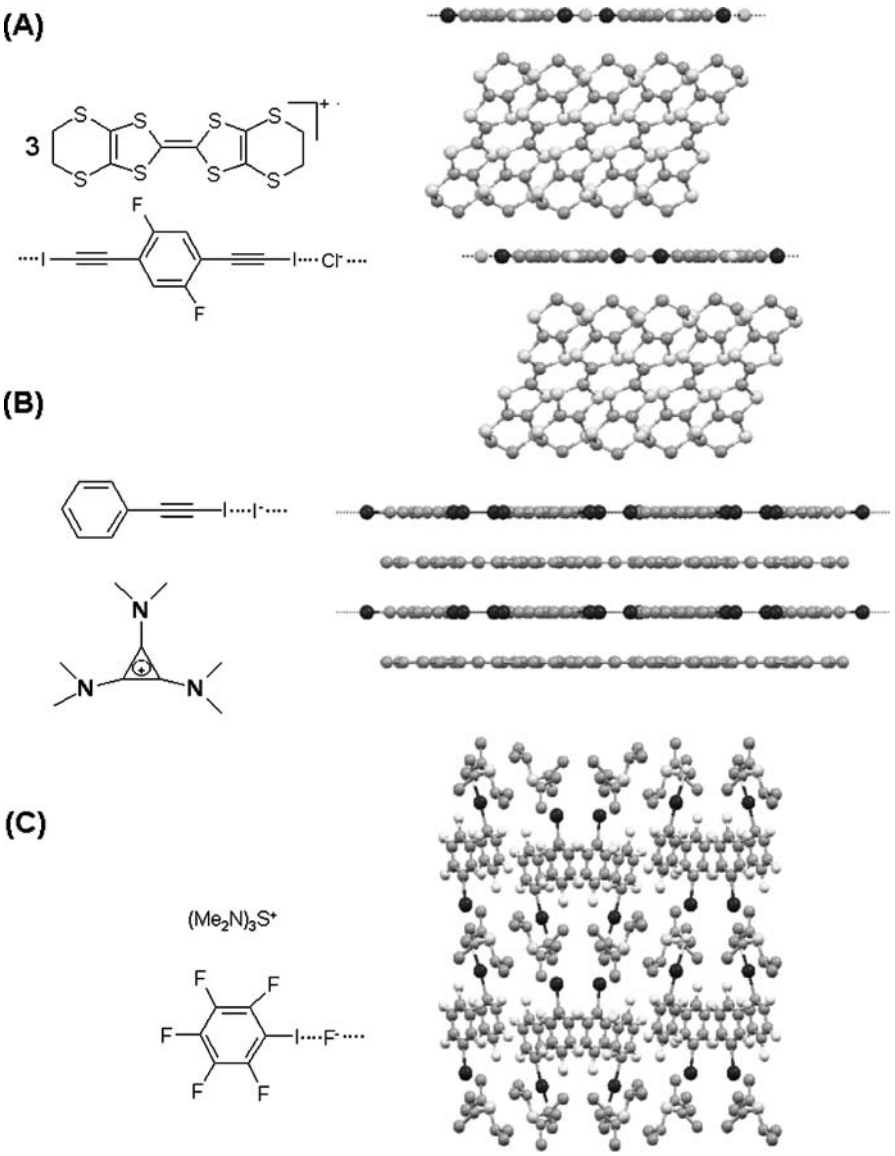


**Fig. 12** Examples of layered crystal packing wherein cationic layers alternate with anionic halogen-bonded layers

From a topological point of view, the homocrystal of 1,3-di(4-pyridyl)-2,4-di(4-iodiotetrafluorophenyl)cyclobutane, which is a self-complementary and tetradentate module, also presents a (4,4) net [176].

An example of 3D architecture is the adamantanoid network that is formed after various self-assembly protocols. This network is in fact present in the

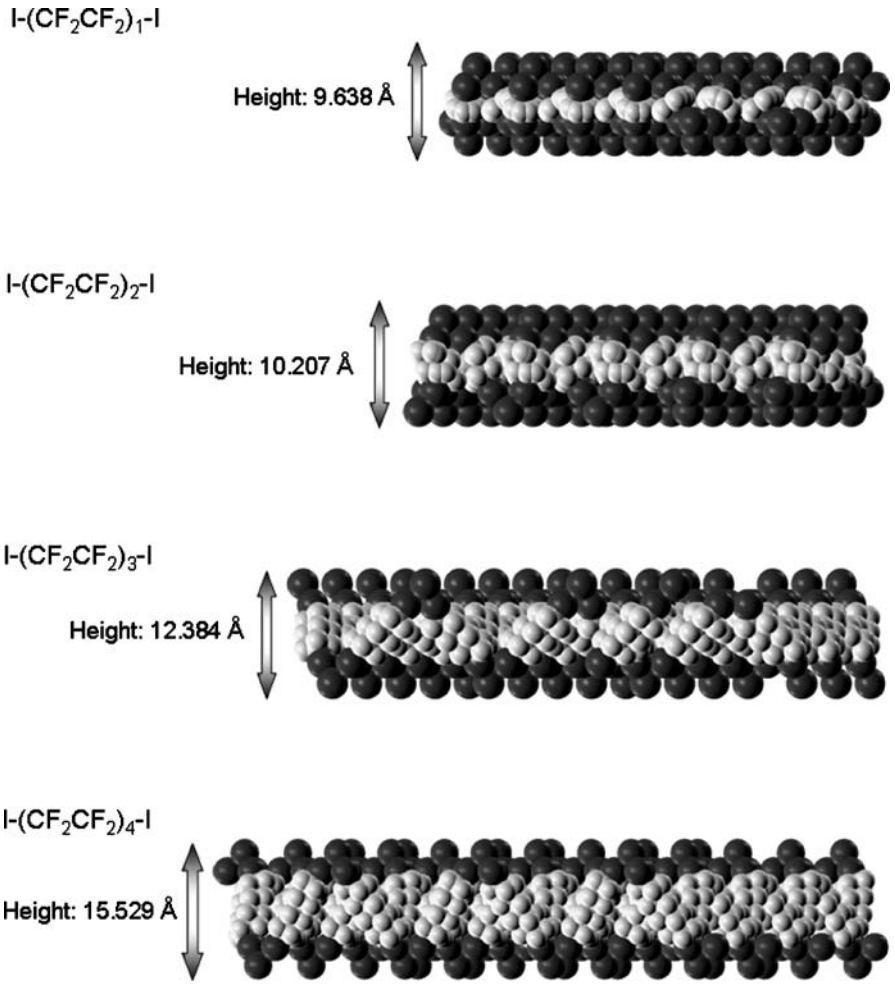


**Fig. 13** Self-assembled architectures wherein the XB acceptor is $I^-$ and the donors are differently sized $\alpha,\omega$-diiodoperfluoroalkanes. The layer thickness depends on the size of the XB donor module, thus allowing an accurate metric engineering of the layers to be realized

homocrystal of self-complementary tetradentate modules (e.g. 4,4′-diiodo-4″,4‴-dinitrotetraphenylmethane [196], and in a variety of co-crystals) (Fig. 14).

For instance, adamantanoid architectures are formed on the self-assembly of tetradentate XB donors with tetradentate XB acceptors, both the complementary tectons alternating at the nodes of the network (this is the case in the complex $CBr_4/Et_4N^+Cl^-$ and its bromide and iodide analogues [192], in the complex tetrakis(4-pyridyl)pentaerythritol/tetrakis(4-iodiotetrafluorophenyl)pentaerythritol [195], and in other systems [197]).

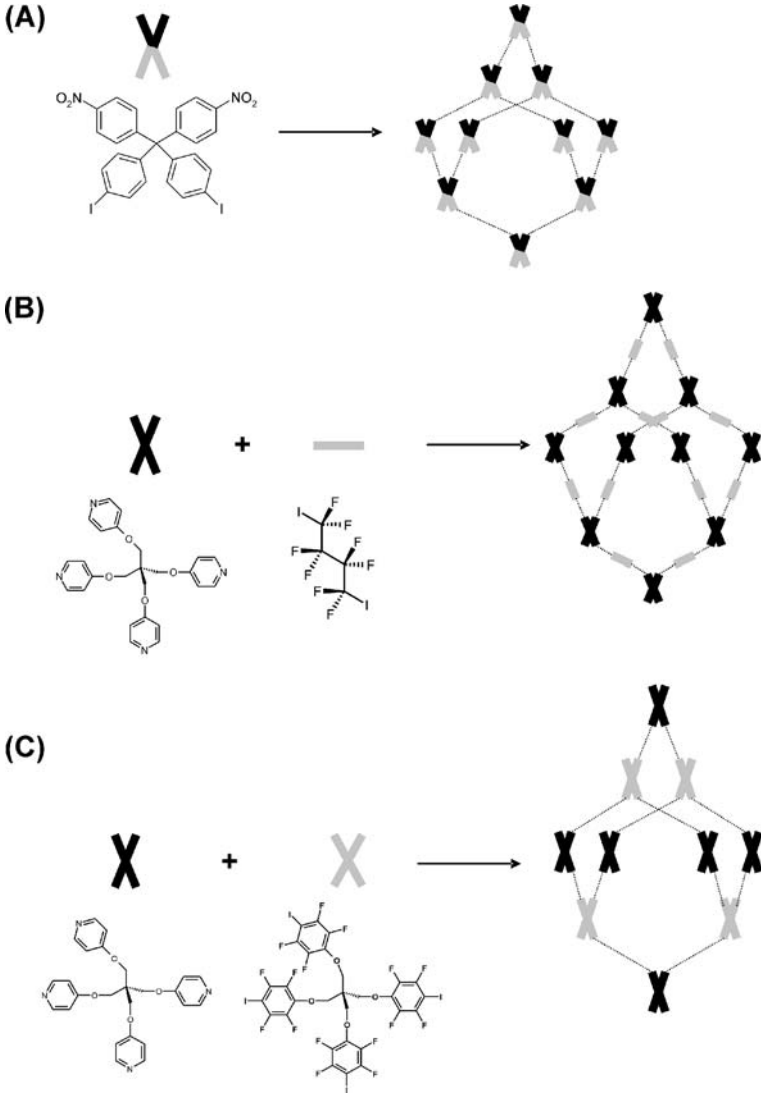


**Fig. 14** Different adamantanoid architectures formed on self-assembly of: *A* a self-complementary tetradentate module; *B* a tetradentate XB acceptor and a bidentate XB donor; *C* a tetradentate XB acceptor and a tetradentate XB donor

Adamantanoid architectures are formed also on the self-assembly of tetradentate XB acceptors, that sit at the nodes, with bidentate XB donors, that work as nodes spacers (e.g. in the complex 1,4-diiodooctafluorobutane/tetrakis(4-pyridyl)pentaerythritol [195]).

The halogen-bonded 2D and 3D networks described above frequently present large meshes. As is the case for similarly sized networks, which are

assembled thanks to hydrogen bonding or other interactions [198–202], the empty space potentially present in the overall crystal packing is filled by solvent molecules or through interpenetration [189, 195, 196]. The XB role and potential with respect to these phenomena of the overall crystal packing still have to be established.

## 4 Conclusions

It has been shown how the XB is a specific, directional, and strong interaction that can be successfully employed as a general protocol to drive the self-assembly of a wide diversity of molecular modules.

Paraphrasing Corey's historic definition of synthon [203], Desiraju defined a supramolecular synthon as a structural unit within a supermolecule that can be formed or assembled by known or conceivable synthetic operations involving intermolecular interactions [204]. The robustness of the XB has allowed several supramolecular synthons based on this interaction to be identified and some examples have been presented in this chapter.

According to Wuest's definition [205, 206], a tecton is a molecule that interacts with its neighbours in strong and well-defined ways, as it inherently possesses the molecular structure and intermolecular recognition features to predictably self-assemble into crystalline networks. Iodine atoms, and to a lesser extent bromine atoms, can be used to build up reliable tectons. In fact, whenever the electropositive crown present in the polar region of these halogens is incremented by electron-withdrawing neighbouring groups, these halogens effectively work as "sticky sites" that direct molecular association. Several cases of such XB-based tectons have been discussed above. Thanks to this potential in identifying and designing supramolecular synthons and tectons, the XB can be considered as a new paradigm in supramolecular chemistry. Halocarbons work as effective XB-based tectons for the construction of a wide and predictable diversity of architectures. Using fancier words, it can be stated that halocarbons are the blocks for the construction of an XB-based Legoland. While XB-based crystal engineering is still in its infancy, the growing interest in the field promises remarkable future advancements.

The ability of XB to control recognition, self-organization, and self-assembly processes in the different phases of matter is clearly emerging in the literature. This chapter focusses on self-assembly in the solid phase, while the chapters of B. Duncan and A. Legon (in this volume) deal with the liquid crystalline phase and gas phase, respectively. Relatively few papers are reported in the literature on self-assembly processes in solution [66–68, 207, 208]. Several analytical techniques have been used to detect XB formation, to define its nature, to establish its energetic and geometric characteristics, and to reveal

the striking similarities between XB and HB (e.g. IR and Raman spectroscopies [209–213], $^{19}$F [67, 68, 213–215], $^{14}$N [67], $^{1}$H [216–220] and $^{13}$C [57, 221, 222] NMR spectroscopies, NQR [223, 224], ESR [225], XPS [226], UV-vis spectroscopy [66, 134, 171, 227, 228], dielectric polarization [229–234], calorimetric analysis [235], GC analysis [236, 237], vapour phase pressure [238, 239]). All these techniques consistently prove the existence and the relevance of XB also in solution, but an XB-based supramolecular chemistry in the liquid phase still remains to be fully developed.

## References

1. Lehn JM (1988) Angew Chem Int Ed 27:89
2. Braga D (2003) Chem Commun 22:2751
3. Metrangolo P, Resnati G (2001) Chem Eur J 7:2511
4. Metrangolo P, Pilati T, Resnati G, Stevenazzi A (2003) Curr Opin Colloid Interface Sci 8:215
5. Metrangolo P, Resnati G, Pilati T, Liantonio R, Meyer F (2007) J Polym Sci Part A Polym Chem 45:1
6. Fox BD, Liantonio R, Metrangolo P, Pilati T, Resnati G (2004) J Fluor Chem 125:271
7. Messina MT, Metrangolo P, Resnati G (2000) Resolution of racemic perfluorocarbons through self-assembly driven by donor–acceptor intermolecular recognition. In: Ramachandran PV (ed) Asymmetric fluoro-organic chemistry: synthesis, applications, and future directions. ACS symposium series 746. American Chemical Society, Washington DC, p 239
8. Metrangolo P, Pilati T, Resnati G (2004) Self-assembly of hybrid fluorous materials. In: Gladysz JA, Curran DP, Horwath IT (eds) Handbook of fluorous chemistry. Wiley, Weinheim, p 507
9. Metrangolo P, Neukirch H, Pilati T, Resnati G (2005) Acc Chem Res 38:386
10. Metrangolo P, Resnati G (2004) Halogen bonding. In: Atwood JL, Steed JW (eds) Encyclopedia of supramolecular chemistry. Dekker, New York, pp 628–635
11. Alkorta I, Rozas I, Elguero J (1998) J Phys Chem A 102:9278
12. Karpfen A (2003) Theor Chem Acc 110:1
13. Syssa-Magalé JL, Boubekeur K, Palvadeau P, Meerschaut A, Schöllhorn B (2005) Cryst Eng Comm 7:302
14. Prout CK, Kamenar B (1973) Crystal structures of electron-donor-acceptor complexes. In: Foster R (ed) Molecular complexes. Elek, London, pp 151–207
15. Foster R (1969) Crystal structures. In: Blomquist AT (ed) Organic charge-transfer complexes. Academic, London, pp 216–251
16. Bent HA (1968) Chem Rev 68:587
17. Hassel O (1970) Science 170:497
18. Legon AC (1999) Angew Chem Int Ed 38:2686
19. Brisdon AK (2006) Annu Rep Prog Chem Sect A Inorg Chem 102:160
20. Blake JA, Devillanova FA, Gould RO, Li WS, Lippolis V, Parson S, Radek C, Schroder M (1998) Chem Soc Rev 27:195
21. Ouvrard C, Le Questel JY, Berthelot M, Laurence C (2003) Acta Crystallogr Sect B: Struct Sci 59:512
22. du Mont WW, Ruthe F (1999) Coord Chem Rev 189:101

23. Amati M, Lelj F, Liantonio R, Metrangolo P, Luzzati S, Pilati T, Resnati G (2004) J Fluor Chem 125:629
24. Lenoir D, Chiappe C (2003) Chem Eur J 9:1037
25. Legon AC (1998) Chem Eur J 4:1890
26. Adams CJ, Bowen LE (2005) Dalton Trans, p 2239
27. Swierczynski D, Luboradzki R, Dolgonos G, Lipkowski J, Schneider HJ (2005) Eur J Org Chem, p 1172
28. Sanrame CN, Suhrada CP, Dang H, Garcia-Garibay MA (2003) J Phys Chem A 107:3287
29. Guthrie F (1863) J Chem Soc 16:239
30. Seamon WH, Mallet JW (1881) Chem N 44:188
31. Roussopoulos O (1883) Ber 16:202
32. Bjorvatten T, Hassel O (1962) Acta Chem Scand 16:249
33. Remsen I, Norris JF (1896) Am Chem J 18:90
34. Dumas JM, Gomel M, Guerin M (1983) Molecular interactions involving organic halides. In: Patai S, Rappoport Z (eds) The chemistry of functional groups, supplement D. Wiley, New York, pp 985–1020
35. Xu K, Ho DM, Pascal RA Jr (1994) J Am Chem Soc 116:105
36. Corradi E, Meille SV, Messina MT, Metrangolo P, Resnati G (2000) Angew Chem Int Ed 39:1782
37. Bernard-Houplain MC, Sandorfy C (1973) Can J Chem 51:3640
38. Di Paolo T, Sandorfy C (1974) Chem Phys Lett 26:466
39. Di Paolo T, Sandorfy C (1974) Can J Chem 52:3612
40. Trudeau G, Cole KC, Massuda R, Sandorfy C (1978) Can J Chem 56:1681
41. Di Paolo T, Sandorfy C (1974) Nature 252:471
42. Massuda R, Sandorfy C (1977) Can J Chem 55:3211
43. Bernard-Houplain MC, Sandorfy C (1973) Can J Chem 51:1075
44. Awwadi FF, Willet RD, Peterson KA, Twamley B (2006) Chem Eur J 12:8952
45. Politzer P, Lane P, Concha MC, Ma Y, Murray JS (2007) J Mol Model 13:305
46. Auffinger P, Hays FA, Westhof E, Ho PS (2004) Proc Natl Acad Sci USA 101:16789
47. Fourmigué M, Betail P (2004) Chem Rev 104:5379
48. Lommerse JPM, Stone AJ, Taylor R, Allen FH (1996) J Am Chem Soc 118:3108
49. De Santis A, Forni A, Liantonio R, Metrangolo P, Pilati T, Resnati G (2003) Chem Eur J 9:3974
50. Walsh RB, Padgett CW, Metrangolo P, Resnati G, Hanks TW, Pennington WT (2001) Cryst Growth Des 1:165
51. Clark T, Hennemann M, Murray JS, Politzer P (2007) J Mol Model 13:291
52. Valerio G, Raos G, Meille SV, Metrangolo P, Resnati G (2000) J Phys Chem A 104:1617
53. Weiss R, Schwab O, Hampel F (1999) Chem Eur J 5:968
54. Brammer L, Bruton EA, Sherwood P (2001) Cryst Growth Des 1:277
55. Dey A, Jetti RKR, Boese R, Desiraju GR (2003) Cryst Eng Comm 5:248
56. Lu YX, Zou JW, Wang YH, Zhang HX, Y QS, Jiang YJ (2006) THEOCHEM 766:119
57. Lohr H-G, Engel A, Josel H-P, Vogale F, Schuh W, Puff H (1984) J Org Chem 49:1621
58. Metrangolo P, Pilati T, Resnati G (2006) Cryst Eng Comm 8:946
59. Ananthavel SP, Manoharan M (2001) Chem Phys 269:49
60. Dunstan S, Henbest HB (1957) J Chem Soc 4905
61. Mulliken RS (1952) J Phys Chem 56:801
62. McAlpine RK (1952) J Am Chem Soc 74:725
63. Chen QY, Li ZT, Zhou CM (1993) J Chem Soc Perkin Trans 1:2457
64. Liantonio R, Luzzati S, Metrangolo P, Pilati T, Resnati G (2002) Tetrahedron 58:4023

65. Neukirch H, Guido E, Liantonio R, Metrangolo P, Pilati T, Resnati G (2005) Chem Commun, p 1534
66. Walsh PL, Ma S, Obst U, Rebek J Jr (1999) J Am Chem Soc 121:7973
67. Messina T, Metrangolo P, Panzeri W, Ragg E, Resnati G (1998) Tetrahedron Lett 39:9069
68. Metrangolo P, Panzeri W, Recupero F, Resnati G (2002) J Fluor Chem 114:27
69. Bjovatten T (1968) Acta Chem Scand 22:410
70. Borgen B, Hassel O, Romming C (1962) Acta Chem Scand 16:2469
71. Desiraju GR, Harlow RL (1989) J Am Chem Soc 111:6757
72. Bond AD, Griffiths J, Rawson JM, Hulliger J (2001) Chem Commun, p 2488
73. Britton D, Gleason WB (1977) Acta Crystallogr Sect B: Struct Sci 33:3926
74. Burdeniuc J, Sanford M, Crabtree RH (1998) J Fluor Chem 91:49
75. Burdeniuc J, Crabtree RH, Rheingold AL, Yap GPA (1997) Bull Soc Chim Fr 134:955
76. Beck CM, Burdeniuc J, Crabtree RH, Rheingold AL, Yap GPA (1998) Inorg Chim Acta 270:559
77. Burdeniuc J, Crabtree RH (1998) Organometallics 17:1582
78. Zou J-W, Jiang Y-J, Guo M, Hu G-X, Zhang B, Liu H-C, Yu Q-S (2005) Chem Eur J 11:740
79. Gao K, Goroff NS (2000) J Am Chem Soc 122:9320
80. Sun A, Lauher JW, Goroff NS (2006) Science 312:1030
81. Goroff NS, Curtis SM, Webb JA, Fowler FW, Lauher J (2005) Org Lett 7:1891
82. Ghassemzadeh M, Harms K, Dehnicke H (1996) Chem Ber 129:115
83. Yamamoto HM, Maeda R, Yamaura J-I, Kato R (2001) J Mater Chem 11:1034
84. Gagnaux P, Susz BP (1960) Helv Chim Acta 43:948
85. Bock H, Holl S (2001) Z Naturforsch B: Chem Sci 56:111
86. Hassel O (1965) Acta Chem Scand 19:2259
87. Dahl T, Hassel O (1965) Acta Chem Scand 19:2000
88. Holmesland O, Rømming C (1966) Acta Chem Scand 20:2601
89. Kuhn N, Abu-Rayyan A, Eichele K, Schwarz S, Steimann M (2004) Inorg Chim Acta 357:1799
90. Logothetis TA, Meyer F, Metrangolo P, Pilati T, Resnati G (2004) New J Chem 28:760
91. Jones PG, Lozano V (2003) Acta Crystallogr Sect E: Struct Rep Online E59:o632
92. Kuhn N, Abu-Rayyan A, Steimann M (2003) Z Anorg Allg Chem 629:2066
93. Freytag M, Jones PG (2001) Z Naturforsch B: Chem Sci 56b:889
94. Freytag M, Jones PG, Ahrens B, Fischer AK (1999) New J Chem 23:1137
95. Imakubo T, Tajima N, Shirahata T, Miyake A, Sawa H, Nakamura T, Ohnuki H, Tamura M, Kato R, Izumi M, Nishio Y, Kajiata K (2003) Synth Met 135–136:601
96. Imakubo T, Tajima N, Kato R, Nishio Y, Kajita K (2003) Synth Met 133–134:181
97. Devic T, Domercq B, Auban-Senzier P, Molinié P, Fourmigué M (2002) Eur J Inorg Chem 2844
98. Yamamoto HM, Maeda R, Yamaura J-I, Kato R (2001) Synth Met 120:781
99. Imakubo T, Sawa H, Kato R (1995) Chem Commun, p 1667
100. Domercq B, Devic T, Fourmigué M, Auban-Senzier P, Canadell E (2001) J Mater Chem 11:1570
101. Devic T, Bertran JN, Domercq B, Canadell E, Avarvari N, Auban-Senzier P, Fourmigué M (2001) New J Chem 11:1418
102. Kato R, Imakubo T, Yamamoto H, Maeda R, Fujwara M, Yamaura JI, Sawa H (2002) Mol Cryst Liq Cryst 380:61
103. Imakubo T, Sawa H, Kato R (1997) Synth Met 86:1847
104. Fourmigué M, Dautel OJ, Devic T, Domercq B (2003) Synth Met 133–134:317

105. Shirahata T, Kibune M, Maesato M, Kawashima T, Saito G, Imakubo T (2006) J Mater Chem 16:3381
106. Imakubo T, Shirahata T, Hervé K, Ouahab L (2006) J Mater Chem 16:162
107. Weiss R, Rechinger M, Hampel F (1994) Angew Chem Int Ed 33:893
108. Leser J, Rabinovich D (1978) Acta Crystallogr Sect B: Struct Sci 34:2250
109. Scherfise KD, Weller F, Dehnicke K (1985) Z Naturforsch B: Chem Sci 40:906
110. Vogt H, Lauritsen K, Riesel L, von Lowis M, Reck G (1993) Z Naturforsch B: Chem Sci 48:1760
111. Bozopoulos A, Kavounis CA (2004) Z Kristallogr – New Cryst Struct 219:501
112. Gustafsson B, Håkansson M, Jagner S (2005) Inorg Chim Acta 358:1309
113. Saha MK, Bernal I, Fronczek FR (2004) Chem Commun, p 84
114. Haberecht M, Lerner HW, Bolte M (2006) Acta Crystallogr Sect E: Struct Rep Online E62:o2836
115. Zhdankin VV, Callies JA, Hanson KJ, Bruno J (1999) Tetrahedron Lett 40:1839
116. Foucaud A (1983) Positive halogen compounds. In: Pattai S, Rappoport Z (eds) The chemistry of functional groups, supplement D. Wiley, New York, pp 441–480
117. Creighton JA, Thomas KM (1972) J Chem Soc Dalton Trans 1972:403
118. Metrangolo P, Meyer F, Resnati G, Ursini M (2005) In: Soloshonok VA (ed) Fluorine-containing synthons. ACS symposium series 911. Oxford University Press/American Chemical Society, Washington, DC, p 514
119. Zhu S, Jiang H, Zhao J, Li Z (2005) Cryst Growth Des 5:1675
120. Vogt H, Frauendorf C, Fischer A, Jones PG (1995) Z Naturforsch B: Chem Sci 50:223
121. Lindner HJ, Kitschke-von Gross B (1976) Chem Ber 109:314
122. Messina MT, Metrangolo P, Panzeri W, Pilati T, Resnati G (2001) Tetrahedron 57:8543
123. Britton D, Gleason WB (2002) Acta Crystallogr Sect E: Struct Rep Online E58:o1375
124. Chu Q, Wang Z, Huang Q, Yan C, Zhu S (2003) New J Chem 27:1522
125. Zhu S, He P (2005) Tetrahedron 61:5679
126. Zhu S, Xu B, Qin C, Xu G (1997) Inorg Chem 36:4909
127. Zongzhen L, Chaozhou N, Yilin M (1984) Huagong Xuebao (Chin Ed) 42:120
128. Liantonio R, Metrangolo P, Pilati T, Resnati G (2003) Cryst Growth Des 3:355
129. Bailey RD, Hook LL, Watson RP, Hanks TW, Pennington WT (2000) Cryst Eng 3:155
130. Tebbe KF, Grafe-Kavoosian A (1996) Z Naturforsch B: Chem Sci 51:1007
131. Tebbe KF, Frohlich R (1983) Z Anorg Allg Chem 505:7
132. Tebbe KF, Frohlich R (1983) Z Anorg Allg Chem 505:19
133. Bock H, Holl S (2002) Z Naturforsch B: Chem Sci 57:843
134. Rosokha SV, Neretin IS, Rosokha TY, Hecht J, Kochi JK (2006) Heteroat Chem 17:449
135. Batsanov AS, Howard JAK (2000) Acta Crystallogr Sect C: Cryst Struct Commun C56:252
136. Romaniello P, Lelj F (2002) J Phys Chem A 106:9114
137. Bondi A (1964) J Phys Chem 68:441
138. Pedireddi VR, Shekhar Reddy D, Satish Goud B, Craig DC, Rae AD, Desiraju GR (1994) J Chem Soc Perkin Trans II 11:2353
139. Chu Q, Zhemin W, Huang Q, Yan C, Zhu S (2001) J Am Chem Soc 123:11069
140. Bjorvatten T, Hassel O (1961) Acta Chem Scand 15:1429
141. Gagnaux P, Susz BP (1960) Helv Chim Acta 43:948
142. Navarrini W, Metrangolo P, Pilati T, Resnati G (2000) New J Chem 24:777
143. Forni A, Metrangolo P, Pilati T, Resnati G (2004) Cryst Growth Des 4:291
144. Padgett CW, Walsh RD, Drake GW, Hanks TW, Pennington WT (2005) Cryst Growth Des 5:745
145. Imakubo T, Maruyma T, Sawa H, Kobayashi K (1998) Chem Commun 1998:2021

146. Imakubo T, Kibune M, Yoshino H, Shirahata T, Yoza K (2006) J Mater Chem 16:4110
147. Crihfield A, Hartwell J, Phelps D, Walsh RB, Harris JL, Payne JF, Pennington WT, Hanks TW (2003) Cryst Growth Des 3:313
148. Leroy J, Schöllhorn B, Syssa-Magalé J-L, Boubekeur K, Palvadeau P (2004) J Fluor Chem 125:1379
149. Pigge FC, Vangala VR, Swenson DC (2006) Chem Commun, p 2123
150. Syssa-Magalé J-L, Boubekeurb K, Schöllhorn B (2005) J Mol Struct 737:103
151. Britton D (2003) Acta Crystallogr, Sect E: Struct Rep Online E59:o1332
152. Naso F, Cardellicchio C, Capozzi MAM, Capitelli F, Bertolasi V (2006) New J Chem 30:1782
153. Syssa-Magalé J-L, Boubekeur K, Palvadeau P, Meerschaut A, Schollhorn B (2004) J Mol Struct 691:79
154. Thaimattam R, Xue F, Sarma JARP, Mak TCW, Desiraju GR (2001) J Am Chem Soc 123:4432
155. Grebe J, Geiseler G, Harms K, Dehnicke K (1999) Z Naturforsch B: Chem Sci 54:77
156. Farnham WB, Dixon DA, Calabrese JC (1988) J Am Chem Soc 110:8453
157. Ahrens B, Jones PG (1999) Acta Crystallogr Sect C: Cryst Struct Commun 55:1308
158. Allen FH, Goud BS, Hoy VJ, Howard JAK, Desiraju GR (1994) Chem Commun, p 2729
159. Sarma JARP, Allen FH, Hoy VJ, Howard JAK, Thaimattam R, Biradha K, Desiraju GR (1997) Chem Commun, p 101
160. Hulliger J, Langley PJ (1998) Chem Commun, p 2557
161. Masciocchi N, Bergamo M, Sironi A (1998) Chem Commun, p 1347
162. Ranganathan A, Pedireddi VR (1998) Tetrahedron Lett 39:1803
163. Lucassen ACB, Vartanian M, Leitus G, van der Boom ME (2005) Cryst Growth Des 5:1671
164. Burton DD, Fontana F, Metrangolo P, Pilati T, Resnati G (2003) Tetrahedron Lett 44:645
165. Corradi E, Mille SV, Messina MT, Metrangolo P, Resnati G (1999) Tetrahedron Lett 40:7519
166. Cardillo P, Corradi E, Lunghi A, Mille SV, Messina MT, Metrangolo P, Resnati G (2000) Tetrahedron 56:5535
167. Dahl T, Hassel O (1968) Acta Chem Scand 22:2851
168. Metrangolo P, Pilati T, Resnati G, Stevenazzi A (2004) Chem Commun, p 1492
169. Liantonio R, Metrangolo P, Pilati T, Resnati G (2002) Acta Crystallogr: Struct Rep Online E58:575
170. Jay JI, Padgett CW, Walsh RDB, Hanks TW, Pennington WT (2001) Cryst Growth Des 1:501
171. Blackstock SC, Kochi JK (1987) J Am Chem Soc 109:2484
172. Blackstock SC, Lorand JP, Kochi JK (1987) J Org Chem 52:1451
173. Dahl T, Hassel O (1971) Acta Chem Scand 25:2168
174. Guardigli C, Liantonio R, Mele ML, Metrangolo P, Resnati G (2003) Supramol Chem 15:177
175. Messina MT, Metrangolo P, Quici S, Manfredi A, Pilati T, Resnati G (2000) Supramol Chem 12:405
176. Marras G, Metrangolo P, Meyer F, Pilati T, Resnati G (2006) New J Chem 30:1397
177. George S, Nangia A, Lam C-K, Mak TCW, Nicoud J-F (2004) Chem Commun, p 1202
178. Yamamoto HM, Yamaura J-I, Kato R (1998) J Mater Chem 8:15
179. Casnati A, Liantonio R, Metrangolo P, Resnati G, Ungaro R, Ugozzoli F (2006) Angew Chem Int Ed 45:1915

180. Thalladi VR, Sathish Goud B, Hoy VJ, Allen FH, Howard JAK, Desiraju GR (1996) Chem Commun, p 401
181. Weiss R, Rechinger M, Hampel F, Wolski A (1995) Angew Chem Int Ed 34:441
182. Gattuso G, Liantonio R, Metrangolo P, Meyer F, Resnati G, Pappalardo A, Parisi MF, Pilati T, Pisagatti I (2006) Supramol Chem 18:235
183. Bock H, Holl S (2001) Z Naturforsch B: Chem Sci 56:152
184. Yamamoto HM, Yamaura J-I, Kato R (1999) Synth Met 102:1448
185. Yamamoto HM, Yamaura J-I, Kato R (1999) Synth Met 102:1515
186. Caronna T, Liantonio R, Logothetis TA, Metrangolo P, Pilati T, Resnati G (2004) J Am Chem Soc 126:4500
187. Guido E, Metrangolo P, Panzeri W, Pilati T, Resnati G, Ursini M, Logothtis TA (2006) J Fluor Chem 126:197
188. Bertani R, Chaux F, Gleria M, Metrangolo P, Milani R, Pilati T, Resnati G, Sansotera M, Venzo A (2007) Inorg Chim Acta 360:1191
189. Liantonio R, Metrangolo P, Meyer F, Pilati T, Navarrini W, Resnati G (2006) Chem Commun, p 1819
190. Dahl T, Hassel O (1970) Acta Chem Scand 24:377
191. du Mont W-W, Stenzel V, Jeske J, Jones PG, Sebald A, Pohl S, Saak W, Batcher M (1994) Inorg Chem 33:1502
192. Lindeman SV, Hecht J, Kochi JK (2003) J Am Chem Soc 125:11597
193. Weiss R, Rechinger M, Hampel F, Wolski A (1995) Angew Chem Int Ed 34:441
194. Ghassemzadeh M, Harms K, Dehnicke K (1996) Chem Ber 129:259
195. Metrangolo P, Meyer F, Pilati T, Proserpio DM, Resnati G (2007) Chem Eur J 13:5765
196. Thaimattam R, Sharma CVK, Clearfield A, Desiraju GR (2001) Cryst Growth Des 1:103
197. Shekhar Reddy D, Craig DC, Desiraju GR (1994) J Chem Soc, Chem Commun, p 1457
198. Blatov VA, Carlucci L, Ciani G, Proserpio DM (2004) Cryst Eng Comm 6:378
199. Baburin IA, Blatov VA, Carlucci L, Ciani G, Proserpio DM (2005) J Solid State Chem 178:2452
200. Carlucci L, Ciani G, Proserpio DM (2006) In: Braga D, Grepioni F (eds) Making crystals by design: methods, techniques and applications. Wiley, Weinheim, pp 58–86
201. Batten S (2007) Interpenetration http://www.chem.monash.edu.au/staff/sbatten/interpen/index.html, last visited: 30 July 2007
202. Batten SR, Robson R (1998) Angew Chem Int Ed 37:1460
203. Corey EJ (1967) Pure Appl Chem 14:19
204. Desiraju GR (1995) Angew Chem Int Ed 34:2311
205. Simard M, Su D, Wuest JD (1991) J Am Chem Soc 113:4696
206. Metrangolo P, Resnati G (2004) Halogen bonding. In: Atwood JL, Steed JW (eds) Encyclopedia of supramolecular chemistry. Dekker, New York, p 1484
207. Mele A, Metrangolo P, Neukirch H, Pilati T, Resnati G (2005) J Am Chem Soc 127:14972
208. Takeuchi T, Minato Y, Takase M, Shinmori H (2005) Tetrahedron Lett 46:9025
209. Messina MT, Metrangolo P, Navarrini W, Radice S, Resnati G, Zerbi G (2000) J Mol Struct 524:87
210. Mishra A, Pullin ADE (1971) Aust J Chem 24:2493
211. Cheetham NF, McNaught IJ, Pullin ADE (1974) Aust J Chem 27:973
212. Cheetham NF, McNaught IJ, Pullin ADE (1974) Aust J Chem 27:987
213. McNaught IJ, Pullin ADE (1974) Aust J Chem 27:1009
214. Van Dyke Tiers G (2000) J Fluor Chem 102:175
215. Larsen DW, Allred AL (1965) J Phys Chem 69:2400

216. Bruno TJ, Martire DE, Harbison MWP, Nikolic A, Hammer CF (1983) J Phys Chem 87:2430
217. Martire DE, Sheridan JP, King JW, O'Donnell SE (1976) J Am Chem Soc 98:3101
218. Green RD, Martin JS (1968) J Am Chem Soc 90:3659
219. Bertrán JF, Rodríguez M (1979) Org Magn Res 12:92
220. Bertrán JF, Rodríguez M (1980) Org Magn Res 14:244
221. Glaser R, Chen N, Wu H, Knotts N, Kaupp M (2004) J Am Chem Soc 126:4412
222. Rege PD, Malkina OL, Goroff NS (2002) J Am Chem Soc 124:370
223. Semin GK, Babushkina TA, Khrlakyan SP, Pervova EY, Shokina VV, Knunyants IL (1968) Teor Exsp Khim 4:275
224. Semin GK, Babushkina TA, Khrlakyan SP, Pervova EY, Shokina VV, Knunyants IL (1968) Chem Abstr 69:72685z
225. Mugnaini V, Punta C, Liantonio R, Metrangolo P, Recupero F, Resnati G, Pedulli GF, Lucarini M (2006) Tetrahedron Lett 47:3265
226. Xu J, Liu X, Ng JK-P, Lin T, He C (2006) J Mater Chem 16:3540
227. Stevenson DP, Coppinger GM (1962) J Am Chem Soc 84:149
228. Haszeldine RN (1953) J Chem Soc 2622
229. Geron C, Gomel M (1979) J Chim Phys 76:411
230. Dumas JM, Gomel M (1975) J Chim Phys 72:953
231. Dumas JM, Geron C, Kribii AR, Lakraimi M (1984) Can J Chem 62:2634
232. Monteau J, Huser H, Guérin M, Gomel M (1978) J Chem Res (S) 256
233. Monteau J, Huser H, Guérin M, Gomel M (1978) J Chem Res (M) 3217
234. Dumas JM, Geron C, Peurichard H, Gomel M (1976) Bull Soc Chim Fr, p 720
235. Davidson AW, VanderWerf CA, Boatright LG (1947) J Am Chem Soc 69:3045
236. Sheridan JP, Martire DE, Tewari YB (1972) J Am Chem Soc 94:3294
237. Sheridan JP, Martire DE, Banda FP (1973) J Am Chem Soc 95:4788
238. Cheetham NF, Pullin ADE (1970) Aust J Chem 24:479
239. McDaniel DH, Deiters SRM (1966) J Am Chem Soc 88:2607
240. Brown RN (1961) Acta Crystallogr 14:711
241. Jabay O, Pritzkow H, Jander J (1977) Z Naturforsch B: Chem Sci 32:1416
242. Padmanabhan K, Paul IC, Curtin DY (1990) Acta Crystallogr C: Cryst Struct Commun 46:88
243. Ghassemzadeh M, Harms K, Dehnicke K, Magull J (1994) Z Naturforsch B: Chem Sci 49:506
244. Ghassemzadeh M, Harms K, Dehnicke K, Fenske D (1994) Z Naturforsch B: Chem Sci 49:593
245. Svensson C, Albertsson J, Eberson L (1988) Acta Chem Scand B 42:596
246. Svensson C, Albertsson J, Eberson L (1986) Acta Crystallogr C: Cryst Struct Commun 42:1500
247. Ghassemzadeh M, Dehnicke K, Goesmann H, Fenske D (1994) Z Naturforsch B: Chem Sci 49:602
248. Elding M, Albertsson J, Svensson G, Eberson L (1990) Acta Chem Scand 44:135
249. Crowston EH, Lobo AM, Prabhakar S, Rzepa HS, Williams DJ (1984) Chem Commun, p 276

Struct Bond (2008) 126: 137–160
DOI 10.1007/430_2007_062

Published online: 19 September 2007

# X-ray Structures and Electronic Spectra of the π-Halogen Complexes between Halogen Donors and Acceptors with π-Receptors

Sergiy V. Rosokha · Jay K. Kochi (✉)

Department of Chemistry, University of Houston, Houston, TX 77204, USA
*jkochi@uh.edu*

**1 Introduction** . . . . . 138

**2 Electronic Spectroscopy and Thermodynamics of Donor/Acceptor Interactions with Halogen Derivatives** . . . . . 139
2.1 Dihalogen Complexes with Arenes and Alkenes . . . . . 139
2.2 Complexes with Halocarbon Acceptors . . . . . 141
2.3 Complexes of Halide Anions with Aromatic and Olefinic π-Acceptors . . . 142
2.4 Unified Mulliken Correlations of Donor/Acceptor Complexes with Halogen Derivatives . . . . . 144

**3 Structural Features of Donor/Acceptor Complexes with Halogen Derivatives** . . . . . 146
3.1 Complexes of Dihalogen Acceptors with Aromatic and Olefinic π-Donors . 146
3.2 Complexes of Polyhalogenated Methanes with π-Donors . . . . . 148
3.3 Complexes of Halide Anions with Aromatic and Olefinic π-Receptors . . . 150
3.4 Donor/Acceptor (Structural) Effects on π-Halogen Interactions . . . . . 155
3.4.1 Intermolecular Separations Relevant to Halogen Bonding . . . . . 155
3.4.2 Molecular Geometries of Donor/Acceptor Moieties . . . . . 155

**4 Summary and Conclusions** . . . . . 156

**References** . . . . . 157

**Abstract** The spectral characteristics and thermodynamics for the formation of intermolecular complexes of dihalogens, halocarbons, and halide anions with various organic (aromatic and olefinic) π-receptors show their direct relationship to the more traditional donor/acceptor complexes. The unified Mulliken dependence indicates the common (charge-transfer) origin of the long-distance π-bonding of the halogen centers. X-ray structural analyses of the molecular complexes of various arene donors with dihalogen ($X_2$) and halocarbon (XR) acceptors reveal that such non-covalent interactions are characterized mostly by over-the-rim halogen coordination, with the intermolecular halogen–carbon contacts shortened by about 0.3–0.4 Å relative to the sum of the van der Waals radii. The location of dihalogen and halocarbon acceptors generally follow the position of highest electron density on the aromatic ring, and the X–X or X–R bonds are directed perpendicular to the aromatic planes. Likewise, the structural arrangements of the halide donors in the molecular complexes with cyano-substituted arenes (by and large) follow the LUMO shape of the aromatic acceptor. Such long-distance π-bondings are attributed to the presence of multiple (close-lying) local energy minima, so that the donor/acceptor arrangements are rather easily modulated by external forces.

**Keywords** Anion–π interaction · Charge transfer · Electronic spectra · Halogen π-bonding · X-ray crystallography

## 1 Introduction

The direct intermolecular (non-covalent) interaction involving a halogen center represents an important example of long-distance bonding [1–4] (see also the chapter by Legon in this volume). Indeed, in the solid-state the interactions of halogen-based (electron-density) acceptors with various organic and inorganic donors are recognized as a powerful motif for the supramolecular design of non-linear optical materials and even pharmaceutical drugs – and also for the control of solid-state reactivity, chiral resolution, etc. [5–11]. On the other hand, solution studies have shown that such interactions are critical for the reactivity of halogenated derivatives [1, 12–14] and in molecular recognition [15, 16]. Halogen interactions also play important roles in biochemical systems [17]. As such, the quantitative characterization of halogen bonding (this generic term is usually reserved for systems involving halogen-based electron acceptors [18, 19])[1]; and in general, the non-covalent interactions involving halogen centers are of prime importance for chemical fundamentals and for a variety of applications in crystal engineering, in biochemistry, and in organic synthesis.

Most of the recent studies of halogen bonding have concentrated on the structural features of solid-state complexes with n-type (electron) donors [2, 20–22]. By comparison, the nature and properties of the π-mode for halogen-centered interactions is much less explored, in spite of their crucial role in the molecular reactivity of aromatic and olefinic compounds, as well as in their synthetic prospects for the development of π-receptors and other applications [1, 12–14, 23–25] (see also the chapter by Legon in this volume). Accordingly, this chapter is focused on the long-distance interactions of halogen centers with organic (olefinic and aromatic) π-receptors. In particular, two basic types of complexes are considered: (i) associates between dihalogens as well as halocarbon acceptors with organic π-donors, and (ii) associates of halide anions with organic π-acceptors.

It is important to recognize that the intermolecular long-distance bonding with the participation of halogen derivatives represents a specific example of the broad general area of donor/acceptor interactions. Moreover, the complexes of molecular iodine, bromine and chlorine with aromatic donors represent classic examples of charge-transfer compounds [26–28] that are vital for the development of Mulliken theory of intermolecular association [29–31]. The latter thus provides the convenient framework for the

[1] For a discussion on usage of the term *halogen bonding*, see [18, 19].

consideration of the electronic spectra, the structures, and the energetics of intermolecular complexes of halogen derivatives; and most importantly, these facets provide significant insight into the electronic nature of halogen donor/acceptor interactions and the reactivity of halogen derivatives.

Accordingly, this chapter begins with a description of the diagnostic features of donor/acceptor associates, as shown by their distinctive charge-transfer absorption bands with the transition energies that are closely correlated with the redox potentials, i.e., the ionization potential and electron affinity of the donor and acceptor, respectively [29–31]. The spectral characterization of the 1 : 1 complexes formed in solution is followed by the structural elucidation of the corresponding associates in the solid-state. (For a review of gas-phase studies, see [1] and chapter by Legon in this volume). In order to avoid obfuscation of the relatively weak long-distance halogen interactions by electrostatics, metal-ion induced effects, etc., principal attention in this work is paid to various halogen complexes with neutral organic (donor/acceptor) π-receptors. Notably, our consideration is focused on the experimental (spectral, structural, thermodynamics) data as well as their implications on the nature and properties of halogen interactions. The high-level quantum mechanical computations (see e.g., [32–38]) of such bondings are beyond the scope of this review.

## 2
## Electronic Spectroscopy and Thermodynamics of Donor/Acceptor Interactions with Halogen Derivatives

### 2.1
### Dihalogen Complexes with Arenes and Alkenes

The (UV-Vis) spectroscopic detection of the interaction of dihalogen acceptors with aromatic π-donors was one of the first studies of intermolecular donor/acceptor complexes. Indeed, more than 50 years ago, Benesi and Hildebrand published their seminal work describing the distinct spectral (UV-Vis) changes that accompany the spontaneous complexation of various aromatic hydrocarbons (ArH) with diiodine in non-polar solvents such as $CCl_4$, $C_6H_{14}$, etc. [39]. Shortly thereafter, these studies were extended to include dibromine, dichlorine and interhalogen acceptors [26–28, 40]. For example, when pure benzene is added incrementally in small amounts to a 5 mM solution of dibromine in carbon tetrachloride, the red-brown color changes almost imperceptibly. However, inspection of the UV-Vis spectrum readily reveals the progressive growth of a new absorption band at $\lambda_{max} = 285$ nm (Fig. 1), while the "local" band of the dibromine moiety is essentially unchanged relative to the absorption of free dibromine, as shown by the series of invariant spectra at $\lambda > 350$ nm [41].

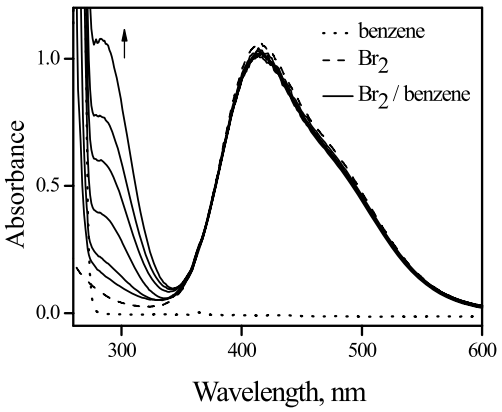


**Fig. 1** Progressive growth of the charge-transfer band ($\lambda_{CT}$ = 285 nm) attendant upon the incremental addition of benzene (from 2 : 1 to 40 : 1 ratio) to 5 mM solution of dibromine in carbon tetrachloride. From [41]

The additions of other (polycyclic) aromatic donors to solutions of dichlorine, dibromine or diiodine afford similar new bands, which show significant red shifts with increasing strength of the arene donor. For example, the absorption maximum of the dibromine complexes varies from 280 nm (with chlorobenzene) to 369 nm (with hexamethylbenzene); and similar variations of the new absorption maxima are observed with diiodine complexes (Fig. 2).

The quantitative (Benesi–Hildebrand) treatment of the spectral data indicated that the equilibrium constants $K_{DA}$ for the formation of these intermolecular (1 : 1) complexes:

$$ArH + X_2 \overset{K_{DA}}{\rightleftarrows} [ArH, X_2], \tag{1}$$

are typically rather small with: $K_{DA} < 3\ M^{-1}$ for $X_2 = I_2$, $Br_2$, and $Cl_2$ or the interhalogens, and the extinction coefficients of these complexes are of the order of $\varepsilon_{CT} \approx 10^4\ M^{-1}\ cm^{-1}$ [26–28]. Furthermore, the temperature dependence of the equilibrium constant affords the enthalpy of the complex formation of $\Delta H_{DA} \approx -3$ to $-5$ kcal $M^{-1}$ [26–28].

The dihalogen complexes with olefin donors were first identified spectroscopically in the mid-1960s [42–45] and extensive experimental and computational studies have been carried out by Chiappe, Lenoir and coworkers in recent years [46–48]. These systems are highly unstable, since the complexation of dihalogens with olefins is followed rapidly by the formation of ionic intermediates and further chemical transformations. Therefore, attention in the corresponding work has mostly focused on hindered olefins, although the spectral characteristics of complexes with less sterically crowded and alkyl- as well as chloro-substituted and cyclic olefins are also reported [44]. The absorption maxima for the dihalogen complexes with olefins (evaluated by the subtraction

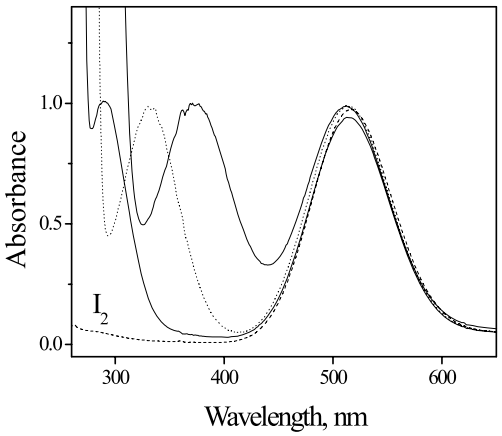


**Fig. 2** Electronic spectra of the carbon tetrachloride solutions of diiodine attendant upon addition of excess amounts of benzene ($\lambda_{CT}$ = 285 nm), mesitylene ($\lambda_{CT}$ = 327 nm) and hexamethylbenzene ($\lambda_{CT}$ = 369 nm) with the charge-transfer band showing significant red-shifts with increasing strength of the aromatic donors

of the spectra of the separate components from the spectrum of the mixture) are found to lie mostly in the range $\lambda_{CT} \approx 260–300$ nm, with the extinction coefficients varying between $\varepsilon_{CT}$ = 2000 and 5000 $M^{-1}$ $cm^{-1}$ [44–48].

## 2.2
## Complexes with Halocarbon Acceptors

In contrast to the dihalogens, there are only a few spectral studies of complex formation of halocarbon acceptors in solution. Indeed, the appearance of new absorption bands is observed in the tetrabromomethane solutions with diazabicyclooctene [49, 50] and with halide anions [5]. The formation of tetrachloromethane complexes with aromatic donors has been suggested without definitive spectral characterization [51, 52]. Moreover, recent spectral measurements of the intermolecular interactions of $CBr_4$ or $CHBr_3$ with alkyl-, amino- and methoxy-substituted benzenes and polycyclic aromatic donors reveal the appearance of new absorption bands only in the case of the strongest donors, viz. $\lambda_{CT}$ = 380 nm with tetramethyl-*p*-phenylendiamine (TMPD) and $\lambda_{CT}$ = 300 nm with 9,10-dimethoxy-1,4 : 5,8-

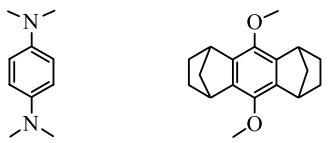


**TMPD** **DMA**

dimethano-1,2,3,4,5,6,7,8-octahydroanthracene (DMA) are examples where distinct bands are observed [53].

No new absorption bands are observed in other cases, largely due to the fact that the strong absorptions of the aromatic donors obstruct the UV-spectral measurements. For the complex between $CBr_4$ and TMPD, the quantitative analyses of the temperature and concentration-dependent absorptions of the new band at 380 nm afford the extinction coefficient of $\varepsilon_{CT} = 3.2 \times 10^3\ M^{-1}\ cm^{-1}$, as well as the thermodynamic parameters for complex formation: $\Delta H = -4.5$ kcal $M^{-1}$, $\Delta S = -14$ e.u., and $K_{DA} = 0.3\ M^{-1}$ at 295 K. Such thermodynamic characteristics are similar to those of the dihalogen complexes of as well as those of other acceptors with aromatic donors. Similar results are also obtained for $CBr_4$ associates with halide and thiocyanide anions [5, 53].

## 2.3
## Complexes of Halide Anions with Aromatic and Olefinic π-Acceptors

Although non-covalent interactions of anions are one of the most actively explored areas of supramolecular chemistry [15], the anion sensing and recognition have up to now relied primarily on electrostatic binding or hydrogen bonding to the receptor [16, 54–61]. However, recent UV-Vis and NMR spectral studies clearly reveal that complex formation takes place in the solutions between halides and neutral olefinic and aromatic π-acceptors such as those in Fig. 3 [23, 62].

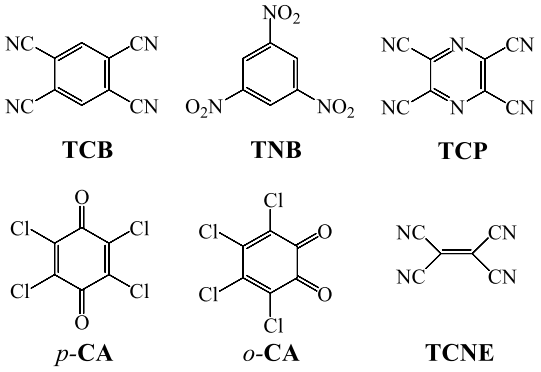


**Fig. 3** π-acceptors and their identification

Solutions of the alkylammonium salts of $Cl^-$, $Br^-$, $I^-$ in acetonitrile show no visible absorptions beyond 300 nm. The aromatic π-acceptor, tetracyanopyrazine (TCP) is characterized by strong absorptions in the 220–300 nm range and a shoulder at 350 nm. However, the electronic spectrum of a mixture of the bromide salt and TCP reveals a new absorption band at $\lambda_{CT} = 400$ nm

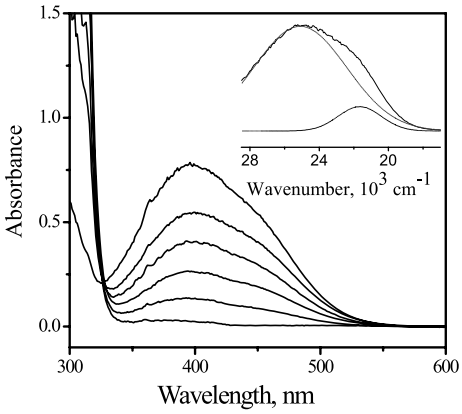


**Fig. 4** Spectral changes upon incremental additions of $Pr_4N^+Br^-$ (from 0 to 208 mM) to the 5 mM solution of TCP in acetonitrile showing the appearance of the new charge-transfer band at $\lambda_{CT} = 400$ nm. *Insert*: deconvolution of the 400-nm band into two Gaussian components [23]

(Fig. 4) related to the 1 : 1 complex [$Br^-$/TCP] [23]. Additions of chloride or iodide salts to the same acceptor also result in the immediate appearance of new absorptions characteristic of the donor/acceptor complexes. Importantly, the band maxima are red-shifted in [$I^-$/TCP] and blue-shifted in [$Cl^-$/TCP] relative to that in [$Br^-$/TCP].

In a similar way, the formation of halide complexes with other π-acceptors in Fig. 3 are revealed by the appearance of new absorption bands in the electronic spectra to reflect the yellow to red colorations of the mixtures. The spectral data thus indicate that halide salts form well-defined electron donor/acceptor complexes with organic π-acceptors, as typified by Eq. 2:

$$Br^- + TCP \overset{K_{DA}}{\rightleftarrows} [Br^-, TCP]\,. \qquad (2)$$

**Table 1** Formation constant and spectral characteristics of bromide (charge-transfer) complexes with various acceptors[a]

| Acceptor | $\lambda_{CT}$ [nm] | $\varepsilon_{CT}$ [$M^{-1}$ $cm^{-1}$] | $K_{DA}$ [$M^{-1}$] |
|---|---|---|---|
| TCB | 355 | 625 | 0.8 |
| *p*-CA | 460 | 1450 | 1.5 |
| TNB | 360 | 1400 | 1.0 |
| TCNE | 465 | 5600 | 8 |
| TCP | 400 | 3900 | 7 |
| $CBr_4$ | 292 | 10 000 | 2.8 |

[a] $Pr_4N^+Br^-$ salt, acetonitrile solution, 22 °C (data from [23, 53])

Quantitative analysis of the absorption intensity affords values of the formation constants ($K_{DA}$) and extinction coefficients ($\varepsilon_{CT}$) listed in Table 1 for comparison with the corresponding characteristics of the bromide complexes with tetrabromomethane.

## 2.4 Unified Mulliken Correlations of Donor/Acceptor Complexes with Halogen Derivatives

According to Mulliken [29–31], the donor/acceptor associates such as those in Eqs 1 and 2, are described via the ground-state ($\Psi_{GS}$) and excited-state ($E_{ES}$) wave functions expressed as the combination of the principal non-bonded van der Waals ($\psi_{D,A}$) and dative ($\psi_{D^+A^-}$) states:

$$\Psi_{GS} = a\,\psi_{D,A} + b\,\psi_{D^+A^-} \tag{3a}$$

$$\Psi_{ES} = b\,\psi_{D,A} - a\,\psi_{D^+A^-}\,, \tag{3b}$$

and the energies of ground and excited states $E_{GS}$ and $E_{ES}$ are:

$$E_{GS,\,ES} = \left(E_{D,A} + E_{D^+A^-}\right)/2 \pm \left(\left(E_{D^+A^-} - E_{D,A}\right)^2 + 4H_{DA}^2\right)^{1/2}/2\,, \tag{4}$$

where $E_{D,A} = \int \psi_{D,A}\mathcal{H}\psi_{D,A}$ and $E_{D^+A^-} = \int \psi_{D^+A^-}\mathcal{H}\psi_{D^+A^-}$ represent the energies of the van der Waals and dative states, respectively, and $H_{DA} = \int \psi_{D,A}\mathcal{H}\psi_{D^+A^-}$ represents the electronic coupling matrix element. The optical (charge-transfer) transition is related to electron promotion from the ground to the excited state:

$$h\nu_{CT} = E_{ES} - E_{GS} = \left(\left(E_{D^+A^-} - E_{D,A}\right)^2 + 4H_{DA}^2\right)^{1/2}\,. \tag{5}$$

In a series of structurally related donors with the same acceptor, or the same donor with various acceptors, the electronic coupling element ($H_{DA}$) as determined mostly by orbital overlap, are usually rather invariant. As such, the changes of the absorption energy in such a series are determined mainly by differences in the energy gap ($E_{D^+A^-} - E_{D,A}$) related to the donor/acceptor properties (i.e., HOMO/LUMO energies). In solution, these properties are quantitatively evaluated as the oxidation and reduction potentials, $E^\circ_{ox}$ and $E^\circ_{red}$, respectively, to represent the conversion energy of the donor to its cation-radical, and the acceptor to its anion-radical. The gas-phase measures of the ionization potential (IP) and electron affinities (EA) represent alternative and closely related measures of donor and acceptor strengths, respectively [63, 64]. Equation 5 thus predicts an essentially linear relationship between the absorption energy for the series of associates involving the same acceptor on the oxidation (or ionization) potential of the donors. Likewise, in

the series of complexes of the same donor, the linear dependence of the transition energy will be observed as a linear function of the reduction potential of the acceptor.

Indeed, the charge-transfer absorption energies of dibromine complexes with various arenes [65] and alkenes [45] both show clear correlations with the ionization potentials of various donors (Fig. 5).

Bromocarbons are weak acceptors, as typically revealed by cyclic voltammetric measurements of tetrabromomethane and bromoform with reduction waves at – 0.96 and – 1.5 V vs. SCE, respectively, in dichloromethane solution [5, 53]. As such, the electronic absorptions of their complexes with most arene and alkene donors are expected to lie in the far-UV region, where they are overshadowed by strong donor absorptions. Therefore among aromatic donors, the charge-transfer bands with the $CBr_4$ acceptor have been unambiguously identified only with TMPD and DMA, since these are characterized by strong donor strengths with $E^{ox} = 0.12$ and 1.11 V, respectively, in combination with their rather high-energy absorptions. By comparison, the absorption band of the $CBr_4$ complexes with halides are relatively easy to identify owing to the spectral transparency of these anions at $\lambda > 250$ nm, combined with the good donor properties of iodide, bromide and chloride that show CV oxidation waves at 0.42, 0.96, and 1.5 V, respectively [53]. Most important, however, is that the clear Mulliken correlations were unambiguously demonstrated in the series of $CBr_4$ associates with different donors, as well as in the series of bromide and iodide complexes with various acceptors [53]. Such correlations confirm the charge-transfer character of the bromocarbon complexes with various donors and their close relationship to the associates with other organic acceptors, as well as the same character as halide complexes.

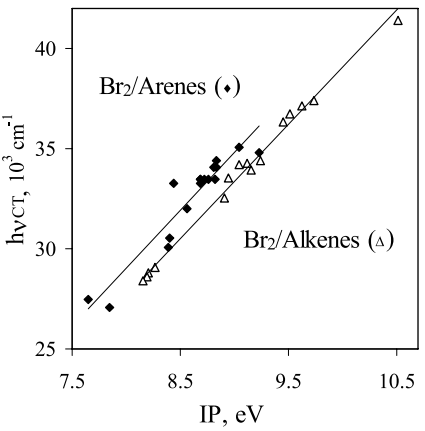


**Fig. 5** Mulliken dependence of the charge-transfer energy in the series of dibromine complexes with alkyl and chloro-substituted arenes and alkene donors (data from [45, 65])

# 3
# Structural Features of Donor/Acceptor Complexes with Halogen Derivatives

## 3.1
## Complexes of Dihalogen Acceptors with Aromatic and Olefinic π-Donors

In spite of the numerous spectral observations of complex formation between aromatic and olefinic donors with the dihalogens, the preparations of the corresponding crystalline complexes have been hindered by their enhanced reactivity (as well as the relatively weak bonding). As such, only few examples of the X-ray structural characterization of the corresponding intermolecular associates are reported, the most notable exception being the dibromine complex with benzene.

According to the earlier X-ray studies of Hassel and Strømme [66, 67], the structure of the isomorphous complexes of dichlorine and dibromine with benzene (measured at 183 K and ~ 230 K, respectively) are characterized by the symmetrical location of the halogen molecules along the sixfold axis of the aromatic ring to form infinite $\cdots$ Ar $\cdots$ Br – Br $\cdots$ Ar $\cdots$ Br – Br $\cdots$ Ar $\cdots$ chains. However, recent X-ray measurements [68] of the $Br_2$/benzene system at lower temperatures (123 K) reveals the less symmetric arrangement of the dihalogen, and a phase transition at 203 K that led to the diffraction pattern originally reported by Hassel and Strømme. In the precise low-temperature structure, the bromine atoms are positioned over the rim of the benzene ring (Fig. 6) and oriented nearly perpendicular to the aromatic planes (with the slight deviation $\alpha$ of typically less than 8°). Furthermore, a pair of dibromines is coordinated to each benzene ring from opposite sides in the *meta*-positions, which are known to be relatively more electron-rich in arenes with acceptor substituents.

The X-ray structure of the dibromine complex with toluene (measured at 123 K) is more complicated, and shows multiple crystallographically independent donor/acceptor moieties [68]. Most important, however, is the fact that in all cases the acceptor shows an over-the-rim location that is similar to that in the benzene complex. In both systems, the acceptor is shifted by ~ 1.4 Å from the main symmetry axis, the shortest Br $\cdots$ C distances of ~ 3.1 Å being significantly less than the sum of the van der Waals radii of 3.55 Å [20]. Furthermore, the calculated hapticity in the benzene/$Br_2$ complex ($\eta$ = 1.52) is midway between the "over-atom" ($\eta$ = 1.0) and "over-bond" ($\eta$ = 2.0) coordination. In the toluene complex, the latter varies from $\eta$ = 1.70 to 1.86 (in four non-equivalent coordination modes) and thus lies closer to the "over-bond" coordination model. Moreover, the "over-bond" bromine is remarkably shifted toward the *ortho*- and *para*-carbons that correspond to the positions of highest electron density (and lead to the transition states for electrophilic aromatic bromination [12]). Such an experimental location of bromine is in good agreement with the results of high level theoretical

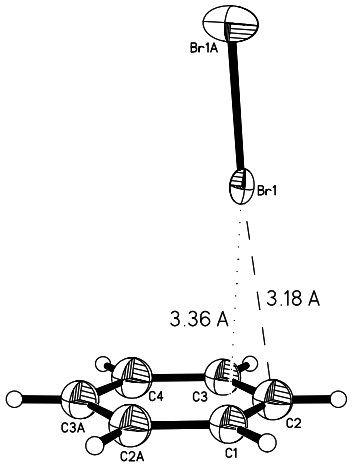


**Fig. 6** Molecular structure of the $Br_2$ complex with benzene (from [68])

calculations, which consistently favor both over-atom and over-bond (i.e., $\eta^1$- and $\eta^2$-) coordinations without a significant energy barrier between them [69–74].

The only reported X-ray structure of a π-bonded diiodine exists in the $I_2$/coronene associate [75], which shows the $I_2$ to be located symmetrically between the aromatic planes and to form infinite donor/acceptor chains. $\eta_2$-Coordination of diiodine over the outer ring in this associate is similar to that observed in the bromine/arene complexes (vide supra), and the I – C separation of 3.20 Å is also significantly contracted relative to the sum of their van der Waals radii [75]. For the highly reactive dichlorine, only X-ray structures of its associates are observed with the n-type coordination to oxygen of 1,4-dioxane [76], and to the chlorinated fullerene [77].

It is should be noted that high reactivity precludes the X-ray structural characterization of the π-complexes between dihalogens and olefinic acceptors. Indeed, quantum mechanical calculation of the interaction between

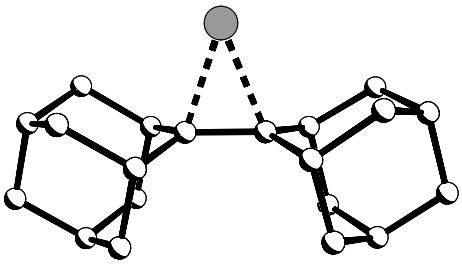

**Fig. 7** Molecular structure of adamantylideneadamantane bromonium, as its salt with $Br_5^-$ counterion (Rosokha et al. unpublished results)

dibromine and ethylene leads to T-shaped structures with $C_{2v}$ symmetry, with a separation of about 3.0 Å between the bromine atom and center of the double C – C bond [13, 14]. However, the low-temperature interaction of bromine with highly sterically encumbered adamantylideneadamantane in dichloromethane results in the (reversible) formation of the crystalline adamantylideneadamantane bromonium adduct shown in Fig. 7 (as the salt with $Br_3^-$ [78] or $Br_5^-$, Rosokha et al. unpublished results) with elongated Br – C bonds of about 2.1–2.2 Å.

### 3.2
### Complexes of Polyhalogenated Methanes with π-Donors

The Cambridge Structural Database [79] contains numerous examples of close contacts of at least 0.2 Å shorter than the sum of the van der Waals radii that exist between aromatic or olefinic donors and the halogen atoms of the halocarbon derivatives – especially in dichloromethane and chloroform solvates. However, most of the structures involve metal-ion complexes or charged species, in which the intrinsic features of the halogen π-bonding might be obscured by electrostatics, hydrogen bonding, crystal packing and other extraneous factors. The intermolecular complexes between a halocarbon and neutral aromatic donors are rather rare; and the structural overview of some complexes of tetrabromomethane with various aromatic donors [53, 80–82] are summarized in Table 2.

Tetrabromomethane shows two types of π-bonding with aromatic donors that are contrasted in Fig. 8a and b, showing over-the-rim coordination to the aromatic C – C bond and over-the-center coordination to the benzene ring. The over-the-rim coordination is generally similar to that observed in the dibromine complexes but the C – Br distance in the former is longer, in agreement with weaker acceptor abilities of tetrabromomethane. Note that picryl bromide shows similar bromine coordination to the outer pyrene C – C bond with Br – C distances of 3.35 and 3.39 Å [83]. A second type of coordination was reported earlier in the *p*-xylene complex [80] and recently in the associate with dimethylnaphtalene [53].

Notably, tetrabromomethane prefers coordination to n-type donors, if available, over the aromatic ring (and such a preference is also observed in complexes of bromoform with *p*-dimethoxybenzene [53], and in diiodopolyfluorocarbons with TMPD or DAM donors [84]) – with the only exception being its complex with triphenylamine. In addition, the bromine separations with n-type oxygen and nitrogen centers are much shorter than the bromine–carbon separation in π-bonded complexes, which indicates (even with a correction for the slightly smaller van der Waals radii of nitrogen and oxygen) stronger bonding of bromine to the former.

Spectroscopic and phase-diagram studies suggest complex formation between tetrachloromethane and chloroform with alkylbenzene donors, and

**Table 2** Overview of crystal structures of $CBr_4$ complexes with aromatic donors

| Donor | Coordination [a,b], | Separation [c] [Å] | C – Br···Ar [d] [deg] |
|---|---|---|---|
| *p*-Xylene [e] | Ar-center [i] | 3.53–3.74 [j] | 179 |
| Durene [f] | Ar-rim [i] | 3.26, 3.34 [k] | 163 |
| DMN [g] | Ar-center [i] | 3.51–3.73 [j] | 173 |
| OMTP [g] | Ar-rim [i] | 3.20, 3.32 [k] | 166, 175 |
| TBA [g] | Ar-rim [i] | 3.38, 3.49 [l] | 179 |
| TPM [h] | Ar-rim [i] | 3.44, 3.58 [l] | 179 |
| TMPD [g] | N | 2.77 | 169 [m] |
| DAM [g] | N | 2.82 | 170 [m] |
| DMA [g] | O | 2.86, 2.82 | 173 [m], 174 [m] |

[a] Donor atom
[b] Each acceptor should have two contacts with the donor and vice versa
[c] Br···X separation
[d] Angle between C – Br bond and normal to aromatic plane
[e] [80]
[f] [81]
[g] [53]
[h] [82]
[i] Halogen π-bonding to benzene ring
[j] Distances to six ring carbons
[k] Distances to two carbon atoms
[l] Distance from Br to aromatic plane
[m] C – Br···X angle

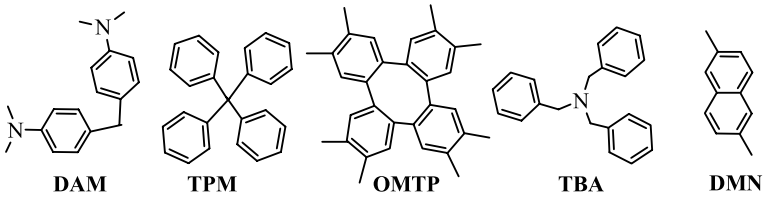


provide values of the enthalpy of their formation (e.g., $-\Delta H = -3.2$, 4.0 and 9.3 kJ $M^{-1}$ for complexes of $CCl_4$ with benzene, toluene and *p*-xylene, respectively) [20]. However, X-ray structural data for the associates of these acceptors with simple arene or olefin donors are lacking, in spite of numerous examples of close chlorine–carbon contacts in chlorocarbon solvates of polycyclic, charged, or metal-complexed aromatic donors. Most frequently, they show over-the-rim π-bonding with the more or less symmetrical arrangement of the chlorine atom over the aromatic C – C bond, although coordination over the ring center and as well as over the carbon atoms are also available. For example, the short and almost identical separations of 3.284 and 3.296 Å between a chlorine atom and the two carbon atoms of ben-

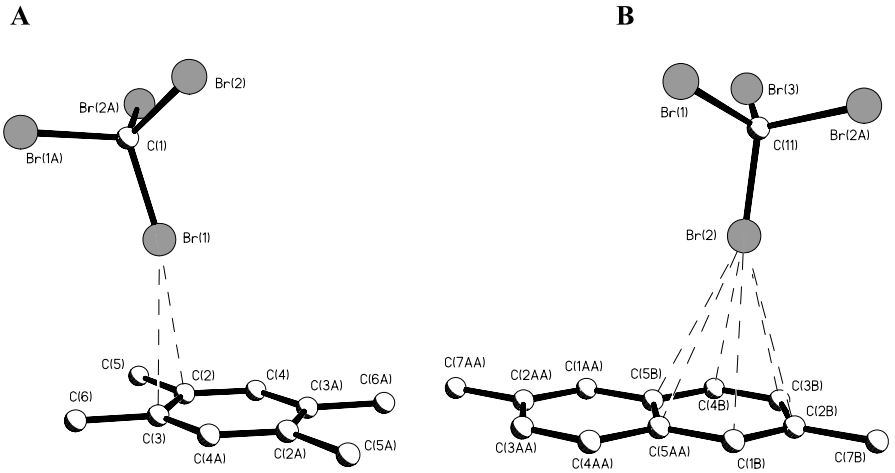


**Fig. 8** Two modes: over-the-rim (**a**) and over-the-center (**b**) coordination of tetrabromomethane to aromatic donors (data from [53, 80])

zene is observed in the complexes of chloroform with calixarene [85]. In the $CHCl_3$ complex with 2,2′-dimethoxy-9,9′-biacridine, one chlorine atom is located over the aromatic bond (with C – Cl separations of 3.25 and 3.33 Å) and another chlorine is coordinated to the carbon (with a 3.33 Å separation) [86] On the other hand, coordination close to the aromatic ring center is observed in the chloroform complex with cobalt-coordinated diphenylphosphinomethane (with Cl – C separations varying from 3.27 to 3.58 Å) or in the tetrachloromethane complex with dicorannulenobarrelene (with Cl – C separations varying from 3.27 to 3.46 Å) [87, 88].

Finally, a weak π-type halogen bonding involving a cyclopentadienyl ring and the iodine atom of an iodofluorocarbon [89] is a rare example of a π-bonded iodocarbon derivative, in contrast to numerous examples of halogen bonding of the latter with n-type electron donors [2, 20].

### 3.3
### Complexes of Halide Anions with Aromatic and Olefinic π-Receptors

X-ray structural information on halide binding to neutral organic π-receptors is limited to a few recent reports [23, 24, 62, 89–91][2]. In fact, the slow diffusion of hexane into a dichloromethane solutions of tetracyanopyrazine containing the alkylammonium salts of either chloride, bromide or iodide affords yellow to red crystals with UV-Vis absorptions closely resembling the elec-

[2] Anion–π interaction is also recognized in halide associates with aromatic rings when the latter represents a part of the (positively charged) metal-ion complex and/or when π-bonding is supported by hydrogen bonding.

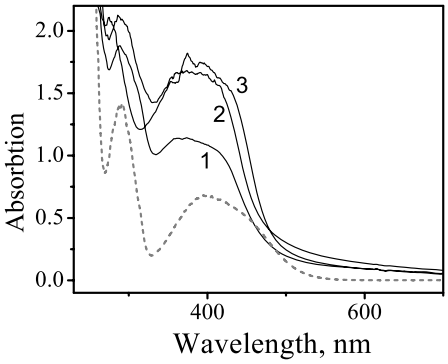


**Fig. 9** Solid-state spectra of bromide complexes with TCP (*solid lines*): *1* $Pr_4N^+[Br^-, (TCP)_4]$, *2* $(Et_4N^+)_2[(Br^-)_2,(TCP)_3]$, *3* $Bu_4N^+$ $[Br^-,(TCP)_4]$. Note: spectra of the corresponding complexes in solution are shown as *gray dashed line* [23]

**Table 3** Solid-state characteristics of halide associates with π-acceptors[a]

| | Molar ratio | $X^-\cdots C$[b] [Å] |
|---|---|---|
| $Br^-$/TCP | 2 : 3[d] | 3.16 |
| | 1 : 4[e] | 3.15 |
| $I^-$/TCP | 1 : 2[d] | 3.52 |
| | 1 : 1[f] | 3.49[c] |
| $Cl^-$/TCP | 1 : 4[f] | 3.07 |
| $NCS^-$/TCP | 1 : 1[f] | 2.951[i] |
| | | 3.288[j] |
| $Br^-$/TCNE | 2 : 1[d] | 3.20 |
| | 1 : 1[e] | 3.11 |
| | 1 : 1[f] | 3.20 |
| $I^-$/TCB[c] | 1 : 2[g] | 3.46 |
| | 1 : 2[h] | 3.45 |
| $Br^-$/TCB[c] | 1 : 2[h] | 3.34 |
| $Br^-$/*o*-CA | 1 : 1[e] | 2.93 |

[a] From [23] unless noted otherwise
[b] Halide–carbon distances with closest contacts.
Note that van der Waals radii are (in Å) 1.70 (C), 1.52 (O), 1.55 (N), 1.80 (S), 1.80 (Cl), 1.85 (Br), 2.1 (I) [20]
[c] From [24]
[d] $Et_4N^+$ salt
[e] $Pr_4N^+$ salt
[f] $Bu_4N^+$ salt
[g] $Na(18\text{-crown-6})^+$ salt
[h] $K(18\text{-crown-6})^+$ salt
[i] C···N separation
[j] C···S separation

tronic spectra of the corresponding of 1 : 1 complexes [$X^-$/TCP] measured in solution (Fig. 9) [23].

However, X-ray analysis of these salts reveals the overall ratio of the acceptor to donor to vary (depending on the counterion and halide) from 4 : 1 to 1 : 1 (Table 3), and they show halide anions in close contact with two to four acceptor moieties, as illustrated in Fig. 10.

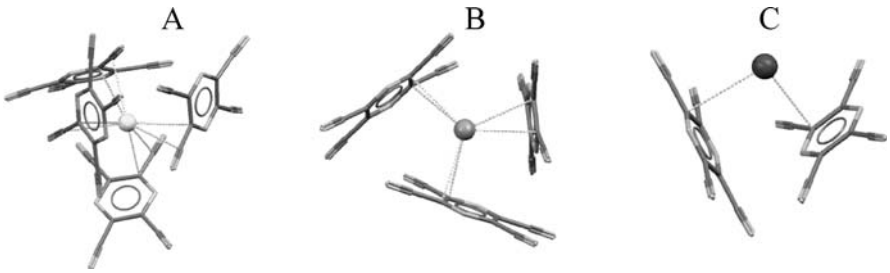


**Fig. 10** Fragment of crystal structures of tetracyanopyrazine complexes with halides showing coordination of anions to four, three or two acceptor moieties in $Bu_4N^+[Cl^-, (TCP)_4]$ (**a**), $Et_4N^+[(Br^-)_2, (TCP)_3]$ (**b**) and $Bu_4N^+[I^-, (TCP)]$ (**c**) salts, respectively [23]

In related complexes of bromide and iodide anions with tetracyanobenzene, the halide anions are also surrounded by four acceptor molecules [24]. The coordination of the halides in two of these moieties is similar to that observed in TCP complexes, i.e., the anion is arranged above (or slightly outside) of the ring and forms close contacts with the cyano-bearing carbons. On the other hand, coordination with the third TCB occurs via the unsubstituted carbon, and the halide is positioned far outside the ring in this case The fourth acceptor moiety is hydrogen-bonded to the halide (Fig. 11).

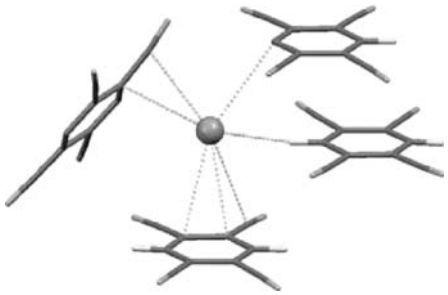

**Fig. 11** Fragment of the crystal structures of tetracyanobenzene/bromide complex showing different modes of anion coordination to the acceptor moieties (coordinates from [24])

Notably, the thiocyanide anion as a pseudohalide forms similar complexes with the aromatic π-acceptors. Indeed, in the recently characterized complex

with tetracyanopyrazine, the $NCS^-$ is arranged over one side of the acceptor moiety (Fig. 12), and the presence of very short nitrogen and sulfur contacts with the cyano-bearing carbons (Table 3) indicate an especially strong donor/acceptor bonding[3].

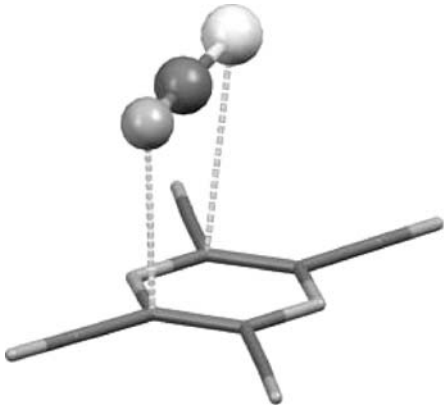

**Fig. 12** Fragment of crystal structure of $Bu_4N^+[NCS^-, TCP]$ salt showing close contact of nitrogen and sulfur atoms with the acceptor moiety (Han et al. private communication)

In anion–π interactions with electron-deficient (neutral) aromatic π-acceptors, the halide lies preferentially over the *periphery* of the aromatic ring (as illustrated in Fig. 13a) and this is apparently related to the shape of the acceptor LUMO (presented for comparison in Fig. 13b).

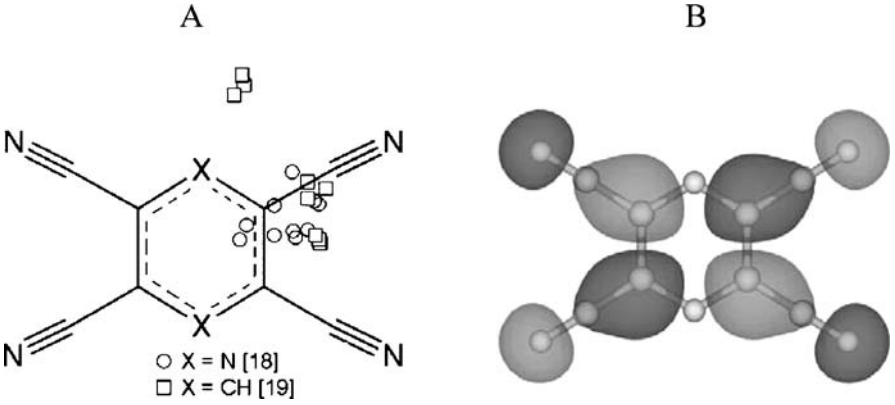


**Fig. 13** **a** Location of the halide anions above the tetracyanopyrazine (○) and tetracyanobenzene (□) π-systems (adapted from [24]) in comparison with **b** the LUMO shape of the TCP acceptor

[3] Han et al. private communication. Note that the S – C distance of 3.29 Å in the complex with TCP is close to separations of 3.16, 3.24 and 3.27 Å measured in the $NCS^-$ associates with $CBr_4$ [53].

On the other hand, the over-the-center coordination in a "carousel" copper(II)-triazine complex (Fig. 14) [92] appears to be the result of multiple hydrogen bonding and steric effects.

**Fig. 14** Fragment of crystal structure of "carousel" copper(II)-triazine complex showing over-the-center coordination of chloride anion to a triazine (coordinates from [92])

In a similar manner, the diffusion of hexane into dichloromethane solutions containing mixtures of the alkylammonium salts of bromide and the olefinic acceptors *o*-CA and TCNE result in the formation of brown-red crystals [23]. X-ray analysis reveals the (1 : 1) complex of bromide with *o*-CA, in which the anion is located over the center of the C – C bond of the acceptor moiety (Fig. 15b) and $Br^{-}\cdots C$ contacts are shortened by as much as 0.6 Å relative to the sum of van der Waals radii (Table 3). In bromide complexes with TCNE, the location of the anion relative to the acceptor is variable. In fact, a 2 : 1 complex $[(Br^{-})_2,TCNE]$ is isolated in which both anions reside over the olefinic bond when the tetraethylammonium salt of bromide is used. In comparison, if the tetrapropyl- or tetrabutylammonium salts of the same anion are employed, the (1 : 1) complexes $[Br^{-},TCNE]$ are formed in which the bromide donors are shifted toward the cyano substituents (Fig. 15a). In both cases however, the short intermolecular separations that are characteris-

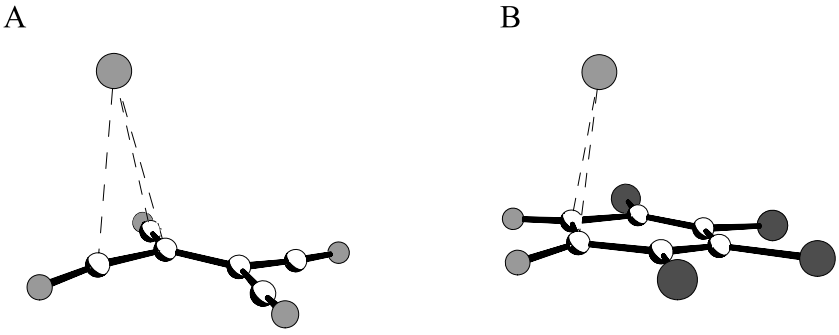


**Fig. 15** Molecular structures of bromide complexes with TCNE (**a**) and *o*-CA (**b**) acceptors

tic of π–π bonded CT complexes [26–28] are indicative of strong anion/TCNE interactions (Table 3).

### 3.4
### Donor/Acceptor (Structural) Effects on π-Halogen Interactions

#### 3.4.1
#### Intermolecular Separations Relevant to Halogen Bonding

Halogen–carbon separations in π-complexes are significantly less than the sum of their van der Waals radii. It is notable, however, that the contractions of ∼ 0.4 Å relative to equilibrium van der Waals separations, which are observed in these $Br_2$ complexes, are somewhat less than those measured earlier with various n-type donors. For example, the X···Br distance contraction (relative to the corresponding equilibrium van der Waals separations) is 0.55 Å in the acetone/$Br_2$ complex (O···Br 2.82 Å), 0.56 Å in the acetonitrile/$Br_2$ complex (N···Br 2.84 Å), 0.57 Å in the $[Te_2Cl_{10}]^{2-}/Br_2$ complex (Cl···Br 3.03 Å), and 0.60 Å in the $[Se_2Br_{10}]^{2-}/Br_2$ complex (Br···Br 3.10 Å) [41]. A similar tendency is observed in tetrabromomethane complexes with π-type (aromatic) vs. n-type donors, with the former showing contractions of up to ∼ 0.3 Å relative to the sum of the van der Waals radii, while the contraction in the oxygen, nitrogen, or halide complexes reach as much as 0.5–0.8 Å. Most importantly, the shortening of the interatomic distances within various halogen complexes apparently correlates with the donor/acceptor strength of the components. Thus, the average C···Br separation of 3.156 Å in the toluene/$Br_2$ complex is somewhat shorter than that in the benzene complex (3.18 Å), as expected from the better donor strength of toluene [63, 64]. In the carbon tetrabromide complexes with π-donors, the separation between the bromine atom and the benzene plane is decreased from 3.34 Å in the tetrabromomethane complex with the weak *p*-xylene donor to 3.21 Å in the associate with the stronger durene donor, and further to 3.14 Å in the complex with OMTP (oxidation potentials for these donors are 2.01, 1.84 and 1.75, respectively [53]. Such data provide clear indications of the increase in the halogen-bonding strength (structurally represented as the interatomic distance) with increasing donor/acceptor strengths that are similar to those observed in halogen bonding with n-type donors [53].

#### 3.4.2
#### Molecular Geometries of Donor/Acceptor Moieties

The C(arene)···Br bonding does not markedly perturbed the geometry of the dibromine, which is rather sensitive to coordination/ polarization effects and the bond readily elongates from 2.284 Å in the non-coordinated molecule to 2.53 Å in the $[Br_3]^-$ anion [41]. Indeed, the Br – Br bond lengths of 2.301(2) Å

in the benzene complex and an average of 2.302(1) Å in the toluene complex do not exhibit significant elongation during complex formation, with the longest Br – Br bond length being 2.307(1) Å. The shortest contact C···Br 3.053(4) Å is found in the toluene complex with unsymmetrical coordination of bromine. Interestingly, a similar asymmetric coordination of dibromine is found in the complex with methanol, in which the O···Br distance is shorter (2.705 vs. 2.723 Å) and the Br – Br bond length is longer (2.324 vs. 2.303 Å) than those in the closely related (but symmetric) dioxane complex. However, the precision of the bond-length determination ($\sigma_{CC}$ = 0.6 pm) is insufficient to allow the detection of (small) polarization effects in the arene donor since such changes in C – C bonds are typically less than 0.5 pm [41].

Minimal changes are also observed in the C – Br bond length of coordinated tetrabromomethane. Indeed, the average C – Br bond length in tetrabromomethane for most of the π-bonded complexes in Table 2 is about 1.930 ± 0.003 Å, i.e., within the accuracy limit of the free acceptor (measured at 123 K) of 1.930 ± 0.006 Å [5]. The somewhat higher tetrabromomethane average bond length of 1.941 in the complex with durene is still within 3$\sigma$ of that in the free acceptor to preclude a reliable conclusion to be drawn. Notably however, in complexes with n-type donors, the elongation of the C – Br bond is more pronounced and shows some correlation with donor strength [53]. In a similar way, the small degree of charge transfer occurring in the halide complexes is insufficient to produce notable changes in the molecular geometry of the aromatic and olefinic acceptors.

## 4 Summary and Conclusions

X-ray structural analyses reveal that the π-bonding of dihalogens, halocarbons and halides to arene donors and acceptors are characterized mostly by over-the-rim coordination in which the dihalogen acceptor generally follows the position of highest electron density on the aromatic donor, and the arrangement of halide donor mostly follows the LUMO shape of the aromatic acceptor.

In the arene complexes of halogen acceptors, the X – X or X – R bonds are directed perpendicular to the aromatic planes, in comparison with nearly 180 deg between these bonds and halogen bonds with n-type donors. The halogen-bond lengths show an apparent correlation with the donor/acceptor strengths: the stronger donor and/or acceptor leading to more significant shortening of the Br···X separation. However, the effects of π-complex formation on the reactant moieties are rather minor, indicating a relatively small degree of donor/acceptor charge transfer.

The structures of the benzene/$Br_2$ and toluene/$Br_2$ complexes at 123 K show over-the-rim coordination with hapticities varying from about 1.5

to 1.9, but X-ray measurements of the benzene/$Br_2$ associate at 230 K are consistent with the symmetrical arrangement of dibromine over the ring center. π-Bonded complexes of tetrabromomethane also show over-the-rim and over-the-center arrangement of the coordinated bromine atom. Furthermore, the halide associates with tetracyanoarenes are characterized by significant scattering of the anion positions over the aromatic ring. In the complexes with tetracyanoethylene, the bromide anion is located over the double bond and also shifted toward the cyano group. Such structural data suggests that various modes of coordination are possible. Such a structural variability on the halogen π-bonding is reminiscent of that observed in the π-complexes of aromatic ion-radicals with their diamagnetic parents [93]. The latter suggests that in long-distance π-bonding, the subtle balance between the attractive interaction of partially occupied frontier orbitals vis á vis the repulsion of filled atomic orbitals led to several shallow, close in energy, local minima involving various mutual donor/acceptor arrangements. As such, we posit that the interactions between halogen acceptors and π-donors (similar to ion-radical π-bonding) can be readily modulated by temperature, electrostatics, crystal packing, solvation, etc., to produce a variety of polymolecular associates within a relatively narrow range of intermolecular separations.

Spectral studies of the intermolecular interaction of dihalogens, halocarbons and halide anions with various organic π-receptors (including the unified Mulliken dependence of their absorption bands) show the direct relationship of the spectral characteristics and formation thermodynamics of the corresponding associates with those of traditional organic donor/acceptors complexes. This indicates the common (charge-transfer) origin of the long-distance bonding of halogen centers. Such a conclusion is of particular interest for the π-interactions of halides, since the formation constants of the halide complexes with neutral π-acceptors, together with their intense absorptions and compression of the intermolecular separations found by X-ray structural analysis, indicate the existence of substantial anion–π interactions. As such, we believe that the relatively strong complex formation together with the distinctive colorations of various anion–π interactions encourage their use in the design of anion-sensing receptors, provided systems with multicentered binding sites are offered for optimal recognition.

**Acknowledgements** We thank the R.A. Welch Foundation for financial support of this study.

## References

1. Legon AC (1999) Angew Chem Int Ed 38:2686
2. Metrangolo P, Resnati G (2001) Chem Eur J 7:2511
3. Metrangolo P, Neukirch H, Pilati T, Resnati G (2005) Acc Chem Res 38:386

4. Dumas JM, Gomel L, Guerin M (1983) Molecualr interactions involving organic halides. In: Patai S, Rappoport Z (eds) The chemistry of functional groups, suppl D. Wiley, New York
5. Lindeman SV, Hecht J, Kochi JK (2003) J Am Chem Soc 125:11597
6. Caronna T, Liantonio R, Logothetis TA, Metrangolo P, Pilati T, Resnati G (2004) J Am Chem Soc 126:4500
7. Crihfield A, Hartwell J, Phelps D, Walsh RB, Harris JL, Payne JF, Pennington WT, Hanks TW (2003) Cryst Growth Des 3:313
8. Goroff NS, Curtis SM, Webb JA, Fowler FW, Lauher JW (2005) Org Lett 7:1891
9. Nguyen HL, Horton PN, Hursthouse MB, Legon AC, Bruce DW (2004) J Am Chem Soc 126:16
10. Farina A, Meille SV, Messina MT, Metrangolo P, Resnati G, Vecchio G (1999) Angew Chem Int Ed 38:2433
11. De Santis A, Forni A, Liantonio R, Metrangolo P, Pilati T, Resnati G (2003) Chem Eur J 9:3974
12. Rosokha S, Kochi JK (2002) J Org Chem 67:1727
13. Lenoir D (2003) Angew Chem Int Ed 42:854
14. Lenoir D, Chiappe C (2003) Chem Eur J 9:1037
15. Beer PD, Gale PA (2001) Angew Chem Int Ed 40:487
16. Bianchi A, Bowman-James K, Garcia-España E (eds) (1997) Supramolecular chemistry of anions. Wiley-VCH, New-York
17. Auffinger P, Hays FA, Westhof E, Ho PS (2004) Proc Natl Acad Sci USA 101:16789
18. Metrangolo P, Pilati T, Resnati G (2006) Cryst Eng Comm 8:946
19. Glaser R, Murphy RF (2006) Cryst Eng Comm 8:948
20. Herbstein FH (2005) Crystalline molecular complexes and compounds: structures and principles, vol 2. Donor–acceptor molecular compounds (essentially localized interactions), Chap 11. Oxford University Press, London
21. Zordan F, Brammer L, Sherwood P (2005) J Am Chem Soc 127:5979
22. Lommerse JPM, Stone AJ, Taylor R, Allen FH (1996) J Am Chem Soc 118:3108
23. Rosokha YS, Lindeman SV, Rosokha SV, Kochi JK (2004) Angew Chem Int Ed 43:4650
24. Berryman OB, Bryantsev VS, Stay DP, Johnson DW, Hay BP (2007) J Am Chem Soc 129:48
25. Fukuzumi S, Kochi JK (1981) J Am Chem Soc 103:7240
26. Foster R (ed) (1969) Organic charge-transfer complexes. Academic, New York
27. Foster R (ed) (1973) Molecular complexes. Crane, Russak, New York
28. Andrews LJ, Keefer RM (1964) Molecular complexes in organic chemistry. Holden-Day, San-Francisco
29. Mulliken RS (1952) J Am Chem Soc 74:811
30. Mulliken RS (1952) J Phys Chem 56:801
31. Mulliken RS, Person WB (1969) Molecular complexes. Wiley, New York
32. Glaser R, Chen N, Wu H, Knotts N, Kaupp M (2004) J Am Chem Soc 126:4412
33. Zou JW, Jiang YJ, Guo M, Hu GX, Zhang B, Liu HC, Yu QS (2005) Chem Eur J 11:740
34. Quiñonero D, Garau C, Rotger C, Frontera A, Ballester P, Costa A, Deyà PM (2002) Angew Chem Int Ed 41:3389
35. Garau C, Frontera A, Quiñonero D, Ballester P, Costa A, Deyà PM (2003) Chem Phys Chem 4:1344
36. Alkorta I, Elguero J (2003) J Phys Chem A 107:9428
37. Kim D, Tarakeshwar P, Kim KS (2004) J Phys Chem A 108:1250
38. Mascal M, Armstrong A, Bartberger MD (2002) J Am Chem Soc 124:6274
39. Benesi HA, Hildebrand JH (1949) J Am Chem Soc 71:2703

40. Kiefer R, Andrews LJ (1950) J Am Chem Soc 72:4677
41. Vasilyev AV, Lindeman SV, Kochi JK (2002) New J Chem 26:582
42. Dubois JE, Garnier F (1967) Spectrochim Acta 23A:2279
43. Dubois JE, Garnier F (1965) Tetrahedron Lett 44:3961
44. Fukuzumi S, Kochi JK (1981) J Am Chem Soc 103:2783
45. Fukuzumi S, Kochi JK (1983) Bull Chem Soc Jpn 56:969
46. Chiappe C, Lenoir D, Pomelli CS, Bianchini R (2004) Phys Chem Phys 6:3235
47. Chiappe C, Detert H, Lenoir D, Pomelli CS, Ruasse MF (2003) J Am Chem Soc 125:2864
48. Chiappe C, De Rubertis A, Jaber A, Lenoir D, Wattenbach C, Pomelli CS (2002) J Org Chem 67:7066
49. Blackstock SC, Kochi JK (1987) J Am Chem Soc 109:2484
50. Blackstock SC, Lorand JP, Kochi JK (1987) J Org Chem 52:1451
51. Anderson R, Prausnitz JM (1963) J Chem Phys 39:1225
52. Weimer RF, Prausnitz JM (1965) J Chem Phys 42:3643
53. Rosokha SV, Neretin IS, Rosokha TY, Hecht J, Kochi JK (2006) Heteroatom Chem 17:449
54. Sessler JL, An D, Cho WS, Lynch V (2003) Angew Chem 42:2278
55. Schmidtchen FP, Berger M (1997) Chem Rev 97:1609
56. Wallace KJ, Belcher WJ, Turner DR, Syed KF, Steed JW (2003) J Am Chem Soc 125:9699
57. Kosower EM, Burbach JC (1956) J Am Chem Soc 78:5838
58. Nakahara A, Wang JH (1963) J Phys Chem 67:491
59. Briegleb G, Liptay W, Fick R (1962) Z Electrochem 66:859
60. Davis KMC (1969) J Chem Soc B 1129
61. de Boer JAAA, Reinhoudt DN, Uiterwijk JWHM, Harkema S (1982) J Chem Soc Chem Chem Commun, p 194
62. Berryman OB, Hof F, Hynes MJ, Johnson DW (2006) Chem Commun, p 506
63. Howell JO, Goncalves JM, Amatore C, Klasinc L, Wightman RM, Kochi JK (1984) J Am Chem Soc 106:3968
64. Rosokha SV, Kochi JK (2002) Charge-transfer effects on arene structure and reactivity. In: Astruc D (ed) Modern arene chemistry. Wiley-VCH, New York, pp 435–478
65. Fukuzumi S, Kochi JK (1981) J Org Chem 46:4116
66. Hassel O, Strømme KO (1958) Acta Chem Scand 12:1146
67. Hassel O, Strømme KO (1959) Acta Chem Scand 13:1781
68. Vasilyev AV, Lindeman SV, Kochi JK (2001) Chem Commun, p 909
69. Grozema FC, Zijlstra RWJ, Swart M, Van Duijhen PT (1999) Int J Quant Chem 75:709
70. Mebel AM, Lin HL, Lin SH Int J (1999) Quantum Chem 75:307
71. Ammal SSC, Ananthavel SP, Venuvanalingam P, Hegde MS (1998) J Phys Chem A 102:532
72. Matsuzawa A, Osamura Y (1997) Bull Chem Soc Jpn 70:1531
73. Milano G, Guerra G. Cavallo E (1998) Eur J Inorg Chem 1513
74. Smith WB (2003) J Phys Org Chem 16:34
75. Mitani S (1986) Annu Rep Res R I Kyoto University 19:1
76. Hassel O, Strømme KO (1959) Acta Chem Scand 13:1775
77. Troshin PA, Lyubovskaya RN, Ioffe IN, Shustova NB, Kemnitz E, Troyanov SI (2005) Angew Chem Int Ed 44:234
78. Slebocka-Tilk H, Ball RG, Brown RS (1985) J Am Chem Soc 107:4504
79. Cambridge Crystallographic Data Centre (2006) CSD version 5.28
80. Strieter FJ, Templeton DH (1962) J Chem Phys 37:161

81. Hubig SM, Lindeman SV, Kochi JK (2000) Coord Chem Rev 200–202:831
82. Reddy DS, Craig DC, Desiraju GR (1996) J Am Chem Soc 118:4090
83. Herbstein FH, Kaftory M (1975) Acta Cryst B31:68
84. Neukirch H, Guido E, Liantonio R, Metrangolo P, Pilati T, Resnati G (2005) Chem Commun, p 1534
85. Juneja RK, Robinson KD, Johnson CP, Atwood JL (1993) J Am Chem Soc 115:3818
86. Boyer G, Lormier T, Galy JP, Llamas-Saiz AL, Foces-Foces C, Fierros M, Elguero J, Virgili A (1999) Molecules 4:104
87. Golovko VB, Hope-Weeks LJ, Mays MJ, McPartlin M, Sloan AM, Woods AD (2004) New J Chem 28:527
88. Sygula A, Sygula R, Ellern A, Rabideau PW (2003) Org Lett 5:2595
89. Amati M, Lelj F, Liantonio R, Metrangolo P, Luzzati S, Pilati T, Resnati G (2004) J Fluor Chem 125:629
90. de Hoog P, Gamez P, Mutikainen I, Turpeinen U, Reedijk J (2004) Angew Chem Int Ed 43:5815
91. Frontera A, Saczewski F, Gdaniec M, Dziemidowicz-Borys E, Kurland A, Deya PM, Quinonero D, Garau C (2005) Chem Eur J 11:6560
92. Demeshko S, Dechert S, Meyer F (2004) J Am Chem Soc 126:4508
93. Rosokha SV, Kochi JK (2007) J Am Chem Soc 129:828

Struct Bond (2008) 126: 161–180
DOI 10.1007/430_2007_068

Published online: 13 October 2007

# Halogen-bonded Liquid Crystals

Duncan W. Bruce

Department of Chemistry, University of York, Heslington, York YO10 5DD, UK
*db519@york.ac.uk*

**1 Preamble** . . . . . 161

**2 An Introduction to Thermotropic Liquid Crystals** . . . . . 162
2.1 Low Molar Mass Liquid Crystals . . . . . 162
2.2 High Molar Mass Liquid Crystals . . . . . 165

**3 Characterisation of Liquid Crystal Mesophases** . . . . . 166

**4 Liquid Crystals Formed Through Non-covalent Interactions** . . . . . 167
4.1 Quadrupolar Interactions . . . . . 167
4.2 Charge-transfer Interactions . . . . . 168

**5 Hydrogen Bonding** . . . . . 169

**6 Halogen-bonded Liquid Crystals** . . . . . 174

**7 Future Prospects** . . . . . 179

**References** . . . . . 179

**Abstract** This chapter discusses the relatively new discovery of liquid crystallinity induced by halogen bonding. Liquid crystals are first introduced and then, to give the work some context, background information is given concerning liquid crystal phases induced by other, non-covalent interactions. In particular, hydrogen bonding is examined, as the two interactions are rather similar as are the molecular components that might be used as the acceptor. Low molar mass and polymeric halogen-bonded mesogens are then described and future prospects are evaluated.

## 1 Preamble

As described most elegantly elsewhere in this volume, the halogen bond is an intermolecular, charge-transfer interaction between a Lewis base and an electron-deficient halogen. Other chapters that accompany this chart its use in, for example, supramolecular chemistry, molecular conductors and coordination chemistry. In this chapter, a much more recent application of halogen bonding is described, namely in the realisation of liquid-crystalline materials.

The literature amounts to few published papers to date, but nonetheless the potential is significant and there is a good deal of work from the author's laboratory that will find its way to publication in the coming period.

It is the author's view that a chapter such as this needs some sort of context and needs to be self-contained. From this point of view, it will begin with a general introduction to liquid crystals themselves and will then introduce *hydrogen*-bonded liquid crystals in order to provide some context. The introduction to liquid crystals will not be referenced or illustrated heavily, so those readers requiring more information are directed to reference [1].

## 2
## An Introduction to Thermotropic Liquid Crystals

The liquid crystal state represents the fourth state of matter and exists between the solid and liquid states, which form its boundaries. The liquid crystal state is reached from the solid state either by the action of temperature (*thermotropic* liquid crystals) or of solvent (*lyotropic* liquid crystals) and it is the former that will be the subject of this chapter.

Being bordered by the solid and liquid states, the liquid crystal state has some of the order of a solid, combined with the fluidity of a liquid. As such, it is an anisotropic fluid and it is this anisotropy that has led to the widespread application of liquid crystals.

The idea of anisotropy in liquid crystals is an important one and indeed, it is shape anisotropy that distinguishes liquid-crystalline molecules (mesogens) from those that are not liquid crystalline. In general, mesogens have one axis that is very different in dimensions to the other two, the most common examples being rod-shaped molecules (one long and two short axes) and disc-like molecules (one short and two long axes). This shape anisotropy leads to additional anisotropic dispersion forces between the molecules and these are sufficiently strong to stabilise phases intermediate in order between the solid and the liquid.

Thermotropic liquid crystals may be classified as either *low molar mass* (i.e. non-polymeric), or *high molar mass* (i.e. polymeric) and within each of these broad classifications, there are several sub-classifications.

### 2.1
### Low Molar Mass Liquid Crystals

There are now three major shape classifications of low molar mass liquid crystals – rod-like (calamitic), disc-like (discotic) and bent-core. The last of these is the most recent, and while examples of bent mesogens have been known for some years, it is only since the mid-1990s that the area has attracted widespread attention [2].

*Calamitic* liquid crystals generally contain two or more rings, at least one flexible chain and often a small, polar function; in some cases, small, lateral groups (normally fluorine) are attached. Some will contain metal

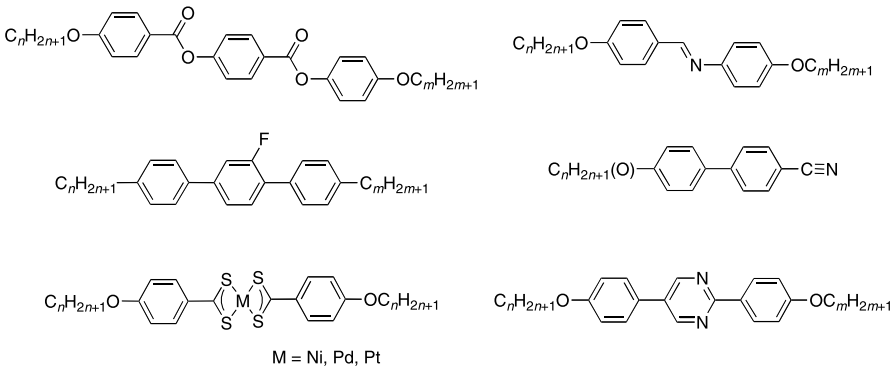


**Fig. 1** Examples of calamitic liquid crystals

atoms [3–6]. The core of the molecule establishes the basic anisotropy and this is reinforced by the flexible, terminal chain, which also acts to reduce the melting point. Some representative examples are given in Fig. 1.

The liquid crystal phases of calamitic mesogens fall into two types – *nematic* (N) and *smectic* (Sm). The nematic phase is the most disordered of the liquid crystal phases and possesses only orientational order, so that the long axes of the molecules are correlated in one direction (known as the director, **n**) while being positioned randomly (Fig. 2A). There are several smectic phases and these differ from the nematic phase in possessing partial posi-

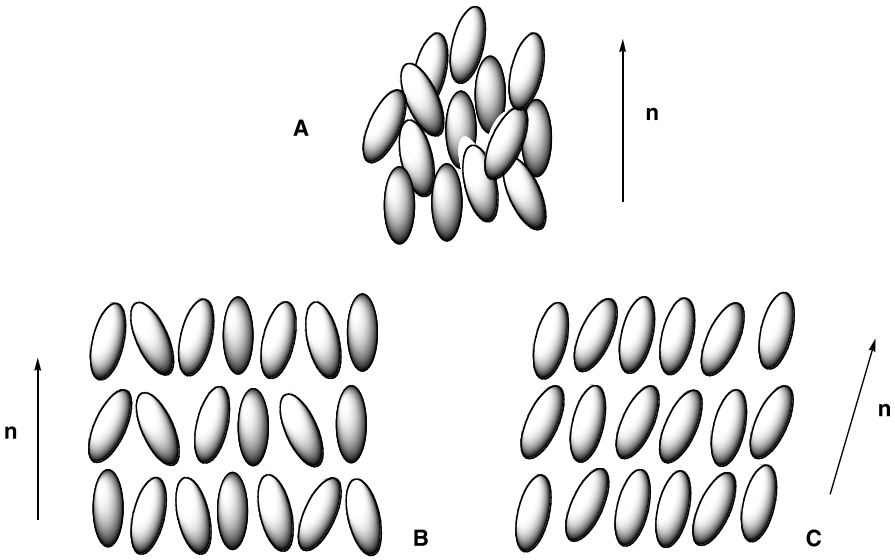


**Fig. 2** Schematic representation of the molecular arrangement in the **A** nematic, **B** smectic A (SmA) and **C** smectic C (SmC) phases

tional order, manifest as a loose ordering of the molecules into layers. There are now very many different smectic phases known, but in general they may be classified as either possessing in-layer order or not. The SmA and SmC phases do not have in-layer order and they are represented as Figs. 2B and 2C. The SmA phases has its molecules orthogonal to the layers, while in the SmC phase they are tilted. The probability for interlayer diffusion of molecules is high and these are truly fluid phases.

In-layer order is normally of the hexagonal kind, so that the SmB phase is an orthogonal, hexagonal phase while the SmF and SmI phases are tilted variants. While, strictly, the symmetry of all of these phases is reduced when the constituent molecules are chiral, the effect is significant only for the nematic phase and the tilted smectic phases (SmC, SmF and SmI). The chiral phase (N*) has a helical structure that arises due to a precession of the director through space. The helical structure confers a periodicity on the phase and it turns out that the pitch ($p$) is often of the order of the wavelength of visible light. As such, the helix can exhibit simple Bragg reflection with the reflected wavelength ($\lambda$) being given by:

$$\lambda = \overline{n}p$$

where $\overline{n}$ is the average refractive index of the phase. Note that the reflected light is circularly polarised. As $p$ changes with temperature ($p$ generally de-

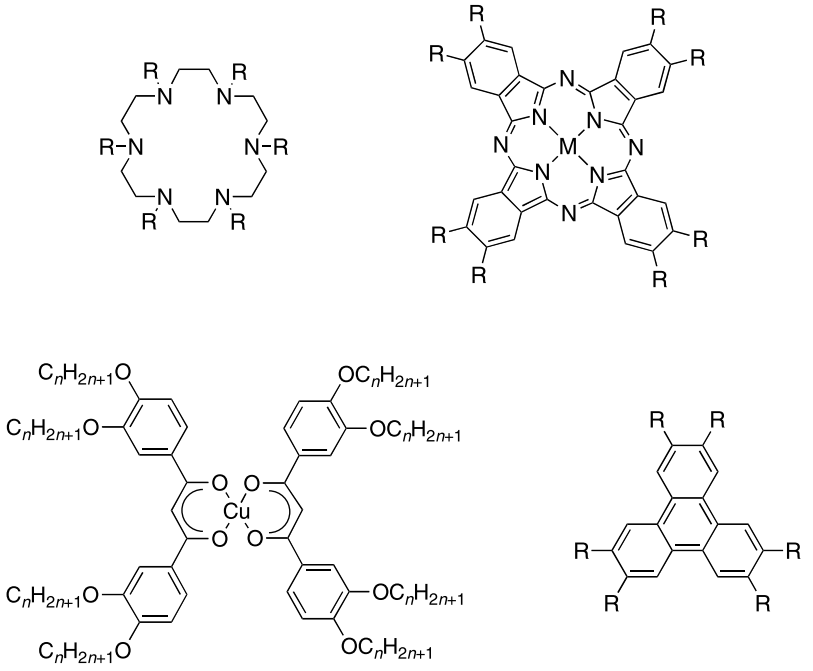


**Fig. 3** Examples of discotic liquid crystals

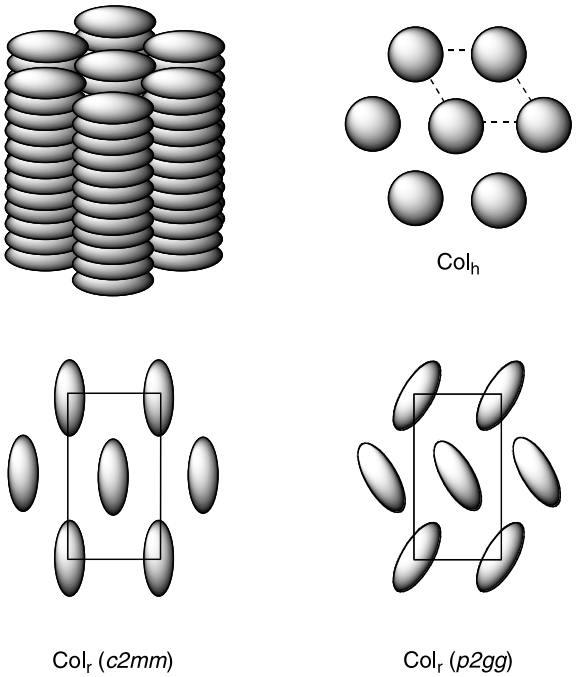


**Fig. 4** Schematic representation of the molecular organisation in three common columnar phases

creases with increasing temperature), then the reflected colour also changes and so chiral nematic liquid crystals (also sometime known as *cholesteric* liquid crystals) find application in temperature sensing.

*Discotic* liquid crystals on the other hand are based around a fairly flat core structure and are generally surrounded by six or eight peripheral alkyl(oxy) chains. Examples are given in Fig. 3.

A nematic phase of discotic molecules exists where the short molecular axes are correlated directionally but this phase is still rather rare. By far and away the most common behaviour is for the molecules to stack in columns, which are then arranged in a particular way with respect to one another [7]. Examples are given in Fig. 4.

## 2.2 High Molar Mass Liquid Crystals

In general terms, high molar mass liquid crystals are classified according to the location of the mesogenic unit in the polymer. Thus, they are either incorporated into the main chain (main-chain liquid crystal polymers – MCLCP; Fig. 5A) or they are pendant from the main chain (side-chain liquid crystal polymers – SCLCP; Fig. 5B).

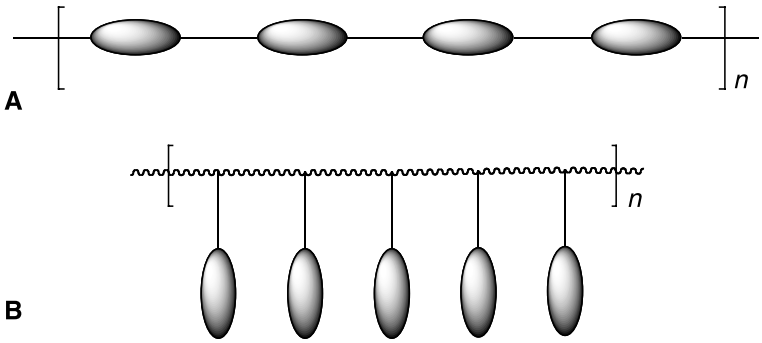


**Fig. 5** Schematic representation of the molecular arrangement in **A** main-chain and **B** side-chain liquid crystal polymers

Many MCLCP are highly insoluble, high-melting materials (if they melt at all) as they are rigid. However, if they can be processed then they make very strong materials, an example of which is Kevlar (Fig. 6) – a copolyamide of terephthalic acid and *p*-phenylene diamine – which is spun into high-strength fibres from its nematic phase in oleum. One way in which MCLCP can be made more tractable is if the rigid link between mesogenic groups is replaced by a flexible chain to give semi-flexible MCLCP.

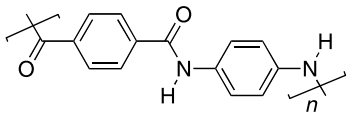


**Fig. 6** Molecular structure of Kevlar®

SCLCP tend to have a conventional backbone, the two most common being methylsiloxane and (meth)acrylate, the former giving low glass transition temperatures ($T_g$), while the latter gives high values of $T_g$. In the case of siloxanes, the mesogenic groups are grafted onto the preformed polymer while for acrylates, the monomeric unit already contains the mesogenic moiety.

## 3
## Characterisation of Liquid Crystal Mesophases

The principal technique is polarised optical microscopy, which exploits the anisotropy in refractive index of the liquid crystal mesophases. Thus, the microscope is configured (Fig. 7) so that the sample is between two polarisers that are crossed (no light would normally pass through) and the sample is placed on a heated stage through which light may pass. Plane, polarised light then impinges on the sample (< 1 mg of sample held between two micro-

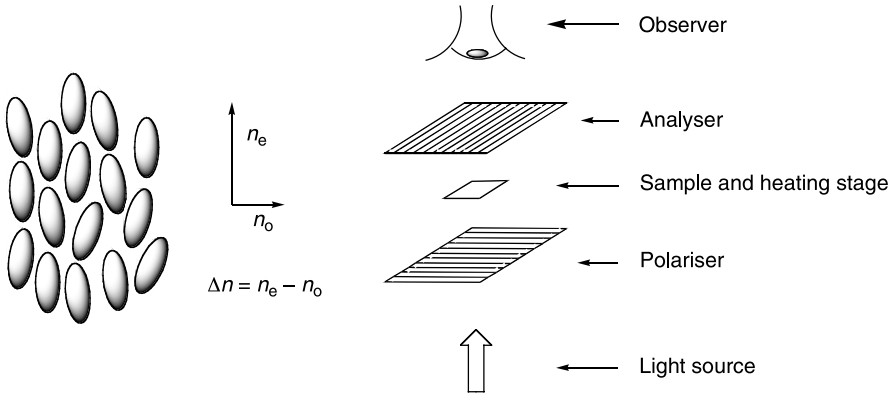


**Fig. 7** Figure to show the origins of birefringence (*left*) and a schematic diagram of a polarised optical microscope (*right*)

scope cover slips) and becomes circularly polarised, generating two refracted rays, $n_e$ and $n_o$, the difference between them ($\Delta n$) being termed the birefringence. These two rays can then interfere with one another and, as the plane polarisation is lost, an interference pattern is seen by the observer [8, 9].

The interference pattern depends both on the symmetry of the liquid crystal mesophase and on the arrangement of the molecules between the glass cover slips. Three examples are given in Fig. 8.

## 4
## Liquid Crystals Formed Through Non-covalent Interactions

### 4.1
### Quadrupolar Interactions

First, it is important to appreciate that all liquid crystal mesophases exist due to non-covalent interactions between molecules, namely the anisotropic dispersion forces mentioned earlier. However, this section will address more specific non-covalent interactions that have been used either to induce liquid-crystalline behaviour or to generate a new species that is liquid crystalline.

For example, Marder and co-workers [10] (among others) have studied liquid crystal mesophases induced by the presence of quadrupolar interactions between non-mesomorphic phenyl- and perfluorophenyl-containing moieties (e.g. **1**).

Quadrupolar interactions (termed *complementary polytopic interactions* by the authors) are also responsible for mesophase induction and modification in a series of disc-like materials (e.g. **2** and **3**) as described by, for example, Bushby and co-workers [11–13].

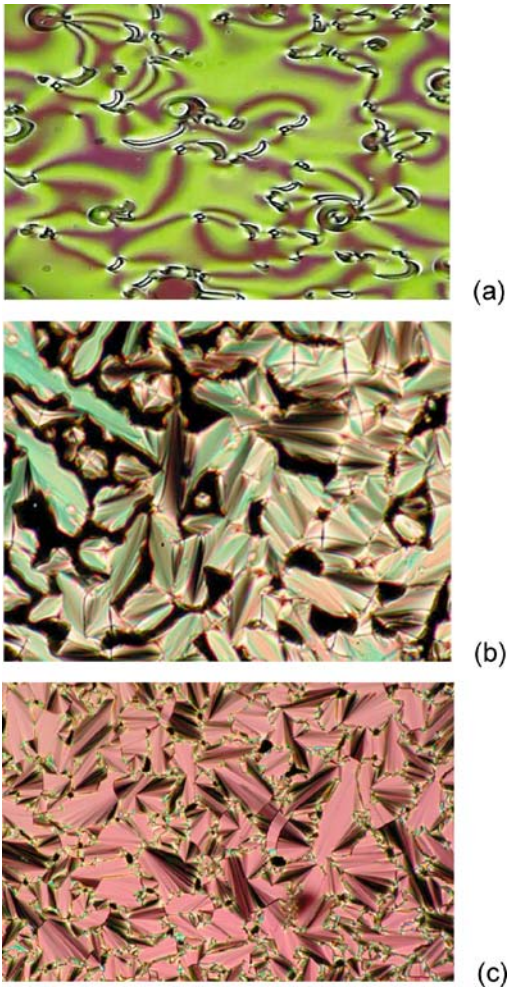


**Fig. 8** Optical micrograph of: **a** a nematic phase, **b** a SmA phase (reproduced with kind permission of the American Chemical Society) and **c** a SmC phase (reproduced with kind permission of the copyright owner, D.W. Bruce)

## 4.2 Charge-transfer Interactions

A different mechanism is that of charge transfer, of which there are many examples based, in particular, on metallomesogens [14]. In these cases, mesophases can be induced by adding the electron-poor TNF (2,4,7-trinitro-9-fluorenone) and Fig. 9 shows Pd mesogen **4**, which shows a particular type of SmA phase when TNF is added [15].

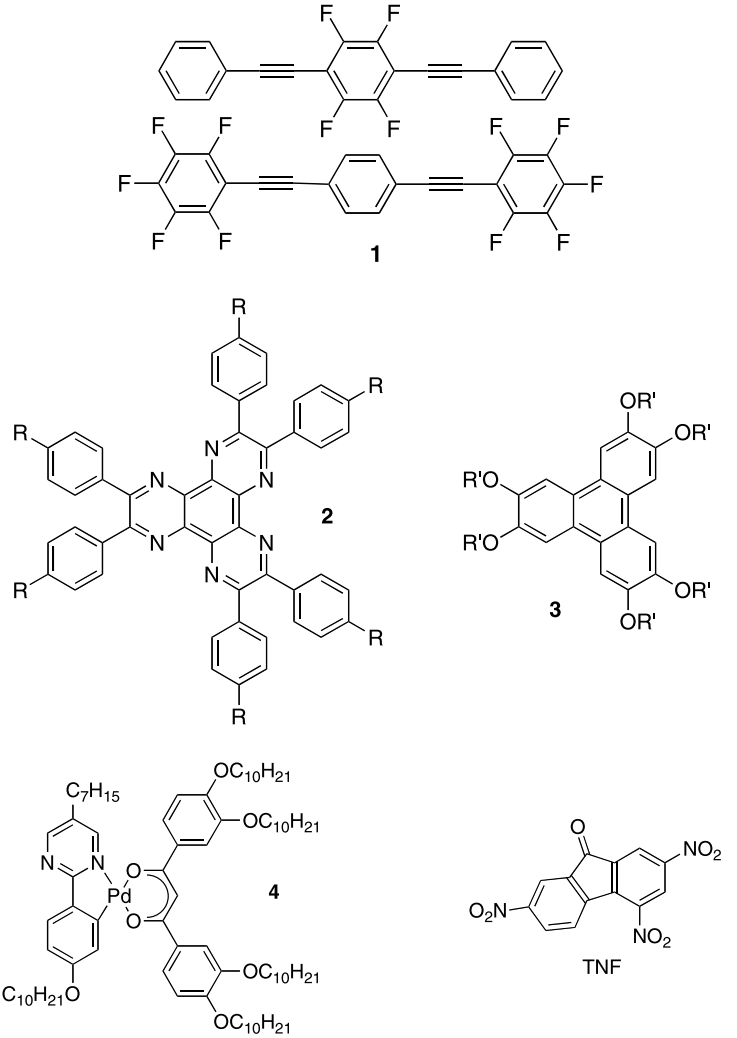


**Fig. 9** The two components that form a charge-transfer complex, which exhibits the biaxial SmA phase

## 5 Hydrogen Bonding

However, by far the most common non-covalent interaction responsible for generating new liquid-crystalline species is the hydrogen bond, and this area has been well reviewed [16, 17]. In fact, hydrogen bonding in liquid crystals is a very old concept and it has been known for some time that, for example, the

mesogenic behaviour of 4-alkoxybenzoic acids, **5**, depends totally on the fact that they exist as hydrogen-bonded dimers.

More exotic systems have also been described and, for example, Lehn and co-workers described the complementary system, **6**, which was found to exhibit a columnar mesophase [18], while neither of the components was mesomorphic.

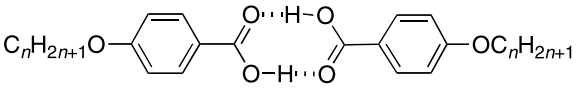

**5**

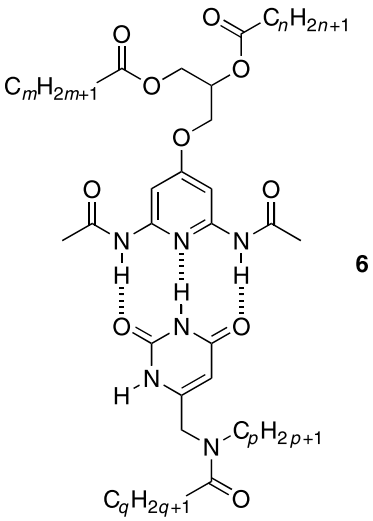

**6**

Diamides such as **7** and **8** (Fig. 10) were described originally by Matsunaga and Terada [19] and then later reinvestigated by Malthête and coworkers [20–23]. In many ways, at first sight it is surprising that these systems are liquid crystalline at all, but the "secret" is in intermolecular hydrogen bonding, which causes the molecules to form columns. These columns can than organise to form nematic and columnar phases.

However, the hydrogen-bonded mesogens that are of most interest in the context of this article are those elaborated initially by Kato and Fréchet in the early 1990s [24–33]. In this approach, a pyridine, which may or may not have liquid crystal properties, was hydrogen bonded with a 4-substituted benzoic acid to form a new species with its own, distinct mesomorphism. For example, complex **9** shows a SmA phase that persists to 238 °C ($n = 2$, $m = 4$), while its free component pyridine is nematic to 213 °C; the component benzoic acid is also nematic (as the H-bonded dimer) to 147 °C (although note that the notional "monomer" would not be liquid crystalline).

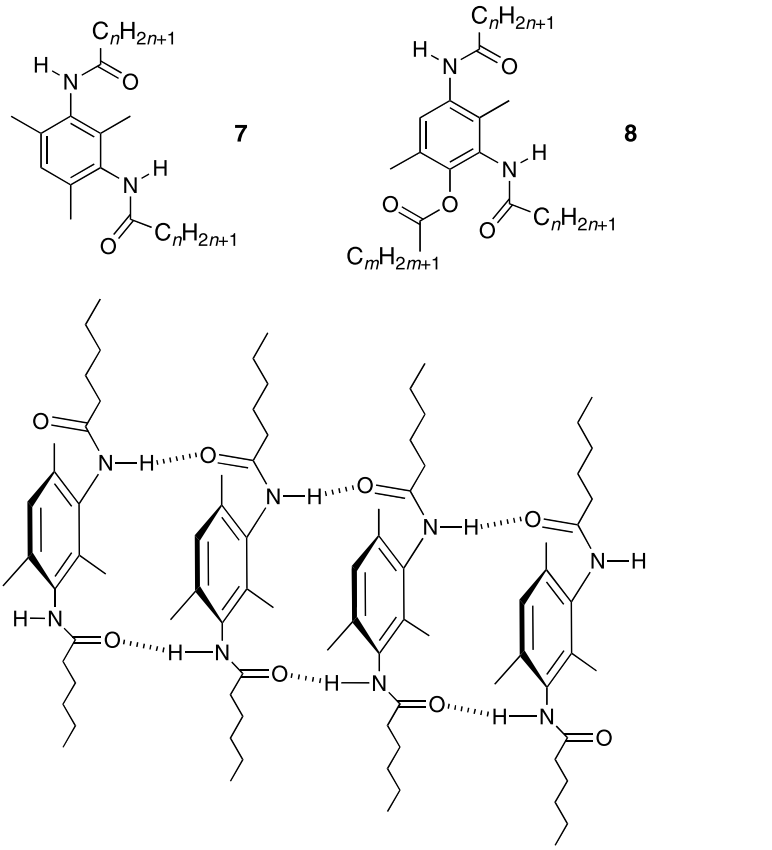


**Fig. 10** The molecules involved in the formation of hydrogen-bonded nematic and columnar phases (*upper part*) and a representation of the arrangement of the molecules in the mesophases (*lower part*)

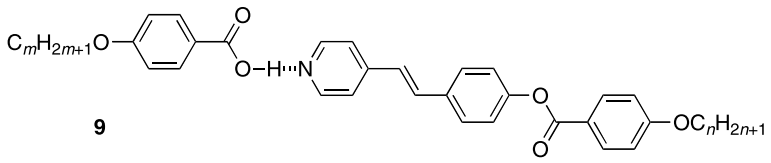


A particularly elegant example of this approach is complex **10**, which represents a very simple situation, namely that of an alkoxybenzoic acid and an alkyl pyridine and which shows a nematic phase at room temperature. There are, of course, very many examples of mesogens constructed in this was using pyridines, benzoic acids and even phenols; these are helpfully collected in the relevant review literature [16, 17].

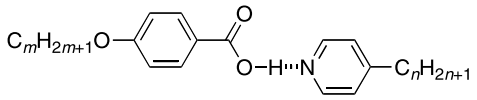


**10**

This work raises some interesting issues. The first is that the stoichiometry of a complex is not necessarily the most obvious. For example, it was reported initially that phthalic acid formed a 2 : 1 complex with alkoxystilbazole [34], when in fact a careful study carried out by constructing a binary phase diagram (Fig. 11) revealed the complex to have a 1 : 1 ratio of the two components [35]. The reluctance of the system to form the more obvious 2 : 1 complex may relate to the presence of intramolecular hydrogen bonding or could even relate to the change in the p$K_a$ of the second acid proton on complexation.

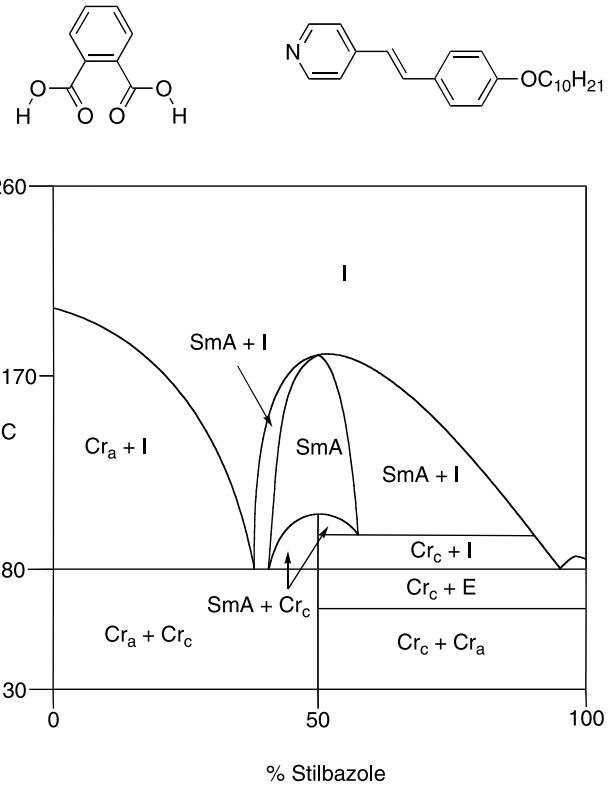


**Fig. 11** Binary phase diagram between phthalic acid and decyloxystilbazole. ($Cr_c$ and $Cr_a$ are the crystal phase of the complex and the acid, respectively; E is the crystal smectic E phase). Adapted from [35]

Note that this phase diagram points to a very useful fact, namely that when a hydrogen-bonded (or, indeed, a halogen-bonded) complex has the two components in the correct ratio, it will melt as a single entity and there will be no biphasic behaviour (indeed, it was the lack of such well-defined behaviour that led to the careful examination of the phthalic acid/stilbazole system in the first place). However, one complication can be the presence of multiple thermal events. For example, complex **11** fails to form from the two components after evaporation of the solvent, rather forming an intimate mixture. On heating, the cyanostilbazole first melts to give a mixture of the crystalline phase of the acid and the isotropic phase of the stilbazole. At a higher temperature, the complex does, however, form giving rise to a nematic material that clears in the normal way. Cooling leads to decomplexation and the whole cycle is repeated [36].

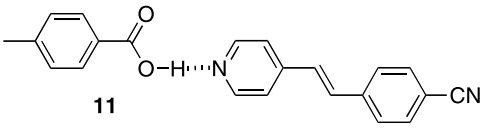


**11**

Another important issue relates to the behaviour at the transition to the isotropic liquid (known as *clearing*) and the question of whether the rupture of the hydrogen bond drives the clearing process or whether the complex passes from mesophase to isotropic as a complete unit. Simple consideration of complex **10** gives an immediate answer, for these materials clear around 50 °C, at which temperature the benzoic acids are solids. Clearing should then lead to immediate crystallisation, which is not observed. This conclusion is reinforced by a variable temperature electronic spectroscopy study of the behaviour of decyloxystilbazole and 2,4-dinitrophenol [37, 38]. 2,4-Dinitrophenol is a relatively strong acid ($pK_a = 3.96$) and the study showed that while at room temperature, a neutral hydrogen-bonded species existed (–N···H–O–), at higher temperature through the SmA phase, proton transfer occurs to give the ionic hydrogen-bonded species ($–NH^+\cdots{}^-O–$) and that this species persists beyond the clearing point. Indeed, there is no reason why hydrogen bond strength should limit the stability of a mesophase, for studies of the hydrogen-bonded complex between the two, non-mesomorphic components, 4-biphenylcarboxylic acid and 4-cyanostilbazole (**12**), have shown the existence of a nematic phase to temperatures above 200 °C [36].

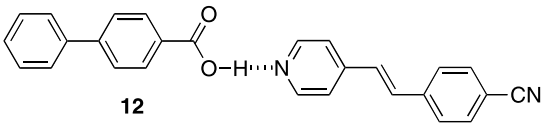


**12**

## 6
## Halogen-bonded Liquid Crystals

It was from this background in hydrogen bonding that our own work in halogen bonding had its genesis. We became aware of the work published by the Milan group [39] and considered whether we could use such a general approach to form new liquid-crystalline species. We had worked with stilbazoles since the mid-1980s and they seemed the obvious choice of Lewis base, with iodopentafluorobenzene a good starting point as a source of electron-poor halide.

The first thing that became immediately apparent is that the synthetic route had to be re-evaluated. In hydrogen-bonded systems, it is normally sufficient to mix the two components in a common solvent and then remove it to leave the pure complex. On occasions when this does not work (often due to the high lattice energy/low solubility of one component), it is necessary only to heat the mixture into the melt for a few minutes and then allow the whole thing to cool down. In the case of the halogen-bonded materials, however, this was often not the case and in many cases attempts to proceed in this way led to materials that were clearly not single component in nature, as evidenced by the observation of more than one melting event and of biphasic behaviour. Clearly then, however stable a halogen bond might be, it would appear to be much more labile than an analogous hydrogen bond. Therefore, the approach adopted by us and followed since has been to try to grow single crystals of the complexes and work exclusively with those, although it is apparent that this is not always necessary. This presents obvious immediate advantages (lots of crystal structures) and disadvantages (some complexes will simply not crystallise). Thus, single crystals were obtained of complex **13**-*n* for $n = 4$, 6, 8, 10 and 12 and the mesomorphism was determined. X-Ray single crystal structures were also obtained for $n = 8$ and 10 [40][1].

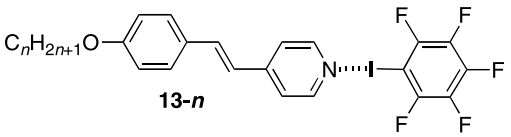


**13-*n***

The molecular structure of **13**-8 (Fig. 12) shows the presence of the halogen bond ($d_{N\cdots I} = 2.811(4)$ Å compared with the sum of the van der Waals' radii of 3.53 Å) with a N···Î–C angle of 168.4°. The structure of **13**-10 was also determined, and this time the following parameters were observed: $d_{N\cdots I} = 2.789$ Å; N···Î–C = 177.9°.

Analysis of the packing of the complexes (e.g. Fig. 13) also showed the absence of quadrupolar phenyl/perfluorophenyl interactions, an observation

[1] Nguyen HL, Horton PN, Hursthouse MB, Bruce DW, unpublished work

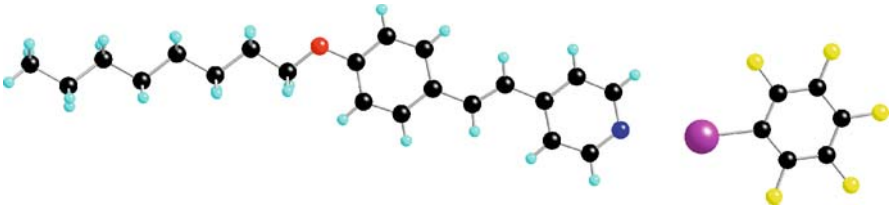

**Fig. 12** Molecular structure of the complex between 4-octyloxystilbazole and iodopentafluorobenzene. Reproduced by kind permission of the American Chemical Society

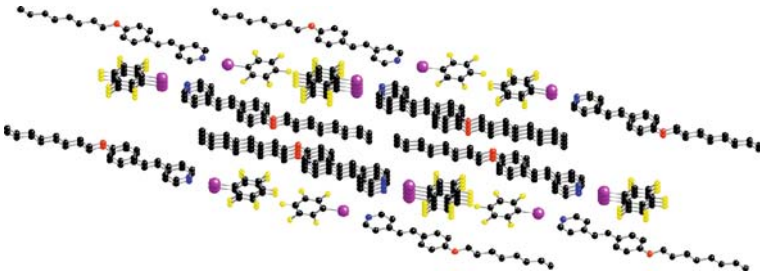

**Fig. 13** One projection of the packing of **13**-8 – hydrogen atoms omitted for clarity

backed up by the lack of any evidence for interactions between stilbazole and hexafluorobenzene [41]. In relation to this, it was observed that while the starting stilbazole was colourless, the halogen-bonded complex was slightly coloured. Such an observation is entirely consistent with a charge-transfer interaction at nitrogen and parallels the red shift observed in the VT electronic spectra for stilbazole and 2,4-dintrophenol (vide supra) [37, 38].

The liquid crystal properties of the complexes were characterised using polarised optical microscopy and showed a nematic phase for $n = 4$ and 6 and a SmA phase for $n = 6$, 8, 10 and 12. The mesophases were monotropic for $n = 4$ and 6 and enantiotropic for the others; the progression from a nematic phase for shorter chain lengths to SmA at longer chain lengths is quite typical for simple, polar mesogens.

Halogen bonding is also observed with electron-poor bromides, and so attempts were made to form complexes between stilbazole and *bromo*pentafluorobenzene. We were never able to find evidence that such a complex formed and indeed, heating crystallised samples only reproduced the thermal behaviour of the stilbazoles themselves. Thus, any halogen bonding is supposed weak (there was no observable colour change in the stilbazole) and unable to sustain the complex at temperatures much above ambient.

Moving on from an aromatic monoiodo species, attention then turned to $\alpha,\omega$-diiodoperfluoroalkanes where it was possible to demonstrate 2 : 1 complex formation (**14**) [42].

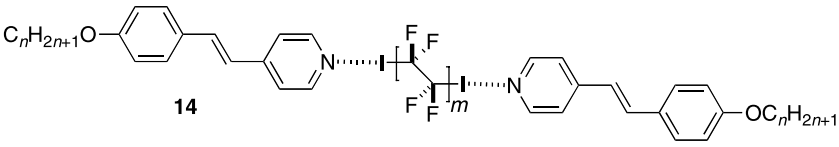


14

The structure and packing of the complex with $n = 8$ and $m = 3$ are shown in Figs. 14 and 15, respectively ($d_{N\cdots I} = 2.746$ Å; N· · ·Î–C = 176.99°). The former shows an expected disposition of the stilbazoles and the perfluoroalkyl entity, while the latter shows an effective segregation of the fluoroalkyl and stilbazole segments.

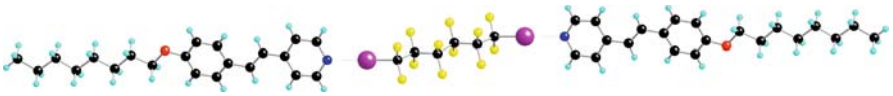

**Fig. 14** Molecular structure of the 2 : 1 complex between 4-octyloxystilbazole and 1,6-diiodoperfluorohexane

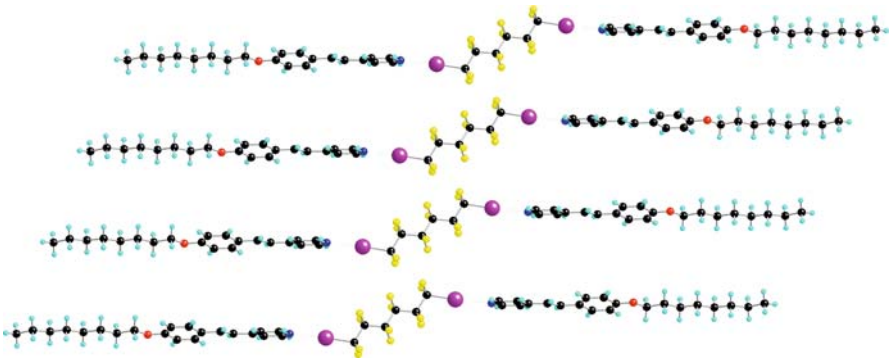

**Fig. 15** Packing in the crystal of the 2 : 1 complex between 4-octyloxystilbazole and 1,6-di-iodoperfluorohexane. Reproduced from [42] by kind permission of the Royal Society of Chemistry

The complexes studied had $n = 8$, 10 and 12 and $m = 2$ and 3. With the exception of the complex with $n = 10$ and $m = 3$, all complexes showed a nematic phase which, in all cases, was monotropic. Thus, melting points were in the range 95 to 108 °C, with clearing points between 90 and 104 °C.

Another series of trimers was reported (**15**-*n*,*m*) that consisted of two stilbazoles halogen bonded to a dimeric iodotetrafluorobenzene unit [43]. Examples were reported for $m = 2$, 4, 6 and 8 and $n = 6$, 8, 10 and 12. In characterising the halogen bonds in these complexes, XPS data were examined and it was reported that the binding energy of the N 1*s* level increased by around 0.9 to 1.1 eV on complexation, while small hypsochromic shifts (typ-

ically 2 to 3 $cm^{-1}$) were seen in the aromatic C–C stretching region of the stilbazole in the infrared spectra on complex formation.

Examination of the thermal behaviour showed that with three exceptions, all complexes showed a monotropic SmA phase with in almost all cases, melting being observed between 88 and 99 °C, with clearing between 82 and 89 °C. Of the three exceptions, **15**-6,8 and **15**-8,10 showed no liquid crystal phase at all, while **15**-12,6 showed an additional monotropic nematic phase. A curious feature of these complexes is the apparent insensitivity of the melting and clearing points to both *n* and *m*.

Simpler examples generated 2 : 1 complexes from alkoxystilbazoles and 1,4-dihalotetrafluorobenzenes (**16** and **17**).

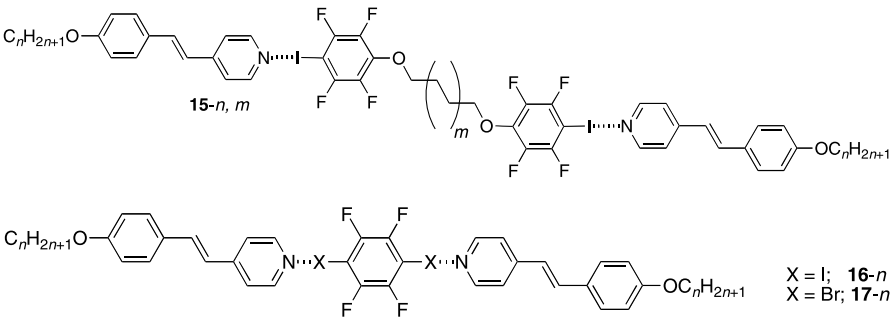


Crystallographic characterisation of **16**-8 showed the expected arrangement and gave an N···I separation of 2.812 Å with an N···I–C angle of 175.09°.

Complexes **16**-6, **16**-8 and **16**-10 all showed monotropic nematic phases with melting points between 115 and 130 °C and N to I transitions around 110 °C; neither **16**-4 nor **16**-12 showed any LC phases. However, enantiotropic mesomorphism was found when mixtures were prepared. Thus, an equimolar mixture of 1,4-diiodotetrafluorobenzene, hexyloxystilbazole and decyloxystilbazole was prepared, which it was assumed contained a statistical mixture of symmetric and unsymmetric complexes. The melting point was 110 °C, with clearing occurring just afterwards at 111.5 °C. However, a mixture consisting of 1 : 2 : 1 : 2 butyloxystilbazole : octyloxystilbazole : dodecyloxystilbazole : diiodotetrafluorobenzene showed a wider range, melting at 100 °C and, once more, clearing at 111.5 °C [44].

The same paper also described an analogous complex of 1,4-dibromotetrafluorobenzene, **17**-8, whose molecular structure, as obtained by single crystal methods, is shown as Fig. 17.

The structure is very similar to that of **16**-8 with N···Br distance was 2.867 Å (again shorter that the sum of van der Waals radii) and the N···Br–C angle at 174.11°. Indeed, the crystals of **17**-8 and **16**-8 are almost isomorphous.

**Fig. 16** Molecular structure of the 2 : 1 complex between octyloxystilbazole and 1,4-diiodotetrafluorobenzene (**16**-8). Reproduced from [44] by kind permission of the Royal Society of Chemistry

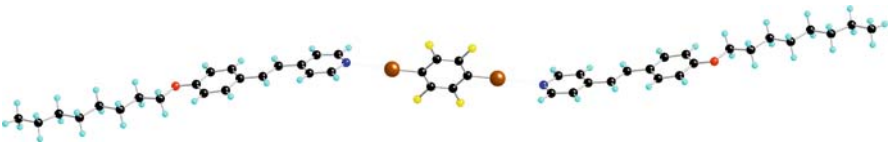

**Fig. 17** Molecular structure of the 2 : 1 complex between octyloxystilbazole and 1,4-dibromotetrafluorobenzene (**17**-8). Reproduced from [44] by kind permission of the Royal Society of Chemistry

Complex **17**-8 melted at 92 to 93 °C – higher than the melting point of dibromotetrafluorobenzene at 78–81 °C – yet no mesophase was seen [24]. It is believed that this is due to the much weaker nature of the N···Br interaction, an observation consistent with those made for complexes between alkoxystilbazoles and bromopentafluorobenzene [20].

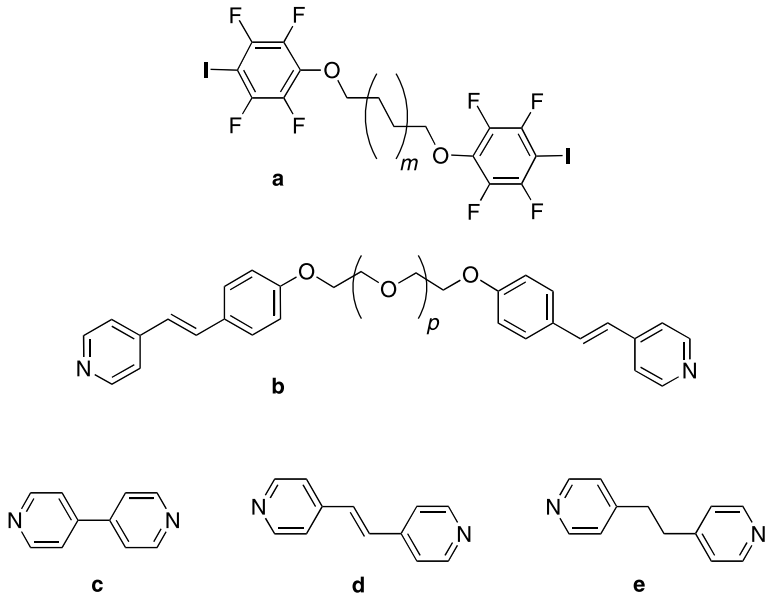


**Fig. 18** Components used to form mesomorphic, halogen-bonded polymers

Polymeric examples have also been reported using similar chemistry. Thus, dimer **a** (Fig. 18) was allowed to react with dimer **b** and also with compounds **c**, **d** and **e** to give polymers whose degree of polymerisation was unreported [45].

Polymers formed between **a** and **c**, **d** and **e** all failed to show any liquid-crystalline behaviour. However, for all **a** examined ($m$ = 2, 4, 6 and 8), nematic phases were observed with **b**-4 (all monotropic) – a further monotropic nematic material was the copolymer of **a**-6 and **b**-3. Unidentified crystal smectic mesophases were reported for a further three examples.

## 7
## Future Prospects

At the time of writing, the five papers described in the preceding section represents the sum total of published work in the area and while this volume is timely in terms of the broader field of halogen bonding, it is slightly premature with respect to liquid crystals. Of course, this is not the end of the story and the author alone and also in collaboration with the Milan group, has a good deal of unpublished work that will come to fruition shortly. For example, it has been shown that iodoperfluoroalkanes will complex with stilbazoles to form mesomorphic materials, again characterised by X-ray methods with some interesting results[2].

This area is just beginning and there is a great deal to learn from previous work with hydrogen-bonded systems. However, the need, in our view, to obtain single crystals in order to be confident about stoichiometry will inevitably limit some of what can be achieved, as this author is only too well aware of the problems associated with crystallising materials containing long and/or multiple alkoxy chains. Nonetheless, there will be systems for which this is not an absolute requirement and there is confidence that other ways will be found to accommodate this issue. It is hoped that the examples given above will whet the appetite and encourage others to join the search for ever more imaginative materials.

## References

1. Demus D, Goodby J, Gray GW, Spiess H-W, Vill V (eds) (1998) Handbook of Liquid Crystals. Wiley-VCH, Weinheim
2. Reddy RA, Tschierske C (2006) J Mater Chem 16:907
3. Donnio B, Guillon D, Deschenaux R, Bruce DW (2003) In: McCleverty JA, Meyer TJ (eds) Comprehensive Coordination Chemistry II, vol 7, chap 7.9. Elsevier, Oxford, UK, pp 357–627
4. Donnio B, Bruce DW (1999) Struct Bonding 95:193

[2] Metrangolo P, Bruce DW, Pilati T, Resnati G, unpublished results

5. Binnemans K, Görller-Walrand C (2002) Chem Rev 102:2303
6. Serrano JL (ed) (1995) Metallomesogens: Synthesis, Properties and Applications. VCH, Weinheim
7. Guillon D (1999) Struct Bonding 95:41
8. Gray GW, Goodby JWG (1984) Smectic Liquid Crystals, Textures and Structures. Blackie, Glasgow
9. Dierking I (2003) Textures of Liquid Crystals. Wiley-VCH, Weinheim
10. Dai C, Nguyen P, Marder TB, Scott AJ, Clegg W, Viney C (1999) Chem Commun, p 2493
11. Boden N, Bushby RJ, Lu Z, Lozman OR (2001) Liq Cryst 5:657
12. Boden N, Bushby RJ, Lu Z, Lozman OR (2001) J Mater Chem 11:1612
13. Boden N, Bushby RJ, Cooke G, Lozman OR, Lu Z (2001) J Am Chem Soc 123:7915
14. Praefcke K, Holbrey JD (1996) J Incl Phenom Mol Recogn Chem 24:19
15. Hegmann T, Kain J, Diele S, Pelzl G, Tschierske C (2001) Angew Chem Int Ed 40:887
16. Paleos C, Tsiourvas D (2995) Angew Chem Int Ed Engl 34:1696
17. Kato T (1998) In: Demus D, Goodby J, Gray GW, Spiess H-W, Vill V (eds) Handbook of Liquid Crystals, Vol. 2B, Chap. XVII. Wiley-VCH, Weinheim
18. Brienne MJ, Galard J, Lehn JM, Stibor I (1989) J Chem Soc Chem Commun, p 1868
19. Matsunaga Y, Terada M (1986) Mol Cryst Liq Cryst 141:321
20. Pucci D, Veber M, Malthête J (1996) Liq Cryst 21:153
21. Garcia C, Malthête J (2002) Liq Cryst 29:1133
22. Albouy PA, Guillon D, Heinrich B, Levelut AM, Malthête J (1995) J Phys II 5:1617
23. Malthête J, Levelut AM, Liebert L (1992) Adv Mater 4:37
24. Kato T, Fréchet JMJ (1989) J Am Chem Soc 111:8533
25. Kato T, Fréchet JMJ (1989) Macromolecules 22:3818
26. Kumar U, Kato T, Fréchet JMJ (1992) J Am Chem Soc 114:6630
27. Kato T, Kihara H, Uryu T, Fuijishima A, Fréchet JMJ (1992) Macromolecules 25:6836
28. Kato T, Kihara H, Kumar U, Uryu T, Fréchet JMJ (1994) Angew Chem Int Ed Eng 33:1644
29. Kato T, Wilson PG, Fuijishima A, Fréchet JMJ (1990) Chem Lett, p 2003
30. Kato T, Fréchet JMJ, Wilson PG, Saito T, Uryu T, Fuijishima A, Sin C, Kaneuch F (1993) Chem Mater 5:1094
31. Kato T, Fuijishima A, Fréchet JMJ (1990) Chem Lett, p 912
32. Fukumassa M, Kato T, Uryu T, Fréchet JMJ (1993) Chem Lett, p 65
33. Kato T, Kihara H, Uryu T, Ujiie S, Iimura K, Fréchet JMJ, Kumar U (1994) Ferroelectrics 148:1303
34. Fukumasa M, Kato T, Uryi T, Fréchet JMJ (1993) Chem Lett, p 65
35. Willis K, Price DJ, Adams H, Ungar G, Bruce DW (1995) J Mater Chem 5:2195
36. Price DJ, Adams H, Bruce DW (1996) Mol Cryst Liq Cryst 289:127
37. Price DJ, Richardson T, Bruce DW (1995) J Chem Soc Chem Commun, p 1911
38. Price DJ, Willis K, Richardson T, Ungar G, Bruce DW (1997) J Mater Chem 7:883
39. Metrangolo P, Neukirch H, Pilati T, Resnati G (2005) Acc Chem Res 38:386
40. Nguyen HL, Horton PN, Hursthouse MB, Legon AC, Bruce DW (2004) J Am Chem Soc 126:16
41. Wasilewska A, Gdaniec M, Polloski T (2007) Cryst Eng Commun 9:203
42. Metrangolo P, Präsang C, Resnati G, Liantonio R, Whitwood AC, Bruce DW (2006) Chem Commun, p 3290
43. Xu J, Liu X, Ng JK-P, Lin T, He C (2006) J Mater Chem 16:3540
44. Bruce DW, Metrangolo P, Meyer F, Präsang C, Resnati G, Terraneo G, Whitwood AC (2007) New J Chem, (in press)
45. Xu J, Liu X, Lin T, Huang J, He C (2005) Macromolecules 38:3554

Struct Bond (2008) 126: 181–207
DOI 10.1007/430_2007_059

Published online: 29 June 2007

# Halogen Bonding in Conducting or Magnetic Molecular Materials

Marc Fourmigué

Equipe Matière Condensée et Systèmes Electroactifs (MaCSE),
Sciences Chimiques de Rennes, UMR 6226 CNRS-Université Rennes 1,
Campus de Beaulieu, 35042 Rennes, France
*marc.fourmigue@univ-rennes1.fr*

**1 Introduction** . . . . . 182

**2 Neutral Radical Nitroxides** . . . . . 183
2.1 Halogenated Neutral Nitroxides . . . . . 183
2.2 Binary Systems Involving Nitroxides . . . . . 185

**3 Conducting Materials Based on Tetrathiafulvalenes** . . . . . 186
3.1 An Introduction to Conducting TTF Salts . . . . . 187
3.2 Neutral Halogenated TTFs . . . . . 188
3.3 Cation Radical Salts of Halogenated TTFs . . . . . 192
3.3.1 Hal···$Hal_{anion}$ Interactions . . . . . 192
3.3.2 Hal···Nitrile Interactions . . . . . 197
3.3.3 Iodopyrazino TTFs, Iododithiapyrenes . . . . . 200
3.4 Ternary Systems . . . . . 202

**4 Summary and Outlook** . . . . . 202

**References** . . . . . 204

**Abstract** The role of halogen bonding interactions in conducting or magnetic molecular systems is evaluated here in various series of halogenated radical molecules, such as neutral nitroxides or tetrathiafulvalene (TTF) salts where short and linear C – Hal···Hal,O,N interactions are identified. Oxidation of halogenated TTFs to the cation radical state activates the halogen bonding interaction with counter ions of Lewis base character, i.e. halide, polyhalide or halometallate anions on the one hand, and polycyanometallate or organic nitrile anions on the other. Iodoperfluoroalkanes or -perfluorarenes can also act as halogen bond donors when associated with neutral nitroxide radicals or with halide anions in cation radical salts of non-halogenated TTFs.

**Keywords** Crystal engineering · Halogen bonding · Nitroxide · Tetrathiafulvalene

**Abbreviations**

| | |
|---|---|
| BEDT-TTF | Bis(ethylenedithio)tetrathiafulvalene |
| CCDC | Cambridge Crystallographic Data Centre |
| DIA | Diiodoacetylene |
| DTPY | 1,6-Dithiapyrene |
| EDO-TTF | Ethylenedioxo-tetrathiafulvalene |

| | |
|---|---|
| EDT-TTF | Ethylenedithio-tetrathiafulvalene |
| SOMO | Singly occupied molecular orbital |
| TEMPO | 2,2,6,6-Tetramethyl(piperidin-1-yloxyl) |
| TSF | Tetraselenafulvalene |
| TTF | Tetrathiafulvalene |

## 1 Introduction

Crystal engineering, defined by Desiraju as "the understanding of intermolecular interactions in the context of crystal packing and the utilization of such understanding in the design of new solids with desired physical and chemical properties", has been the subject of several excellent reviews [1–3]. As a favourite tool to build such supramolecular crystalline systems, directional intermolecular interactions, such as the prototypical hydrogen bond [4], have demonstrated their remarkable efficiency, extended since to the weaker C – H···X hydrogen bonds [5]. However, among these desired physical properties invoked by Desiraju, a metallic conductivity or a magnetic ordering are not considered to possibly derive solely from the structural requirements brought by hydrogen or halogen bonding interactions in molecular solids. Indeed, molecular conductors are primarily based on *radical molecules* interacting more or less strongly with each other in one-, two- or three-dimensional structures, allowing for the formation of partially filled conduction bands and their associated metallic behaviour through the overlap interaction of the singly occupied molecular orbitals (SOMOs) [6–8]. Similarly, a magnetic ordering in molecular solids requires a precise distribution and topology of spin density interactions between radical molecules [9]. However, it was soon discovered that the band structures of molecular conductors are excessively sensitive to minute structural modifications [10], and hence that intermolecular interactions as weak as C – H···X interactions could bring dramatic effects on the conduction properties [11]. Similarly, magnetic interactions, much weaker in essence, can possibly be transmitted through such weak C – H···X intermolecular interactions [12, 13].

The combination of both approaches, toward a *crystal engineering of radical molecules*, has led to numerous conducting or magnetic molecular materials which exhibit normal hydrogen bond interactions thanks to their functionalization with hydrogen bond donor groups (– OH, N – H). This has been recently reviewed in the field of molecular conductors [14, 15], while many examples can also be found in the family of nitroxide radicals [16]. Therefore, it is not totally surprising that halogen bonding, once identified as a powerful structural tool, would also be considered in the frame of molecular conductors and magnets. This is the topic of the present review article, which will be divided into two parts, a shorter one dedicated to halogen bonding

in neutral radical nitroxides, and a longer one involving conducting materials derived from halogenated tetrathiafulvalenes (TTFs). We will particularly show that halogen bonding is not only compatible with a metallic conductivity in molecular solids, but also that it is activated in these salts where it might contribute to the conductivity itself through its involvement in the conduction band dispersion.

## 2
## Neutral Radical Nitroxides

In the search for molecular magnetic materials, nitroxide free radicals have been widely used as materials in their own right [16] or in combination with paramagnetic ions [17]. The first organic ferromagnetic material was reported in 1991 in these series, namely the *p*-nitrophenyl nitronyl nitroxide [18]. The overall magnetic behaviour of these radical molecules is controlled not only by the distribution of the spin density in the molecule and the interactions between spins if there is more than one electron, but also by the intermolecular interactions, through space and/or through non-covalent bonds. In that respect, hydrogen bonding interactions between nitroxide-based radical molecules have been extensively investigated as they bring a strong control over the supramolecular arrangement of the radical species. Let us mention, for example, the TANOL (**1**) [19, 20] or the 4-hydroxyimino derivative **3** of TEMPO (**2**) [21] (Scheme 1) where O – H···O – N interactions were unambiguously identified. Similarly, OH···O – N [22, 23] or C – H···O – N [12, 24, 25] interactions were observed in various nitronyl nitroxide derivatives. It is therefore highly surprising that halogen bonding interactions were not used purposely in these extensive series as the N – O groups, which proved to be good hydrogen bond acceptors, can also be considered as potential good halogen bond acceptors.

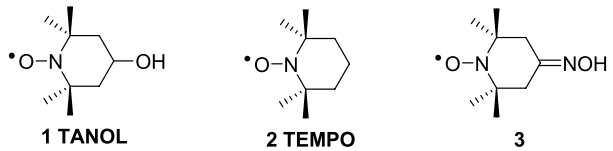


**Scheme 1** Examples of neutral nitroxide radicals

### 2.1
### Halogenated Neutral Nitroxides

A survey of the CCDC database on halogenated nitroxides revealed only a few examples of structures showing halogen bonded motifs, which will be

described below. Among the simplest halogenated nitronyl nitroxides **4a–c** (Scheme 2), only the bromo (**4b**) and iodo (**4c**) derivatives have been described and structurally characterized [26]. These are isostructural and exhibit short N – O···Br (2.970(3) Å) and N – O···I (2.928(3) Å) interactions. Despite a similar molecular packing, the dominant magnetic interactions in **4b** and **4c** are antiferromagnetic and ferromagnetic, respectively, with Curie–Weiss temperatures above 150 K of – 2 (**4b**) and + 5 K (**4c**). The three *p*-halophenyl derivatives **5a–c** have also been structurally characterized [27–29]. In the chloro compound **5a** (Fig. 1) [27], a type I Cl···Cl halogen interaction is identified rather than a Cl···O – N interaction, with the following structural characteristics: Cl···Cl 3.360(2) Å, C – Cl···Cl 154.22(7)°.

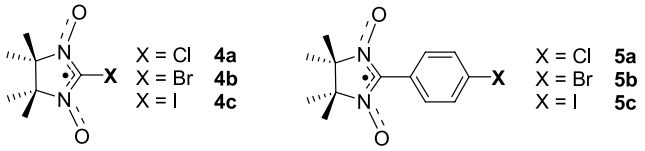


**Scheme 2** Halogenated nitronyl nitroxides

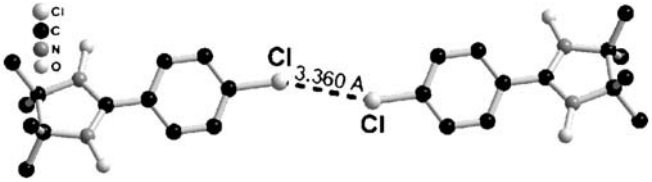


**Fig. 1** Type I Cl···Cl interaction in the *p*-chlorophenyl nitronyl nitroxide **5a**

The iodo derivative **5c** (Fig. 2) is characterized by a linear N – O···I interaction with a relatively long O···I distance (3.412(4) Å) and N – O···I angle (167.9(2)°) [29]. The iodine atom lies on the plane defined by the nitronyl

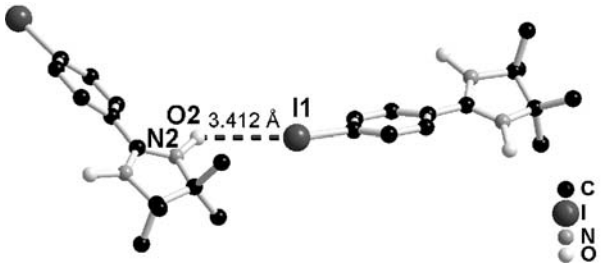


**Fig. 2** N – O···I interaction in the *p*-iodophenyl nitronyl nitroxide **5c**

nitroxide heterocycle while the N – O···I angle amounts to 136.3(3)°, indicating that the interaction is directed toward one of the lone pairs of the oxygen atom.

## 2.2 Binary Systems Involving Nitroxides

An alternative to broaden the possible X-ray crystal structures adopted by a given radical molecule lies in the possibility to associate it with other radical or diamagnetic molecules through strong intermolecular interactions. This approach has been successfully investigated by taking advantage of the known capacity of the oxygen atoms of the nitronyl nitroxide molecules to act as hydrogen bond acceptors, for example when co-crystallized in the presence of hydroquinone [30]. Very recently, a similar concept based on halogen bonding has been explored by Boubekeur and Schöllhorn upon co-crystallization of nitroxide radicals with 1,4-diiodotetrafluorobenzene (*p*TFDIB) [31]. As shown in Scheme 3, a trimeric entity was obtained with the 4-phenyl-2,2,5,5-tetramethyl-3-imidazolin-1-yloxyl radical **6**, however through a N···I interaction rather than an O···I interaction as anticipated. Alternatively, the co-crystallization of *p*TFDIB with the 4-amino-2,2,6,6-tetramethyl(piperidin-1-yloxyl) radical **7** afforded one-dimensional polymer chains where one *p*TFDIB molecule is halogen bonded to the N – O groups of two radicals, while another crystallographically independent *p*TFDIB molecule is hydrogen bonded to the $NH_2$ groups of **7**.

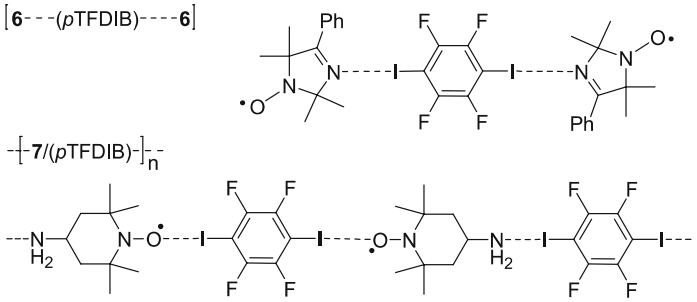


**Scheme 3** The trimeric (*top*) and polymeric (*bottom*) organization of the neutral radicals **6** and **7** with *p*-diiodotetrafluorobenzene (*p*TFDIB)

In the former case, the nearly linear arrangement of C – I···N (176.75(9)°) is consistent with the presence of N···I halogen bonding, albeit the I···N distance (3.209(3) Å), which is shorter than the sum of van der Waals radii (3.68 Å), is longer than in comparable systems involving imines (2.89 Å) [32, 33], indicating a relatively weak interaction. In the 1 : 1 *p*TFDIB–**7** complex (Fig. 3), the C – I···O – N interaction is probably stronger as the I···O dis-

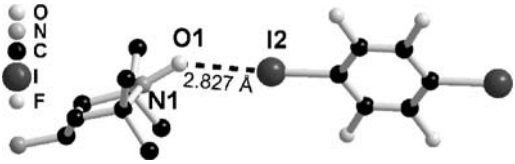


**Fig. 3** Detail of the O···I interaction in the binary system associating the 4-amino-2,2,6,6-tetramethyl(piperidin-1-yloxyl) radical **7** with *p*TFDIB

tance (2.827(9) Å) is much shorter than the sum of the van der Waals radii (3.48 Å), and comparable to the I···O distances found in halogen bonded systems with pyridine *N*-oxide (2.75 Å) [34]. The C – I···O bond is approximately linear (175°) and the N – O···I characteristics indicate that the halogen bond forms along the lone pair direction of the oxygen. These two recent examples demonstrate that halogen bonding is a promising, largely unexplored tool for the construction of novel nitroxide assemblies, comparable in that respect to hydrogen bonding and transition-metal coordination.

The attractive possibility of spin delocalization through the halogen bond was not specifically addressed for these compounds, because the central carbon atom of the ONCNO moiety is known to be a node of the SOMO of nitronyl nitroxides, hence little delocalization is expected from substitution at this point. However, the influence of halogen bonding on the – N – O$^{\bullet}$ group was investigated recently in solution by EPR spectroscopy [35]. Indeed, addition of an iodoperfluorocarbon to the TEMPO radical molecule **2** causes a substantial increase of the nitrogen hyperfine splitting, $a_N$, of the nitroxide, a behaviour related to an increase of the spin density on the nitrogen atom upon halogen bond formation. Furthermore, the equilibrium constants ($K_1$) for the formation of the halogen bonded systems were determined, since, at the timescale of the EPR spectroscopy, the experimental spectrum represents the concentration-weighted average of the spectra due to the free and halogen bonded radicals. The strongest interaction was found with iodoperfluoroalkanes and the temperature dependence of $K_1$ afforded the corresponding thermodynamic parameters, $\Delta H^\circ = -7.0 \pm 0.4$ kcal mol$^{-1}$ and $\Delta S^\circ = -18.1 \pm 1.4$ kcal mol$^{-1}$ K$^{-1}$. Note that this $\Delta H^\circ$ value of – 7 kcal mol$^{-1}$ compares favourably with strong hydrogen bonded systems.

## 3
## Conducting Materials Based on Tetrathiafulvalenes

The involvement of halogen bonding in conducting molecular materials is essentially based on the use of halogenated TTFs in electrocrystallization experiments with counter ions of Lewis base character prone to act as halogen bond acceptors. This concept was first successfully introduced by Imakubo

and Kato in 1995 [36] as they described the 2 : 1 cation radical salts of EDT-TTF-I with $Br^-$ and $[Ag(CN)_2]^-$ (Scheme 4). In these two salts, each anion is "coordinated" by two partially oxidized EDT-TTF-I molecules.

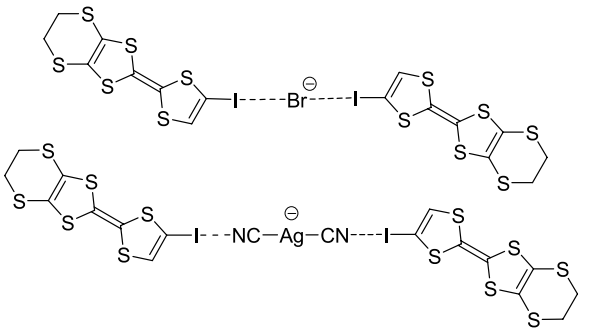


**Scheme 4** Typical halogen bonded motifs involving a partially oxidized TTF molecule such as EDT-TTF-I with halide (*top*) or cyanometallate (*bottom*) counter ions

This original report prompted the preparation of numerous salts based on halogenated TTFs. Reviews on this topic have recently appeared [15, 37], showing the generality of this concept and even the activation of halogen bonding in these salts. In the following, we will therefore recall the essential conclusions that were reached from these compilations and then highlight the most recent developments. Indeed, following a first period where halogen bonding interactions were shown to be able to coexist with the overlap interactions of open-shell molecules to afford conducting organic salts, efforts have been pursued to demonstrate that the halogen bonding interaction itself could carry some "information" by eventually (1) contributing to the band dispersion of the organic stacks, (2) transmitting magnetic interactions if both halogen bond donor and acceptor are themselves paramagnetic, or (3) allowing for the formation of porous materials.

### 3.1 An Introduction to Conducting TTF Salts

Since the discovery of the first organic conductors based on TTF, [TTF]Cl in 1972 [38] and TTF – TCNQ in 1973 [39], TTF has been the elementary building block of hundreds of conducting salts [40]: (1) charge-transfer salts if an electron acceptor such as TCNQ is used, and (2) cation radical salts when an "innocent" anion is introduced by electrocrystallization [41]. In both cases, a mixed-valence state of the TTF is required to allow for a metallic conductivity (Scheme 5), as the fully oxidized salts of $TTF^+$ cation radicals most often either behave as Mott insulators (weakly interacting spins) or associate into

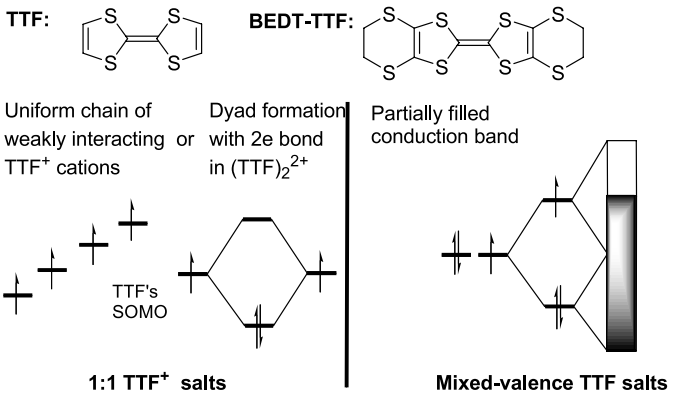


**Scheme 5** Electronic structures of TTF salts, showing charge localization into uniform chains or dicationic dimers in the $TTF^{+\cdot}X^{-}$ salts (*left*) or the partially filled conduction bands in mixed-valence $(TTF)_2X$ salts (*right*)

dicationic dyads (strongly interacting spins in the bonding combination of the two SOMOs).

The role of weak C – H···O hydrogen bonds in the neutral-to-ionic phase transition in TTF – chloranil [42] and the importance of C – H···Hal (Hal = halogen) contacts in the superconductivity of BEDT-TTF salts [11] have served as an incentive to develop the chemistry of TTFs functionalized with hydrogen bonding groups, such as alcohols [43, 44], acids [45], phosphonic acids [46] or amides [47–49]. This topic was reviewed by Bryce in 1995 [14] and by Fourmigué and Batail in 2004 [15]. It was demonstrated not only that the hydrogen bond can coexist with the formation of partially filled conduction bands, but also that the hydrogen bond itself was *activated* in those salts when the hydrogen bond donor group is conjugated with the π system of the TTF core. In this situation, the positive charge carried by the partially oxidized TTF enhances the O – H or N – H hydrogen bond donor ability. The identification in the crystal engineering domain of a similar interaction based on halogen atoms to take part in halogen bond interactions has prompted a similar development of halogen-substituted TTFs, as discussed below.

### 3.2 Neutral Halogenated TTFs

The synthesis of halogenated TTF is most often based on the lithiation/electrophilic halogenation of either the TTF core itself [50] or the five-membered 1,3-dithiole-2-thione [36, 51]. This procedure has been recently expanded to the analogous 1,3-diselenole-2-thione [52, 53], allowing for the formation of a wide variety of iodo- and bromotetraselenafulvalenes or dithiadiselenafulvalenes shown in Schemes 6 and 7.

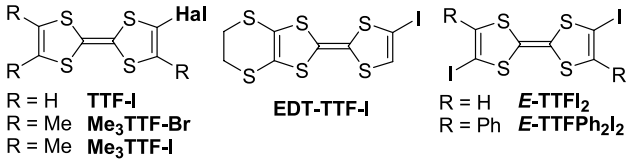


**Scheme 6** Mono- or *E*-dihalo TTFs

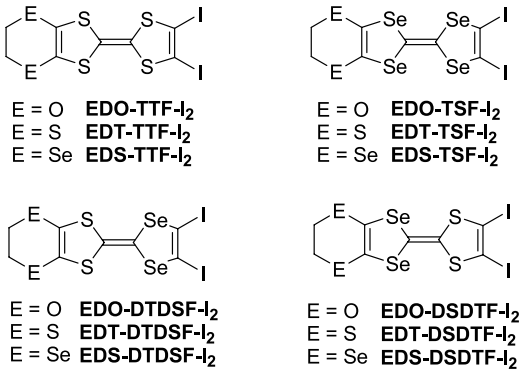


**Scheme 7** Examples of *ortho*-diiodo TTFs and selenium analogues used in cation radical salts

Considering the eventual presence of halogen bonding interactions in the X-ray crystal structures of these *neutral* molecules, one observes different behaviours depending on the substitution pattern and number of halogen atoms on the TTF core. Monohalo TTFs often exhibit a Me/halogen disorder indicative of the absence of any strong directional halogen bonding interaction. Among dihalo TTFs, the *E*-$TTFI_2$ [54] and *E*-$TTFPh_2I_2$ [55] exhibit intermolecular I···I interactions. They are characterized by relatively short I···I intermolecular distances (4.12(2) Å) and a type I motif ($\theta_1 = \theta_2 = 120°$) in *E*-$TTFPh_2I_2$, while much shorter I···I distances with type II motifs (I···I 3.676(3) Å, $\theta_1 = 88.7(6)°$, $\theta_2 = 175.9(5)°$ and 3.817(3) Å, $\theta_1 = 87.7(5)°$, $\theta_2 = 175.9(6)°$) are found in *E*-$TTFI_2$. Note that the evaluation of "short" Hal···Hal intermolecular distances is based here and in the following on the polar flattening model [56], which attributes to each halide an $r_{min}$ and $r_{max}$ rather than one single van der Waals radius. In this anisotropic model, the contact distance ($D_{anis}$ in Table 1) for a type I interaction C – X···Y corresponds to the sum ($r_{max}$(X) + $r_{max}$(Y), while the contact distance for a type II interaction corresponds to $r_{min}$(X) + $r_{max}$(Y) (Scheme 8). Representative values are collected in Table 1 for comparison with experimental data. Halogen bonding will be considered as relevant when the X···Y distance is shorter than

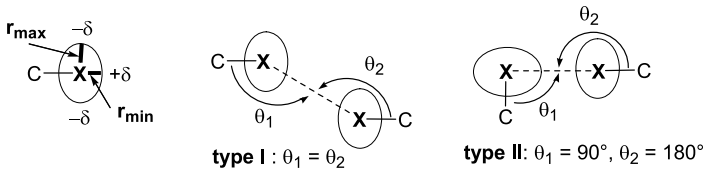


**Scheme 8** The two main types of halogen bond interactions

**Table 1** Contact distances predicted by the anisotropic model [56] (reproduced from ref [15], with permission of the ACS)

| Interaction | $D_{anis}$ (type I) (Å) | $D_{anis}$ (type II) Å |
|---|---|---|
| C – Cl···Cl | 3.56 | 3.36 |
| C – Br···Br | 3.68 | 3.38 |
| C – Br···I | 3.97 | 3.67 |
| C – I···Cl | 3.91 | 3.54 |
| C – I···Br | 3.97 | 3.60 |
| C – I···I | 4.26 | 3.89 |
| C – Cl···N | – | 3.18 |
| C – Br···N | – | 3.14 |
| C – I···N | – | 3.36 |
| C – I···O | 3.67 | 3.30 |
| C – I···S | 4.16 | 3.79 |

the corresponding $D_{anis}$ value. Note that I···I distances reported above for *E*-TTFPh$_2$I$_2$ (type I, 4.12 Å) and *E*-TTFI$_2$ (type II, 3.7–3.8 Å) are indeed shorter than the $D_{anis}$ values for a C – I···I interaction reported in Table 1 as 4.26 Å for a type I and 3.89 Å for a type II interaction, respectively.

In the numerous examples of *ortho*-dihalo TTFs described so far (Scheme 7) [53, 57–62], one observes the formation of inversion-centred dyads with strong S···S, S···Se or Se···Se interactions (Fig. 4), a recurrent motif among TTFs with $C_{2v}$ symmetry [63]. This dyadic motif eventually interacts with neighbouring ones through short Hal···Hal contacts and also Hal···S(Se) contacts, demonstrating that the favoured packing of such TTFs into dyads with the associated S(Se)···S(Se) van der Waals interactions overcomes in most cases possible Hal···Hal interactions. The situation is reversed in the tetrahalotetrathiafulvalenes [57, 64] where the larger size of the halogen atoms hinders such dyadic association. As a consequence, type I motifs can now be observed in the chloro and bromo derivatives, while type II motifs are found in the structure of tetraiodotetrathiafulvalene (Fig. 5) with the following structural characteristics: I···I 3.85 Å, $\theta_1 = 87°$, $\theta_2 = 166°$ and 3.99 Å,

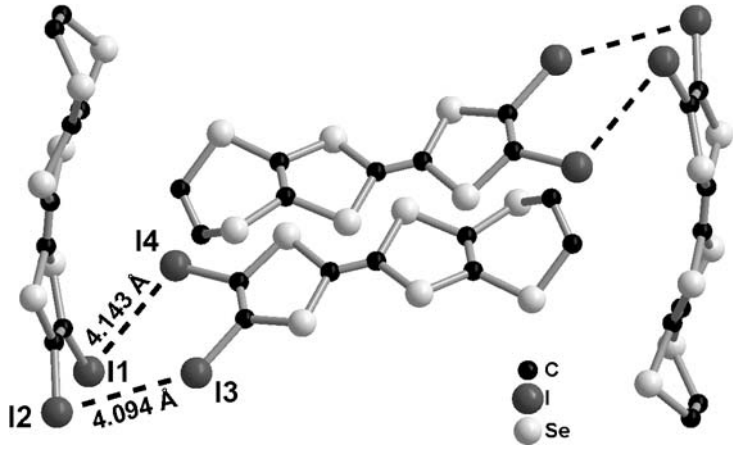


**Fig. 4** Illustration of the head-to-tail dyadic association of *ortho*-dihalo TTFs in the structure of neutral EDS-TSF-$I_2$

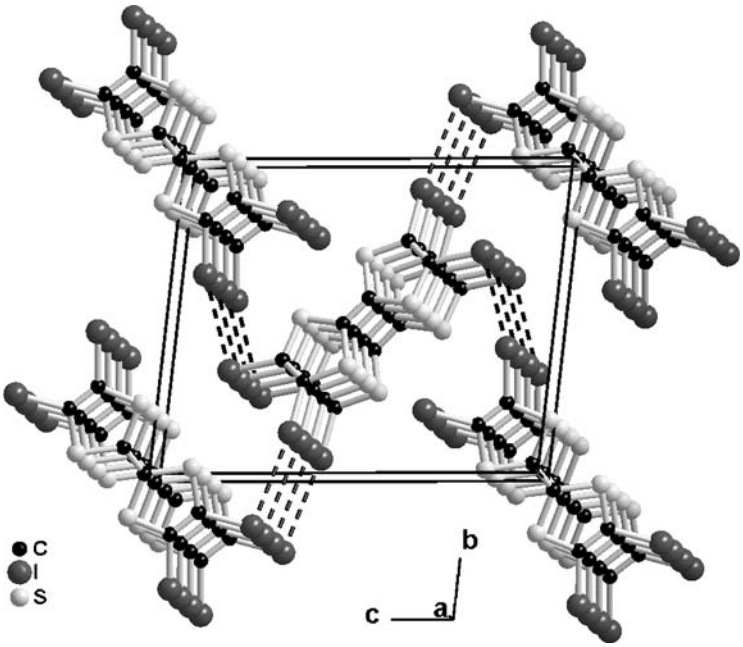


**Fig. 5** A view of the two crystallographically independent $TTFI_4$ stacks, halogen bonded through two type II I···I interactions (*dotted lines*)

$\theta_1 = 101°$, $\theta_2 = 174°$. Note that the I···I distances are, however, close to the $D_{anis}$ value for such a type II C – I···I interaction.

## 3.3
## Cation Radical Salts of Halogenated TTFs

As mentioned above, (EDT-TTF-I)$_2$Br was the first, beautiful example of halogen bonding in TTF salts (Scheme 4) [36]. It possesses most of the characteristics of the other salts described so far, that is, a linear C – Hal···Hal$^-$ interaction with short Hal···Hal distance, found at 3.213 Å and to be compared with the corresponding type II $D_{anis}$ value (Table 1) for C – I···Br interaction (3.60 Å). The other salt described by the same authors (Scheme 4) involved the linear $[Ag(CN)_2]^-$, affording upon electrocrystallization of EDT-TTF-I a similar 2 : 1 salt where now each nitrile of the $[Ag(CN)_2]^-$ anion is halogen bonded to the iodine atom of the partially oxidized EDT-TTF-I molecule [36]. A linear C≡N···I interaction was observed with N···I distance at 2.88 Å, to be compared with the corresponding type II $D_{anis}$ value (3.36 Å). The remarkably short halogen interactions found in these two examples demonstrate that, upon oxidation of the TTF derivative to the radical cation state, the positive charge density in the polar region of the iodine atom is enhanced, for a stronger interaction with the negatively charged counter ion [15]. The other examples which have been described since can thus be organized into two such series, one involving halide, polyhalide or polyhalometallate anions through C – Hal···Hal interactions, the other involving polycyanometallate or organic nitrile anions through C – Hal···N≡C interactions. They will be presented successively in the following sections.

### 3.3.1
### Hal···Hal$_{anion}$ Interactions

#### 3.3.1.1
#### Halide Anions as Halogen Bond Acceptors

The (EDT-TTF-I)$_2$Br salt described above [36] and the 1 : 1 (TTFI$_4$)I salt reported by Gompper [51] were the only structurally characterized salts with simple halide anions until Imakubo recently described an extensive series of Cl$^-$ and Br$^-$ salts from several *ortho*-diiodo tetrathiafulvalene, tetraselenafulvalene and dithiadiselenafulvalene derivatives (Scheme 8) [62]. The X-ray crystal structure analysis of the nine salts described there show a variety of halogen bonded motifs, demonstrating the adaptability of the supramolecular interactions to other structural requirements imposed by the nature of the heteroatoms (O, S, Se) in the TTF frame. Indeed, in (EDT-TTF-I$_2$)$_2$X·(H$_2$O)$_2$ (X = Cl, Br), a bimolecular motif (Fig. 6) associates two partially oxidized EDT-TTF-I$_2$ molecules with one Br$^-$ anion and one water molecule.

Note that the acute (C –)I···Br$^-$···I(– C) angle observed here (85.35(2)°) has already been observed in similar situations where one Br$^-$ or Cl$^-$ anion is bonded to two activated iodine atoms, as reported, for example,

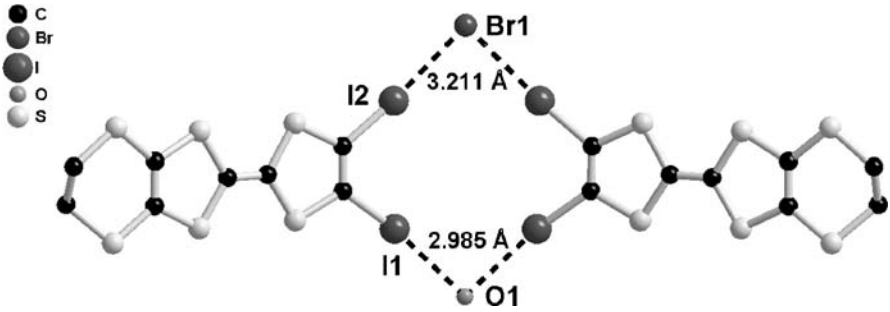


**Fig. 6** Detail of the halogen bonded motif in $(EDT\text{-}TTF\text{-}I_2)_2Br\cdot(H_2O)_2$

in the adducts of tetraphenylphosphonium chloride or bromide with 1,4-diiodotetrafluorobenzene [65]. The corresponding salts with the tetraselenafulvalene analogue, EDT-TSF-$I_2$, are not isostructural, as no water molecules are included in the structure but rather a methylene chloride one. As a consequence, one halide anion links two EDT-TSF-$I_2$ molecules with short $I\cdots Cl^-(Br^-)$ distances and an $I\cdots Br^-\cdots I$ angle of 121.11(2) Å. The two molecules with the ethylenedioxo substituents, that is, EDO-TTF-$I_2$ and EDO-DTDSF-$I_2$, gave isomorphous salts with $Cl^-$ and $Br^-$. The four salts are characterized by a halide anion bonded to four TTF molecules in a distorted tetrahedral environment (Fig. 7)

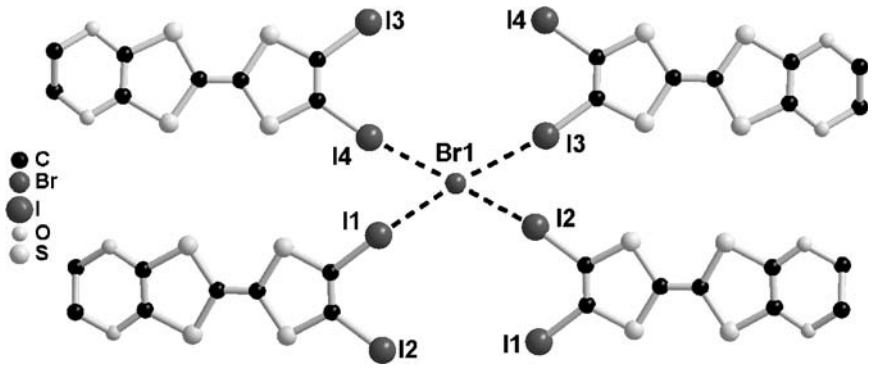


**Fig. 7** Detail of the halogen bonded motif in $(EDO\text{-}TTF\text{-}I_2)_2Br$

In all these salts, the intermolecular $I\cdots Cl^-(Br^-)$ distances are much shorter than the corresponding $D_{anis}$ distances (Table 2), indicating very strong interactions, most probably attributable to an important electrostatic contribution. Furthermore, these salts are highly conducting and exhibit a variety of electronic structures, from completely two-dimensional to quasi one-dimensional, with original $TTF\cdots TTF$ overlap patterns observed here

**Table 2** Intermolecular halogen bond distances (in Å) in the iodotetrathiafulvalene salts with $Cl^-$ or $Br^-$ anions, measured at 293 K

| | C–I···$Cl^-$ ($D_{anis}$ = 3.54 Å) | C–I···$Br^-$ ($D_{anis}$ = 3.60Å) | Refs. |
|---|---|---|---|
| $(IET)_2X$ | – | 3.213 | [36] |
| $(DIET)_2X{\cdot}(H_2O)_2$ | 3.313(1) | 3.211(2) | [62] |
| $(DIETSe)_2X{\cdot}CH_2Cl_2$ | 3.074(5) | 3.136(1) | [62] |
| $(DIEDO)_2X$ | 3.252(2) | 3.3569(9) | [62] |
| | 3.213(2) | 3.362(1) | |
| | 3.521(2) | 3.5872(8) | |
| | 3.113(2) | 3.2720(8) | |
| $(DIEDO-STF)_2X$ | 3.316(11) | 3.382(12) | [62] |
| | 3.235(8) | 3.372(9) | |
| | 3.603(10) | 3.611(11) | |
| | 3.213(12) | 3.268(14) | |

because of the structural requirements of the strong halogen bonding interactions.

#### 3.3.1.2 Polyhalide Anions as Halogen Bond Acceptors

After the description of halogen bonded systems with the simplest $Cl^-$ or $Br^-$ anions, we now describe those salts involving complex polyhalide anions such as $I_3^-$ or $IBr_2^-$ as halogen bond acceptors. Several salts have been obtained upon electrocrystallization with EDT-TTF-$Br_2$ [66], BTM-TTF-$Br_2$ [61, 64], EDO-TTF-$I_2$ [67] or EDT-TTF-$I_2$ [66], which all exhibit type II C – Br(I)···Br(I) interactions. A good example is offered by the 2 : 1 salt (EDT-TTF-$I_2$)($I_3$) where halogen bonding interactions are identified, not only between the iodo TTF and $I_3^-$ but also between iodo TTFs (Fig. 8). As shown in Table 3, the intermolecular distances, albeit shorter than the corresponding $D_{anis}$, are not as short as observed above in Sect. 3.3.1.1, the signature of a weaker halogen bonding interaction with anions where the negative charge is now delocalized on three rather than on one atom.

Moreover, it was shown that the presence of Hal···Hal interactions between the partially oxidized molecules also contribute to the electronic delocalization. Indeed, the presence of non-zero atomic coefficients on the halogen atoms in the HOMO of EDT-TTF-$Br_2$ or EDT-TTF-$I_2$ [66], together with the short Hal···Hal contacts, leads to a sizeable increase of the band dispersion and stabilizes a rare β′ structure through the side-by-side arrangement of the inversion-centred dyads connected by Hal···Hal interactions. Both $I_3^-$ salts are semiconductors with room temperature conductivities around

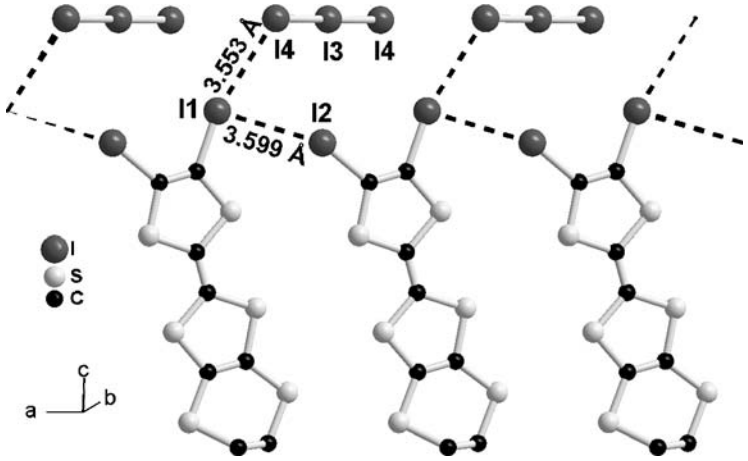


**Fig. 8** A view of both types of I···I interactions in (EDT-TTF-$I_2$)($I_3$)

**Table 3** Halogen bond distances and angles in various salts with $I_3^-$

| | Interaction | $D_{anis}$ (Å) | Br(I)I (Å) | $\theta_1$ (°C) | $\theta_2$ (°C) | Refs. |
|---|---|---|---|---|---|---|
| (BTM – TTF – $Br_2$)$_2$($I_3$) | C – Br···I | 3.67 | 3.635(1) | 163.6(3) | 72.08(3) | [61, 64] |
| (EDT – TTF – $Br_2$)$_2$($I_3$) | C – Br···I | 3.67 | 3.51(5) | 165.3(1) | 110.48(2) | [66] |
| (EDO – TTF – $I_2$)($I_3$) | C – I···I | 3.89 | 3.40(2) | 173.2(2) | 133.1(3) | [67] |
| | | | 3.399(8) | 163.4(2) | 71.54(2) | |
| (EDT – TTF – $I_2$)$_2$($I_3$) | C – I···I | 3.89 | 3.55(5) | 164.8(2) | 107.21(2) | [66] |

1 S $cm^{-1}$, a large value when compared with other β′ structures such as β′-(BEDT-TTF)$_2$($ICl_2$).

#### 3.3.1.3 Halometallate Anions as Halogen Bond Acceptors

Only a few recent examples of halogen bonding of halogenated TTFs with halometallate anions have been described and this most probably represents a broad development field in this area. Indeed, these halometallate salts offer a wide variety of complexes and specifically here a large variation of the ratio of anion charge vs number of halide atoms, as already discussed above in the comparison between $Br^-$ and $I_3^-$ salts. This point is illustrated by the superb structures of two salts of EDT-TTF-$I_2$ with the polymeric one-dimensional $PbI_3^-$ (Fig. 9) and two-dimensional $(Pb_{5/6}\square_{1/6}I_2)_3^-$ anions where shorter C – I···$I_{anion}$ contacts are observed with the linear $PbI_3^-$ chains

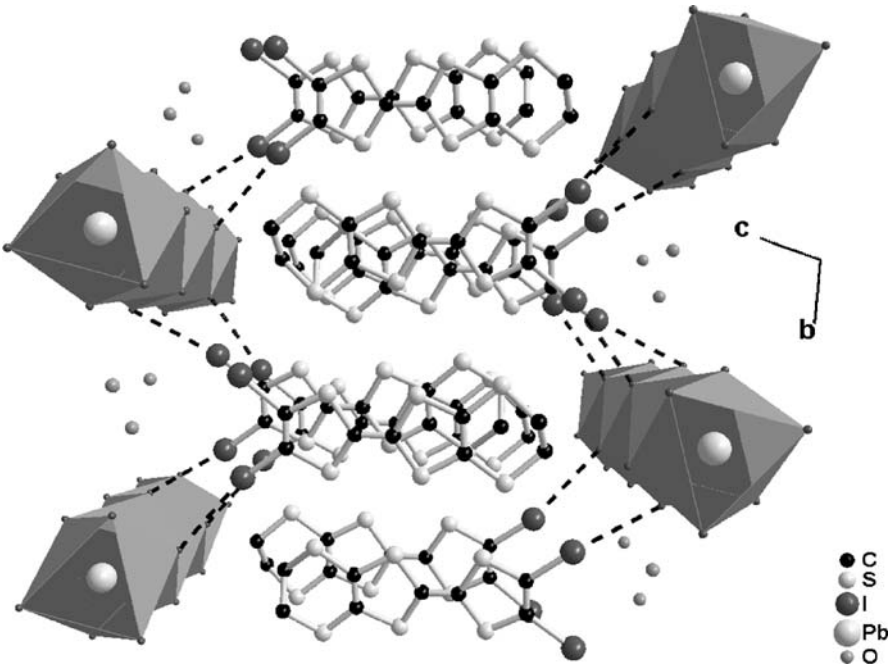


**Fig. 9** I···I interactions in (EDT-TTF-$I_2$)$_2$($PbI_3$) with the polymeric $(PbI_3)_\infty^-$ anionic chains

with a charge per iodine atom of – 0.33 [68], when compared with the two-dimensional $(Pb_{5/6}\square_{1/6}I_2)_3^-$ layers [69] where the charge per iodine atom amounts to – 0.17 for the same oxidation state of EDT-TTF-$I_2$ ($\rho = 0.5$). In the latter, the inorganic layers exhibit the $CdI_2$ structure type while the exact negative charge of the layer is governed by the presence of a specific number of lead vacancies. The shortest $I_{donor}\cdots I_{anion}$ distances (3.81, 4.09 Å), albeit longer than in the other salts described above, are still much shorter than the I···I separation across the van der Waals gap in 2H-$PbI_2$ (4.95 Å).

Polyhalometallates are also particularly interesting since they often exist in a paramagnetic state, allowing for investigation of possible π–d interaction in these salts between the conducting, delocalized electrons of the organic slabs (the π electrons) and the localized spins of the counter ions, for example, the $S = 5/2$ $FeCl_4^-$ ions [71–73]. Enoki et al. have reported the very first approach aimed at associating halogen bonding to the π–d interaction, first in the (EDO-TTF-$Br_2$)$_2$($FeBr_4$) salt [74], then in two salts of EDT-TTF-$Br_2$ with paramagnetic $FeBr_4^-$ and diamagnetic $GaBr_4^-$ [75]. These three systems are isostructural and exhibit $Br_{donor}\cdots Br_{anion}$ interactions at distances (3.65–3.68 Å) associated with a weaker, type I halogen interaction. Nevertheless, the antiferromagnetic ordering of the $FeBr_4^-$ anion lattice was shown to affect the transport properties of the conducting π electrons, demonstrating

the usefulness of the π–d interaction mediated here by the halogen bonding. This approach was extended to the tetraselenafulvalene analogues, EDT-TSF-$Br_2$ and EDT-TSF-$I_2$, by Imakubo who electrocrystallized these two donor molecules with $FeCl_4^-$ and $FeBr_4^-$ and their diamagnetic analogues $GaCl_4^-$ and $GaBr_4^-$ [76].

In conclusion, because of the highly delocalized charge of the anion on several halide atoms, the halogen bonding with polyhalometallate anions appears to be much weaker than with the simplest anions. The π–d interactions identified in several of these salts suggest, however, that the organic and inorganic lattices are indeed interconnected, with a probable contribution of the through-bond halogen bonding interactions. Contrariwise, we will see in the following that the marked directionality of the C – Hal···N≡C – interaction will be very useful to favour such interactions with polycyanometallates or organic nitriles, even when the negative charge of the anion is also strongly delocalized.

### 3.3.2
### Hal···Nitrile Interactions

#### 3.3.2.1
#### Inorganic Cyanometallate Anions

Following the first described example reported by Imakubo and Kato with the linear $Ag(CN)_2^-$ anion [36], various polycyanometallates have been investigated as electrolytes in electrocrystallization experiments with essentially iodotetrathiafulvalenes, such as the square-planar $[M(CN)_4]^{2-}$, $[Pt(CN)_4]^{2-}$ or $[Au(CN)_4]^-$ or the octahedral $[Cr(CN)_6]^{3-}$ or $[Fe(CN)_5NO]^{2-}$ [15]. From the halogen bonding point of view, this approach is very successful as short, linear C – I···N≡C contacts are observed in every salt. More recently, larger cluster anions such as $[Re_6Se_8(CN)_6]^{4-}$ were also associated with *E* – TTF-$I_2$ and EDT-TTF-I [77], affording one- or two-dimensional halogen bonded systems where two or four of the six possible CN groups of the anions enter into halogen bond interactions with the fully oxidized cation radical of *E*-TTF-$I_2$ or EDT-TTF-I, respectively (Fig. 10). In these salts, the (C –)I···N(≡C) distances amount to 2.79 and 2.83 Å, with C – I···N(≡) angles of 177 and 176°, respectively. These distances are far shorter than the $D_{anis}$ value (Table 1) estimated at 3.36 Å, but also shorter than those observed in $[EDT\text{-}TTF\text{-}I]_2[Ag(CN)_2]$ (2.88 Å) [36].

The association of magnetic ions through halogen bonding, already investigated with the hexacyanometallate anions, has been extended to more complex ions such as the low spin, $S = 1/2$, $[Fe(bpca)(CN)_3]^-$ (bpca: bis(2-pyridylcarbonyl)amide) anion [78]. Associated with EDT-TTF-$I_2$ or EDO-TTF-$I_2$, it gives rise to 2 : 1 salts characterized by two halogen bonding interactions with the anion, one involving one cyano substituent and

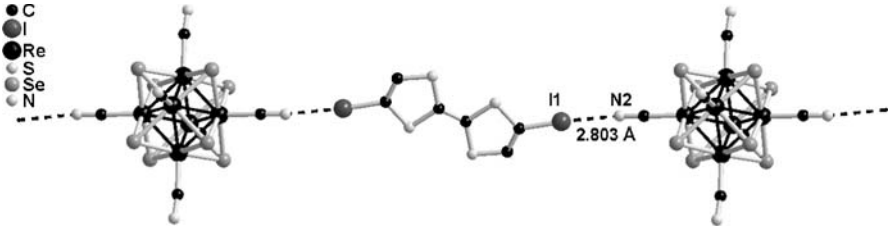


**Fig. 10** One-dimensional halogen bonded system involving *E*-TTFI$_2$ and the octahedral polycyano cluster anion $[Re_6Se_6(CN)_6]^{4-}$

the other involving the oxygen atom of a carbonyl (Fig. 10). This work was further extended by the same authors to thiocyanate anions such as the $S = 3/2$ $[Cr(isoq)_2(NCS)_4]^-$ ion where, upon association with EDT-TTF-I$_2$ or EDT-TSF-I$_2$, C – I···SCN – interactions can now be identified [79].

### 3.3.2.2 Organic Nitrile-Containing Anions

The most popular organic nitrile-containing anions used so far in their salts with halogenated TTFs are the square-planar metal dithiolene complexes of the mnt dithiolate, formulated as $[M(mnt)_2]^-$, M = Ni, Pt, Pd (Scheme 9). Dithiolene complexes have been extensively used for the elaboration of conducting [80] or magnetic materials [81–83]. The non-innocent character of the dithiolate ligand allows for multiple redox states, some of them paramagnetic. Let us mention the $[M(mnt)_2]$ complexes, known in their dianionic ($S = 0$) or monoanionic ($S = 1/2$) states, or the $[M(dmit)_2]$ complexes, known as dianion, monoanion or mixed-valence, formally – 0.5 ions in conducting systems. The presence of nitrile substituents combined with their negative charge make the $[M(mnt)_2]$ complexes ideal counter ions to favour halogen bond interactions with halogenated TTFs. There are, however, only five reported examples of such salts, which are collected in Table 4 with their structural characteristics. Note the short and strongly linear C – I···N≡C interaction in all of them.

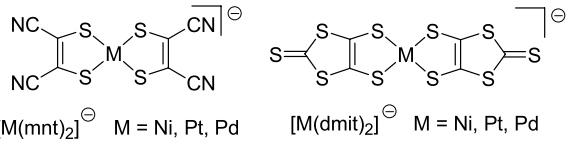


**Scheme 9** Metal dithiolene complexes

In $(TTF – I)_2[Pd(mnt)_2]$, dyads of fully oxidized $(TTF\text{-}I)^{+\bullet}$ radical cations alternate with the dianionic $[Pd(mnt)_2]^{2-}$ affording an insulating salt [84]. On the other hand, the EDO-TTF-I$_2$ salts of $[Ni(mnt)_2]^-$ and $[Pt(mnt)_2]^-$

**Table 4** Structural characteristics of the metal dithiolene salts of halogenated TTFs

| Compound | I···N (Å) | C – I···N (°C) | I···N≡C (°C) | Refs. |
|---|---|---|---|---|
| $(TTF-I)_2[Pd(mnt)_2]$ | 3.04 | 175 | 173 | [84] |
| $(EDO-TTF-I_2)_2[Ni(mnt)_2]$ | 3.04 | 169 | 165 | [85] |
| $(EDO-TTF-I_2)_2[Pt(mnt)_2]$ | 3.05 | 169 | 167 | [85] |
| $(EDT-TTF-I)_2[Ni(mnt)_2]$ | 2.93 | 178 | 172 | [86] |
| $(EDT-TTF-I_2)_2[Ni(mnt)_2]$ | 2.93 | 177 | 172 | [86] |

organize into segregated stacks of cations and anions [85], linked together by the C – I···N≡C interaction (Fig. 11), giving rise to a salt with metallic conductivity while the localized spins of the dithiolene complexes behave as a one-dimensional ferromagnet. Finally, the $[Ni(mnt)_2]$ salts of the monoiodo EDT-TTF-I and diiodo EDT-TTF-$I_2$ molecules provide examples of both behaviours [86]. Indeed, based on the magnetic, electrical and structural properties, the 2 : 1 salts obtained with both TTF derivatives were formulated as $(EDT\text{-}TTF\text{-}I^{+\bullet})_2[Ni(mnt)_2]^{2-}$ and $[EDT\text{-}TTF\text{-}I_2]_2^{+\bullet}[Ni(mnt)_2]^{-}$, respectively, with diamagnetic dicationic dyad and dianion with EDT-TTF-I, and paramagnetic mixed-valence dyad and monoanion with EDT-TTF-$I_2$. These few examples demonstrate that the delocalization of the anionic charge is not a drawback when nitrile substituents are involved in the halogen bonding interaction, by contrast with its weakening in larger polyhalometallates (see Sects. 3.3.1.2 and 3.3.1.3). This observation opens new promising routes for the elaboration of such salts since dithiolene complexes are known with a wide variety of geometries and stoichiometries, not only as square-planar complexes but also within tris(dithiolene) complexes with geometries in between octahedral and trigonal-prismatic [81].


**Fig. 11** The trimeric motif formed upon halogen bonding interaction between the partially oxidized EDT-TTF-$I_2$ and the dithiolene complex $[Ni(mnt)_2]^{-}$

### 3.3.2.3 Inverting the Polarity with Cyanotetrathiafulvalenes

As already mentioned above, the oxidation of halogenated TTFs to the radical cation state is found to activate the halogen atom for entering into a halo-

gen bond as the charge depletion along the C – Hal bond is enhanced. This adds a strong electrostatic contribution to the halogen bond, besides the important polarizability component. In order to test this assumption, a TTF substituted with a CN group, that is, EDT-TTF-CN (Scheme 10), was prepared and its electrocrystallization investigated in the presence of various halide, polyhalide or polyhalometallate anions [87].

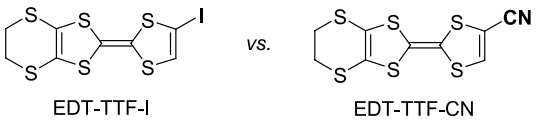


**Scheme 10** Inverting the polarity of halogen bonding with EDT-TTF-CN

Six different salts of EDT-TTF-CN were obtained upon oxidation in the presence of $I_3^-$, $FeBr_4^-$, $InBr_4^-$, $AuBr_4^-$, $Mo_6Br_{14}^{2-}$ and $Mo_6Cl_8Br_6^{2-}$. In none of them was an interaction between the EDT-TTF-CN and the halogen atom of one anion identified, demonstrating at least by the negative that the oxidation of the cyano TTF does favour such an interaction, while is known to occur in neutral systems such as in *p*-halobenzonitrile [88].

### 3.3.3 Iodopyrazino TTFs, Iododithiapyrenes

Another very beautiful illustration of halogen bonding in TTF-based molecular conductors is found in Imakubo's work on dihalopyrazinodithiafulvalene and analogues [89]. The neutral chloroiodopyrazinotetrathiafulvalene, denoted **ClIPS** in Scheme 11, crystallizes in the neutral state with a short N···I halogen bond (3.08(3) Å), demonstrating that this interaction is indeed favoured with iodine rather than chlorine [90]. Most probably here in **ClIPS**, the chlorine atom, with its electron-withdrawing character, partly activates the neighbouring iodine atom for entering into the C – I···N interaction.

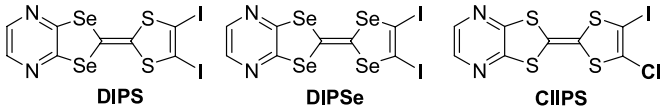


**Scheme 11** The dihalopyrazinotetrathiafulvalenes and analogues involved in threefold symmetry salts

Furthermore, electrocrystallization of the diodo derivatives **DIPS** and **DIPSe** afforded original salts with threefold symmetry and varying stoichiometries, such as $(\mathbf{DIPS})_3(PF_6)(PhCl)_{1.15}$ or $(\mathbf{DIPSe})_3(PF_6)_{1.33}(CH_2Cl_2)_{1.2}$ [91]. In these salts, the halogen bond is further enhanced as

the (C–)I···N distance is now found at 2.84–2.88 Å in the **DIPS** salts $(\mathbf{DIPS})_3(PF_6)(S)_x$ with S = PhCl, $CH_2Cl_2$ or $ClCH_2CHCl_2$, and at 2.85–2.87 Å in the **DIPSe** salts $(\mathbf{DIPSe})_3(X)_{1.33}(CH_2Cl_2)_{1.2}$ with X = $PF_6$, $AsF_6$ or $SbF_6$. The halogen bond network affords a lacunary crystal structure with two types of channels (denoted A and B in Fig. 12) where the counter ion and solvent molecules are dispersed. These extraordinary porous materials exhibit high conductivities, with $\sigma_{RT}$ = 10 S cm$^{-1}$ and $E_{act}$ = 50 meV for the **DIPS** salts, and $\sigma_{RT}$ = 100 S cm$^{-1}$ and a metallic behaviour for the **DIPSe** salts.

Recently, the ability of halogenated TTFs to enter into halogen bond interactions was also extended to other families of donor molecules such as the dithiapyrenes (DTPYs) (Scheme 12) [92]. The better solubility of

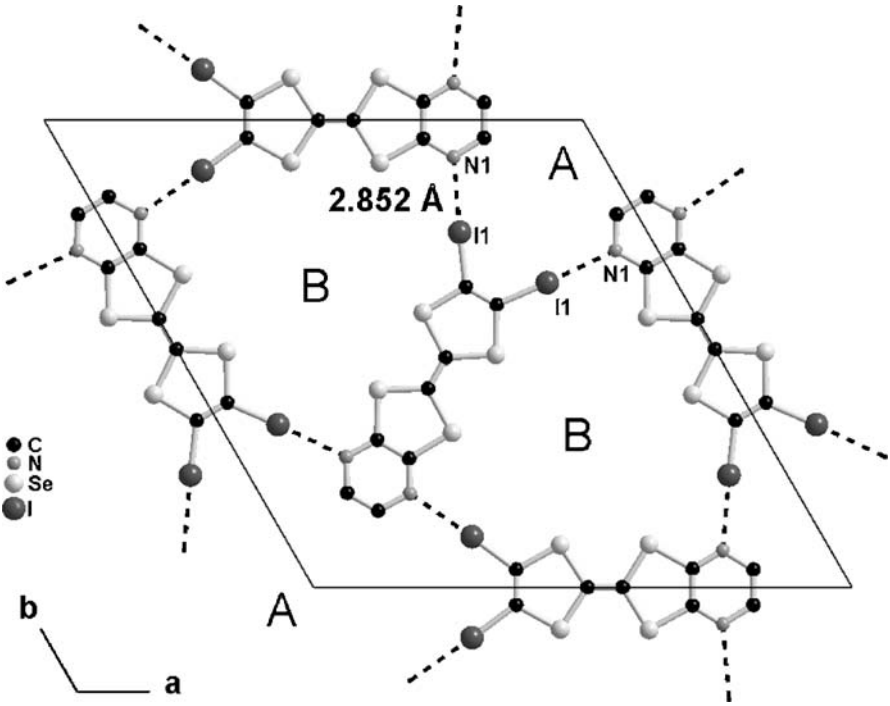


**Fig. 12** The threefold symmetry rigid structure adopted by the **DIPSe** salts with $PF_6^-$, $AsF_6^-$ or $SbF_6^-$, showing the two types of channels (denoted A and B) occupied by the anions and solvent molecules

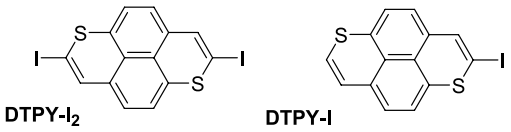


**Scheme 12** Mono- and diiododithiapyrenes

the monoiododithiapyrene DTPY-I, when compared with the diodo derivative DTPY-$I_2$, allowed for its successful electrocrystallization with $NO_3^-$ or chemical oxidation with various quinones (Fig. 13). The short and linear $C-I\cdots O-NO_2^-$ interaction identified in its 1 : 1 nitrate salt demonstrates that any donor molecule substituted with a bromide or iodine atom is potentially able to enter into a halogen bond interaction upon oxidation to the cation radical state.

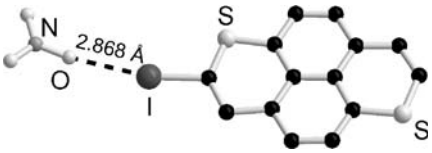


**Fig. 13** A detail of the $C-I\cdots O-NO_2^-$ interaction in $(DTPY\text{-}I)NO_3$

## 3.4 Ternary Systems

Following Dehnicke's report in 1996 on the co-crystallization of diiodoacetylene (DIA) with various halide anions to form two-dimensional networks through $C-I\cdots X^-$ interactions [93], Kato et al. investigated these supramolecular anions in the electrocrystallization of classical TTFs such as BEDT-TTF.

Highly conducting 2 : 1 BEDT-TTF salts were obtained with diiodoacetylene with chains of alternating DIA neutral molecules and $X^-$ anions (Scheme 13) [94]. Increasing the size of the neutral molecules with difluorotetraiodobenzene (DFTIB) or 1,4-(bisiodoethynyl)benzene (pBIB) decreases the overall charge per surface unit in the anionic layer, thus affording 3 : 1 salts such as $(BEDT\text{-}TTF)_3X(DFTIB)$ or $(BEDT\text{-}TTF)_3X(pBIB)$, X = Cl, Br [95]. These salts exhibit a two-dimensional character and a metallic conductivity down to 1.6 K. Other donor molecules derived from BEDT-TTF are also currently being investigated, such as bis(methylenedithio)-tetrathiafulvalene (BMDT-TTF) [96]. With the latter, slightly smaller than BEDT-TTF, a 4 : 1 salt was isolated in the presence of difluorobis(iodoethynyl) benzene and $Cl^-$ or $Br^-$.

## 4 Summary and Outlook

This short review has demonstrated that halogen bonding interactions have already been used in many ways in the field of magnetic or conducting organic systems. Only a few examples are available in the nitroxide family, but

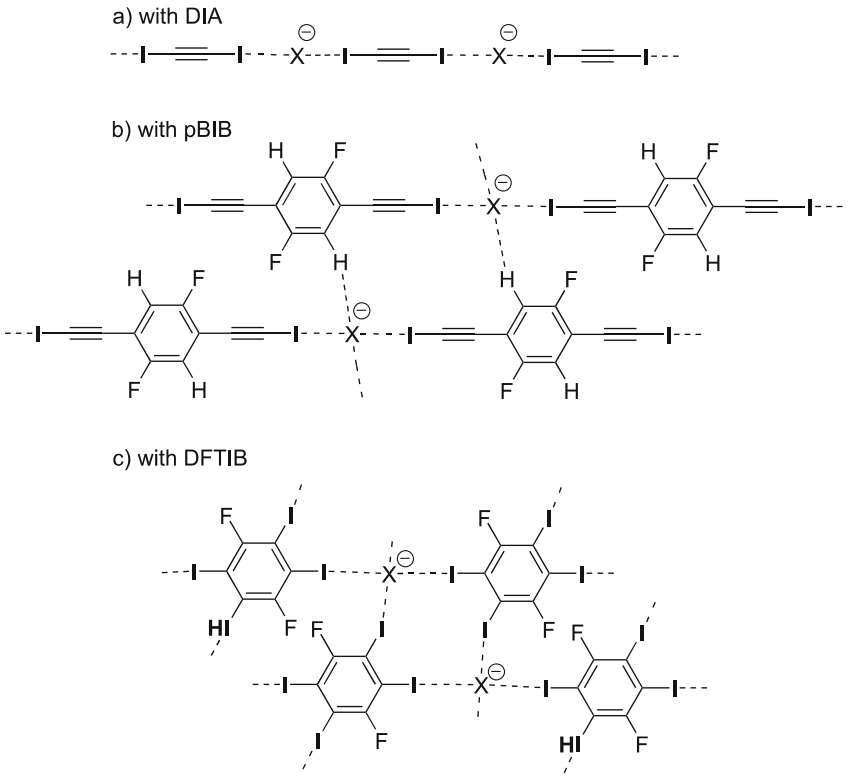


**Scheme 13** Polymeric anionic networks formed upon electrocrystallization of BEDT-TTF with $X^-$ ($Cl^-$, $Br^-$) in the presence of iodoalkynes or iodoperfluoroarenes

the formation of binary systems with perfluoroiodoalkanes or -arenes offers new perspectives for the elaboration of original structures based on the extensive library of such neutral radicals investigated so far. In the cation radical salts of halogenated TTFs, a strong electrostatic component is added to the halogen bonding interaction, as the oxidation of the TTF to the cation radical state enhances the partial positive charge along the C – Hal bond toward the anion. As a consequence, halogen bonds in these salts, when present, are strongly directional and systematically shorter than in neutral systems. This charge effect decreases when replacing small halide ($Cl^-$, $Br^-$) anions by larger polyhalide ($IBr_2^-$, $I_3^-$) or polyhalometallate ($FeBr_4^-$, $PbI_3^-$, ...) anions. On the other hand, C – Hal···N≡C halogen interaction of partially oxidized halogenated TTFs with polycyanometallate anions or organic anionic nitriles is systematically strong, offering probably a more predictable structural tool than the Hal···Hal interactions. Also, beyond this reliable *structural* role, we have shown that halogen bonding could also play an important *electronic* role, by contributing to the band dispersion of the organic stacks, or by transmit-

ting magnetic interactions indicating that part of the spin density is most probably delocalized on the halogen atoms involved in the halogen bonding. This assumption still remains to be validated, on the basis of experimental and theoretical determinations of the spin density in such conducting or magnetic halogen bonded systems.

## References


1. Desiraju GR (1989) In: Crystal engineering: the design of organic solids. Elsevier, Amsterdam
2. Desiraju GR (1995) Angew Chem Int Ed Engl 34:2311
3. Atwood JL, Lehn JM, Davies JED, MacNicol DD, Vogtle F (1996) Comprehensive supramolecular chemistry: 11-volume set. Pergamon, Oxford
4. Jeffrey GA, Saenger W (1991) Hydrogen bonding in biological structures. Springer, Berlin
5. Desiraju GR, Steiner T (1991) The weak hydrogen bond. Oxford University Press, Oxford
6. Jérome D (2004) Chem Rev 104:5565
7. Hoffmann R (1987) Angew Chem Int Ed Engl 26:846
8. Canadell E, Whangbo MH (1991) Chem Rev 91:965
9. Kahn O (1993) In: Molecular magnetism. Wiley, Weinheim
10. Davison A, Boubekeur K, Pénicaud A, Auban P, Lenoir C, Batail P, Hervé G (1989) J Chem Soc Chem Commun, p 1373
11. Whangbo MH, Williams JM, Schultz AJ, Emge TJ, Beno MA (1987) J Am Chem Soc 109:90
12. Romero FM, Ziessel R, Drillon M, Tholence JL, Paulsen C, Kyritsakas N, Fisher J (1996) Adv Mater 8:826
13. Deumal M, Cirujeda J, Veciana J, Kinoshita M, Hosokoshi Y, Novoa JJ (1997) 265:190
14. Bryce MR (1995) J Mater Chem 5:1481
15. Fourmigué M, Batail P (2004) Chem Rev 104:5379
16. Amabilino DB, Veciana J (2001) In: Miller JS, Drillon M (eds) Magnetism: molecules to materials II, chap. 1. Wiley-VCH, Weinheim
17. Iwamura H, Inoue K (2001) In: Miller JS, Drillon M (eds) Magnetism: molecules to materials II, chap. 2. Wiley-VCH, Weinheim
18. Turek P, Nozawa K, Shiomi D, Awaga K, Inabe T, Maruyama Y, Kinoshita M (1991) Chem Phys Lett 180:327
19. Lajzerowicz-Bonneteau JP (1968) Acta Cryst B24:196
20. Berliner LJ (1970) Acta Cryst B26:1198
21. Bordeaux PD, Lajzerowicz J (1977) Acta Cryst B33:1837
22. Cirujeda J, Mas M, Molins E, Lanfranc de Panthou F, Laugier J, Park JG, Paulsen C, Rey P, Rovira C, Veciana J (1995) J Chem Soc Chem Commun, p 709
23. Hernandez E, Mas M, Molins E, Rovira C, Veciana J (1993) Angew Chem Int Ed Engl 32:882
24. Hosokoshi Y, Tamura M, Nozawa K, Susuki S, Sawa H, Kato R, Kinoshita M (1995) Mol Cryst Liq Cryst 271:115
25. Romero FM, Ziessel R, De Cian A, Fisher J, Turek P (1996) New J Chem 20:919
26. Hosokoshi Y, Tamura M, Nozawa K, Suzuki S, Kinoshita M, Sawa H, Kato R (1995) Synth Met 71:1795

27. Zakrassov A, Shteiman V, Sheynin Y, Botoshansky M, Kapon M, Kraftory M, Del Sesto RE, Miller JS (2003) Helv Chim Acta 86:1234
28. Tamura M, Shiomi D, Hosokoshi Y, Iwasawa N, Nozawa K, Kinoshita M, Sawa H, Kato R (1993) Mol Cryst Liq Cryst A232:45
29. Wagner B, Gompper R, Polborn K (2002) Private Communication CCDC 198532 (CSD VADFOW)
30. Otsuka T, Okuno T, Awaga K, Inabe T (1998) J Mater Chem 8:1157
31. Boubekeur K, Syssa-Magalé JL, Palvadeau P, Schöllhorn B (2006) Tetrahedron Lett 47:1249
32. Metrangolo P, Resnati G (2001) Chem Eur J 7:2511
33. Syssa-Magalé JL, Boubekeur K, Palvadeau P, Meerschaut A, Schöllhorn B (2004) J Mol Struct 691:79
34. Messina MT, Metrangolo P, Panzeri W, Pilati T, Resnati G (2001) Tetrahedron 57:8543
35. Mugnaini V, Punta C, Liantonio R, Metrangolo P, Recupero F, Resnati G, Pedulli GF, Lucarini M (2006) Tetrahedron Lett 47:3265
36. Imakubo T, Sawa H, Kato R (1995) Synth Met 73:117
37. Imakubo T (2004) In: Yamada J, Sugimoto T (eds) TTF chemistry: fundamentals and applications of tetrathiafulvalenes, halogenated TTFs, chap. 3. Kodansha and Springer, Tokyo
38. Wudl F, Wobschall D, Hufnagel EJ (1972) J Am Chem Soc 94:670
39. Ferraris J, Cowan DO, Walakta VV, Perlstein JF (1973) J Am Chem Soc 95:948
40. Batail P (ed) (2004) Thematic Issue on Molecular Conductors. Chem Rev 104(11)
41. Batail P, Boubekeur K, Fourmigué M, Gabriel JCP (1998) Chem Mater 10:3005
42. Batail P, LaPlaca SJ, Mayerle JJ, Torrance JB (1981) J Am Chem Soc 103:951
43. Dolbecq A, Fourmigué M, Batail P, Coulon C (1994) Chem Mater 6:1413
44. Dolbecq A, Guirauden A, Fourmigué M, Boubekeur K, Batail P, Rohmer MM, Bénard M, Coulon C, Sallé M, Blanchard P (1999) J Chem Soc Dalton Trans, p 1241
45. Heuzé K, Fourmigué M, Batail P (1999) J Mater Chem 9:2373
46. Dolbecq A, Fourmigué M, Krebs FC, Batail P, Canadell E, Clérac R, Coulon C (1996) Chem Eur J 2:1275
47. Heuzé K, Mézière C, Fourmigué M, Batail P, Coulon C, Canadell E, Auban-Senzier P, Jérome D (2000) Chem Mater 12:1898
48. Heuzé K, Fourmigué M, Batail P, Canadell E, Auban-Senzier P (1999) Chem Eur J 5:2971
49. Baudron SA, Avarvari N, Batail P, Coulon C, Clérac R, Canadell E, Auban-Senzier P (2003) J Am Chem Soc 125:11583
50. Jørgensen M, Bechgaard K (1989) Synthesis 207
51. Gompper R, Hock J, Pollborn K, Dormann E, Winter H (1995) Adv Mater 7:41
52. Imakubo T, Shirahata T (2003) Chem Commun, p 1940
53. Shirahata T, Imakubo T (2004) Org Biomol Chem 2:1685
54. Wang C, Ellern A, Khodorkovsky V, Bernstein J, Becker JY (1994) J Chem Soc Chem Commun, p 983
55. Shimizu T, Koizumi T, Yamaguchi I, Osakada K, Yamamoto T (1998) Synthesis, p 259
56. Nyburg SC, Faerman CH (1985) Acta Crystallogr B41:274
57. Wang C, Becker JY, Bernstein J, Ellern A, Khodorkovsky V (1995) J Mater Chem 5:1559
58. Iyoda M, Kuwatani Y, Ogura E, Hara K, Suzuki H, Takano T, Takeda K, Takano J, Ugawa K, Yoshida M, Matsuyama H, Nishikawa H, Ikemoto I, Kato T, Yoneyama N, Nishijo J, Miyazaki A, Enoki T (2001) Heterocycles 54:833
59. Kux U, Suzuki H, Sasaki S, Iyoda M, (1995) Chem Lett, p 183

60. Becker JY, Bernstein J, Bittner S, Shalal L, Shaik SS (1991) J Chem Soc Chem Commun, p 92
61. Iyoda M, Kuwatani Y, Hara K, Ogura E, Suzuki H, Ito H, Mori T (1997) Chem Lett, p 599
62. Imakubo T, Shirahata T, Hervé K, Ouahab L (2006) J Mater Chem 16:162
63. Mézière C, Fourmigué M, Fabre JM (2000) CR Acad Sci IIc 3:387
64. Batsanov AS, Bryce MR, Chesney A, Howard JAK, John DE, Moore AJ, Wood CL, Gershtenman H, Becker JY, Khodorkovsky VY, Ellern A, Bernstein J, Perepichka IF, Rotello V, Gray M, Cuello AO (2001) J Mater Chem 11:2181
65. Grebe J, Geiseler G, Harms K, Dehnicke K (1999) Z Naturforsch 54b:77
66. Domercq B, Devic T, Fourmigué M, Auban-Senzier P, Canadell E (2001) J Mater Chem 11:1570
67. Kuwatani Y, Ogura E, Nishikawa H, Ikemoto I, Iyoda M (1997) Chem Lett, p 817
68. Devic T, Canadell E, Auban-Senzier P, Batail P (2004) J Mater Chem 14:135
69. Devic T, Evain M, Moëlo Y, Canadell E, Auban-Senzier P, Fourmigué M, Batail P (2003) J Am Chem Soc 125:3295
70. Trigunayat GC (1991) Solid State Ionics 48:3
71. Fujiwara H, Fujiwara B, Nakazawa Y, Nrymbetov BZ, Kato K, Kobayashi H, Kobayashi A, Tokumoto M, Cassoux P (2001) J Am Chem Soc 123:306
72. Uji H, Shinagawa H, Terashima T, Yakabe T, Terai Y, Tokumoto M, Kobayashi A, Tanaka H, Kobayashi H (2001) Nature 410:908
73. Brossard L, Clérac R, Coulon C, Tokumoto M, Ziman T, Petrov DK, Laukhin VN, Naughton MJ, Audouard A, Goze F, Kobayashi A, Kobayashi H, Cassoux P (1998) Eur Phys J B 1:439
74. Miyazaki A, Enomoto K, Okabe K, Yamazaki H, Nishijo J, Enoki T, Ogura E, Ugawa K, Kuwatani Y, Iyoda M (2002) J Solid State Chem 168:547
75. Nishijo J, Miyazaki A, Enoki T, Watanabe R, Kuwatani Y, Iyoda M (2005) Inorg Chem 44:2493
76. Shirahata T, Kibune M, Maesato M, Kawashima T, Saito G, Imakubo T (2006) J Mater Chem 16:3381
77. Ranganathan A, El-Ghayoury A, Mézière C, Harté E, Clérac R, Batail P (2006) Chem Commun, p 2878
78. Ouahab L, Setifi F, Golhen S, Imakubo T, Lescouezec R, Lloret F, Julve M, Swietlik R (2005) CR Chim 8:1286
79. Hervé K, Cador O, Golhen S, Costuas K, Halet JF, Shirahata T, Muto T, Imakubo T, Miyazaki A, Ouahab L (2006) Chem Mater 18:790
80. Kato R (2004) Chem Rev 104:5319
81. Stiefel EI (ed) (2004) Dithiolene chemistry. Prog Inorg Chem 52:399
82. Fourmigué M (2004) Acc Chem Res 37:179
83. Robertson N, Cronin L (2002) Coord Chem Rev 227:93
84. Batsanov AS, Moore AJ, Robertson N, Gree A, Bryce MR, Howard JAK, Underhill AE (1997) J Mater Chem 7:387
85. Nishijo J, Ogura E, Yamaura J, Miyazaki A, Enoki T, Takano T, Kuwatani Y, Iyoda M (2000) Solid State Commun 116:661
86. Devic T, Domercq B, Auban-Senzier P, Molinié P, Fourmigué M (2002) Eur J Inorg Chem, p 2844
87. Devic T, Bertran JN, Domercq B, Canadell E, Avarvari N, Auban-Senzier P, Fourmigué M (2001) New J Chem 25:1418
88. Desiraju GR, Harlow RL (1989) J Am Chem Soc 111:6757
89. Imakubo T, Maruyama T, Sawa H, Kobayashi K (1998) Chem Commun, p 2021

90. Suizi R, Imakubo T (2003) Org Biomol Chem 1:3629
91. Imakubo T, Kibune M, Yoshino H, Shirahata T, Yoza K (2006) J Mater Chem 16:4110
92. Miyazaki E, Morita Y, Nakasuji K (2005) Polyhedron 24:2632
93. Ghassemzadeh M, Harms K, Dehnicke K (1996) Chem Ber 129:259
94. Yamamoto HM, Yamaura JI, Kato R (1998) J Mater Chem 8:15
95. Yamamoto HM, Yamaura JI, Kato R (1998) J Am Chem Soc 120:5905
96. Kosaka Y, Yamamoto HM, Nakao A, Kato R (2006) Bull Chem Soc Jpn 79:1148

# Author Index Volumes 101–126

Author Index Vols. 1–100 see Vol. 100

*The volume numbers are printed in italics*


Alajarin M, see Turner DR (2004) *108*: 97–168
Aldinger F, see Seifert HJ (2002) *101*: 1–58
Alessio E, see Iengo E (2006) *121*: 105–143
Alfredsson M, see Corà F (2004) *113*: 171–232
Aliev AE, Harris KDM (2004) Probing Hydrogen Bonding in Solids Using State NMR Spectroscopy *108*: 1–54
Alloul H, see Brouet V (2004) *109*: 165–199
Amstutz N, see Hauser A (2003) *106*: 81–96
Anitha S, Rao KSJ (2003) The Complexity of Aluminium-DNA Interactions: Relevance to Alzheimer's and Other Neurological Diseases *104*: 79–98
Anthon C, Bendix J, Schäffer CE (2004) Elucidation of Ligand-Field Theory. Reformulation and Revival by Density Functional Theory *107*: 207–302
Aramburu JA, see Moreno M (2003) *106*: 127–152
Arčon D, Blinc R (2004) The Jahn-Teller Effect and Fullerene Ferromagnets *109*: 231–276
Arman HD, see Pennington WT (2007) *126*: 65–104
Aromí G, Brechin EK (2006) Synthesis of 3*d* Metallic Single-Molecule Magnets. *122*: 1–67
Atanasov M, Daul CA, Rauzy C (2003) A DFT Based Ligand Field Theory *106*: 97–125
Atanasov M, see Reinen D (2004) *107*: 159–178
Atwood DA, see Conley B (2003) *104*: 181–193
Atwood DA, Hutchison AR, Zhang Y (2003) Compounds Containing Five-Coordinate Group 13 Elements *105*: 167–201
Atwood DA, Zaman MK (2006) Mercury Removal from Water *120*: 163–182
Autschbach J (2004) The Calculation of NMR Parameters in Transition Metal Complexes *112*: 1–48

Baerends EJ, see Rosa A (2004) *112*: 49–116
Balch AL (2007) Remarkable Luminescence Behaviors and Structural Variations of Two-Coordinate Gold(I) Complexes. *123*: 1–40
Baranoff E, Barigelletti F, Bonnet S, Collin J-P, Flamigni L, Mobian P, Sauvage J-P (2007) From Photoinduced Charge Separation to Light-Driven Molecular Machines. *123*: 41–78
Barbara B, see Curély J (2006) *122*: 207–250
Bard AJ, Ding Z, Myung N (2005) Electrochemistry and Electrogenerated Chemiluminescence of Semiconductor Nanocrystals in Solutions and in Films *118*: 1–57
Barigelletti F, see Baranoff E (2007) *123*: 41–78
Barriuso MT, see Moreno M (2003) *106*: 127–152
Beaulac R, see Nolet MC (2004) *107*: 145–158

Bebout DC, Berry SM (2006) Probing Mercury Complex Speciation with Multinuclear NMR *120*: 81–105
Bellamy AJ (2007) FOX-7 (1,1-Diamino-2,2-dinitroethene). *125*: 1–33
Bellandi F, see Contreras RR (2003) *106*: 71–79
Bendix J, see Anthon C (2004) *107*: 207–302
Berend K, van der Voet GB, de Wolff FA (2003) Acute Aluminium Intoxication *104*: 1–58
Berry SM, see Bebout DC (2006) *120*: 81–105
Bianconi A, Saini NL (2005) Nanoscale Lattice Fluctuations in Cuprates and Manganites *114*: 287–330
Biella S, see Metrangolo P (2007) *126*: 105–136
Blinc R, see Arcčon D (2004) *109*: 231–276
Blinc R (2007) Order and Disorder in Perovskites and Relaxor Ferroelectrics. *124*: 51–67
Boča R (2005) Magnetic Parameters and Magnetic Functions in Mononuclear Complexes Beyond the Spin-Hamiltonian Formalism *117*: 1–268
Bohrer D, see Schetinger MRC (2003) *104*: 99–138
Bonnet S, see Baranoff E (2007) *123*: 41–78
Bouamaied I, Coskun T, Stulz E (2006) Axial Coordination to Metalloporphyrins Leading to Multinuclear Assemblies *121*: 1–47
Boulanger AM, see Nolet MC (2004) *107*: 145–158
Boulon G (2004) Optical Transitions of Trivalent Neodymium and Chromium Centres in $LiNbO_3$ Crystal Host Material *107*: 1–25
Bowlby BE, Di Bartolo B (2003) Spectroscopy of Trivalent Praseodymium in Barium Yttrium Fluoride *106*: 193–208
Braga D, Maini L, Polito M, Grepioni F (2004) Hydrogen Bonding Interactions Between Ions: A Powerful Tool in Molecular Crystal Engineering *111*: 1–32
Brechin EK, see Aromí G (2006) *122*: 1–67
Brouet V, Alloul H, Gàràj S, Forrò L (2004) NMR Studies of Insulating, Metallic, and Superconducting Fullerides: Importance of Correlations and Jahn-Teller Distortions *109*: 165–199
Bruce DW (2007) Halogen-bonded Liquid Crystals. *126*: 161–180
Buddhudu S, see Morita M (2004) *107*: 115–144
Budzelaar PHM, Talarico G (2003) Insertion and $\beta$-Hydrogen Transfer at Aluminium *105*: 141–165
Burrows AD (2004) Crystal Engineering Using Multiple Hydrogen Bonds *108*: 55–96
Bussmann-Holder A, Dalal NS (2007) Order/Disorder Versus or with Displacive Dynamics in Ferroelectric Systems. *124*: 1–21
Bussmann-Holder A, Keller H, Müller KA (2005) Evidences for Polaron Formation in Cuprates *114*: 367–386
Bussmann-Holder A, see Dalal NS (2007) *124*: 23–50
Bussmann-Holder A, see Micnas R (2005) *114*: 13–69
Byrd EFC, see Rice BM (2007) *125*: 153–194

Canadell E, see Sánchez-Portal D (2004) *113*: 103–170
Cancines P, see Contreras RR (2003) *106*: 71–79
Caneschi A, see Cornia A (2006) *122*: 133–161
Cartwright HM (2004) An Introduction to Evolutionary Computation and Evolutionary Algorithms *110*: 1–32
Chapman RD (2007) Organic Difluoramine Derivatives. *125*: 123–151
Christie RA, Jordan KD (2005) *n*-Body Decomposition Approach to the Calculation of Interaction Energies of Water Clusters *116*: 27–41

Clérac R, see Coulon C (2006) *122*: 163–206
Clot E, Eisenstein O (2004) Agostic Interactions from a Computational Perspective: One Name, Many Interpretations *113*: 1–36
Collin J-P, see Baranoff E (2007) *123*: 41–78
Conley B, Atwood DA (2003) Fluoroaluminate Chemistry *104*: 181–193
Contakes SM, Nguyen YHL, Gray HB, Glazer EC, Hays A-M, Goodin DB (2007) Conjugates of Heme-Thiolate Enzymes with Photoactive Metal-Diimine Wires. *123*: 177–203
Contreras RR, Suárez T, Reyes M, Bellandi F, Cancines P, Moreno J, Shahgholi M, Di Bilio AJ, Gray HB, Fontal B (2003) Electronic Structures and Reduction Potentials of Cu(II) Complexes of [N,N′-Alkyl-bis(ethyl-2-amino-1-cyclopentenecarbothioate)] (Alkyl = Ethyl, Propyl, and Butyl) *106*: 71–79
Cooke Andrews J (2006) Mercury Speciation in the Environment Using X-ray Absorption Spectroscopy *120*: 1–35
Corà F, Alfredsson M, Mallia G, Middlemiss DS, Mackrodt WC, Dovesi R, Orlando R (2004) The Performance of Hybrid Density Functionals in Solid State Chemistry *113*: 171–232
Cornia A, Costantino AF, Zobbi L, Caneschi A, Gatteschi D, Mannini M, Sessoli R (2006) Preparation of Novel Materials Using SMMs. *122*: 133–161
Coskun T, see Bouamaied I (2006) *121*: 1–47
Costantino AF, see Cornia A (2006) *122*: 133–161
Coulon C, Miyasaka H, Clérac R (2006) Single-Chain Magnets: Theoretical Approach and Experimental Systems. *122*: 163–206
Crespi VH, see Gunnarson O (2005) *114*: 71–101
Curély J, Barbara B (2006) General Theory of Superexchange in Molecules. *122*: 207–250

Dalal NS, Gunaydin-Sen O, Bussmann-Holder A (2007) Experimental Evidence for the Coexistence of Order/Disorder and Displacive Behavior of Hydrogen-Bonded Ferroelectrics and Antiferroelectrics. *124*: 23–50
Dalal NS, see Bussmann-Holder A (2007) *124*: 1–21
Daul CA, see Atanasov M (2003) *106*: 97–125
Day P (2003) Whereof Man Cannot Speak: Some Scientific Vocabulary of Michael Faraday and Klixbüll Jørgensen *106*: 7–18
Deeth RJ (2004) Computational Bioinorganic Chemistry *113*: 37–69
Delahaye S, see Hauser A (2003) *106*: 81–96
Deng S, Simon A, Köhler J (2005) Pairing Mechanisms Viewed from Physics and Chemistry *114*: 103–141
Di Bartolo B, see Bowlby BE (2003) *106*: 191–208
Di Bilio AJ, see Contreras RR (2003) *106*: 71–79
Ding Z, see Bard AJ (2005) *118*: 1–57
Dovesi R, see Corà F (2004) *113*: 171–232
Duan X, see He J (2005) *119*: 89–119
Duan X, see Li F (2005) *119*: 193–223

Egami T (2005) Electron-Phonon Coupling in High-$T_c$ Superconductors *114*: 267–286
Egami T (2007) Local Structure and Dynamics of Ferroelectric Solids. *124*: 69–88
Eisenstein O, see Clot E (2004) *113*: 1–36
Ercolani G (2006) Thermodynamics of Metal-Mediated Assemblies of Porphyrins *121*: 167–215
Evans DG, see He J (2005) *119*: 89–119
Evans DG, Slade RCT (2005) Structural Aspects of Layered Double Hydroxides *119*: 1–87

Ewing GE (2005) $H_2O$ on NaCl: From Single Molecule, to Clusters, to Monolayer, to Thin Film, to Deliquescence *116*: 1–25

Flamigni L, Heitz V, Sauvage J-P (2006) Porphyrin Rotaxanes and Catenanes: Copper(I)-Templated Synthesis and Photoinduced Processes *121*: 217–261
Flamigni L, see Baranoff E (2007) *123*: 41–78
Fontal B, see Contreras RR (2003) *106*: 71–79
Forrò L, see Brouet V (2004) *109*: 165–199
Fourmigué M (2007) Halogen Bonding in Conducting or Magnetic Molecular Materials. *126*: 181–207
Fowler PW, see Soncini A (2005) *115*: 57–79
Frenking G, see Lein M (2003) *106*: 181–191
Frühauf S, see Roewer G (2002) *101*: 59–136
Frunzke J, see Lein M (2003) *106*: 181–191
Furrer A (2005) Neutron Scattering Investigations of Charge Inhomogeneities and the Pseudogap State in High-Temperature Superconductors *114*: 171–204

Gao H, see Singh RP (2007) *125*: 35–83
Gàràj S, see Brouet V (2004) *109*: 165–199
Gatteschi D, see Cornia A (2006) *122*: 133–161
Gillet VJ (2004) Applications of Evolutionary Computation in Drug Design *110*: 133–152
Glazer EC, see Contakes SM (2007) *123*: 177–203
Golden MS, Pichler T, Rudolf P (2004) Charge Transfer and Bonding in Endohedral Fullerenes from High-Energy Spectroscopy *109*: 201–229
Goodin DB, see Contakes SM (2007) *123*: 177–203
Gorelesky SI, Lever ABP (2004) *107*: 77–114
Grant GJ (2006) Mercury(II) Complexes with Thiacrowns and Related Macrocyclic Ligands *120*: 107–141
Grätzel M, see Nazeeruddin MK (2007) *123*: 113–175
Gray HB, see Contreras RR (2003) *106*: 71–79
Gray HB, see Contakes SM (2007) *123*: 177–203
Grepioni F, see Braga D (2004) *111*: 1–32
Gritsenko O, see Rosa A (2004) *112*: 49–116
Güdel HU, see Wenger OS (2003) *106*: 59–70
Gunnarsson O, Han JE, Koch E, Crespi VH (2005) Superconductivity in Alkali-Doped Fullerides *114*: 71–101
Gunter MJ (2006) Multiporphyrin Arrays Assembled Through Hydrogen Bonding *121*: 263–295
Gunaydin-Sen O, see Dalal NS (2007) *124*: 23–50
Gütlich P, van Koningsbruggen PJ, Renz F (2004) Recent Advances in Spin Crossover Research *107*: 27–76
Guyot-Sionnest P (2005) Intraband Spectroscopy and Semiconductor Nanocrystals *118*: 59–77

Habershon S, see Harris KDM (2004) *110*: 55–94
Han JE, see Gunnarson O (2005) *114*: 71–101
Hanks TW, see Pennington WT (2007) *126*: 65–104
Hardie MJ (2004) Hydrogen Bonded Network Structures Constructed from Molecular Hosts *111*: 139–174
Harris KDM, see Aliev (2004) *108*: 1–54

Harris KDM, Johnston RL, Habershon S (2004) Application of Evolutionary Computation in Structure Determination from Diffraction Data *110*: 55–94
Hartke B (2004) Application of Evolutionary Algorithms to Global Cluster Geometry Optimization *110*: 33–53
Harvey JN (2004) DFT Computation of Relative Spin-State Energetics of Transition Metal Compounds *112*: 151–183
Haubner R, Wilhelm M, Weissenbacher R, Lux B (2002) Boron Nitrides – Properties, Synthesis and Applications *102*: 1–46
Hauser A, Amstutz N, Delahaye S, Sadki A, Schenker S, Sieber R, Zerara M (2003) Fine Tuning the Electronic Properties of $[M(bpy)_3]^{2+}$ Complexes by Chemical Pressure (M = $Fe^{2+}$, $Ru^{2+}$, $Co^{2+}$, bpy = 2,2′-Bipyridine) *106*: 81–96
Hays A-M, see Contakes SM (2007) *123*: 177–203
He J, Wei M, Li B, Kang Y, G Evans D, Duan X (2005) Preparation of Layered Double Hydroxides *119*: 89–119
Heitz V, see Flamigni L (2006) *121*: 217–261
Herrmann M, see Petzow G (2002) *102*: 47–166
Herzog U, see Roewer G (2002) *101*: 59–136
Hoggard PE (2003) Angular Overlap Model Parameters *106*: 37–57
Höpfl H (2002) Structure and Bonding in Boron Containing Macrocycles and Cages *103*: 1–56
Hubberstey P, Suksangpanya U (2004) Hydrogen-Bonded Supramolecular Chain and Sheet Formation by Coordinated Guranidine Derivatives *111*: 33–83
Hupp JT (2006) Rhenium-Linked Multiporphyrin Assemblies: Synthesis and Properties *121*: 145–165
Hutchison AR, see Atwood DA (2003) *105*: 167–201

Iengo E, Scandola F, Alessio E (2006) Metal-Mediated Multi-Porphyrin Discrete Assemblies and Their Photoinduced Properties *121*: 105–143
Itoh M, Taniguchi H (2007) Ferroelectricity of $SrTiO_3$ Induced by Oxygen Isotope Exchange. *124*: 89–118
Iwasa Y, see Margadonna S (2004) *109*: 127–164

Jansen M, Jäschke B, Jäschke T (2002) Amorphous Multinary Ceramics in the Si-B-N-C System *101*: 137–192
Jäschke B, see Jansen M (2002) *101*: 137–192
Jäschke T, see Jansen M (2002) *101*: 137–192
Jaworska M, Macyk W, Stasicka Z (2003) Structure, Spectroscopy and Photochemistry of the $[M(\eta^5\text{-}C_5H_5)(CO)_2]_2$ Complexes (M = Fe, Ru) *106*: 153–172
Jenneskens LW, see Soncini A (2005) *115*: 57–79
Jeziorski B, see Szalewicz K (2005) *116*: 43–117
Johnston RL, see Harris KDM (2004) *110*: 55–94
Jordan KD, see Christie RA (2005) *116*: 27–41

Kabanov VV, see Mihailovic D (2005) *114*: 331–365
Kang Y, see He J (2005) *119*: 89–119
Karpfen A (2007) Theoretical Characterization of the Trends in Halogen Bonding. *126*: 1–15
Keller H (2005) Unconventional Isotope Effects in Cuprate Superconductors *114*: 143–169
Keller H, see Bussmann-Holder A (2005) *114*: 367–386
Khan AI, see Williams GR (2005) *119*: 161–192

Kind R (2007) Evidence for Ferroelectric Nucleation Centres in the Pseudo-spin Glass System $Rb_{1-x}(ND_4)_xD_2PO_4$: A $^{87}Rb$ NMR Study. *124*: 119–147
Klapötke TM (2007) New Nitrogen-Rich High Explosives. *125*: 85–121
Kobuke Y (2006) Porphyrin Supramolecules by Self-Complementary Coordination *121*: 49–104
Koch E, see Gunnarson O (2005) *114*: 71–101
Kochelaev BI, Teitel'baum GB (2005) Nanoscale Properties of Superconducting Cuprates Probed by the Electron Paramagnetic Resonance *114*: 205–266
Kochi JK, see Rosokha SV (2007) *126*: 137–160
Köhler J, see Deng (2005) *114*: 103–141
van Koningsbruggen, see Gütlich P (2004) *107*: 27–76
Kume S, Nishihara H (2007) Metal-Based Photoswitches Derived from Photoisomerization. *123*: 79–112

Legon AC (2007) The Interaction of Dihalogens and Hydrogen Halides with Lewis Bases in the Gas Phase: An Experimental Comparison of the Halogen Bond and the Hydrogen Bond. *126*: 17–64
Lein M, Frunzke J, Frenking G (2003) Christian Klixbüll Jørgensen and the Nature of the Chemical Bond in HArF *106*: 181–191
Leroux F, see Taviot-Gueho C (2005) *119*: 121–159
Lever ABP, Gorelesky SI (2004) Ruthenium Complexes of Non-Innocent Ligands; Aspects of Charge Transfer Spectroscopy *107*: 77–114
Li B, see He J (2005) *119*: 89–119
Li F, Duan X (2005) Applications of Layered Double Hydroxides *119*: 193–223
Liebau F, see Santamaría-Pérez D (2005) *118*: 79–135
Linton DJ, Wheatley AEH (2003) The Synthesis and Structural Properties of Aluminium Oxide, Hydroxide and Organooxide Compounds *105*: 67–139
Lo KK-W (2007) Luminescent Transition Metal Complexes as Biological Labels and Probes. *123*: 205–245
Lux B, see Haubner R (2002) *102*: 1–46

Mackrodt WC, see Corà F (2004) *113*: 171–232
Macyk W, see Jaworska M (2003) *106*: 153–172
Mahalakshmi L, Stalke D (2002) The R2M+ Group 13 Organometallic Fragment Chelated by P-centered Ligands *103*: 85–116
Maini L, see Braga D (2004) *111*: 1–32
Mallah T, see Rebilly J-N (2006) *122*: 103–131
Mallia G, see Corà F (2004) *113*: 171–232
Mannini M, see Cornia A (2006) *122*: 133–161
Margadonna S, Iwasa Y, Takenobu T, Prassides K (2004) Structural and Electronic Properties of Selected Fulleride Salts *109*: 127–164
Maseras F, see Ujaque G (2004) *112*: 117–149
Mattson WD, see Rice BM (2007) *125*: 153–194
McInnes EJL (2006) Spectroscopy of Single-Molecule Magnets. *122*: 69–102
Merunka D, Rakvin B (2007) Anharmonic and Quantum Effects in KDP-Type Ferroelectrics: Modified Strong Dipole–Proton Coupling Model. *124*: 149–198
Meshri DT, see Singh RP (2007) *125*: 35–83
Metrangolo P, Resnati G, Pilati T, Biella S (2007) Halogen Bonding in Crystal Engineering. *126*: 105–136

Micnas R, Robaszkiewicz S, Bussmann-Holder A (2005) Two-Component Scenarios for Non-Conventional (Exotic) Superconstructors *114*: 13–69
Middlemiss DS, see Corà F (2004) *113*: 171–232
Mihailovic D, Kabanov VV (2005) Dynamic Inhomogeneity, Pairing and Superconductivity in Cuprates *114*: 331–365
Millot C (2005) Molecular Dynamics Simulations and Intermolecular Forces *115*: 125–148
Miyake T, see Saito (2004) *109*: 41–57
Miyasaka H, see Coulon C (2006) *122*: 163–206
Mobian P, see Baranoff E (2007) *123*: 41–78
Moreno J, see Contreras RR (2003) *106*: 71–79
Moreno M, Aramburu JA, Barriuso MT (2003) Electronic Properties and Bonding in Transition Metal Complexes: Influence of Pressure *106*: 127–152
Morita M, Buddhudu S, Rau D, Murakami S (2004) Photoluminescence and Excitation Energy Transfer of Rare Earth Ions in Nanoporous Xerogel and Sol-Gel $SiO_2$ Glasses *107*: 115–143
Morsch VM, see Schetinger MRC (2003) *104*: 99–138
Mossin S, Weihe H (2003) Average One-Center Two-Electron Exchange Integrals and Exchange Interactions *106*: 173–180
Murakami S, see Morita M (2004) *107*: 115–144
Müller E, see Roewer G (2002) *101*: 59–136
Müller KA (2005) Essential Heterogeneities in Hole-Doped Cuprate Superconductors *114*: 1–11
Müller KA, see Bussmann-Holder A (2005) *114*: 367–386
Myung N, see Bard AJ (2005) *118*: 1–57

Nazeeruddin MK, Grätzel M (2007) Transition Metal Complexes for Photovoltaic and Light Emitting Applications. *123*: 113–175
Nguyen YHL, see Contakes SM (2007) *123*: 177–203
Nishibori E, see Takata M (2004) *109*: 59–84
Nishihara H, see Kume S (2007) *123*: 79–112
Nolet MC, Beaulac R, Boulanger AM, Reber C (2004) Allowed and Forbidden d-d Bands in Octa-hedral Coordination Compounds: Intensity Borrowing and Interference Dips in Absorption Spectra *107*: 145–158

O'Hare D, see Williams GR (2005) *119*: 161–192
Ordejón P, see Sánchez-Portal D (2004) *113*: 103–170
Orlando R, see Corà F (2004) *113*: 171–232
Oshiro S (2003) A New Effect of Aluminium on Iron Metabolism in Mammalian Cells *104*: 59–78

Pastor A, see Turner DR (2004) *108*: 97–168
Patkowski K, see Szalewicz K (2005) *116*: 43–117
Patočka J, see Strunecká A (2003) *104*: 139–180
Peng X, Thessing J (2005) Controlled Synthesis of High Quality Semiconductor Nanocrystals *118*: 137–177
Pennington WT, Hanks TW, Arman HD (2007) Halogen Bonding with Dihalogens and Interhalogens. *126*: 65–104
Petzow G, Hermann M (2002) Silicon Nitride Ceramics *102*: 47–166
Pichler T, see Golden MS (2004) *109*: 201–229
Pilati T, see Metrangolo P (2007) *126*: 105–136

Polito M, see Braga D (2004) *111*: 1–32
Popelier PLA (2005) Quantum Chemical Topology: on Bonds and Potentials *115*: 1–56
Power P (2002) Multiple Bonding Between Heavier Group 13 Elements *103*: 57–84
Prassides K, see Margadonna S (2004) *109*: 127–164
Prato M, see Tagmatarchis N (2004) *109*: 1–39
Price LS, see Price SSL (2005) *115*: 81–123
Price SSL, Price LS (2005) Modelling Intermolecular Forces for Organic Crystal Structure Prediction *115*: 81–123

Rabinovich D (2006) Poly(mercaptoimidazolyl)borate Complexes of Cadmium and Mercury *120*: 143–162
Rakvin B, see Merunka D (2007) *124*: 149–198
Rao KSJ, see Anitha S (2003) *104*: 79–98
Rau D, see Morita M (2004) *107*: 115–144
Rauzy C, see Atanasov (2003) *106*: 97–125
Reber C, see Nolet MC (2004) *107*: 145–158
Rebilly J-N, Mallah T (2006) Synthesis of Single-Molecule Magnets Using Metallocyanates. *122*: 103–131
Reinen D, Atanasov M (2004) The Angular Overlap Model and Vibronic Coupling in Treating s-p and d-s Mixing – a DFT Study *107*: 159–178
Reisfeld R (2003) Rare Earth Ions: Their Spectroscopy of Cryptates and Related Complexes in Glasses *106*: 209–237
Renz F, see Gütlich P (2004) *107*: 27–76
Resnati G, see Metrangolo P (2007) *126*: 105–136
Reyes M, see Contreras RR (2003) *106*: 71–79
Ricciardi G, see Rosa A (2004) *112*: 49–116
Rice BM, Byrd EFC, Mattson WD (2007) Computational Aspects of Nitrogen-Rich HEDMs. *125*: 153–194
Riesen H (2004) Progress in Hole-Burning Spectroscopy of Coordination Compounds *107*: 179–205
Robaszkiewicz S, see Micnas R (2005) *114*: 13–69
Roewer G, Herzog U, Trommer K, Müller E, Frühauf S (2002) Silicon Carbide – A Survey of Synthetic Approaches, Properties and Applications *101*: 59–136
Rosa A, Ricciardi G, Gritsenko O, Baerends EJ (2004) Excitation Energies of Metal Complexes with Time-dependent Density Functional Theory *112*: 49–116
Rosokha SV, Kochi JK (2007) X-ray Structures and Electronic Spectra of the **π**-Halogen Complexes between Halogen Donors and Acceptors with **π**-Receptors. *126*: 137–160
Rudolf P, see Golden MS (2004) *109*: 201–229
Ruiz E (2004) Theoretical Study of the Exchange Coupling in Large Polynuclear Transition Metal Complexes Using DFT Methods *113*: 71–102

Sadki A, see Hauser A (2003) *106*: 81–96
Saini NL, see Bianconi A (2005) *114*: 287–330
Saito S, Umemoto K, Miyake T (2004) Electronic Structure and Energetics of Fullerites, Fullerides, and Fullerene Polymers *109*: 41–57
Sakata M, see Takata M (2004) *109*: 59–84
Sánchez-Portal D, Ordejón P, Canadell E (2004) Computing the Properties of Materials from First Principles with SIESTA *113*: 103–170
Santamaría-Pérez D, Vegas A, Liebau F (2005) The Zintl–Klemm Concept Applied to Cations in Oxides II. The Structures of Silicates *118*: 79–135

Sauvage J-P, see Flamigni L (2006) *121*: 217–261
Sauvage J-P, see Baranoff E (2007) *123*: 41–78
Scandola F, see Iengo E (2006) *121*: 105–143
Schäffer CE (2003) Axel Christian Klixbüll Jørgensen (1931–2001) *106*: 1–5
Schäffer CE, see Anthon C (2004) *107*: 207–301
Schenker S, see Hauser A (2003) *106*: 81–96
Schetinger MRC, Morsch VM, Bohrer D (2003) Aluminium: Interaction with Nucleotides and Nucleotidases and Analytical Aspects of Determination *104*: 99–138
Schmidtke HH (2003) The Variation of Slater-Condon Parameters $F^k$ and Racah Parameters B and C with Chemical Bonding in Transition Group Complexes *106*: 19–35
Schubert DM (2003) Borates in Industrial Use *105*: 1–40
Schulz S (2002) Synthesis, Structure and Reactivity of Group 13/15 Compounds Containing the Heavier Elements of Group 15, Sb and Bi *103*: 117–166
Scott JF (2007) A Comparison of Magnetic Random Access Memories (MRAMs) and Ferroelectric Random Access Memories (FRAMs). *124*: 199–207
Seifert HJ, Aldinger F (2002) Phase Equilibria in the Si-B-C-N System *101*: 1–58
Sessoli R, see Cornia A (2006) *122*: 133–161
Shahgholi M, see Contreras RR (2003) *106*: 71–79
Shinohara H, see Takata M (2004) *109*: 59–84
Shreeve JM, see Singh RP (2007) *125*: 35–83
Sieber R, see Hauser A (2003) *106*: 81–96
Simon A, see Deng (2005) *114*: 103–141
Singh RP, Gao H, Meshri DT, Shreeve JM (2007) Nitrogen-Rich Heterocycles. *125*: 35–83
Slade RCT, see Evans DG (2005) *119*: 1–87
Soncini A, Fowler PW, Jenneskens LW (2005) Angular Momentum and Spectral Decomposition of Ring Currents: Aromaticity and the Annulene Model *115*: 57–79
Stalke D, see Mahalakshmi L (2002) *103*: 85–116
Stasicka Z, see Jaworska M (2003) *106*: 153–172
Steed JW, see Turner DR (2004) *108*: 97–168
Strunecká A, Patočka J (2003) Aluminofluoride Complexes in the Etiology of Alzheimer's Disease *104*: 139–180
Stulz E, see Bouamaied I (2006) *121*: 1–47
Suárez T, see Contreras RR (2003) *106*: 71–79
Suksangpanya U, see Hubberstey (2004) *111*: 33–83
Sundqvist B (2004) Polymeric Fullerene Phases Formed Under Pressure *109*: 85–126
Szalewicz K, Patkowski K, Jeziorski B (2005) Intermolecular Interactions via Perturbation Theory: From Diatoms to Biomolecules *116*: 43–117

Tagmatarchis N, Prato M (2004) Organofullerene Materials *109*: 1–39
Takata M, Nishibori E, Sakata M, Shinohara M (2004) Charge Density Level Structures of Endohedral Metallofullerenes by MEM/Rietveld Method *109*: 59–84
Takenobu T, see Margadonna S (2004) *109*: 127–164
Talarico G, see Budzelaar PHM (2003) *105*: 141–165
Taniguchi H, see Itoh M (2007) *124*: 89–118
Taviot-Gueho C, Leroux F (2005) In situ Polymerization and Intercalation of Polymers in Layered Double Hydroxides *119*: 121–159
Teitel'baum GB, see Kochelaev BI (2005) *114*: 205–266
Thessing J, see Peng X (2005) *118*: 137–177
Trommer K, see Roewer G (2002) *101*: 59–136
Tsuzuki S (2005) Interactions with Aromatic Rings *115*: 149–193

Turner DR, Pastor A, Alajarin M, Steed JW (2004) Molecular Containers: Design Approaches and Applications *108*: 97–168

Uhl W (2003) Aluminium and Gallium Hydrazides *105*: 41–66
Ujaque G, Maseras F (2004) Applications of Hybrid DFT/Molecular Mechanics to Homogeneous Catalysis *112*: 117–149
Umemoto K, see Saito S (2004) *109*: 41–57
Unger R (2004) The Genetic Algorithm Approach to Protein Structure Prediction *110*: 153–175

van der Voet GB, see Berend K (2003) *104*: 1–58
Vegas A, see Santamaría-Pérez D (2005) *118*: 79–135
Vilar R (2004) Hydrogen-Bonding Templated Assemblies *111*: 85–137

Wei M, see He J (2005) *119*: 89–119
Weihe H, see Mossin S (2003) *106*: 173–180
Weissenbacher R, see Haubner R (2002) *102*: 1–46
Wenger OS, Güdel HU (2003) Influence of Crystal Field Parameters on Near-Infrared to Visible Photon Upconversion in $Ti^{2+}$ and $Ni^{2+}$ Doped Halide Lattices *106*: 59–70
Wheatley AEH, see Linton DJ (2003) *105*: 67–139
Wilhelm M, see Haubner R (2002) *102*: 1–46
Williams GR, Khan AI, O'Hare D (2005) Mechanistic and Kinetic Studies of Guest Ion Intercalation into Layered Double Hydroxides Using Time-resolved, In-situ X-ray Powder Diffraction *119*: 161–192
de Wolff FA, see Berend K (2003) *104*: 1–58
Woodley SM (2004) Prediction of Crystal Structures Using Evolutionary Algorithms and Related Techniques *110*: 95–132

Xantheas SS (2005) Interaction Potentials for Water from Accurate Cluster Calculations *116*: 119–148

Zaman MK, see Atwood DA (2006) *120*: 163–182
Zeman S (2007) Sensitivities of High Energy Compounds. *125*: 195–271
Zerara M, see Hauser A (2003) *106*: 81–96
Zhang H (2006) Photochemical Redox Reactions of Mercury *120*: 37–79
Zhang Y, see Atwood DA (2003) *105*: 167–201
Zobbi L, see Cornia A (2006) *122*: 133–161

# Subject Index


Ab initio calculations 1, 31
Acridine 87
Adamantanoid architectures 127
Alkenes, dihalogen complexes 139
Allene···HCl 42
Angular geometries 17, 23
Anion–$\pi$ interaction 137
Arenes, dihalogen complexes 139
Arsenic electron donors 89

B···ClF, angular geometries 25
B···HCl, angular geometries 25
B···XY 21
Basis set superposition error (BSSE) 3
Benzene···HCl 39
Binding strength 50
Bis(2-pyridylcarbonyl)amide) 197
4,5-Bis(bromomethyl)-1,3-dithiole-2-thione-diiodine diiodine (HAMCAA) 87
1,4-(Bisiodoethynyl)benzene (pBIB) 202
Bromotetraselenafulvalenes 188
Bumps-in-hollows 67
Butadiene 39

CCSD(T) 3
Charge transfer 65, 137
Charge-transfer complexes/interactions 1, 67, 168
9-Chloroacridine 87
*p*-Chlorophenyl nitronyl nitroxide 184
Complex resonance 67
Counterpoise (CP) 3
Crystal engineering 105, 181
–, radical molecules 182
Crystal structures 69
Crystallography 65
C–X···B 11
C–X···H-C 12
C–X···N 12
Cyanotetrathiafulvalenes 199
Cyclopropane···ClF 38

Density functional theory (DFT) 3
Dibromine 139
Difluorotetraiodobenzene (DFTIB) 202
Dihalogen acceptors, aromatic/olefinic $\pi$-donors 146
Dihalogen complexes, arenes/alkenes 139
Dihalogens 17
–, halogen bonding 68
Dihalopyrazinodithiafulvalene 200
Diiodine 139
Diiododithiapyrenes 201
1,4-Diiodooctafluorobutane/tetrakis(4-pyridyl)pentaerythritol 128
*p*-Diiodotetrafluorobenzene (*p*TFDIB) 184
1,3-Diselenole-2-thione 188
Dithiadiselenafulvalenes 188
Dithiapyrenes (DTPYs) 201
Dithiole thiones 69, 188
Dithiolene complexes 198
Donor/acceptor complexes, halogen derivatives, unified Mulliken correlations 144
Donor/acceptor interactions 67
–, halogen derivatives 139
Donor/acceptor moieties, molecular geometries 155
DOXABR 87

Electric charge transfer 17
Electron clutching 67
$\pi$ –Electron donors 97
Electronic spectra 137
Electrophilicities 49

Ethene 36
Ethyne 37
Exaltation of valency 67

Filling of antibonding orbitals 67
Fourier-transform (F-T) 21
Furan 45

Hal···halanion interactions 192
Hal···nitrile interactions 197
Halide anions, aromatic/olefinic $\pi$-acceptors 142
–, aromatic/olefinic $\pi$-receptors 150
Halocarbon acceptors 141
Halocarbon, role 114
Halogen bonding 1, 17, 19, 65, 105, 181
–, intermolecular separations 155
$\pi$-Halogen interactions, donor/acceptor (structural) effects 155
Halogen $\pi$-bonding 137
Halogen-bonded supramolecular architectures 118
Halo-PFCs 109
Hartree–Fock, restricted (RHF) 4
Hydrogen bonding 1, 19, 169

Imidazole selones 69
Imidazole thiones 69
Iododithiapyrenes 200
*p*-Iodophenyl nitronyl nitroxide 184
Iodopyrazino TTFs, iododithiapyrenes 200

LCs 161
LCAO 67
Lewis bases 17
Liquid crystals, halogen-bonded 161, 174
–, high molar mass 165
–, low molar mass 162
–, mesophases 166
–, non-covalent interactions 167
–, thermotropic 162

Mesogens, halogen-bonded 161
Methylenecyclopropane 42
4-Methylpyridine-$I_2$ 93
Microwave spectroscopy 21
Molecular beam electric resonance spectroscopy (MBERS) 21
Molecular modeling 65
Møller–Plesset second-order (MP2) 3
Monoiododithiapyrene 202

Nitrogen electron donors 87, 93
Nitronyl nitroxides, halogenated 184
Nitroxides 181
–, binary systems 185
–, halogenated neutral 183
–, neutral radical 183
Nuclear quadrupole coupling constants (NQCCs) 4
Nucleophilicities 49

Oxazole thiones 69
Oxetane 34
Oxirane···ClF/···HCl 32
Oxygen electron donors 87, 92

Pairsin-pockets 67
PAQKIB 70, 87
Phosphorus electron donors 88
Polycyanometallates 197
Polyhalogenated methanes, $\pi$-donors 148
Polyhalometallates 196
Potential energy (PE) 26
Prereactive complexes 3, 20
Pseudo-$\pi$-pairs 38
Pyridine 46
Pyridine-ICl 93

Quadrupolar interactions 167

Radial geometries, halogen-bonded complexes 23
Radical molecules 182

Selenium electron donors 89, 95
Selenoamides 69
Selenoethers 69
SOMOs 182
Sulfur dioxide 35
Sulfur electron donors 88, 95
Supramolecular chemistry 105

TANOL 183
TCNQ 187
Tecton 105
TEMPO 183
Tetra-2′-pyridylpyrazine 87

Tetramethylethylenediamine (TMEDA) 109
Tetrathiafulvalenes (TTFs) 181
–, conducting materials 186
Thermotropic liquid crystals 162
Thiazole selones 69
Thiazole thiones 69
Thiirane···ClF/···HCl 35
Thiophene···HCl 45
Thiourea derivatives 69
Topology 105
Tris(diethylamino)phosphine selenide 70
TTFs, iodopyrazino, iododithiapyrenes 200
–, neutral halogenated 188
–, salts 187

Vinyl fluoride 45

X-ray crystallography 137
XB 107
–, directionality 116
–, electron density, halogen atoms 110
XB vs. HB 109
XY···amine 10
XY···B 3
XY···$NH_3$ 4